Simulating SCWR thermal-hydraulics with the modified COBRA-TF subchannel code

SIMULATING SCWR THERMAL-HYDRAULICS WITH THE MODIFIED COBRA-TF SUBCHANNEL CODE

BY

DINUSHA LOKULIYANA, B.Eng.Mgt

A THESIS

SUBMITTED TO THE DEPARTMENT OF ENGINEERING PHYSICS

AND THE SCHOOL OF GRADUATE STUDIES

OF MCMASTER UNIVERSITY

IN PARTIAL FULFILMENT OF THE REQUIREMENTS

FOR THE DEGREE OF

MASTER OF APPLIED SCIENCE

Master of Applied Science (2014) McMaster University

(Engineering Physics) Hamilton, Ontario, Canada

TITLE:	Simulating SCWR thermal-hydraulics with the modified COBRA-TF subchannel code
AUTHOR:	Dinusha Lokuliyana B.Eng.Mgt, (Engineering Physics) McMaster University, Hamilton,Canada
SUPERVISOR:	Dr. D.R. Novog
NUMBER OF PAGES:	xviii, 296

Abstract

Among the six GEN-IV reactor concepts recommended by the Gen-IV International Forum, supercritical water-cooled reactors (SCWR) have gained significant interests due to its economic advantage, technology and experience continuity. According to the Generation IV International Forum (GIF), the use of supercritical water in nuclear reactors will significantly increase the efficiency of modern nuclear power plants from 33%-35% to about 40%-45% and decrease capital and operational costs [19]. Extensive R&D activities have been launched covering the various aspects of SCWR development, especially in thermal-hydraulic analysis. In Canada, most R&D projects are led by AECL or NRCan.

SCWR design and development require the modification of simulation codes used for design and safety demonstration of subcritical water-cooled reactors. Subchannel codes predict the detailed thermalhydraulic behaviour of coolant within fuel assemblies. This study modifies the subchannel code COBRA-TF, applicable to only subcritical water-cooled reactors, to a new version COBRA-TF-SC, applicable to both supercritical and subcritical water-cooled reactors. Supercritical water property data tables and supercritical water property formulations are implemented. Supercritical water heat transfer and pressure drop correlations are also added. The saturation curve in the subcritical model is extended by introducing a pseudo two-phase region at supercritical

pressures to avoid any numerical instabilities consistent with other studies.

Some simple fuel bundle experimental data on the flow and temperature distribution are used to evaluate the code. The fuel bundle experiment is simulated with both COBRA-TF-SC and AECL's modified ASSERT-PV-SC. The COBRA-TF-SC predicted results show good agreement with the experimental data and results obtained from ASSERT-PV-SC, demonstrating good feasibility and accuracy of this code. COBRA-TF-SC is then used to predict the detailed thermalhydraulic behaviour of the 62-element Canadian SCWR fuel bundle design. The advantage of COBRA-TF-SC is that it can accommodate transcritical flow conditions whereas the existing subchannel codes for SCWRs cannot.

Acknowledgements

I am very grateful to those who have supported me with my research and completion of this thesis. First and foremost, I would like to extend my gratitude to my graduate supervisor, Dr. David Novog, for providing me with the opportunity to perform this study and guiding me throughout the entire process. The experiences I have had over the past two years were truly amazing.

I would also like to thank everyone at the Atomic Energy of Canada Limited for warmly welcoming me during my 2 months stay. My most sincere thanks go to Armando Nava-Dominguez, Thomas Beuthe, and Lawrence Leung at AECL for their help, expertise and advice.

Finally, and most importantly I would like to thank my family and friends for all their love and support. None of this would have been possible without them.

Contents

List of Tables

List of Figures

Chapter 1

Introduction and Problem Statement

In the Generation IV International Forum (GIF) program, the Supercritical Water-Cooled Reactor (SCWR) concept is among the six innovative reactor types selected for development [19]. A Supercritical Water-Cooled Reactor (SCWR) is high-temperature, high-pressure water-cooled reactor that operates at pressures above the critical pressure of water. This gives a number of advantages over current Subcritical Water-Cooled Reactors; increase in thermal efficiency due to higher operating parameters, no boiling crisis due to the single phase nature of supercritical water, and a better economics due to the absence of steam separators and steam dryers as well as steam generators and a smaller containment building [19]. There are currently two types of SCWR concepts; (a) reactor pressure vessel containing the reactor core heat source, similar to conventional PWRs and BWRs, and (b) distributed pressure tubes or channels containing fuel bundles, similar to conventional CANDU [19]. The distributed pressure tubes concept is investigated in more detail in the current study.

Operating above the critical pressure of water brings about new technical challenges. The thermalhydraulics behaviour of water at supercritical conditions is different compared to water at subcritical conditions. The thermophysical properties of water undergo rapid fluctuations with steep changes at supercritical pressures especially near the pseudocritical line [19]. The heat transfer and pressure drop characteristics are strongly affected by steep changes of thermophysical properties [19]. The steep variations in thermophysical properties of water along the core height can result in hot spots leading to high local cladding temperatures challenging the cladding integrity [19]. Therefore, an exhaustive knowledge of the thermalhydraulic behaviour at supercritical water conditions is required for SCWR fuel assembly design.

System codes, Subchannel codes, and CFD codes are used to simulate nuclear reactor thermalhydraulics. Subchannel codes are typically used to simulate thermal-hydraulic behaviour within a fuel bundle in nuclear reactors. Subchannel codes must be able to simulate these supercritical water conditions when analysing fuel assemblies in Supercritical Water-Cooled Reactors. Currently, only a few existing subchannel codes are capable of simulating supercritical water conditions. The COBRA-TF code belongs to the series of the COBRA (COolant Boiling in Rod Arrays) subchannel analysis computer codes which were originally developed by Pacific Northwest Laboratories (PNL). COBRA-TF can only simulate subcritical water conditions observed in existing nuclear reactors. Therefore in the current study, a modified subchannel analysis code COBRA-TF-SC is developed to simulate supercritical water conditions inherent to Supercritical Water-Cooled Reactors by modifying the existing subchannel analysis code COBRA-TF. The subchannel analysis code COBRA-TF is modified to simulate both subcritical and supercritical water

conditions. Several modifications are implemented in the code. The operating pressure range of the existing COBRA-TF code is extended by introducing a pseudo two-phase region at supercritical pressures to maintain the two-fluid structure of the code. The existing property formulations and intrinsic property table of COBRA-TF only cover the subcritical pressure region. Therefore, new property formulations and intrinsic property tables based on the IAPWS Industrial Formulation 1997 for the Thermodynamic Properties of Water and Steam are added to the code. The heat transfer and frictional pressure drop characteristics are strongly affected by the sharp change of the thermophysical properties (specific heat and density among the others) in the vicinity of the pseudocritical line. Therefore, new heat transfer and pressure drop correlations are integrated for the supercritical pressure region in the code.

The COBRA-TF-SC subchannel analysis code is verified by comparing with experimental data and other numerical results. Experimental data for the validation of the code are obtained from the experimental studies on heat transfer to supercritical water flowing upward in seven-rod test bundle carried out by the Japanese Atomic Energy Agency (JAEA). The main objective of this study is to perform thermalhydraulics analysis on the 62-element Canadian Supercritical Water Reactor (SCWR) fuel bundle. The 62-element Canadian SCWR fuel bundle is simulated with modified COBRA-TF-SC.

The thesis comprises of a number of sections. The Background and Literature Review section provides an overview of the Supercritical Water Cooled Nuclear Reactors. A literature review on supercritical water heat transfer and supercritical water hydraulics resistance correlations are also provided. This section also provides an overview of subchannel analysis codes and a literature review on subchannel and

system codes applicable for SCWRs. The Theory section provides the structure and basic theory behind the subchannel analysis code COBRA-TF. It also provides a brief overview of fundamental equations used in IAPWS-IF97. The Methodology section provides a detailed description of modifications done to upgrade the COBRA-TF code to perform supercritical water flow simulations. The Results section outlines the code assessment and the thermalhydraulics analysis of the 62-element Canadian SCWR fuel bundle. The results of the thermalhydraulics analysis of the 62-element Canadian SCWR fuel bundle are presented along with a sensitivity analysis. Finally the conclusion and recommendations for future work are provided.

To summarize, the objectives of this study are to:

- Modify the existing COBRA-TF subchannel analysis code to be able to simulate supercritical water conditions;
- Verify and validate the modified COBRA-TF-SC code by comparing with the experimental data and other numerical results;
- Perform thermalhydraulics analysis and sensitivity analysis on the 62-element Canadian SCWR fuel bundle using the modified COBRA-TF-SC code;

Chapter 2

Background and Literature Review

2.1 Supercritical Water Cooled Nuclear Reactors (SCWR)

A supercritical fluid is a fluid that is at pressures higher than its thermodynamic critical values. A supercritical water reactor operates at pressures above the critical point of water (22.064 MPa, 374°C) [19]. According to the the Generation IV International Forum (GIF), the use of supercritical water in nuclear reactors will:

- increases the thermal efficiency of modern nuclear plants from 33%-35% up to 40%-45%;
- provides a simplified flow circuit in which steam generators, steam separators, steam dryers and re-circulation pumps can be reduced or eliminated;
- allows the direct thermo-chemical or indirect electrolysis production of hydrogen at low cost due to high coolant outlet temperatures;

- offers low coolant mass flow rates which would significantly decrease reactor coolant pumping power;
- eliminates dryout.

The design of supercritical water cooled nuclear reactors is seen as the natural and ultimate evolution of present day conventional reactors due to:

- some designs of modern Pressurized Water Reactors (PWRs) work at pressures of about 16 MPa;
- some designs of modern Boiling Water Reactors (BWRs) are a once-through or a direct-cycle design;
- some experimental reactors used nuclear steam superheaters with outlet steam temperatures well beyond the critical temperature but at pressures below the critical pressure;
- modern supercritical turbines are capable of operating successfully at pressures of about 25 MPA and inlet temperatures of about 600°, operating parameter of SCWRs.
- operating experience obtained with supercritical water cooled coal power plants. [19]

The SCWR design concepts follow two main types; the use of either a large pressure vessel to contain the reactor core similar to conventional PWRs and BWRs or distributed pressure tubes or channels similar to conventional CANDU nuclear reactors [19]. The pressure-vessel SCWR design is developed largely in the EU, Japan,

Korea, and China [19]. This design allows using a traditional high-pressure circuit layout [19]. The pressure-channel SCWR design is developed largely in Canada and in Russia [19]. This design allows the key features of passive accident and decay heat removal by radiation and convection from the distributed channels even with no active cooling and fuel melting and use of multi-pass reactor flows making reheating and superheating possible while keeping the pressure tube cool [19]. The Canadian SCWR design is described below in more detail.

The Canadian SCWR is designed to generate 2540 MW of thermal power corresponding to 1200 MW of electric power assuming a 48% thermodynamic cycle efficiency [23]. The core consists of 336 fuel channels, each containing a 500 cm long fuel assembly arranged in a 25 cm square lattice pitch [23]. The core diameter is 625 cm and the core height is 600 cm with 50 cm thick lower and upper axial D_2O reflectors [23]. A cross-sectional view of the 62-element Canadian SCWR fuel assembly is given in Figure 2.1. The fuel channel has a high-efficiency re-entrant channel (HERC) or double flow pass configuration as illustrated in Figure 2.2.

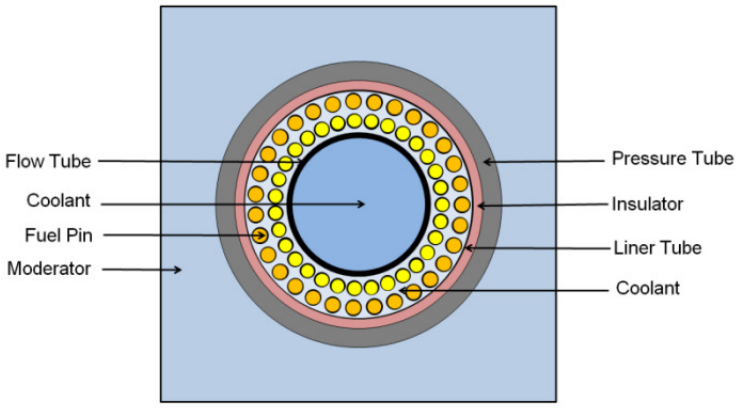

Figure 2.1: Cross-sectional view of the 62-element Canadian SCWR fuel bundle design, channel, and lattice cell (Spencer 2013).

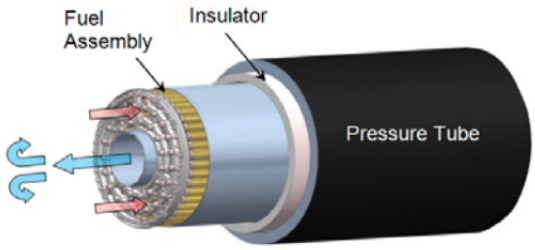

Figure 2.2: Cut-away view of the 62-element Canadian SCWR fuel bundle design (Spencer 2013).

The coolant enters the top of the channel into the central coolant tube and flows down the channel through the central coolant tube and reaches the closed bottom of the channel [23]. The coolant is then directed upwards into the outer fuel-containing annulus, where it is heated up by fuel [23]. Table 2.1 illustrates the geometric specifications for the channel.

Table 2.1: 62-element Canadian SCWR Fuel Bundle and Channel Specifications (Spencer 2013).

Component	Dimension	Material
Central coolant	4.45 cm radius	Light water
Flow tube	4.45 cm IR 0.1 cm thick	Zr-modified 310 Stainless Steel
Inner Pins (31)	0.415 cm radius	15 wt% PuO_2/ThO_2
Outer Pins (31)	0.465 cm radius	12 wt% PuO_2/ThO_2
Cladding	0.06 cm thick	Zr-modified SS
Linear Tube	7.20 cm IR 0.05 cm thick	Zr-modified SS
Insulator	7.25 cm IR 0.55 cm thick	Zirconia (ZrO_2)
Outer Linear	7.80 cm IR 0.05 cm thick	Excel (Zirconium Alloy)
Pressure Tube	7.85 cm IR 1.2 cm thick	Excel (Zirconium Alloy)
Moderator	25 cm square lattice pitch	D_2O

2.1.1 Supercritical Water Property

Fluids in the supercritical domain exhibit properties sometimes similar to those of gases and sometimes similar to those of liquids. The most significant property variations occur near the critical and pseudocritical points [19]. The critical point of water occurs at a pressure of 22.064 MPa and a temperature of 374°C. Pseudocritical point is a point at a pressure above the critical pressure and at a temperature ($T_{pc} > T_{cr}$) corresponding to the maximum value of the specific heat at the given pressure. Figures 2.3-2.5 illustrate the behaviour of thermophysical properties of water near the critical (22.1MPa) and pseudocritical (25MPa) points. Near the critical point these property changes are dramatic. In the vicinity of the pseudocritical point at 25 MPa, these property changes become less pronounced. At 25 MPa the most significant property changes occur within ±25°C around pseudocritical point (389.4°C) [19].

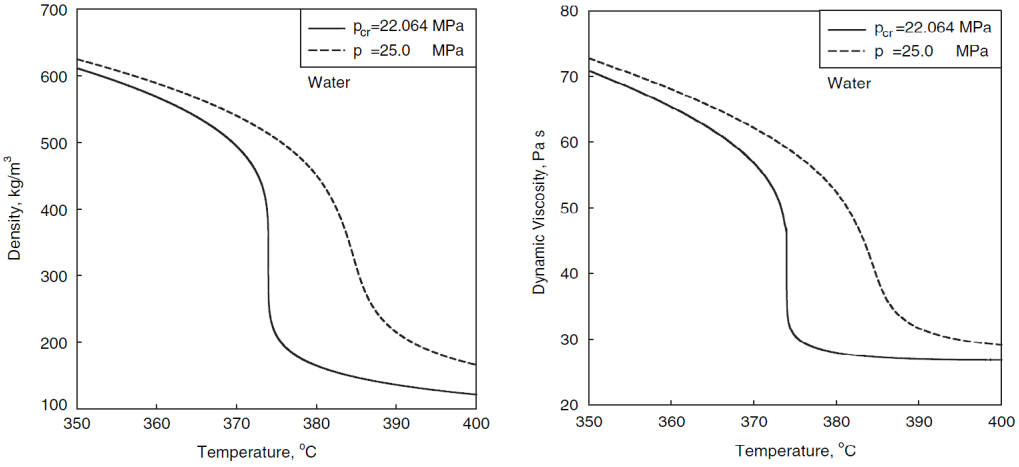

Figure 2.3: Density and Dynamic viscosity as a function of temperature (Pioro 2007).

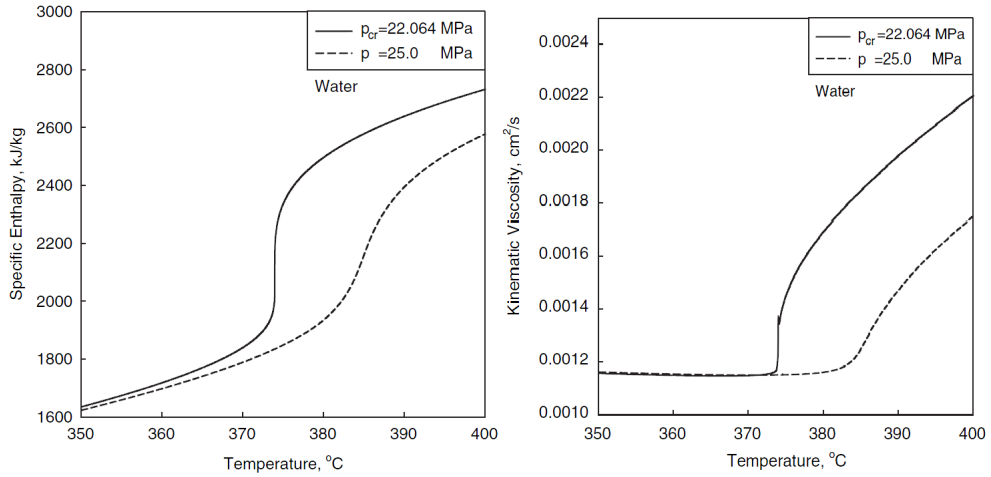

Figure 2.4: Specific enthalpy and Kinematic viscosity as a function of temperature (Pioro 2007).

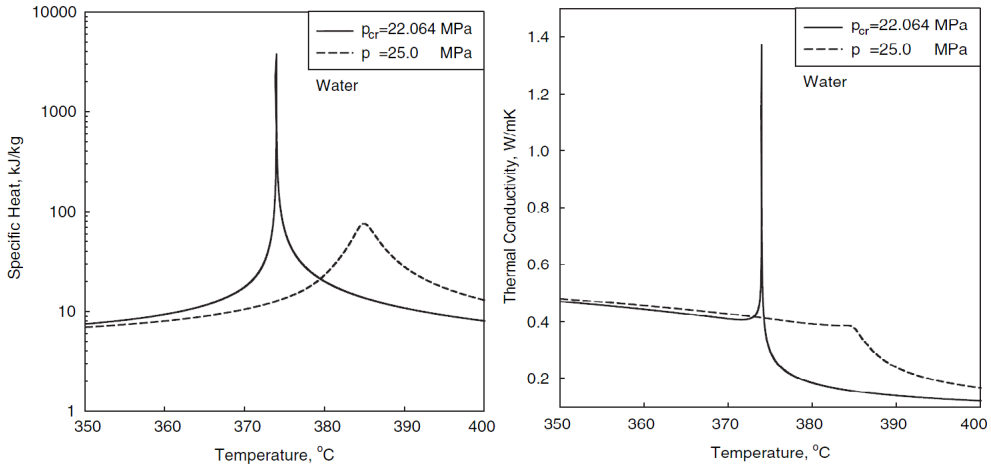

Figure 2.5: Specific heat and Thermal conductivity as a function of temperature (Pioro 2007).

The IAPWS Industrial Formulation 1997 (IAPWS-IF97) for the Thermodynamic Properties of Water and Steam can be used to calculate thermodynamic properties of water at supercritical conditions. The International Association for the Properties of Water and Steam (IAPWS) provides internationally accepted formulations for the properties of light and heavy water and steam [28]. The thermophysical properties of water at different pressures and temperatures can also be calculated using the miniREFPROP software by National Institute of Standard and Technology (NIST). The miniREFPROP software calculates thermophysical properties of water using the IAPWS-IF97 property formulations [28].

At subcritical pressures, there is a saturated region for water where vapour and liquid exist simultaneously[7]. In this region the fluid temperature stays constant and void fraction varies between zero and unity where the void fraction is defined as the fraction of a given volume that is occupied by vapour. At supercritical pressures the fluid behaves as a single phase fluid and there is no phase transformation. For convenience, below the pseudocritical point fluid properties are considered to show liquid-like behaviour and above the pseudocritical point they are considered to show gas-like behaviour. These properties can then be considered to have pseudo void fractions of 0 and 1 respectively. However the void fraction change of supercritical fluids in this regard is not continuous as observed in the subcritical case [7]. This is illustrated in Figure 2.6 below.

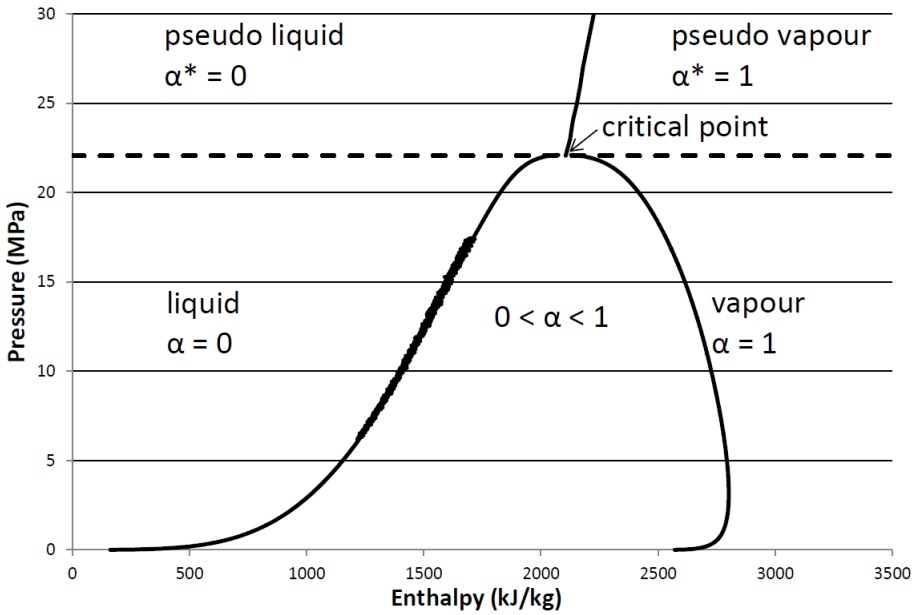

Figure 2.6: Pseudocritical line.

The apparent discontinuity of void fraction will affect the numerical calculation of two fluid models such as COBRA-TF and result in termination of the simulation [7]. The discontinuity can be avoided by introducing a pseudo two-phase region at supercritical pressures as suggested in the two fluid model APROS, developed by VTT Technical Research Centre of Finland, and in the system analysis code ATHLET-SC, developed by Shanghai Jiao Tong University [7, 8]. Figure 2.7 illustrates the scheme of the pseudo two-phase method.

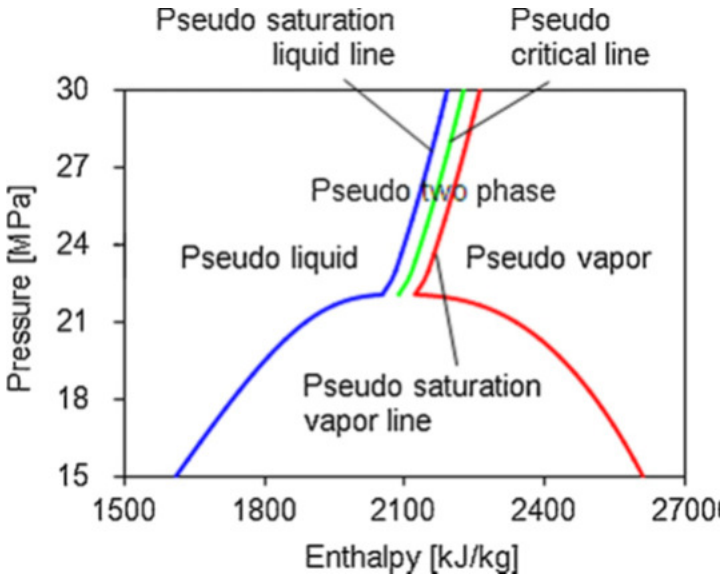

Figure 2.7: Scheme of the pseudo two-phase method (Fu 2007).

The pseudo two-phase region is created by using a fictitious region of latent heat at supercritical pressures [7]. This fictitious region is based on the detachment of the pseudocritical line, which is an extension of the saturation curve to the supercritical pressure region, to get a narrow band of the pseudo two-phase region [7]. The pseudo two-phase method connects the liquid, two-phase, and vapour regions at subcritical pressures with pseudo-liquid, pseudo two-phase, and pseudo vapour regions at supercritical pressures smoothly maintaining the two-fluid numerical structure of the code. Fluid properties change significantly near the critical point. The specific heat capacity of water goes to infinity at the critical point leading to numerical instabilities in the simulation. In pseudo two-phase scheme the critical point lies within the pseudo two-phase region. Therefore, in pseudo two-phase scheme the specific heat capacity at the critical point is not simulated maintaining the numerical stability of the code. These give the modified subchannel analysis code the ability to perform transcritical flow simulations, where the working fluid goes through both subcritical

and supercritical state.

2.1.2 Supercritical Water Heat Transfer

Heat transfer at supercritical pressures is influenced by the significant changes in thermophysical properties at these conditions [19]. Several heat transfer correlations have been developed for various geometries and flow conditions for supercritical water heat transfer. However, satisfactory analytical methods have not yet been developed due to the difficulty in dealing with these significant property variations [19]. Therefore, empirical generalized correlations based on experimental data are used for heat transfer coefficient calculations at supercritical pressures [19].

Circular tubes

Majority of publications devoted to the forced convective heat transfer to supercritical water are related to heat transfer in circular tubes [19]. McAdams (1942) modified the Dittus-Boelter correlation to calculate forced convective heat transfer in turbulent flows at subcritical pressures [16].

$$Nu_b = 0.0243 Re_b^{0.8} Pr_b^{0.4} \tag{2.1}$$

According to Shnurr et al.(1976), the above equation also shows good agreement with the experimental data of supercritical water flowing inside circular tubes at a pressure of 31 MPa and at low heat fluxes [19]. However, this equation can give unrealistic results near the critical and pseudocritical points because it is sensitive to property variations [19]. This classical equation is used as the base model for modified supercritical water heat transfer correlations [19].

Kransnoshchekov and Protopopov (1959, 1960) proposed a correlation for forced convective heat transfer in water and carbon dioxide at supercritical pressures [13],

$$Nu = Nu_0 \left(\frac{\mu_b}{\mu_w}\right)^{0.231} \left(\frac{k_b}{k_w}\right)^{-0.33} \left(\frac{\bar{c_p}}{c_{p,b}}\right)^{0.35} \tag{2.2a}$$

$$Nu_0 = \frac{\frac{\xi}{8} Re_b \bar{Pr}}{12.7\sqrt{\frac{\xi}{8}}\left(\bar{Pr}^{\frac{2}{3}} - 1\right) + 1.07} \tag{2.2b}$$

$$\xi = \frac{1}{\left(1.82 \log Re_b - 1.64\right)^2} \tag{2.2c}$$

The Prandtl number ($\bar{Pr}$) and the specific heat capacity were averaged over the ranges to account for the thermophysical property variations [13]. The Average Prandtl number is defined as,

$$\bar{Pr} = \mu \bar{c_p} / k \tag{2.3}$$

where the average specific heat capacity ($\bar{c_p}$) is defined as,

$$\bar{c_p} = \left(H_w - H_b\right) / \left(T_w - T_b\right) \tag{2.4}$$

The majority of their experimental data and experimental data of Miropolskiy and Shitman (1957), Dickinson and Welch (1958), Petukhov and Kirillov (1958) can be generalized using the above correlation with discrepancies within ±15% [13]. This correlation is valid for following ranges [13].

$$2 \times 10^{04} < Re_b < 8.6 \times 10^{05}, 0.85 < \bar{Pr_b} < 65, 0.90 < \frac{\mu_b}{\mu_w} < 3.60,$$

$$1.00 < \frac{k_b}{k_w} < 6.00, 0.07 < \frac{\bar{c_p}}{c_{p,b}} < 4.50$$

Bishop et al. (1964) conducted experiments with supercritical water flowing upward inside tubes and annuli within operating parameters: pressure 22.8-27.6MPa, bulk-fluid temperature 282-527°C, mass flux 651-3662 kg/m^2s and heat flux 0.31-3.46 MW/m^2 [3]. The experimental data for heat transfer in tubes of the above experiment were generalized with a fit of ±15% using the correlation [3],

$$Nu_x = 0.0693 Re_x^{0.9} \bar{Pr}_x^{0.66} \left(\frac{\rho_w}{\rho_b}\right)_x^{0.43} \left(1 + 2.4\frac{D}{x}\right) \tag{2.5}$$

where x is the axial location along the heated length. The Prandtl number is averaged over the ranges to account for thermophysical property variations and is given Equation 2.3.

Swenson et al. (1965) investigated local heat transfer coefficients in supercritical water flowing inside smooth tubes [24]. They determined that conventional heat transfer correlations did not work well at supercritical pressures due to rapid thermophysical property changes near the critical and pseudocritical points [24]. They recommended the correlation [24],

$$Nu_w = 0.00459 Re_w^{0.923} \bar{Pr}_w^{0.613} \left(\frac{\rho_w}{\rho_b}\right)^{0.231} \tag{2.6}$$

They conducted experiments with supercritical water flowing inside smooth tubes within operating parameters: pressure 22.8-41.6 MPa, bulk-fluid temperature 75-576°C, wall temperature 93-649°C and mass flux 542-2150 kg/m^2s [24]. The correlation reproduced the experimental data to within ±15% [24]. However, Swenson et al. (1965) assumed that thermal conductivity was a smoothly decreasing function of temperature near the critical and pseudocritical points, which is not the case [19].

Jackson et al. (1975) presented the following correlation to define the ranges for negligible buoyancy effects in supercritical water heat transfer [11].

$$\frac{\bar{Gr}_b}{Re_b^{2.7}} < 5 \times 10^{-06} \; for \; upward \; flow \; in \; vertical \; tubes \tag{2.7a}$$

$$\frac{\bar{Gr}_b}{Re_b^{2.7}} < 2 \times 10^{-05} \; for \; downward \; flow \; in \; vertical \; tubes \tag{2.7b}$$

$$\frac{\bar{Gr}_b}{Re_b^{2}} \left(\frac{\rho_b}{\rho_w}\right) \left(\frac{x}{D}\right)^2 < 10 \; for \; horizontal \; tubes \tag{2.7c}$$

Kirillov et al. (1990) investigated the role of free convection heat transfer near the critical and pseudocritical points [12]. They determined that the role of free convection heat transfer near the critical and pseudocritical points can be taken into account using [12],

$$k^* = \left(1 - \frac{\rho_w}{\rho_b}\right) \frac{Gr}{Re^2} \tag{2.8}$$

The effects of free convection can be observed for $k^* < 0.4$, which results in deteriorated heat transfer [12]. At larger values of k^* the effects of free convection disappears resulting in improved heat transfer [12]. For the heating of a supercritical fluid flowing inside a circular tube at a constant heat flux Kirillov et al. proposed the correlation [12],

$$\frac{Nu}{Nu_0} = \left(\frac{\bar{c_p}}{c_{p,b}}\right)^n \left(\frac{\rho_w}{\rho_b}\right)^m \; for \; k^* < 0.01 \tag{2.9a}$$

$$\frac{Nu}{Nu_0} = \left(\frac{\bar{c_p}}{c_{p,b}}\right)^n \left(\frac{\rho_w}{\rho_b}\right)^m \varphi(k^*) \; for \; k^* > 0.01 \tag{2.9b}$$

$$Nu_0 = \frac{\frac{\xi}{8} Re \bar{Pr}}{1 + \frac{900}{Re} + 4.5\xi^{0.5}\left(\bar{Pr}^{2/3} - 1\right)} \tag{2.9c}$$

The values of $\varphi(k^*)$ are given in Table 2.2. The exponent m is 0.4 for upward flow in

vertical tubes and 0.3 for horizontal tubes [12]. The values of exponent n are provided in Table 2.3.

Table 2.2: Values of $\varphi(k^*)$ (Kirillov 1990)

k^*	0.01	0.02	0.04	0.06	0.08	0.1	0.2	0.4
$\varphi(k^*)$	1	0.88	0.72	0.67	0.65	0.65	0.74	1

Table 2.3: Values of exponent n (Kirillov 1990)

Region	n
$\frac{T_w}{T_{pc}} < 1 \; and \; \frac{T_b}{T_{pc}} > 1.2$	0.4
$\frac{T_w}{T_{pc}} < 1 \; and \; \frac{\bar{T}_b}{T_{pc}} < 1$	$0.22 + 0.18\left(\frac{T_w}{T_{pc}}\right)$
$\frac{T_w}{T_{pc}} > 1 \; and \; 1 < \frac{\bar{T}_b}{T_{pc}} < 1.2$	$0.9\frac{\bar{T}_b}{T_{pc}}\left(1 - \frac{T_w}{T_{pc}}\right) + 1.08\left(\frac{T_w}{T_{pc}}\right) - 0.68$

Equation 2.9a can be used to calculate the deteriorated heat transfer for $k^* < 0.01$ [12]. In this region, the bulk temperature is lower than the pseudocritical temperature and a peak in wall temperature appears in the tube cross section [12]. The deteriorated heat transfer can be associated with the effects of acceleration and variability of physical properties over the flow cross section in the process of turbulent transport [12]. Additional deterioration in heat transfer occurs in the range $k^* = 0.01 - 0.4$ due to the effect of free or natural convection [12]. As the effects of free convection disappears ($k^* > 0.4$) the heat transfer increases and the improved heat transfer regime begins [12]. This correlation is valid for following ranges[12].

$$Re = (20 - 800) \times 10^3, \bar{Pr} = 0.85 - 55, \frac{\rho_w}{\rho_b} = 0.09 - 1, \frac{\bar{c_p}}{c_{p,b}} = 0.02 - 4$$

$$q = 0.023 - 2.6\frac{MW}{m^2}, \frac{p}{p_{crit}} = 1.01 - 1.33, \frac{T_b}{T_{pc}} = 1 - 1.2, \frac{T_w}{T_{pc}} = 0.6 - 2.6$$

Jackson (2002) modified the original correlation of Kransnoshchekov et al. (Equation 2.2a) for forced convective heat transfer in supercritical water to employ the Dittus-Boelter type form for Nu_0 [10]. This correlation can be expected to follow trends of the correlation predicted by Kransnoshchekov et al. [10].

$$Nu = 0.0183 Re_b^{0.82} Pr_b^{0.5} \left(\frac{\rho_w}{\rho_b}\right)^{0.3} \left(\frac{\bar{c_p}}{c_{p,b}}\right)^n \tag{2.10}$$

The values of exponent n are provided in Table 2.4.

Table 2.4: Values of exponent n (Jackson 2002)

Region	n
$T_b < T_w < T_{pc}$ *and* $1.2T_{pc} < T_b < T_w$	0.4
$T_b < T_{pc} < T_w$	$0.4 + 0.20\left(\frac{T_w}{T_{pc}} - 1\right)$
$T_{pc} < T_b < 1.2T_{pc}$ *and* $T_b < T_w$	$0.4 + 0.20\left(\frac{T_w}{T_{pc}} - 1\right)\left(1 - 5\left(\frac{T_b}{T_{pc}} - 1\right)\right)$

The Mokry et al. (2009) correlation is based on a set of experimental data at the State Scientific Centre of Russian Federation and the latest thermophysical properties of water (NIST,2007) [18]. The experimental data set used for this correlation falls within the operating conditions of supercritical water reactors: $P = 24\ MPa$, $T_{in} = 320 - 350°C$, $G = 200 - 1500\ kg/m^2s$, and $q = 70 - 1250\ kW/m^2$ [18]. The data for this correlation is obtained within the following conditions: Vertical stainless-steel smooth tube; $D = 10mm$, $\delta_w = 2mm$, and $L_h = 4m$; tube internal surface roughness $R_a = 0.63 - 0.8\mu m$; and upward flow [18]. The Mokry et al. correlation can be defined as [18],

$$Nu_b = 0.0061 Re_b^{0.904} \bar{Pr}_b{}^{0.684} \left(\frac{\rho_w}{\rho_b}\right)^{0.564} \tag{2.11}$$

The Prandtl number is averaged over the ranges to account for thermophysical property

variations and is given Equation 2.3. This correlation has an uncertainty of about ±25% for calculated heat transfer coefficient values and about ±15% for calculated wall temperatures [18].

A recent study was conducted by Zahan et al. (2010) to develop a heat transfer look-up table for critical/supercritical pressures. An extensive literature review was conducted, which included 28 data sets and 6663 trans-critical heat transfer data [18]. Table 2.5 summarizes the results obtained, in the form of the overall weighted average and root mean square (RMS) errors, within the three supercritical sub-regions for several supercritical heat transfer correlations discussed in this section [18].

Table 2.5: Overall weighted average and RMS errors within three supercritical sub-regions (Zahan et al., 2010).

	Liquid-like		Gas-like		Critical & pseudocritical	
Correlation	Ave. Er(%)	RMS(%)	Ave. Er(%)	RMS(%)	Ave. Er(%)	RMS(%)
Dittus-Boelter	32.5	46.7	87.7	131.0	-	-
Bishop et al.	6.3	24.2	5.2	18.4	20.9	28.9
Swenson et al.	1.5	25.2	-15.9	20.4	5.1	23.0
Jackson	13.5	30.1	11.5	28.7	22.0	40.6
Mokry et al.	-3.9	21.3	-8.5	16.5	-2.3	17.0

According to Table 2.5 the Mokry et al. correlation gives the lowest overall weighted average and root mean square (RMS) errors for each supercritical sub-region investigated. Therefore, the Mokry et al. correlation provides the best prediction for the experimental data within the three sub-regions of supercritical flow investigated.

Annuli

McAdams et al. (1950) conducted experiments in an annulus with internal heating and their data can be generalized with the correlation [15],

$$Nu_f = 0.0214 Re_f^{0.8} Pr_f^{0.33} \left(1 + \frac{2.3}{\frac{L}{D_{hy}}}\right) \tag{2.12}$$

All properties are evaluated at the film temperature t_f which is given by [15],

$$t_f = \frac{t_b + t_w}{2} \tag{2.13}$$

This correlation is valid for following ranges of each parameter [15],

$$D_{hy} = 3.32mm, \frac{L}{D_{hy}} = 14.7 - 80.0, p = 0.8 - 24MPa, G = 75 - 224\frac{kg}{m^2 s},$$

$$t_w = 319 - 544°C, t_b = 221 - 544°C, h = 0.52 - 2\frac{kW}{m^2 K}$$

The correlation has a maximum error of $\pm 17\%$ [15].

Bishop et al. (1964) conducted experiments with supercritical water flowing upward inside annuli and obtained the correlation given in Equation 2.5 to calculate heat transfer [3].

Bundles

There are very few publications devoted to heat transfer in bundles cooled with supercritical water [19]. Dyadyakin and Popov (1977) conducted experiments with a tight 7-rod bundle with helical fins cooled with supercritical water and obtained the

correlation [6],

$$Nu_x = 0.021 Re_x^{0.8} \bar{Pr}_x^{0.7} \left(\frac{\rho_w}{\rho_b}\right)_x^{0.45} \left(\frac{\mu_b}{\mu_{in}}\right)_x^{0.2} \left(\frac{\rho_b}{\rho_{in}}\right)_x^{0.1} \left(1 + 2.5\frac{D_{hy}}{x}\right) \tag{2.14}$$

This correlation fits their experimental data to within ±20% [6].

2.1.3 Supercritical Water Hydraulic Resistance

The total pressure drop for forced convection flow inside a closed-loop system can be determined using the expression,

$$\Delta P = \sum \Delta P_{fr} + \sum \Delta P_l + \sum \Delta P_{ac} + \sum \Delta P_g \tag{2.15}$$

where $\Delta P_{fr}, \Delta P_l, \Delta P_{ac}, \Delta P_g$ are the pressure drop due to fictional resistance, local flow obstruction, acceleration of flow, and gravity respectively. The pressure drop due to frictional resistance can be calculated using,

$$\Delta P_{fr} = \xi_{fr} \frac{LG^2}{2D\rho} \tag{2.16}$$

where the frictional resistance coefficient ($_{fr}$) is defined as,

$$\xi_{fr} = \frac{1}{(1.82 + \log Re_b - 1.64)^2} \tag{2.17}$$

This frictional resistance (ξ_{fr}) coefficient is valid only at subcritical pressures [19]. The frictional resistance coefficient changes at supercritical pressures due to significant property changes near the critical and pseudocritical points [19]. There are only limited number of studies devoted to pressure drop in flow geometries at supercritical

pressures compared to studies devoted to heat transfer at supercritical pressures [19]. Satisfactory analytical and numerical methods have not yet been developed due to the difficulty in dealing with steep property variations near the critical and pseudocritical points [19]. Kirillov et al. (1990) proposed a correlation to calculate the frictional resistance coefficient at supercritical pressures [12]. Kirillov suggested that the frictional resistance coefficient for an isothermally stabilized turbulent fluid flow at supercritical water conditions can be approximated with the same equation that is used to calculate the frictional resistance coefficient at subcritical pressures [12]. They also showed that the frictional resistance coefficient within the same range of parameters for a heated tube in the normal and deteriorated supercritical heat transfer regimes can be approximated with [12],

$$\left(\frac{\xi}{\xi_{iso}}\right)_{fr} = \left(\frac{\rho_w}{\rho_b}\right)^{0.4} \tag{2.18}$$

where ξ_{iso} is calculated using Equation 2.17. The pressure drop due to local flow obstructions is defined as,

$$\Delta P_l = \xi_l \frac{G^2}{2D} \tag{2.19}$$

where the local resistance coefficient, ξ_l, is determined using appropriate correlations for different flow obstructions. Significant property changes at supercritical flow conditions also affect the local resistance coefficients. However, there are no satisfactory correlations for different flow obstructions at supercritical flow conditions in the literature. Therefore, subcritical pressure local resistance coefficients are used for supercritical flow simulations in the current study. The pressure drop due to

acceleration of flow is defined as,

$$\Delta P_{ac} = G^2 \left(\frac{1}{\rho_{out}} - \frac{1}{\rho_{in}} \right) \tag{2.20}$$

There is a strong non-linear dependency of the density on temperature variation at supercritical pressures, especially within the critical and pseudocritical regions [19]. Therefore the arithmetic average of densities can only be used to calculate the pressure drop due to gravity in short test sections [19]. In long test sections at high heat fluxes and within the critical and pseudocritical regions, the integral value of densities should be used to calculate the gravitational pressure drop as suggested by Ornatskiy et al. (1980) and Razumovskiy (2003) [19].

$$\Delta P_g = \pm g \left(\frac{H_{out}\rho_{out} + H_{in}\rho_{in}}{H_{out} + H_{in}} \right) L \sin\theta \tag{2.21}$$

where θ is the test-section inclination angle to the horizontal plane.

2.2 Subchannel Codes

The single phase and two-phase flow behaviour of a fuel channel can be simulated through System codes, Subchannel codes, and CFD codes. Subchannel codes offer higher spatial resolution than System codes and lower spatial resolution than CFD codes. Subchannel codes are typically used to model thermalhydraulic behaviour within a fuel bundle while System codes are used to model the entire primary and secondary systems of nuclear reactors. CFD codes are used to model small complex geometries.

In subchannel codes a reactor core can be represented by several sub-assemblies. Each sub-assembly can be represented by several subchannels and other water channels and fuel rods. A fully three-dimensional model can then be represented by simply connecting the subchannels in a three-dimensional array. However, the subchannel analysis approach is not a fully three-dimensional representation of the flow due to the treatment of lateral exchanges between adjacent subchannels [25]. It is assumed that any lateral flow through the gap region between subchannels loses its sense of direction after leaving the gap [25]. Subchannels are therefore connected arbitrarily since no fixed lateral coordinate is required [25]. This treatment is advantageous from both physical and computational point of view as it simplifies the lateral convective terms of the linear momentum balance equation [25]. However, this approximation limits subchannel code's ability to predict some phenomena such as swirl-flow.

The subchannel volume can be defined using either the coolant-centered approach or the rod-centered approach as illustrated in Figure 2.8 [25]. The traditional approach in rod bundle analysis has been the coolant-centered approach in which the actual subchannel volume encompasses only the coolant [25]. The rod-centered approach is more suitable to model the liquid flow around the rod in two-phase flow, particularly in the annular flow regime, as suggested by Gaspari et al [25].

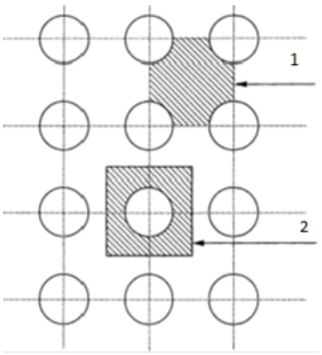

Figure 2.8: 1.Coolant-centered 2.Rod-centered Subchannels (Todreas 2001)

This control volume is then used to solve the mass, axial momentum and energy conservation equations. Transverse momentum conservation equation is solved on a separate control volume between adjacent subchannels. In addition to conservation equations, constitutive equations and fluid properties are specified to develop a closed set of equations for the solution [25]. Constitutive equations are used for input parameters such as friction factors, heat transfer coefficients, and lateral mass, momentum, and energy exchanges between adjacent subchannels [25]. Some subchannel codes currently in use are summarized in Table 2.6.

Table 2.6: Partial list of Subchannel Level Codes currently in use

Code	Acronym	Origin
COolant Boiling in Rod Arrays	COBRA	PNL - USA
Advanced Solution of Subchannel Equations in Reactor Thermal-hydraulics	ASSERT	AECL - Canada
Multichannel Analyzer for steady states and Transients in Rod Arrays	MATRA	KAERI - Korea
Sub-channel Thermal-hydraulic Analysis of Fuel Assembly under Supercritical Conditions	STAFAS	Cheng et al.

2.2.1 Subchannel and System Codes Applicable for Supercritical Water-Cooled Reactors (SCWR)

Subchannel code development and validation for SCWR is a difficult task due to the complex flow channels and the strong property variations of water near the critical and pseudocritical points. This section briefly outlines some subchannel and system codes developed for supercritical water-cooled reactors. The modified COBRA-TF code incorporates features of both supercritical water subchannel and supercritical water system codes.

Chen et al.(2003) developed the subchannel analysis code Sub-channel Thermal-hydraulic Analysis in Fuel Assemblies under Supercritical conditions (STAFAS) to investigate the effect of design parameters of the High Performance Light Water Reactor (HPLWR) fuel bundles on the thermalhydraulic behaviour in subchannels at supercritical water conditions .The main features of the STAFAS code are a high feasibility for complex fuel bundle configuration, the capacity of the macro subchannel approach, and high numerical stability and convergence [4]. Based on their results, they recommended two fuel assembly configurations for supercritical water cooled reactors; tight square lattice and semi-tight hexagonal lattice [4].

Shan et al. (2009) developed the subchannel analysis code known as Advanced Thermal-Hydraulics Analysis Subchannel (ATHAS) for preliminary analyses of flow distributions, enthalpy distributions, and cladding temperatures at supercritical water conditions. Their code is equipped with a number of heat transfer correlations, frictional resistance correlations and mixing models as options for sensitivity analyses. They also introduced a 3D heat conduction model to establish the cladding temperature [21]. Their results indicated that a CANFLEX bundle is appropriate for use in the

Canadian supercritical water-cooled reactor based on heat transfer analysis. They determined that the selection of heat transfer, friction, and mixing models has a significant impact on the prediction of the maximum cladding surface temperature and the inclusion of the 3D heat conduction in the calculation has provided a more realistic prediction of the maximum cladding-surface temperature [21].

Atomic Energy of Canada Limited modified its subchannel analysis code ASSERT-PV to simulate supercritical flow conditions. However, that code is only capable of simulating either subcritical or supercritical flow conditions. It is not capable of performing transcritical flow simulations, where the working fluid goes through both subcritical and supercritical state. Atomic Energy of Canada Limited currently uses this code to perform thermalhydraulic analysis of the Canadian SCWR fuel bundles.

Hänninnen and Kurki (2008) modified the two-fluid system code known as Advanced Process Simulation Environment (APROS) to simulate thermalhydraulic behaviour of flow at supercritical water conditions [8]. The modified APROS code incorporates a pseudo two-phase region at supercritical pressures to preserve the two-fluid numerical structure of the original code [8]. They determined that the code is capable of simulating the transition from subcritical to supercritical water conditions and the transition from pseudo liquid to pseudo gas at supercritical pressures without any numerical instabilities [8].

Zhou et al.(2009) modified the system code Analysis of Thermal-hydraulics of Leaks and Transients (ATHLET) to simulate rapid decrease from supercritical to subcritical water conditions during the loss of coolant accident (LOCA) of supercritical water-cooled reactors [30]. This model also incorporates a pseudo two-phase region at supercritical pressures to preserve the two-fluid numerical structure of the original

code [30]. The modified ATHLET model is applied to simulate the blowdown process of a simplified model [30]. The results obtained indicated a good applicability of the modified code for the tans-critical transient [30].

Chapter 3

Theory

This section provides the structure and basic theory behind the subchannel analysis code COBRA-TF. It also provides a brief overview of fundamental equations used in IAPWS-IF97.

3.1 Subchannel Model COBRA-TF

3.1.1 Generalized Conservation Equations

Subchannel code COBRA-TF employs a two-fluid model with consideration for three separate flow fields; liquid film, liquid droplets, and vapour [1]. The two-fluid model accounts for thermal and mechanical non-equilibrium. Each of the three fields is modelled with a separate set of conservation equations with the exception of the liquid and droplet fields sharing an energy equation. COBRA-TF assumes that the liquid and droplets fields are in thermal equilibrium [1].

The general mass conservation equation can be expressed as,

$$\frac{\partial\left(\alpha_k\rho_k\right)}{\partial t}+\nabla\cdot\left(\alpha_k\rho_k\overrightarrow{V_k}\right)=L_k+M_e^T \tag{3.1}$$

The k subscript denotes the field under consideration. It can be liquid (l), vapour (v), or entrained droplets (e). The first term on the left-hand side (LHS) of the equation is the change of mass with time and the second term is the advection of field mass into or out of the control volume, where $\overrightarrow{V_k}$ is the field velocity. The first term on the right-hand side (RHS) is the mass transfer into or out of phase k. The inter-phase mass transfer can occur either by evaporation/condensation or by entrainment/de-entrainment. The second term on the RHS represents mass transfer due to turbulent mixing and void drift. COBRA-TF does not employ advance turbulence models to determine turbulent mixing due to the axially-dominated subchannel flow assumption [1].

The general momentum conservation equation can be given as,

$$\begin{aligned}&\frac{\partial\left(\alpha_k\rho_k\overrightarrow{V_k}\right)}{\partial t}+\frac{\partial\left(\alpha_k\rho_k u_k\overrightarrow{V_k}\right)}{\partial x}+\frac{\partial\left(\alpha_k\rho_k v_k\overrightarrow{V_k}\right)}{\partial y}+\frac{\partial\left(\alpha_k\rho_k w_k\overrightarrow{V_k}\right)}{\partial z}\\&\quad=\alpha_k\rho_k\overrightarrow{g}-\alpha_k\nabla P+\nabla\cdot\left[\alpha_k\left(\tau_k^{ij}+T_k^{ij}\right)\right]+\overrightarrow{M_k^L}+\overrightarrow{M_k^d}+\overrightarrow{M_k^T}\end{aligned} \tag{3.2}$$

The terms on the LHS are the change of control volume momentum with time and the advection of momentum into or out of the control volume. The terms on the RHS are the gravitational force, pressure force, viscous and turbulent shear stress, momentum source/sink due to phase change and entrainment, interfacial drag forces, and momentum transfer due to turbulent mixing respectively. The turbulent shear stress is not modelled in COBRA-TF [1]. COBRA-TF also assumes the pressure to be

equal in all phases within each volume and the gravity to be the only body force [1].

The general energy conservation equation can be given as,

$$\frac{\partial\left(\alpha_k \rho_k h_k\right)}{\partial t} + \nabla \cdot \left(\alpha_k \rho_k h_k \overrightarrow{V_k}\right) = -\nabla \cdot \left[\alpha_k \left(\overrightarrow{Q_k} + \overrightarrow{q_k^T}\right)\right] + \Gamma_k h_k^i + q_{wk}''' + \alpha_k \frac{\partial P}{\partial t} \quad (3.3)$$

The terms on the LHS of the equation are the change of phase energy with respect to time and the advection of phase energy into or out of the control volume. The RHS terms are the k-phase conduction and turbulent heat flux, energy transfer due to phase change, volumetric wall heat transfer, and the pressure work term respectively. COBRA-TF assumes that there is no heat generation occurring in the fluid and radiative heat transfer can only occurs between solid surfaces and the vapour/droplet fields [1]. COBRA-TF does not model heat conduction in fluids; therefore the term $\overrightarrow{Q_k}$ is assigned a zero [1]. The energy exchange by both turbulent mixing and void drift is only considered in the lateral and orthogonal directions [1].

These conservation equations are applied to the modeling geometry. This is performed by generating a mesh of volumes and then setting up the mass, momentum, and energy conservation equations for each flow field in each of these mesh cells. In COBRA-TF, two axial meshes which are staggered from each other are used to solve the axial momentum, mass, and energy conservation equations [1]. One mesh, which is called the scalar mesh, is used to define the scalar variables (P, h, and fluid properties). The second mesh, which is called the momentum mesh, is used to define the fluid velocity field [1]. The momentum mesh cell is centered on the scalar mesh cell as illustrated in Figure 3.1. The transverse momentum equation is solved on a separate mesh between adjacent subchannels as illustrated in Figure 3.2.

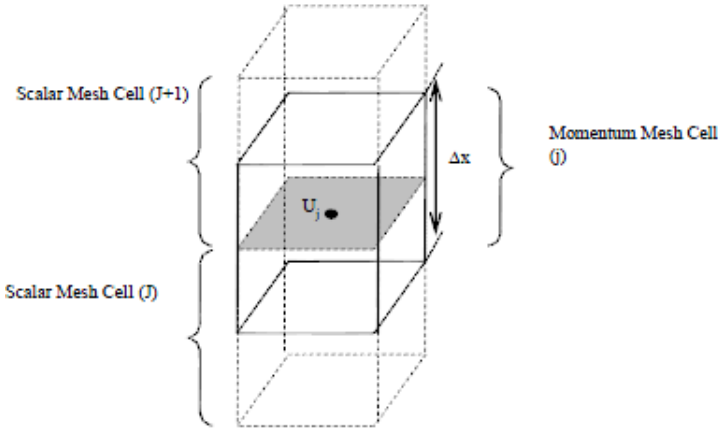

Figure 3.1: Axial momentum and Scalar mesh cells (Avramova 2011).

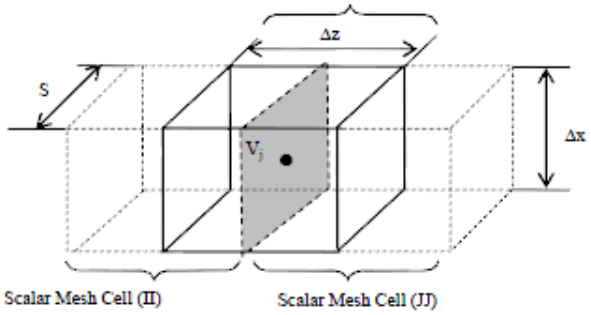

Figure 3.2: Transverse momentum mesh cell (Avramova 2011).

The conservation equations contain several terms that link similar conservation equations located in different spatial locations due to the physical phenomena such as void drift and turbulent mixing [1]. They also have terms that link conservation equations in the same spatial location due to inter-phase effects such as phase change and entrainment [1]. These terms are called closure terms or constitutive equations because they define the remaining conservation equation terms and allow them to be solved for the independent variables. These closure terms must be solved prior to solving the conservation equations. There are two general types of closure terms in

COBRA-TF; field interactions that arise from outside of the mesh cell that a given conservation equation is defined in (macro) and field interactions that arise from within the mesh cell that a given conservation equation is defined in (micro) [1]. The macro-mesh cell closure terms include the wall shear stress, inter-cell shear, wall heat transfer, turbulent mixing, and void drift [1]. The micro-mesh cell closure terms include interfacial drag, interfacial heat transfer, and entrainment and de-entrainment [1]. These closure terms are discussed in more detail in subsequent sections.

After defining the closure terms and determining fluid properties, the set of conservation equations can be solved simultaneously using the Semi-implicit Method for Pressure-Linked Equation (SIMPLE) [1].

3.1.2 Water Property

Thermophysical properties of water are required to define terms in both conservation equations and closure terms. Most subchannel analysis codes such as COBRA and ASSERT use both intrinsic property data tables and property formulations to determine thermophysical properties of water. The saturation curve of COBRA-TF is defined in the SAT subroutine and is illustrated in Figure 3.3. The SAT subroutine calculates the liquid and vapour saturation enthalpies of water for a given pressure.

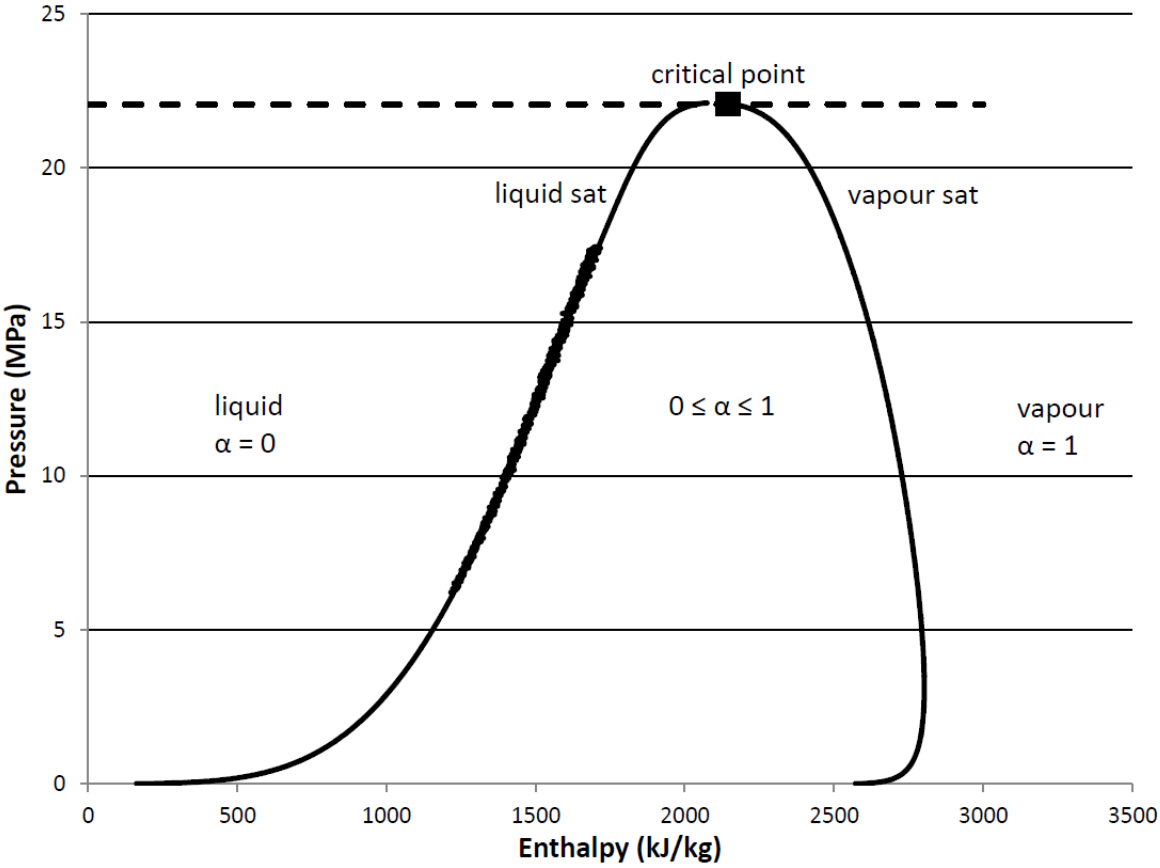

Figure 3.3: COBRA-TF saturation curve

The IPROP subroutine in COBRA-TF calculates most of the required liquid and vapour properties of water. COBRA-TF uses an intrinsic property table to determine water properties when the enthalpy of water is below the liquid saturation enthalpy. This intrinsic property table is used to determine temperature, heat capacity, thermal conductivity, and dynamic viscosity of subcooled liquid water at a given enthalpy h. These subcooled liquid properties do not depend on pressure. COBRA-TF uses the same intrinsic property table to determine the saturated liquid and saturated vapour properties of water at a given liquid saturation enthalpy h_f and a vapour saturation enthalpy h_g. COBRA-TF uses property formulations, obtained from the

IAPWS-IF97, to determine water properties when the enthalpy of water is above the vapour saturation enthalpy. The IPROP subroutine calls three different subroutines to determine vapour properties of water. The HGAS subroutine determines the enthalpy and specific volume of superheated vapour as a function of temperature and pressure. The TGAS subroutine calculates the temperature and specific heat capacity of vapour as a function of enthalpy and pressure. Finally the TRANSP subroutine calculates the thermal conductivity and viscosity of superheated vapour as a function of temperature and density.

The specific volume of liquid and vapour are calculated using the VOLVAP and VOLLIQ subroutines respectively. These subroutines use IAPWS-IF97 property formulations to determine the specific volume of water. Some terms in the conservation equations and constitutive equations require the calculation of partial derivatives of thermophysical properties of water. The partial derivatives of liquid and vapour specific volumes with respect to pressure are calculated in the XTRA1 and DVDPV subroutines respectively. The partial derivatives of liquid and vapour specific volumes with respect to enthalpy are calculated in the DVDHL and DVDHV subroutines respectively. These variables are calculated using the partial derivatives of specific volume property formulations obtained from the IAPWS-IF97.

COBRA-TF uses IAPWS-IF97 region 2 property formulations to determine the specific volume of vapour and partial derivatives of specific volume of vapour when the enthalpy of water is greater than the vapour saturation enthalpy. COBRA-TF uses IAPWS-IF97 region 1 property formulations to determine the specific volume of liquid water and the partial derivative of specific volume of liquid water when the enthalpy of water is less than the liquid saturation enthalpy. In COBRA-TF the IAWPS-IF97

region 1 and region 2 property formulations are simplified to improve computational time.

3.1.3 Flow Regime Map

Prior to modelling macro- and micro- closure terms, it is required to determine the behaviour of two-phase flow in the mesh cell being modelled. This is done by utilizing a flow regime map to categorize the two-phase flow behaviour into one of several classification of two-phase flow. The two-phase flow behaviour depends on the pressure, channel geometry, and flow rates of vapour and liquid. COBRA-TF defines flow regimes for momentum mesh cells [1]. Linear averaging of values of adjacent axial momentum mesh cells is performed to define flow regimes for scalar mesh cells [1]. The INTFR subroutine in COBRA-TF determines the flow regime applicable to a given mesh cell. COBRA-TF contains two different types of flow regimes; the normal wall flow regime and the hot wall flow regime [1]. The normal wall flow regime is used when the maximum wall temperature (T_w) is below the critical heat flux temperature [1].

$$T_w < \min\left(705.3°F, T_{CHF}\right)$$

The upper limit of 705.3°F (647.20 K) corresponds to the critical temperature of water. The hot wall flow regime is selected when the maximum wall temperature is above the critical heat flux temperature [1].

$$T_w > \min\left(705.3°F, T_{CHF}\right)$$

The calculation of critical heat flux temperature is discussed in Section 3.1.5.

Normal Wall Flow Regime

The main flow regimes identified in co-current upward vertical two-phase flows are bubbly, slug, churn, and annular. The bubbly or small bubble regime is identified by the presence of small dispersed gas bubbles in a continuous liquid phase. The bubbles can be of variable sizes and shapes. Slug flow is distinguished by the presence of gas plugs or large bubbles separated by liquid slugs. The liquid film encompassing the gas plugs usually moves downward. In this regime, it is also possible to have several small bubbles dispersed within the liquid. COBRA-TF identifies this flow regime as small-to-large bubble flow regime [1]. The churn flow has similar characteristics as the slug flow but more chaotic in nature. The churn flow behaviour can be captured by combining the slug and the annular/mist flow regime characteristics [1]. Annular flow is characterized by the presence of a continuous gas core surrounded by an annulus of the liquid phase. If the gas flow in the core is sufficiently high, it may be carrying liquid droplets. In this case, the annular-dispersed flow regime is said to exist. COBRA-TF combines the annular and the annular-dispersed flow regimes to form the annular/mist flow regime [1]. The annular/mist flow regime ends at the onset of single phase vapour flow at which point the continuous liquid film surrounding the vapour core is completely depleted. COBRA-TF normal wall flow regimes are shown graphically in Figure 3.4.

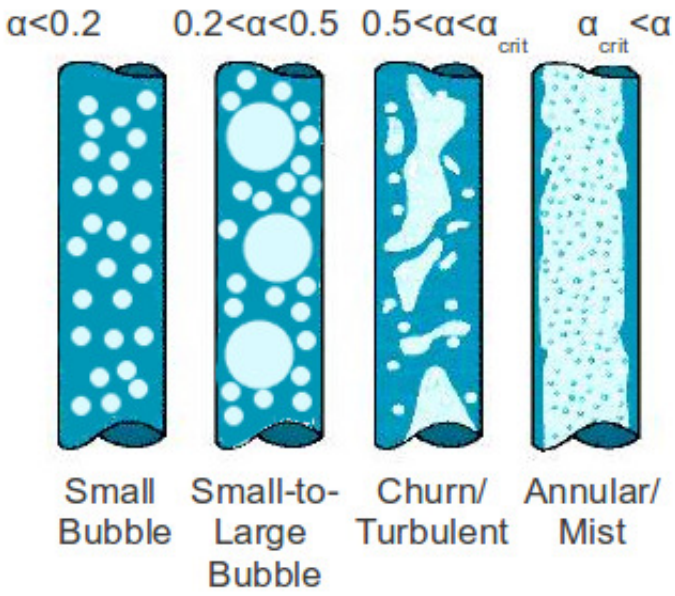

Figure 3.4: Normal wall flow regimes in COBRA-TF (Avramova 2011).

COBRA-TF determines the appropriate normal wall flow regime using the control volume void distribution (α). The normal wall flow regime selection logic is shown in Figure 3.5.

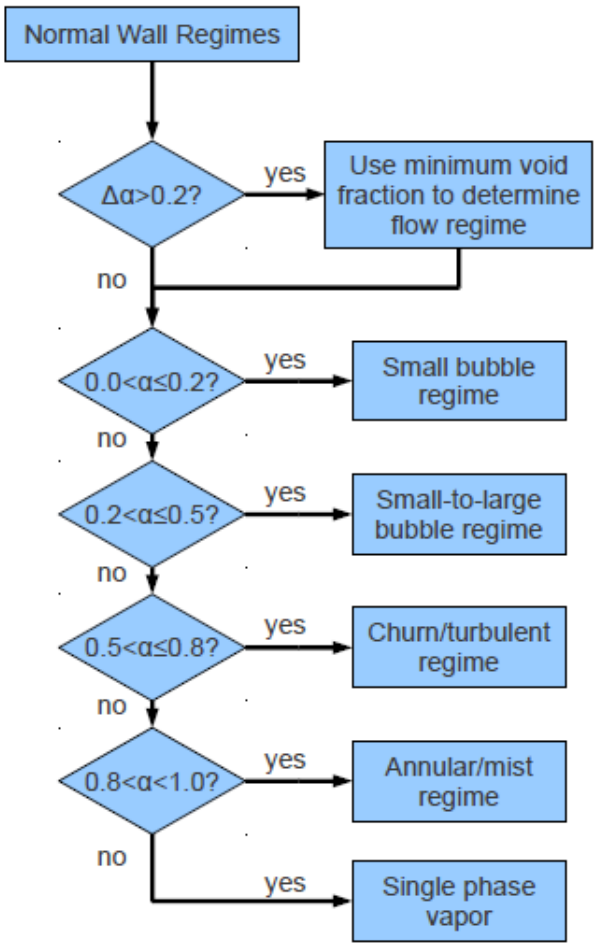

Figure 3.5: Normal wall flow regime selection logic in COBRA-TF (Avramova 2011).

Hot Wall Flow Regime

In hot wall flow regime, the vapour keeps the liquid from contacting the heated surface; therefore the liquid can only partially wet the wall. In nuclear reactor fuel channels, the wall temperature could exceed the Critical Heat Flux (CHF) temperature during accident scenarios such as the blowdown phase of a large-break LOCA. The hot wall flow regimes recognized by COBRA-TF are [1],

- Inverted annular flow
- Inverted slug flow
- Dispersed droplet flow
- Falling film flow
- Top deluge flow

The hot wall flow regimes are shown graphically in Figure 3.6. The COBRA-TF hot wall flow regime selection logic is illustrated in Figure 3.7.

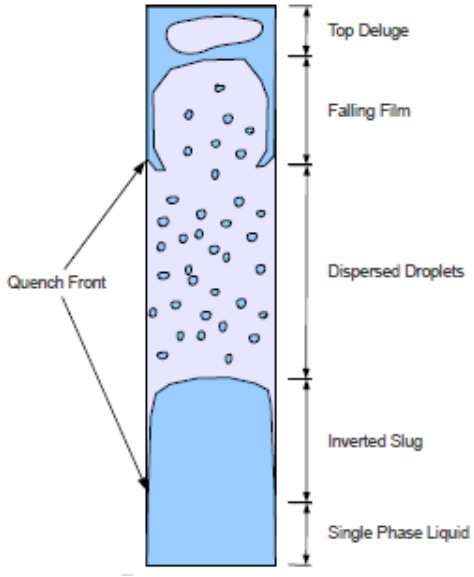

Figure 3.6: Hot wall flow regimes in COBRA-TF (Avramova 2011).

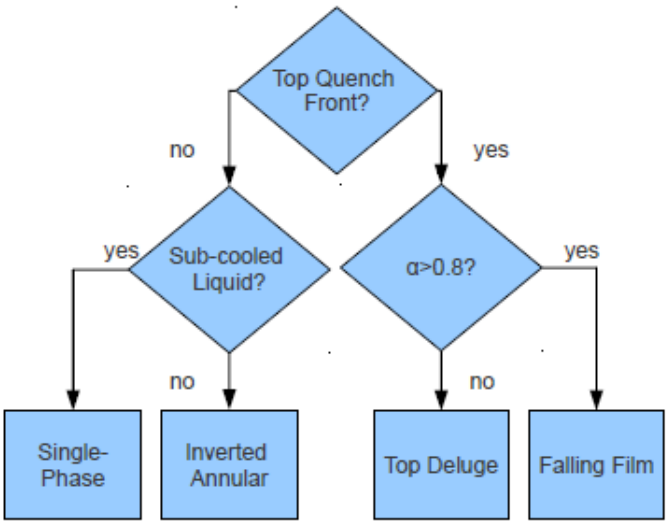

Figure 3.7: Hot wall flow regime selection logic in COBRA-TF (Avramova 2011).

The inverted annular flow regime consists of an annular film of vapour surrounding a liquid core. According to the selection logic, the inverted annular flow regime exists in the absence of a top quench front if the liquid is subcooled [1]. A top quench front occurs when the mesh cell under consideration is in the hot wall flow regime and the mesh cell above it is in the normal wall flow regime. The presence of a top quench front also results in falling film and top deluge flow regimes [1]. Falling film flow regime consists of liquid film flowing down and vapour flowing up. The top deluge flow regime is identified by the presence of large liquid slugs with a diameter equal to the channel hydraulic diameter. Finally the dispersed droplet flow regime is distinguished by the presence of a continuous vapour field with entrained droplets throughout. Dispersed droplets can exist in all hot wall flow regimes [1].

3.1.4 Wall Shear and Form Loss

The viscous shear stress term in the general momentum conservation equation can be expanded into a wall shear and a fluid-fluid shear components,

$$\nabla \cdot \left(\alpha \tau_e^{ij}\right) = \overrightarrow{\tau_{we}}''' \tag{3.4a}$$

$$\nabla \cdot \left(\alpha \tau_v^{ij}\right) = \overrightarrow{\tau_{wv}}''' + \nabla \cdot \left(\alpha_v \sigma_v^{ij}\right) \tag{3.4b}$$

$$\nabla \cdot \left(\alpha \tau_l^{ij}\right) = \overrightarrow{\tau_{wl}}''' + \nabla \cdot \left(\alpha_l \sigma_l^{ij}\right) \tag{3.4c}$$

where $\overrightarrow{\tau_{we}}'''$, $\overrightarrow{\tau_{wv}}'''$, and $\overrightarrow{\tau_{wl}}'''$ are the volumetric wall drag and form losses of the entrained, vapour, and liquid phases respectively. The liquid-liquid shear stresses are not modelled in COBRA-TF, so they are eliminated from the viscous shear stress term. The wall shear in COBRA-TF is modelled as a combination of frictional losses and flow form losses.

$$\tau_{w,x} = \left[\left(\frac{dP}{dx}\right)_{fric} + \left(\frac{dP}{dx}\right)_{form}\right] \Delta X \tag{3.5}$$

The frictional pressure loss for single phase flow within a pipe of constant flow area can be expressed as,

$$\left(\frac{dP}{dx}\right)_{fric} = \frac{f_k G_{m,x}^2}{2 D_h \rho} \tag{3.6}$$

where G_m is the single phase mass flux and f_k is the single phase friction factor. The friction factor is defined using a correlation suggested by Wallis [29].

$$f_k = \{ \underbrace{\frac{64}{Re_k}}_{\text{laminar}}, \underbrace{0.0055 + 0.55 Re_k^{-1/3}}_{\text{turbulent}} \} \tag{3.7}$$

The frictional pressure loss for two-phase flow can be expressed in a general form similar to the single-phase flow.

$$\left(\frac{dP}{dx}\right)_{fric} = \frac{f_{TP} G_{m,x}^2}{2 D_h \rho} \tag{3.8}$$

where G_m is the total two-phase mass flux and f_{TP} is the two-phase friction factor. The general approach for determining the two-phase friction factor is to relate it to a friction factor and a multiplier defined for a single-phase flow, flowing at the same mass flux as the total two-phase mass flux and with a temperature corresponding to bulk flow conditions [26]. If the single phase is liquid, the relevant flow parameters are f_{lo} and ϕ_{lo}^2, whereas if the single phase is vapour, the relevant parameters are f_{vo} and ϕ_{vo}^2 [26]. These parameters are related as [26],

$$\left(\frac{dP}{dx}\right)_{fric}^{TP} = \phi_{lo}^2 \left(\frac{dP}{dx}\right)_{fric}^{lo} = \phi_{vo}^2 \left(\frac{dP}{dx}\right)_{fric}^{vo} \tag{3.9}$$

COBRA-TF utilizes a two-phase frictional pressure drop model based on the work of Wallis [29]. In pre-CHF or normal wall two-phase flow, the entire pipe wall is still in contact with the liquid. Therefore the liquid phase is assumed to carry all the wall drag and the liquid only flow parameters are used to calculate the two-phase frictional pressure drop [1].

$$\phi_{lo} = \frac{1}{\alpha_l} \tag{3.10a}$$

$$f_{lo} = \{\frac{64}{Re_l}, 0.0055 + 0.55 Re_l^{-1/3}\} \tag{3.10b}$$

In post-CHF or hot wall two-phase flow, the liquid phase is no longer in contact with the surface. Therefore the vapour phase is assumed to carry all the wall drag and the vapour only flow parameters are used to calculate the two-phase frictional pressure drop [1].

$$\phi_{vo} = \frac{1}{\alpha_v} \tag{3.11a}$$

$$f_{vo} = \{\frac{64}{Re_v}, 0.0055 + 0.55Re_v^{-1/3}\} \tag{3.11b}$$

The wall friction factors are calculated in the INTFR subroutine in COBRA-TF.

The pressure drop due to abrupt change in the flow direction and/or geometry is called a form loss. The form loss is defined as,

$$\left(\frac{dP}{dx}\right)_{form} = K_x \frac{\alpha_k \rho_k}{2\Delta X} |U_k| U_k \tag{3.12}$$

where K_x is the form loss coefficient and U_k is the field velocity of phase k. According to the modelling circumstances, the form loss coefficient can be user supplied, code calculated, or a combination of both [1]. The code-modelled form loss coefficient is calculated using the expression [1],

$$K_{grid} = \min\left(20, 196Re_{mix}^{-1/3}\right) f_{loss} A_{block}^2 \tag{3.13}$$

where Re_{mix} is the droplets/bubbles mixture Reynolds number, f_{loss} is the user defined pressure loss coefficient multiplier, and A_{block} is the user defined ratio of blocked area to the flow area. The form loss coefficients are determined in the GRID subroutine in COBRA-TF.

3.1.5 Wall Heat Transfer

The energy conservation equation requires the determination of volumetric wall heat transfer. The wall heat transfer to the liquid phase closure term is passed to the liquid energy conservation equation and the wall heat transfer to the vapour phase closure term is passed to the vapour energy conservation equation.

$$Q_{wl} = h_l A_w \left(T_w - T_l\right) \tag{3.14a}$$

$$Q_{wv} = h_v A_w \left(T_w - T_v\right) \tag{3.14b}$$

where h_l and h_v are the liquid and vapour heat transfer coefficients and A_w is the wall area. The liquid and vapour heat transfer coefficients are dependent on the flow heat transfer regime. The liquid heat transfer coefficient is comprised of two different components; sensible heat transfer between the wall and liquid (h_{wl}) and latent heat transfer resulting from vaporization of the liquid (h_{wb}) [1].

Heat Transfer Regime

The heat transfer regimes in a flowing system depend on a number of variables: fluids employed, wall materials, geometry of the system, heat flux magnitude and distribution, and mass flow rate [26]. Different models are used to calculate the heat transfer coefficient for each heat transfer regime. Heat transfer correlations used for each heat transfer regime are not included here for conciseness. The HCOOL subroutine in COBRA-TF determines the appropriate heat transfer regime for a given mesh cell and the BOILING subroutine determines the heat transfer coefficients applicable to the given heat transfer regime. Heat transfer regimes are illustrated in

Figure 3.8, which depicts the boiling curve.

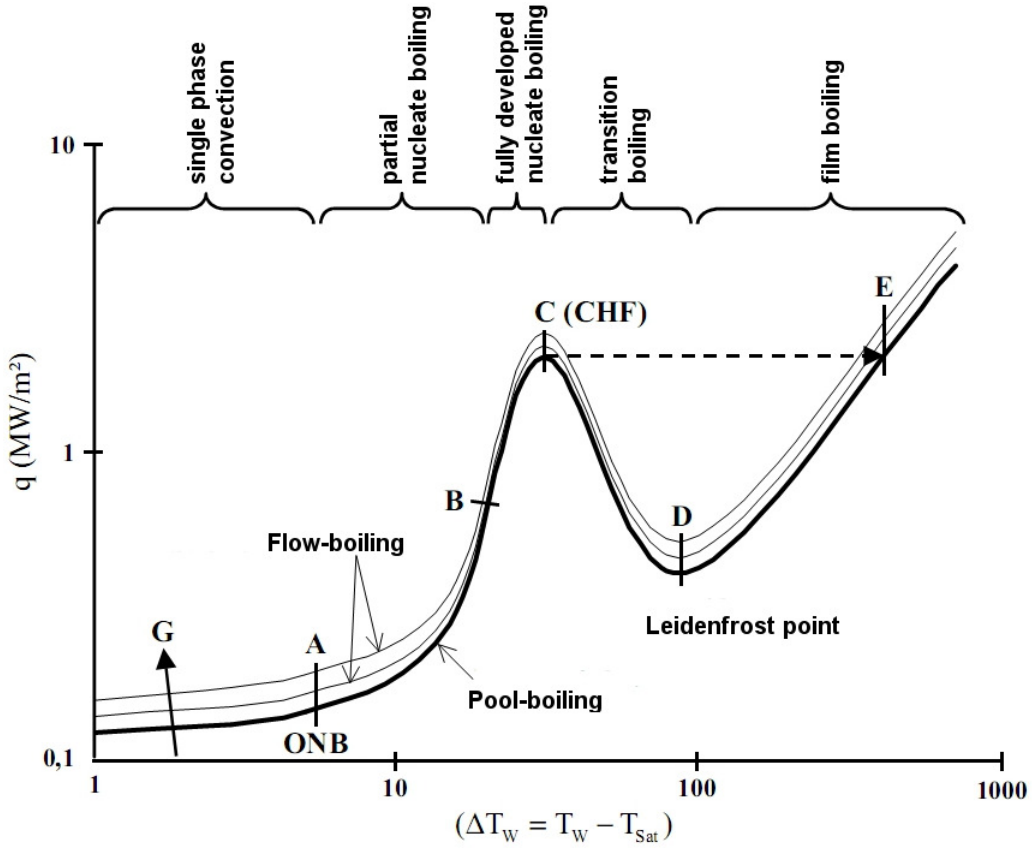

Figure 3.8: Boiling curve (Gregor Bloch)

In single-phase liquid convection regime the liquid is in a subcooled state ($T_{in} < T_{sat}$). As more heat is added, the liquid near the wall becomes superheated and can nucleate a vapour bubble. This initiates the nucleate boiling regime. In this regime the boiling process and the turbulence caused by the boiling improve heat transfer and the wall temperature ceases to rise as fast as in the single phase liquid convection regime. The nucleate boiling regime can be further sub divided into subcooled nucleate boiling and saturated nucleate boiling regimes. The bulk fluid temperature is below the saturation temperature in the subcooled nucleate boiling regime and the bulk fluid

temperature is at the saturation temperature in the saturated nucleate boiling regime. In the saturated nucleate boiling regime bubbles becomes numerous and may start to agglomerate into larger bubbles as they detach. As more heat is added the vapour phase begins to blanket the heated surface. This occurrence is known as the critical heat flux or the departure from nucleate boiling (DNB). Higher heat fluxes lead to the formation of a continuous vapour film at the surface initiating the film boiling heat transfer regime. Film boiling can also be established at lower heat fluxes if the surface temperature is sufficiently high. However, at low wall superheat the formation of the film is unstable giving rise to the transition boiling heat transfer regime. COBRA-TF identifies the following heat transfer regimes [1]:

- Single-phase liquid convection (SPL)
- Single-phase vapour convection (SPV)
- Sub-cooled nucleate boiling (SCB)
- Saturated nucleate boiling (SB)
- Transition boiling (TRAN)
- Inverted annular film boiling (IAFB)
- Dispersed droplet film boiling (DFFB)
- Dispersed droplet deposition heat transfer (DDFB)

COBRA-TF identifies two basic heat transfer zones: pre-CHF and post-CHF. The pre-CHF heat transfer zone is selected if the wall temperature is 0.1°F below the critical heat flux temperature [1]. The pre-CHF heat transfer zone consists of

single-phase liquid convection, subcooled nucleate boiling, and saturated nucleate boiling heat transfer regimes [1]. The post-CHF heat transfer zone is selected if the wall temperature is 0.1°F above the critical heat flux temperature [1]. The post-CHF heat transfer zone consists of transition boiling, inverted annular film boiling, dispersed droplet film boiling, and dispersed droplet deposition heat transfer regimes [1]. The transition boiling regime is selected if the heated wall temperature is below the minimum film boiling temperature and other post-CHF heat transfer regimes are selected if the heated wall temperature is above the minimum film boiling temperature [1]. The single-phase vapour heat transfer regime is selected if the void fraction is above 0.999, regardless of the heated wall temperature [1]. The COBRA-TF heat transfer regime selection algorithm is outlined in Figure 3.9.

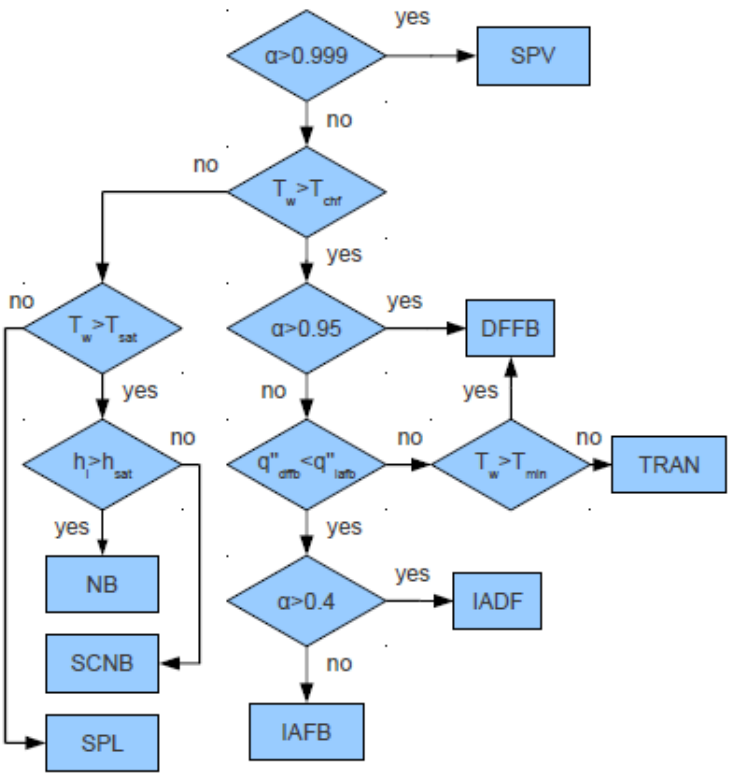

Figure 3.9: COBRA-TF heat transfer regime selection algorithm (Avramova 2011).

It is required to first define the critical heat flux temperature and the minimum film boiling temperature before determining the heat transfer regime.

Critical Heat Flux

COBRA-TF consists of three different critical heat flux calculation models; the W-3 model suggested by Tong et al. [27], the standard COBRA-TF model [1], and a constant CHF of $10^9 BTU/hr.ft^2$. The user can select the appropriate CHF model for the modelling circumstances at hand. The details of each CHF model are not included here for conciseness. The critical heat flux temperature is then calculated iteratively

using the calculated critical heat flux. The BOILING subroutine in COBRA-TF calculates the critical heat flux and the critical heat flux temperature according to the selected CHF calculation model.

Minimum Film Boiling Temperature

The minimum film boiling temperature is the temperature at which a stable vapour film forms on the heated surface. The minimum film boiling temperature separates the transition film boiling regime, where liquid intermittently contacts the heated surface, and the film boiling regime, where a continuous vapour film blankets the heater surface. It is set to a minimum value of 900°F (755.37 K) for unheated conductors [1]. It is set to a minimum value of 900°F (755.37 K) for void fractions less than 0.8 and to a minimum value of 700°F (644.26 K) for void fractions greater than 0.8 for heated conductors [1]. The minimum film boiling temperature is calculated using two different methods. The first method assumes that it equals the wall temperature that results in an instantaneous contact temperature equal to the homogeneous nucleation temperature [1]. The second method uses the Henry′s modification of the Berenson correlation [9]. The criteria for selecting the minimum film boiling temperature can be summarized as,

$$T_{min} = max \begin{cases} min \begin{cases} 1158 \\ max \begin{cases} T_{min,hn} \\ T_{min,henry} \end{cases} \end{cases} \\ 900 & \text{if } \alpha_v < 0.8 \\ 700 & \text{if } \alpha_v \geq 0.8 \end{cases} \tag{3.15}$$

The minimum film boiling temperature is calculated in the HEAT subroutine in COBRA-TF.

3.1.6 Interfacial Drag

The shear force between different flow fields (vapour/droplets and vapour/liquid) is required during the momentum equation solution. The interfacial drag force term in the general momentum equation is calculated using the expression,

$$M_k^d = \frac{1}{2}\rho v^2 C_D A \tag{3.16}$$

where C_D is the interfacial drag coefficient and A is the interfacial area. Both interfacial drag coefficient and interfacial are highly dependent on the nature of flow. Therefore, COBRA-TF includes different models to calculate these terms according to the prevailing flow regime in the mesh cell under consideration [1]. These correlations are not presented here for conciseness. Interfacial drag force calculations are performed for the axial momentum cells and then for the transverse momentum cells [1]. Interfacial drag force calculations are performed in the INTFR subroutine.

3.1.7 Interfacial Heat Transfer

The interfacial heat transfer terms are used to calculate the mass transfer due to phase change (L_k) in the mass conservation equation and the energy transfer due to phase change ($\Gamma_k h_k^i$) in the energy conservation equation. The calculated mass transfer is then used in the momentum conservation equation to calculate momentum transfer due to phase change (M_k^L) in the next time step. Interfacial heat transfer

coefficients are calculated for droplet/vapour and liquid/vapour field interfaces [1]. They are considered for four different possible scenarios [1];

- Subcooled Liquid (scl)
- Superheated Liquid (shl)
- Subcooled Vapour (scv)
- Superheated Vapour (shv)

All four interfacial heat transfer coefficients are calculated for both field interfaces in the INTFR subroutine. The interfacial heat transfer coefficients and the interfacial area for heat transfer are dependent on the flow regime. Models for calculating interfacial heat transfer coefficients are different for different flow regimes and are not included here for conciseness.

Subcooled liquid and subcooled vapour lead to condensation while superheated liquid and superheated vapour lead to evaporation. Then the mass transfer rate can be calculated as [1],

$$\Gamma_{evap,shl} = \frac{h_{int,shl}}{(h_g - h_f)\, C_{p,l}} |h_l - h_f| \tag{3.17a}$$

$$\Gamma_{evap,shv} = \frac{h_{int,shv}}{(h_g - h_f)\, C_{p,v}} |h_v - h_g| \tag{3.17b}$$

$$\Gamma_{cond,scl} = \frac{h_{int,scl}}{(h_g - h_f)\, C_{p,l}} |h_l - h_f| \tag{3.17c}$$

$$\Gamma_{cond,scv} = \frac{h_{int,scv}}{(h_g - h_f)\, C_{p,v}} |h_v - h_g| \tag{3.17d}$$

where $h_{int,shl}, h_{int,shv}, h_{int,scl}$, and $h_{int,scv}$ are the interfacial heat transfer coefficients. The total mass transfer is then obtained by subtracting condensation terms from

evaporation terms as follows [1].

$$\Gamma_{net} = [\Gamma_{evap,shl} + \Gamma_{evap,shv}] - [\Gamma_{cond,scl} + \Gamma_{cond,scv}] \tag{3.18}$$

When mass changes phases, it takes energy along with it. Then energy exchange by phase mass transfer is calculated as [1],

$$\Gamma_{net} H = [\Gamma_{evap,shl} - \Gamma_{cond,scl}]\, h_f + [\Gamma_{evap,shv} - \Gamma_{cond,scv}]\, h_g \tag{3.19}$$

3.1.8 Turbulent Mixing and Void Drift

Turbulent Mixing

The mass, momentum, and energy transfer due to turbulence mixing must be defined prior to the conservation equations solution. COBRA-TF utilizes a simple turbulent diffusion model to capture the effects of turbulent mixing [1]. The momentum transfer due to turbulent mixing in the momentum conservation equation is calculated as [1],

$$W_{ij}^{M} = V_{ij}^{T} \left(G_{iz} - G_{jz}\right) S_k \Delta X \tag{3.20}$$

The difference in axial mass flux between the adjacent subchannels i and j, $G_{iz} - G_{jz}$, is used to drive the axial momentum transfer. This difference is then multiplied by the transverse velocity causing turbulent mixing (V_{ij}^{T}), the gap width (S_k), and the axial mesh cell height (ΔX) to obtain the axial momentum transfer rate. The mass transfer due to turbulent mixing in the mass conservation equation is defined as [1],

$$W_{ij}^{D} = V_{ij}^{T} \left(\rho_i - \rho_j\right) S_k \Delta X \tag{3.21}$$

The difference in density between the adjacent subchannels i and j, $\rho_i - \rho_j$, is used to drive the turbulent mass exchange. This difference is then multiplied by the transverse velocity causing turbulent mixing (V_{ij}^T), the gap width (S_k), and the axial mesh cell height (ΔX) to obtain the mass transfer rate. The energy transfer due to turbulent mixing is calculated similarly, but with the density terms multiplied by the respective subchannel energies [1].

$$W_{ij}^E = V_{ij}^T \left(\rho_i h_i - \rho_j h_j\right) S_k \Delta X \tag{3.22}$$

The mass, momentum, and energy turbulent mixing terms are then broken into separate equations for vapour and droplets fields [1]. In COBRA-TF turbulent exchange is not considered for the liquid field [1].

The turbulent mixing transverse velocity depends on the average mass flux between the adjacent subchannels and a turbulent mixing coefficient, β_{tp}. [1].

$$V_{ij}^T = \beta_{tp} \frac{\overline{G}}{\overline{\rho_{mix}}} \tag{3.23}$$

The mass flux is divided by the mixture density to convert it to transverse velocity. The turbulent mixing coefficient can be completely user-defined or it can be calculated using one of two methods [1]. The first method is to calculate the single phase turbulent mixing coefficient using the Rogers and Rosehart correlation and calculate the two-phase turbulent mixing coefficient using the Beus correlation [1]. The second method is to use a user-defined single phase mixing coefficient and calculate the two-phase mixing coefficient using the Beus correlation [1]. The COBRA-TF turbulent mixing coefficient selection logic illustrated in Figure 3.10.

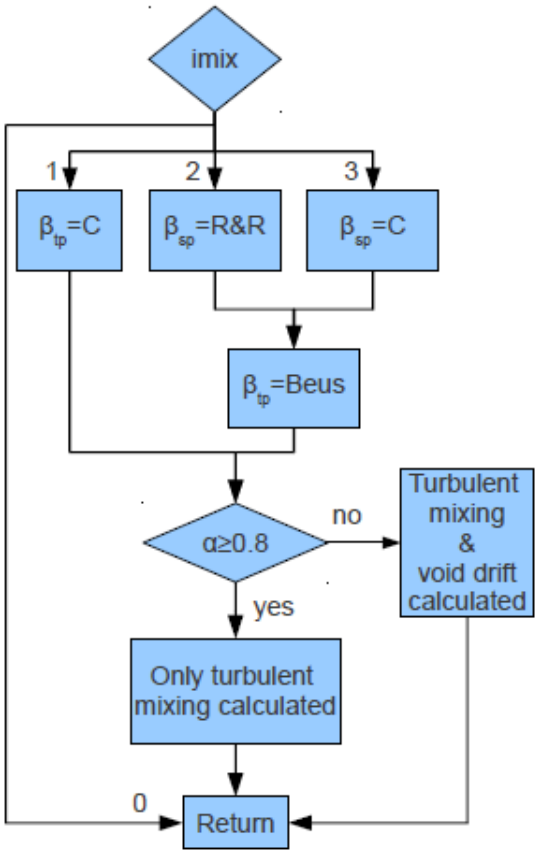

Figure 3.10: Flow chart for the application of the turbulent mixing and void drift model in COBRA-TF (Avramova 2011).

The Rogers and Rosehart correlation for turbulent exchange in bundle geometries can be expressed as [20],

$$\beta_{sp} = 0.5\lambda Re^{-0.1}\left[1+\left(\frac{D_{h,jj}}{D_{h,ii}}\right)^{1.5}\right]\frac{D_{h,ii}}{D_{rod}},\ if\ D_{h,ii} < D_{h,jj} \tag{3.24a}$$

$$\beta_{sp} = 0.5\lambda Re^{-0.1}\left[1+\left(\frac{D_{h,ii}}{D_{h,jj}}\right)^{1.5}\right]\frac{D_{h,jj}}{D_{rod}},\ if\ D_{h,jj} < D_{h,ii} \tag{3.24b}$$

where $D_{h,ii}$ and $D_{h,jj}$ are hydraulic diameters of adjacent subchannels ii and jj. The

coefficient, λ, is calculated as [20],

$$\lambda = 0.0058 \left(\frac{S_k}{D_{rod}} \right)^{-1.46} \tag{3.25}$$

Beus demonstrated that the behaviour of the two-phase turbulent mixing coefficient is highly dependent on the flow regime [2]. He determined that the mixing coefficient increases linearly with respect to flow quality up until the flow regime change from slug to annular and then decreases in a hyperbolic fashion [2]. The Beus correlation can be defined as [2],

$$\beta_{tp} = 1 + (\beta_{tp,M} - 1) \left(\frac{x}{x_M} \right), \; if \; x < x_M \tag{3.26a}$$

$$\beta_{tp} = 1 + (\beta_{tp,M} - 1) \left(\frac{x_M - x_0}{x - x_0} \right), \; if \; x > x_M \tag{3.26b}$$

where x_M is the quality at the slug to annular transition point, $\beta_{tp,M}$ is the two-phase mixing coefficient at the transition point, and x_0 is the asymptote to which the hyperbola converges.

Void Drift

Void drift is the phenomena by which void migrates from lower velocity subchannels to higher velocity subchannels. It is caused by the higher velocity vapour phase seeking the path of least resistance, which are the higher velocity subchannels. Void drift causes a transfer of mass, momentum, and energy between subchannels. COBRA-TF considers void drift if the void fraction is lower than the churn and annular flow boundary ($\alpha < 0.8$) [1]. There is an equilibrium distribution of void, when achieved will cause the void migration to cease. COBRA-TF expresses this equilibrium void

distribution using a model suggested by Lahey and Moody [14],

$$(\alpha_i - \alpha_j)_{equil} = K_a \frac{(G_i - G_j)_{equil}}{G_{avg}} \tag{3.27}$$

where $(G_i - G_j)_{equil}$ is the fully developed equilibrium mass flux difference between subchannels i and j [1]. This is simply taken as the actual mass flux difference between subchannels i and j [1]. The proportionality constant, K_a, is usually taken to be 1.4, but the user can select any value according to the modelling circumstance [1].

The mass transfer due to void drift in the mass conservation equation is calculated by multiplying the equilibrium void distribution parameter by the density of the fluid in the adjacent subchannels and the turbulent mixing transverse velocity.

$$W_{ij}^D = -V_{ij}^T \left(\rho_i \alpha_i + \rho_j \alpha_j\right) \left(\alpha_i - \alpha_j\right)_{equil} S_{ij} \Delta X \tag{3.28}$$

The negative sign is used to preserve the global coordinate system in COBRA-TF. Similarly the momentum transfer by void drift in the momentum conservation equation is determined by multiplying the equilibrium void distribution parameter by the total mass flux in the adjacent subchannels and the turbulent mixing transverse velocity.

$$W_{ij}^M = -V_{ij}^T \left(G_i + G_j\right) \left(\alpha_i - \alpha_j\right)_{equil} S_{ij} \Delta X \tag{3.29}$$

The energy transfer by void drift in the energy conservation equation is determined by,

$$W_{ij}^E = -V_{ij}^T \left(\rho_i \alpha_i h_i + \rho_j \alpha_j h_j\right) \left(\alpha_i - \alpha_j\right)_{equil} S_{ij} \Delta X \tag{3.30}$$

These void drift mixing terms are directly added to the turbulent mixing terms

calculated in the previous section to determine the mass, momentum, and energy transfer due to turbulent mixing and void drift in the mass, momentum, and energy conservation equations.

$$M_e^T = W_{ij,turbulent}^D + W_{ij,void}^D \tag{3.31a}$$

$$M_k^T = W_{ij,turbulent}^M + W_{ij,void}^M \tag{3.31b}$$

$$q_k^T = W_{ij,turbulent}^E + W_{ij,void}^E \tag{3.31c}$$

In COBRA-TF all the turbulent mixing and void drift calculations are done in the VDRIFT subroutine.

3.2 IAPWS-IF97

The IAPWS Industrial Formulation 1997 consists of a set of equations for different regions that cover range of validity [28],

$$273.15K \leq T \leq 1073.15K \ , \ P \leq 100MPa \text{ and}$$

$$1073.15K < T \leq 2273.15K \ , \ P \leq 50MPa$$

The entire region of validity is divided into five regions [28]. Figure 3.11 illustrates the assignment of the five basic equations to the corresponding regions. It is thermodynamically reasonable to establish the corresponding equations of state as a function of pressure p and temperature T for regions 1, 2, and 5 [28]. The equations are formulated explicit in the specific Gibbs free energy $g(p,T)$, a fundamental equation [28]. Region 3 contains the critical point [28]. This region can't be covered by an equation with

pressure and temperature as independent variables [28]. However, it is possible to represent it by an equation as a function of density ρ and temperature T [28]. Then Region 3 is covered by a fundamental equation for the Helmholtz free energy $f(\rho, T)$ [28]. Region 4 or the saturation curve is defined by a saturation pressure equation $ps(T)$ [28].

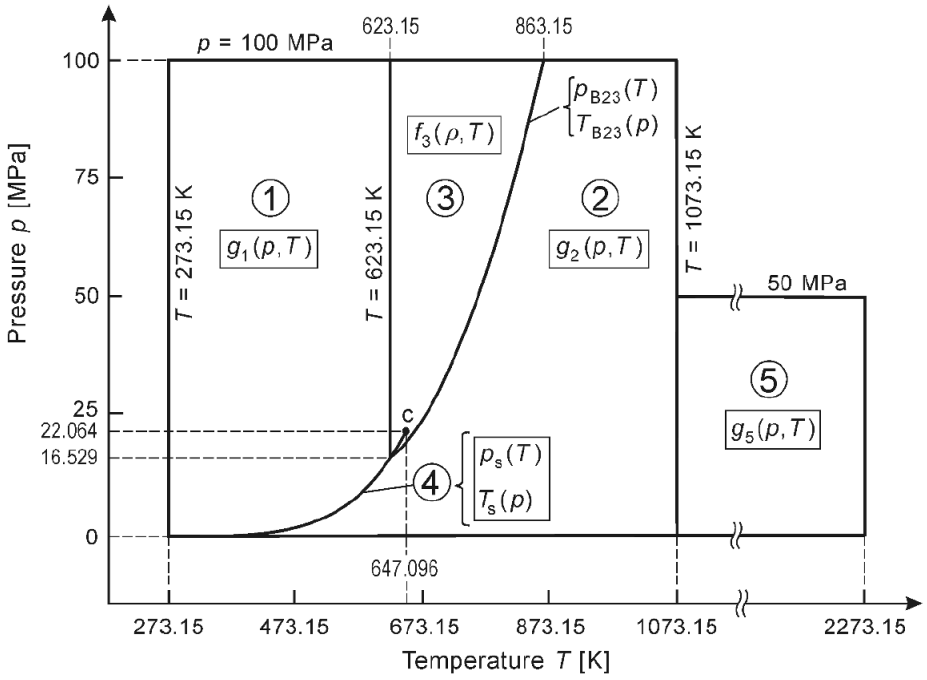

Figure 3.11: Regions and equations of IAPWS-IF97 (Wagner 2008).

The boundary between regions 1 and 3 is the isotherm at 623.15 K [28].The boundary between regions 2 and 3 is defined using a simple quadratic pressure-temperature relation [28].

$$p_{B23}(T) = n_1 + n_2\theta + n_3\theta^2 \tag{3.32}$$

where $\theta = T/T^*$ with $p* = 1$ MPa. The coefficients n_1,n_2, and n_3 are provided in the IAPWS-IF97 and are not included here for conciseness. The $p_s(T)$ is the

saturation-pressure equation. COBRA-TF defines this in the SAT subroutine.

3.2.1 Basic equations of IAPWS-IF97

IAPWS-IF97 Region 1

The basic equation for region 1 is a fundamental equation for specific Gibbs free energy g [28]. This equation is expressed in dimensionless form, $\gamma = g/(RT)$, and reads [28]

$$\frac{g_1(p,T)}{RT} = \gamma(\pi,\tau) = \sum_{i=1}^{34} n_i (7.1-\pi)^{I_i} (\tau - 1.222)^{J_i} \tag{3.33}$$

where $\pi = p/p^*$ and $\tau = T^*/T$ with $p^* = 16.53\ MPa$, $T^* = 1368\ K$, and $R = 0.461526\ kJ \cdot kg^{-1} \cdot K^{-1}$. The coefficients n_i and exponents I_i and J_i are given in the IAPWS-IF97 and are omitted here for conciseness. All thermodynamic properties for region 1 can be derived from Equation 3.33, by using the appropriate combination of the dimensionless Gibbs free energy, γ, and its derivatives [28].

IAPWS-IF97 Region 2

The basic equation for region 2 is a fundamental equation for specific Gibbs free energy as well [28]. This equation is expressed in dimensionless form, $\gamma = g/(RT)$, and is separated into two parts, an ideal gas part γ^0 and a residual part γ^r [28].

$$\frac{g_2(p,T)}{RT} = \gamma(\pi,\tau) = \gamma^0(\pi,\tau) + \gamma^r(\pi,\tau) \tag{3.34}$$

where $\pi = p/p^*$ and $\tau = T^*/T$ with $R = 0.461526\ kJ \cdot kg^{-1} \cdot K^{-1}$. The equation for the dimensionless ideal-gas part γ^0 of the basic equation reads [28],

$$\gamma^0(\pi, \tau) = ln\pi + \sum_{i=1}^{9} n_i^0 \tau^{J_i^0} \tag{3.35}$$

where $\pi = p/p^*$ and $\tau = T^*/T$ with $p^* = 1\ MPa$ and $T^* = 540\ K$. The coefficients n_i^0 and exponents J_i^0 are provided in the IAPWS-IF97 and are omitted here for conciseness. The form of the dimensionless residual part, γ^r, of the basic equation is as follows [28].

$$\gamma^r(\pi, \tau) = \sum_{i=1}^{43} n_i \pi^{I_i} (\tau - 0.5)^{J_i} \tag{3.36}$$

where $\pi = p/p^*$ and $\tau = T^*/T$ with $p^* = 1\ MPa$ and $T^* = 540\ K$. The coefficients n_i and exponents I_i and J_i are provided in the IAPWS-IF97 and are omitted here for conciseness. All thermodynamic properties for region 2 can be derived from Equation 3.34 by using the appropriate combination of the ideal gas part γ^0 and the residual part γ^r of the dimensionless Gibbs free energy and their derivatives [28].

IAPWS-IF97 Region 3

The basic equation for region 3 is a fundamental equation for the specific Helmholtz free energy [28]. This equation is expressed in dimensionless form, $\phi = f/(RT)$, and reads [28],

$$\frac{f_3(\rho, T)}{RT} = \phi(\delta, \tau) = n_1 ln\delta + \sum_{i=2}^{40} n_i \delta^{I_i} \tau^{J_i} \tag{3.37}$$

where $\delta = \rho/\rho^*$ and $\tau = T^*/T$ with $\rho^* = \rho_c = 322\ kg/m^3$, $T^* = T_c = 647.096$ K and $R = 0.461526\ kJ/kgK$. The coefficients n_i and exponents I_i and J_i are listed in the IAPWS-IF97 and are omitted here for conciseness. All thermodynamic properties for

region 3 can be derived from Equation 3.37 by using the appropriate combinations of the dimensionless Helmholtz free energy ϕ and its derivatives [28].

3.2.2 Backward Equations of IAPWS-IF97

This section summarizes only the backward equations used in the modified COBRA-TF-SC code for conciseness. The full list of backward equations can be seen at the IAPWS-IF97. All forms of backward equations (marked in grey) assigned to the corresponding regions of IAPWS-IF97 are illustrated in Figure 3.12. The basic equations for these regions are shown in rectangular boxes.

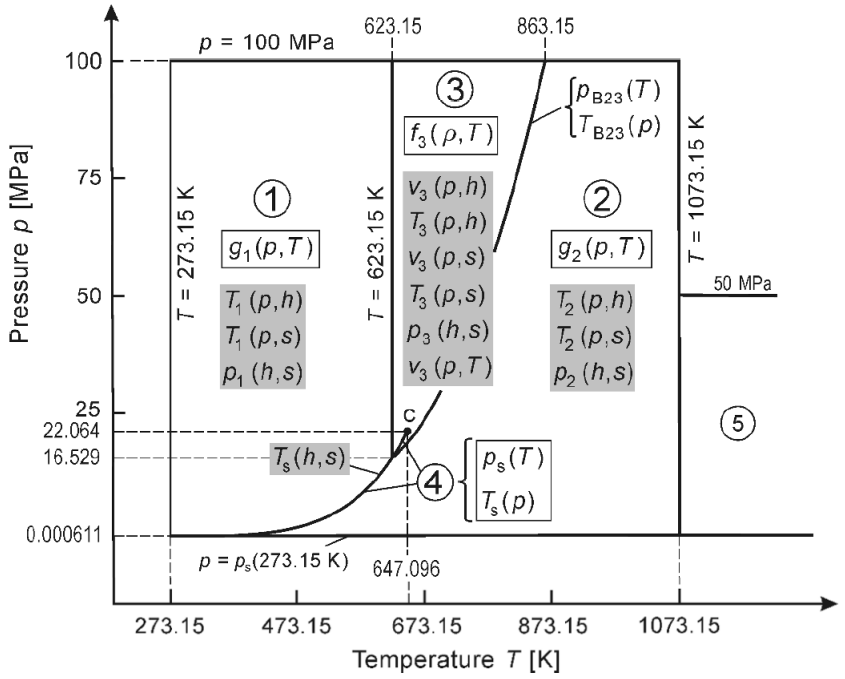

Figure 3.12: Backward equations (marked in grey) assigned to the corresponding regions of IAPWS-IF97 (Wagner 2008).

Backward Equation T(p,h) for Region 1

Figure 3.13 illustrates the assignment of the backward equation $T_1(p,h)$ to region 1 in a p-h diagram.

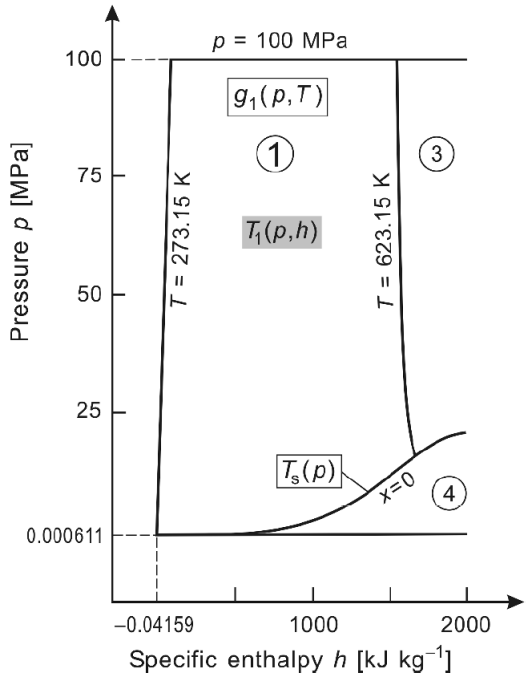

Figure 3.13: Assignment of the backward equation $T_1(p,h)$ to region 1 in a p-h diagram (Wagner 2008).

The backward equation $T_1(p,h)$ for region 1 has the following dimensionless form [28]:

$$\frac{T_1(p,h)}{T^*} = \theta(\pi,\eta) = \sum_{i=1}^{20} n_i \pi^{I_i} (\eta+1)^{J_i} \tag{3.38}$$

where $\theta = T/T^*$, $\pi = p/p^*$, and $\eta = h/h^*$ with $T^* = 1\ K$, $p^* = 1\ MPa$, and $h^* = 2500\ kJ \cdot kg^{-1}$. The coefficients n_i and exponents I_i and J_i are listed in the IAPWS-IF97 and are omitted here for conciseness.

Backward Equation T(p,h) for Region 2

Figure 3.14 illustrates how region 2 is divided into three subregions for the backward equation $T\,(p,h)$.

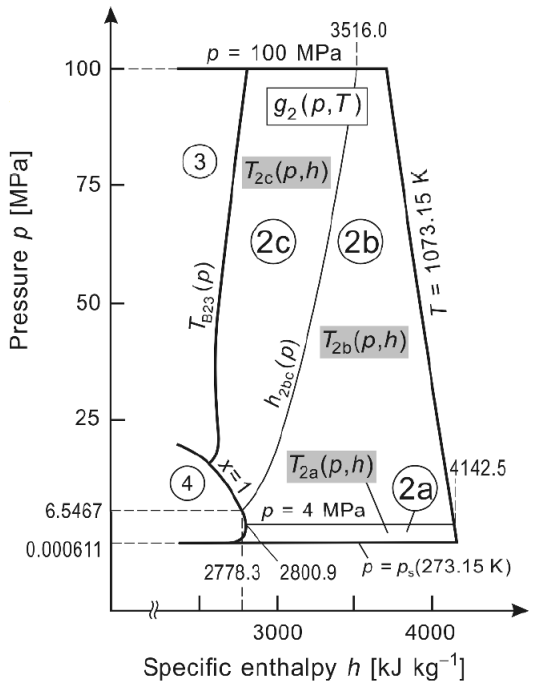

Figure 3.14: Division of region 2 into subregions 2a, 2b, and 2c and the assignment of the backward equation $T\,(p,h)$ to these subregions (Wagner 2008).

The boundary between subregions 2a and 2b is the isobar p = 4 MPa, and the boundary between subregions 2b and 2c is described by the equation [28],

$$\frac{h_{2bc}\,(p)}{h^*} = \eta\,(\pi) = n_4 + \left[(\pi - n_5)\,/n_3\right]^{0.5} \tag{3.39}$$

where $\eta = h/h^*$ and $\pi = p/p^*$ with $p^* = 1\ MPa$ and $h^* = 1\ kJ \cdot kg^{-1}$. The coefficients n_3 to n_5 are listed in the IAPWS-IF97 and are omitted here for conciseness. The

backward equation for subregion 2a in its dimensionless form reads [28],

$$\frac{T_{2a}(p,h)}{T^*} = \theta(\pi,\eta) = \sum_{i=1}^{34} n_i \pi^{I_i} (\eta - 2.1)^{J_i} \tag{3.40}$$

The backward equation for subregion 2b in its dimensionless form reads [28],

$$\frac{T_{2b}(p,h)}{T^*} = \theta(\pi,\eta) = \sum_{i=1}^{38} n_i (\pi - 2)^{I_i} (\eta - 2.6)^{J_i} \tag{3.41}$$

The backward equation for subregion 2c in its dimensionless form reads [28],

$$\frac{T_{2c}(p,h)}{T^*} = \theta(\pi,\eta) = \sum_{i=1}^{23} n_i (\pi + 2.5)^{I_i} (\eta - 1.8)^{J_i} \tag{3.42}$$

where $\theta = T/T^*$, $\pi = p/p^*$, and $\eta = h/h^*$ with $T^* = 1\ K$, $p^* = 1\ MPa$, and $h^* = 2000\ kJ \cdot kg^{-1}$. The coefficients n_i and exponents I_i and J_i are listed in the IAPWS-IF97 and are omitted here for conciseness.

Backward Equations ν(p,h) and T(p,h) for Region 3

Figure 3.15 illustrates that region 3 is divided into two subregions for the backward equations $T(p,h)$ and $\nu(p,h)$. The boundary between subregions 3a and 3b is defined by the dimensionless equation [28],

$$\frac{h_{3ab}(P)}{h^*} = n_1 + n_2\pi + n_3\pi^2 + n_4\pi^3 \tag{3.43}$$

where $p = p/p^*$ with $p^* = 1$ MPa and $h^* = 1$ kJ/kg. The coefficients n_1 to n_4 are listed in the IAPWS-97 and are omitted here for conciseness.

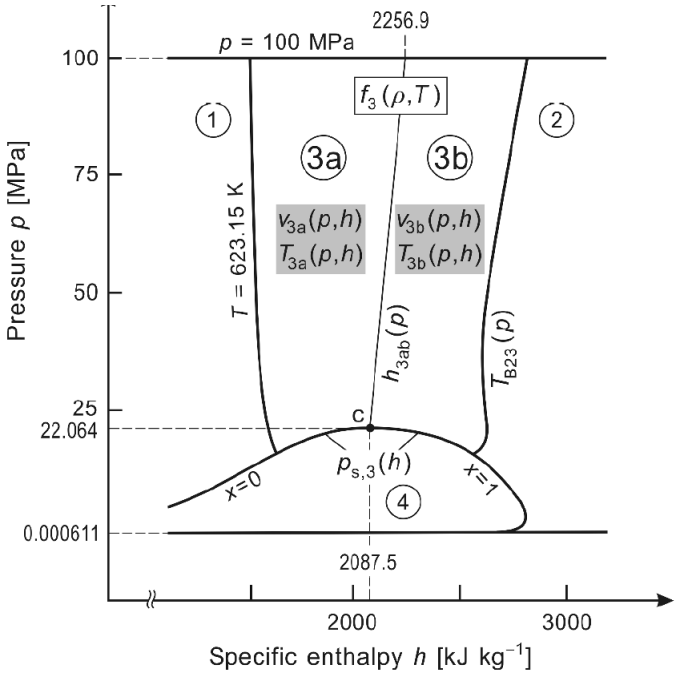

Figure 3.15: Division of region 3 into subregions 3a and 3b and the assignment of the backward equations $T(p,h)$ and $\nu(p,h)$ to these subregions (Wagner 2008).

The backward equation $\nu_{3a}(p,h)$ for subregion 3a has the following dimensionless form [28]:

$$\frac{\nu_{3a}(p,h)}{\nu^*} = \omega(\pi,\eta) = \sum_{i=1}^{32} n_i (\pi + 0.128)^{I_i} (\eta - 0.727)^{J_i} \tag{3.44}$$

where $\omega = \nu/\nu^*$, $\pi = p/p^*$, and $\eta = h/h^*$ with $\nu^* = 0.0028\ m^3/kg$, $p^* = 100\ MPa$, and $h^* = 2100\ kJ/kg$. The backward equation $\nu_{3b}(p,h)$ for subregion 3b has the following dimensionless form [28]:

$$\frac{\nu_{3b}(p,h)}{\nu^*} = \omega(\pi,\eta) = \sum_{i=1}^{30} n_i (\pi + 0.0661)^{I_i} (\eta - 0.720)^{J_i} \tag{3.45}$$

where $\omega = \nu/\nu^*$, $\pi = p/p^*$, and $\eta = h/h^*$ with $\nu^* = 0.0088\ m^3/kg$, $p^* = 100\ MPa$, and $h^* = 2800\ kJ/kg$. The coefficients n_i and exponents I_i and J_i are listed in the

IAPWS-IF97 and are omitted here for conciseness.

The backward equation $T_{3a}(p,h)$ for subregion 3a has the following dimensionless form [28]:

$$\frac{T_{3a}(p,h)}{T^*} = \theta(\pi,\eta) = \sum_{i=1}^{31} n_i (\pi + 0.240)^{I_i} (\eta - 0.615)^{J_i} \tag{3.46}$$

where $\theta = T/T^*$, $\pi = p/p^*$, and $\eta = h/h^*$ with $T^* = 760\ K$, $p^* = 100\ MPa$, and $h^* = 2300\ kJ/kg$. The backward equation $T_{3b}(p,h)$ for subregion 3b has the following dimensionless form [28]:

$$\frac{T_{3b}(p,h)}{T^*} = \theta(\pi,\eta) = \sum_{i=1}^{33} n_i (\pi + 0.298)^{I_i} (\eta - 0.720)^{J_i} \tag{3.47}$$

where $\theta = T/T^*$, $\pi = p/p^*$, and $\eta = h/h^*$ with $T^* = 860\ K$, $p^* = 100\ MPa$, and $h^* = 2800\ kJ/kg$. The coefficients n_i and exponents I_i and J_i are listed in the IAPWS-IF97 and are omitted here for conciseness.

3.2.3 The IAPWS-IF97 Equations for Transport Properties

The IAPWS-IF97 equations for the dynamic viscosity and thermal conductivity are presented in this section. The correlation equation for the dynamic viscosity η is given in dimensionless form, $\Psi = \eta/\eta^*$, and consists of two functions Ψ_0 and Ψ_1 that are multiplied with each other.

$$\frac{\eta(\rho,T)}{\eta^*} = \Psi(\delta,\theta) = \Psi_0(\theta) \cdot \Psi_1(\delta,\theta) \tag{3.48}$$

where $\delta = \rho/\rho^*$ and $\theta = T/T^*$ with $\eta^* = 1 \times 10^6\ Pa \cdot s$. The first function of Equation 3.48 represents the viscosity in the ideal-gas limit and has the form,

$$\Psi_0(\theta) = \theta^{0.5} \left[\sum_{i=1}^{4} n_i^o \theta^{1-i} \right]^{-1} \tag{3.49}$$

where $\theta = T/T^*$ with $T^* = T_c = 647.096\ K$. The coefficients n_i^o are listed in IAPWS-IF97 and are omitted here for conciseness. The equation for the second function of Equation 3.48 reads,

$$\Psi_1(\delta, \theta) = exp \left[\delta \sum_{i=1}^{21} n_i (\delta - 1)^{I_i} \left(\theta^{-1} - 1 \right)^{J_i} \right] \tag{3.50}$$

where $\delta = \rho/\rho^*$ and $\theta = T/T^*$ with $\rho^* = \rho_c = 322\ kg \cdot m^{-3}$ and $T^* = T_c = 647.096\ K$. The coefficients n_i and the exponents I_i and J_i are listed in the IAPWS-IF97 and are omitted here for conciseness.

The correlation equation for the thermal conductivity λ is given in dimensionless form, $\Lambda = \lambda/\lambda^*$, and consists of the sum of three functions.

$$\frac{\lambda(\rho, T)}{\lambda^*} = \Lambda(\delta, \theta) = \Lambda_0(\theta) + \Lambda_1(\delta) + \Lambda_2(\delta, \theta) \tag{3.51}$$

where $\delta = \rho/\rho^*$ and $\theta = T/T^*$ with $\lambda^* = 1\ W \cdot m^{-1} \cdot K^{-1}$. The first function represents the thermal conductivity in the ideal gas limit and has the form,

$$\Lambda_0(\theta) = \theta^{0.5} \sum_{i=1}^{4} n_i^o \theta^{i-1} \tag{3.52}$$

where $\theta = T/T^*$ with $T^* = 647.26\ K$. The coefficients n_i^o are listed in the IAPWS-IF97

are omitted here for conciseness. The correlation equation for the second function is,

$$\Lambda_1(\delta) = n_1 + n_2\delta + n_3 exp\left[n_4(\delta + n_5)^2\right] \tag{3.53}$$

where $\delta = \rho/\rho^*$ and $\theta = T/T^*$ with $\rho^* = 317.7\ kg \cdot m^{-3}$ and $T^* = 647.26\ K$. The coefficients n_i are listed in IAPWS-IF97 and are omitted here for conciseness. The third function is defined as,

$$\Lambda_2(\delta,\theta) = \left(n_1\theta^{-10} + n_2\right)\delta^{1.8} exp\left[n_3\left(1-\delta^{2.8}\right)\right] + n_4 A\delta^B exp\left[\left(\frac{B}{1+B}\right)\left(1-\delta^{1+B}\right)\right] + n_5 exp\left[n_6\delta^{1.5} + n_7\delta^{-5}\right] \tag{3.54}$$

where $\delta = \rho/\rho^*$ and $\theta = T/T^*$ with $\rho^* = 317.7\ kg \cdot m^{-3}$ and $T^* = 647.26\ K$. The functions A and B have the form,

$$A(\theta) = 2 + n_8(\Delta\theta)^{-0.6} \tag{3.55a}$$

$$B(\theta) = \begin{cases} (\Delta\theta)^{-1} & \text{for } \theta \geq 1 \\ n_9(\Delta\theta)^{-0.6} & \text{for } \theta < 1 \end{cases} \tag{3.55b}$$

$$\Delta\theta = |\theta - 1| + n_{10} \tag{3.55c}$$

The coefficients n_i are listed in IAPWS-IF97 and are omitted here for conciseness.

Chapter 4

Methodology

This section provides a detailed description of modifications done to upgrade the COBRA-TF subchannel analysis code to perform supercritical water flow simulations. An explanation of how the modifications are implemented to the code is also provided. Modified source codes of COBRA-TF-SC are given in Appendix C.

4.1 Water Property

The variations in thermophysical properties of water in the vicinity of the critical and pseudocritical points require the implementation of new formulations to determine water properties at supercritical pressures. COBRA-TF property tables and property formulations are only valid for subcritical water flow and must be updated to simulate supercritical water flow.

4.1.1 Saturation Curve

The saturation curve must be updated prior to updating intrinsic property table and property formulations in COBRA-TF. Supercritical water behaves as a single phase fluid and no boiling is experienced. Therefore the pseudo void fraction should be zero or unity at supercritical pressures as shown in Figure 4.1.

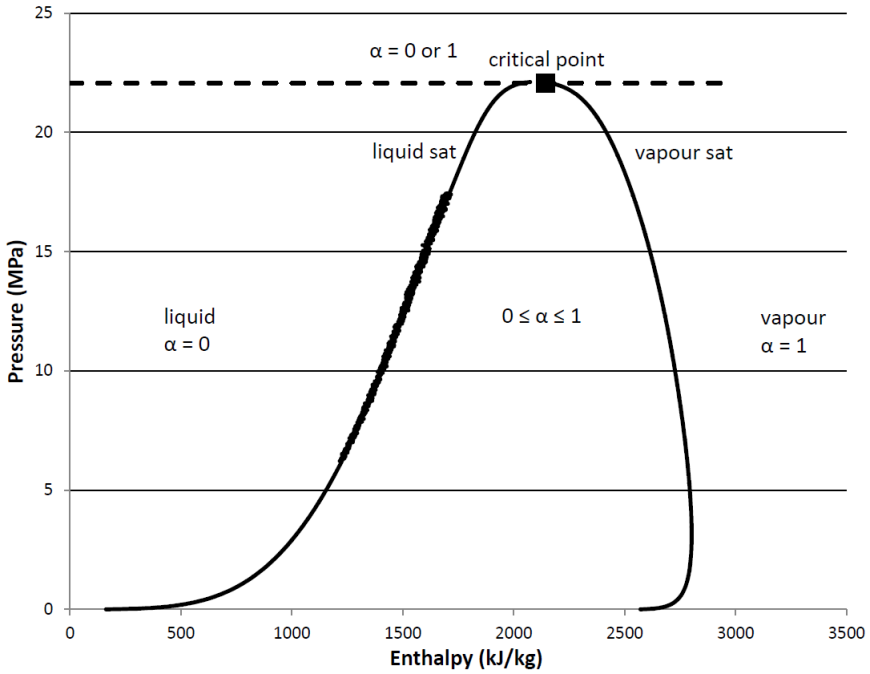

Figure 4.1: Saturation curve at supercritical pressure.

In order to avoid discontinuities in void fraction when fluid conditions transfer between supercritical and subcritical pressure regions, the pseudo two-phase method is adopted to the solution [7]. A pseudo two-phase region is introduced into the supercritical region and a constant latent heat of vaporization is set artificially as the pseudo latent heat of vaporization [7]. This pseudo latent heat of vaporization determines the width of the pseudo two-phase zone [7]. The pseudo saturated liquid and pseudo saturated vapour lines are obtained by detaching the pseudocritical line. The pseudo liquid zone,

pseudo two-phase zone, and pseudo vapour zone in supercritical pressure region are connected to the liquid zone, two-phase zone, and vapour zone in subcritical pressure region smoothly [7]. In this case, all field equations of COBRA-TF can be solved in supercritical pressure region in the same way as in subcritical pressure region without any discontinuities. The width of the pseudo two-phase region or the choice of the pseudo latent heat value is the key to this whole numerical treatment [7]. From the physical point of view, the width of the pseudo two-phase region should be as small as possible to minimize property errors introduced by the pseudo two-phase zone. From the numerical feasibility point of view, a narrower pseudo two-phase zone means a sharper change in void fraction during transition through the pseudo two-phase zone, which might lead to numerical instability. The decision of the pseudo latent heat of vaporization value should be a compromise between property accuracy and feasibility and stability of the numerical treatment [7]. The value of the pseudo latent heat of vaporization adopted in this model results from a large number of test calculations.

The width of the pseudo two-phase region or the value of the pseudo latent heat (L_{pc}) is determined by the difference between the vapour saturation enthalpy ($h_{vap,sat}$) and the liquid saturation enthalpy ($h_{liq,sat}$) at pressure at the onset of the pseudo two-phase region.

$$L_{pc} = h_{vap,sat} - h_{liq,sat} \tag{4.1}$$

This ensures that the saturation curve extends to the supercritical pressure region smoothly. It is advisable to begin the pseudo two-phase region slightly below the critical point again to ensure that the saturation curve extends to the supercritical pressure region smoothly. Then the liquid and vapour saturation enthalpies at the onset of the pseudo two-phase region can be determined using the subcritical saturation

curve in COBRA-TF. After a fair amount of test calculation, the onset of the pseudo two-phase zone is set to a pressure of 3200psi or 22.063 MPa. At this pressure, the width of the pseudo two-phase region is minimized while maintaining feasibility and stability of the numerical treatment. The error introduced by the pseudo two phase method in supercritical region is mainly temperature error for keeping the fluid temperature in the pseudo two phase zone constant at the pseudo saturation temperatures, as it increases with the pressure. In the pressure range from 22.064 MPa to 30 MPa, the maximum absolute temperature error is about 2.00°C, which is negligible. Then the pseudo latent heat of vaporization at supercritical pressures is calculated to be,

$$L_{pc} = h_{vap,sat}\,(3200psi) - h_{liq,sat}\,(3200psi) = 56.11\ Btu/lbm = 130.51\ kJ/kg$$

After determining the appropriate pseudo latent heat of vaporization, the pseudo liquid and pseudo vapour saturation enthalpies can be defined as,

$$h_{liq,sat}\,(p) = h_{pc}\,(p) - \frac{L_{pc}}{2} \tag{4.2a}$$

$$h_{vap,sat}\,(p) = h_{pc}\,(p) + \frac{L_{pc}}{2} \tag{4.2b}$$

where $h_{pc}\,(p)$ is the pseudocritical enthalpy. Table 4.1 provides the pseudocritical enthalpies at different pressures. The saturation curve in COBRA-TF is defined in British units, therefore any updates to the saturation curve must also be defined in British units.

Table 4.1: Pseudocritical enthalpies

Pressure (psi)	3200.1	3335.9	3480.9	3625.9	3771	3916
Enthalpy (Btu/lbm)	905.34	913.8	918.27	926.22	932.05	936.86

The modified COBRA-TF-SC code calculates the pseudocritical enthalpy at a given pressure using a line of best fit to the data set in Table 4.1 as illustrated in Figure 4.2.

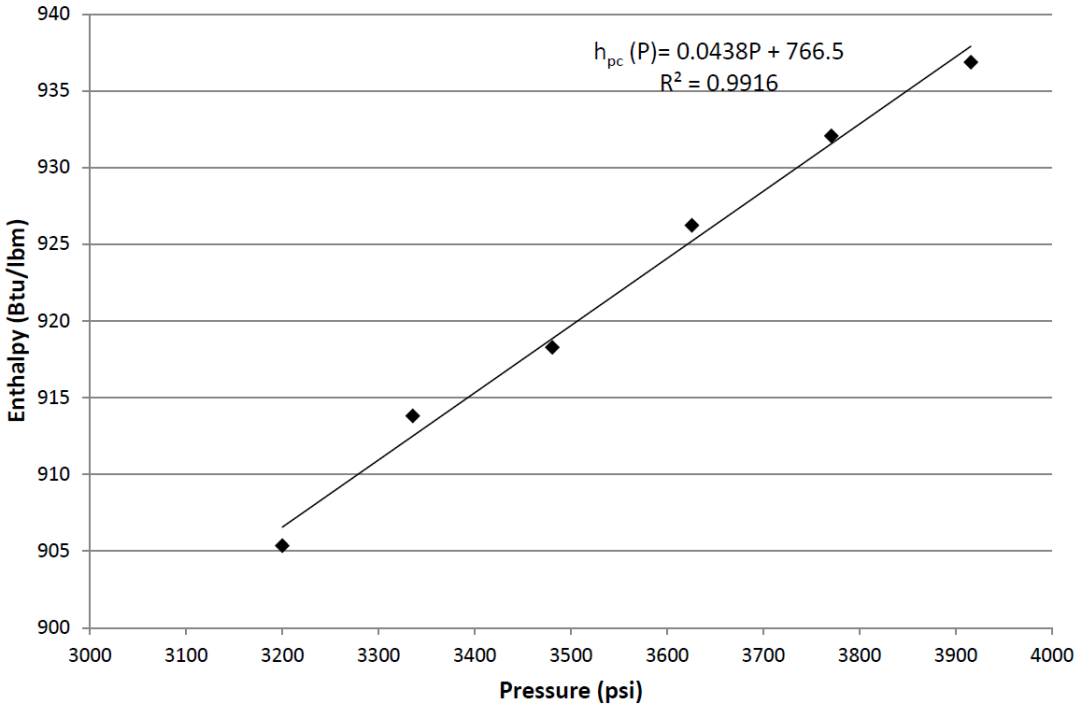

Figure 4.2: Pseudocritical enthalpy at a given pressure

After determining the pseudocritical enthalpy and the pseudo latent heat of vaporization, the saturation curve can be extended to the supercritical pressure region as illustrated in Figure 4.3.

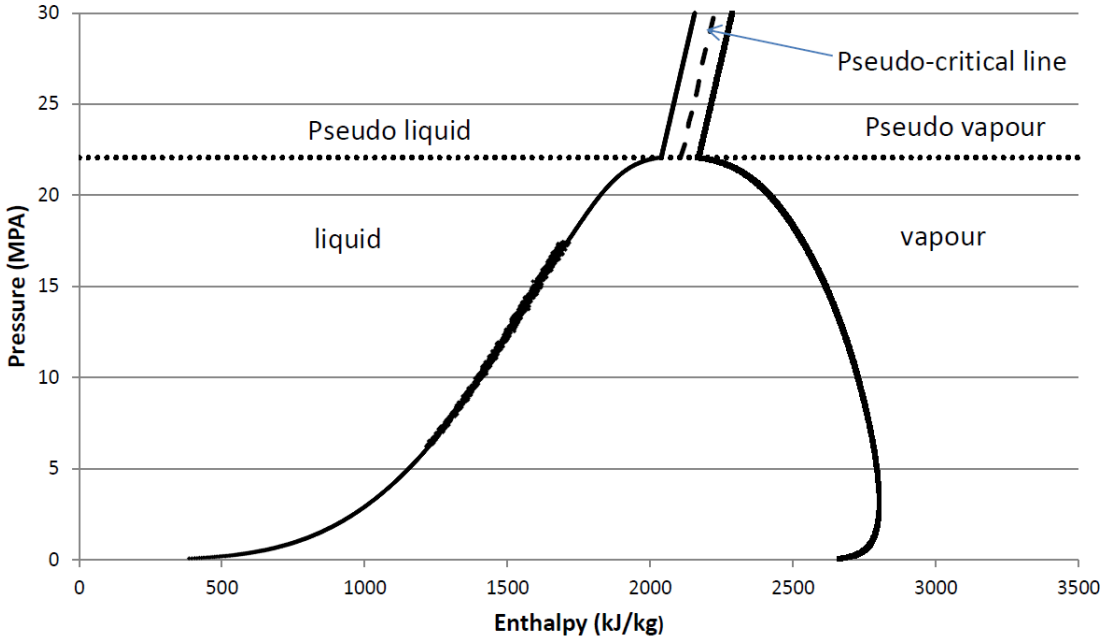

Figure 4.3: Saturation curve extended to the supercritical pressure region.

Modifications done to the SAT subroutine source code are given in Appendix C.1.

The intrinsic property table and property formulations in COBRA-TF are then updated using the IAPWS-IF97. First the IAPWS-IF97 regions in the updated saturation curve need to be identified. Figure 4.4 illustrates that there are three IAPWS-IF97 regions in the updated saturation curve.

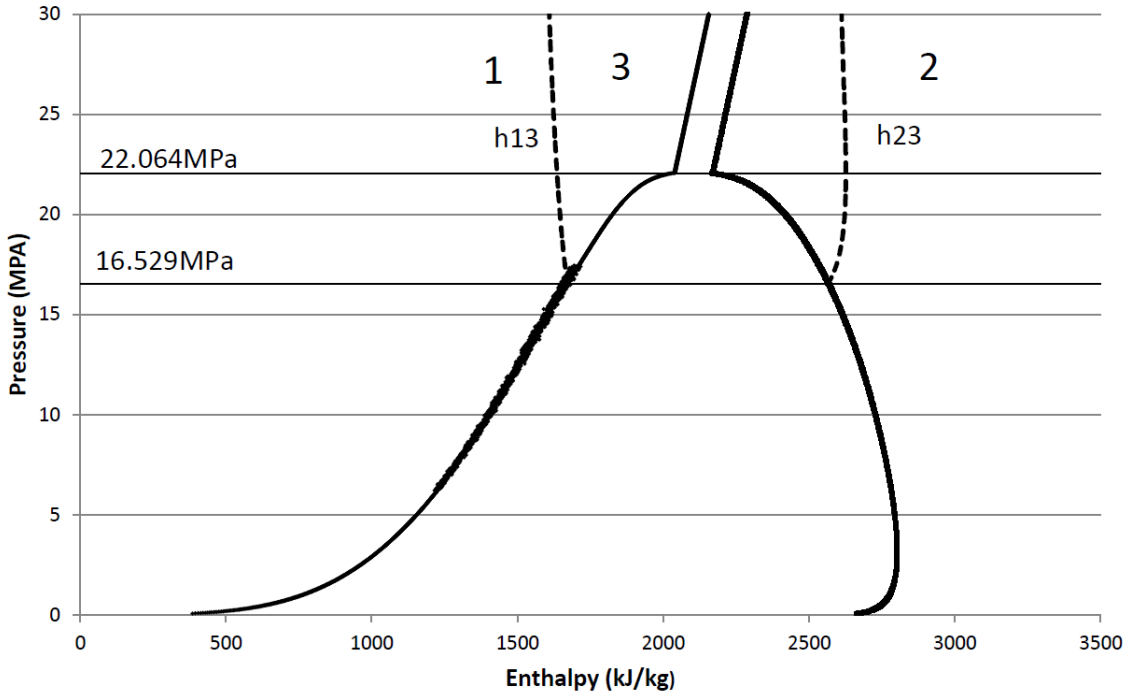

Figure 4.4: IAPWS-IF97 regions in the updated saturation curve.

The region boundaries are defined in Section 3.2. A new subroutine, named VBOUNDARY, is defined to determine all the IAPWS-IF97 region boundaries.

4.1.2 Intrinsic Property Tables

The subcritical model of COBRA-TF incorporates one intrinsic property table to determine temperature, heat capacity, thermal conductivity, and dynamic viscosity of subcooled liquid water. Figure 4.4 illustrates that subcooled liquid properties at subcritical pressures falls within IAPWS-IF97 region 1. The intrinsic property table is also used to determine all the saturated liquid and saturated vapour properties of water at subcritical pressures as well. For equilibrium, in the two phase mixture region, the liquid phase is assumed as saturated liquid and the vapour phase is assumed as

saturated vapour. The two-phase mixture is simply a mixture of saturated liquid and saturated vapour. Quality defines the proportions of the liquid and vapour phases in the two-phase mixture. Therefore, the saturated liquid and saturated vapour properties are weighted by quality to determine water properties in the two-phase region. Figure 4.5 illustrates the region at which the intrinsic property table is used to calculate water properties in COBRA-TF.

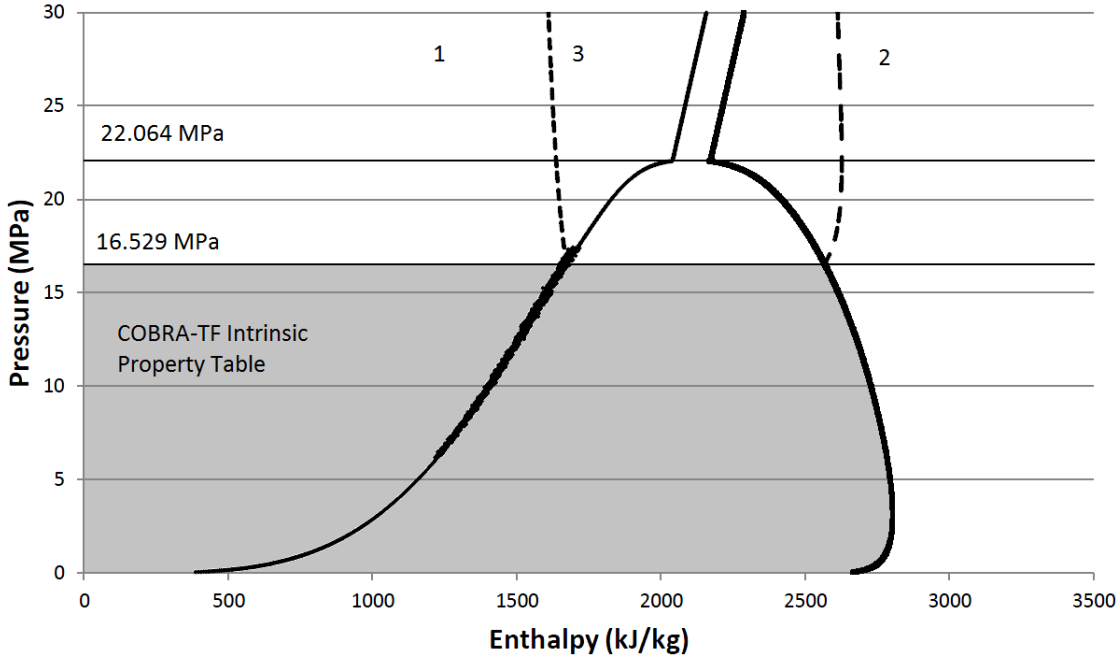

Figure 4.5: Region at which the intrinsic property table is used to calculate water properties.

It is acceptable to use just one intrinsic property table to determine subcooled liquid and saturated properties of water for subcritical flow as subcooled liquid and saturated properties of water do not change significantly with pressure at these conditions. However, water properties change significantly with pressure specially near the critical and pseudocritical points at supercritical pressures. Therefore the intrinsic property

table in COBRA-TF needs to be updated to simulate supercritical flow. This is achieved by adding 7 additional intrinsic property tables to the COBRA-TF source code. Each intrinsic property table is obtained by holding the pressure constant while varying the fluid enthalpy using the miniREFPROP software by National Institute of Standard and Technology (NIST). They are included in the SUPERCRITDATA module. Each property table is used in the IPROP subroutine to calculate subcooled liquid and saturated properties of water at the specified pressure range. The pressure at which each property table is defined and the pressure range at which each property table is used are summarized in Table 4.2.

Table 4.2: Pressure at which each property table is defined and the pressure range at which each property table is used in the modified code.

Pressure Defined (MPa)	17.0	21.9	22.1	23.0	24.0	25.0	26.0
Pressure Range (MPa)	16.5-21.0	21.0-22.0	22.0-22.5	22.5-23.5	23.5-24.5	24.5-25.5	25.5-up

The intrinsic property table in COBRA-TF is valid only up to a pressure of 16.529 MPa, the starting point of IAPWS-IF97 region 3. Above this point a new property table need to be implemented to take into account region 3 property variations. Therefore an intrinsic property table defined at 17 MPa is used to determine water properties for the pressure range 16.5-21.0 MPa. Thermophysical properties of water changes significantly near the critical (22.064 MPa and 374°C) and pseudocritical points of water. These property changes are more pronounced near the critical point of water. Therefore, a property table defined at 21.9 MPa is used to determine water properties for the pressure range 21.0-22.0 MPa and a property table defined at 22.1 MPa is used to determine water properties for the pressure range 22.0-22.5 MPa to capture this significant property changes near the critical point of water. Property tables

defined at 23.0 MPA, 24.0 MPA, 25.0 MPA, and 26.0 MPA are used to determine water properties for the pressure ranges 22.5-23.5, 23.5-24.5, 24.5-25.5,and 25.5-up respectively to capture property changes near the pseudocritical points of water. A pressure ramp named *pramp* as defined by Equation 4.3 is used to ensure smooth property transitions between intrinsic property tables.

$$pramp = \frac{p - p_{low}}{p_{rr}} \tag{4.3}$$

where p_{low} is the starting point of the pressure range of the intrinsic property table and p_{rr} is the pressure range at which the pressure ramp is applied to. p_{rr} equals to 0.5 MPa for pressure ranges 16.5-21.0 MPa, 22.5-23.5 MPa, 23.5-24.5MPa, 24.5-25.5 MPa, and 25.5-up MPa. p_{rr} equals to 0.1 MPa for pressure ranges 21.0-22.0 MPa and 22.0-22.5 MPa. Figure 4.6 illustrates the region at which the 7 additional property tables are used to calculate water properties in the modified code.

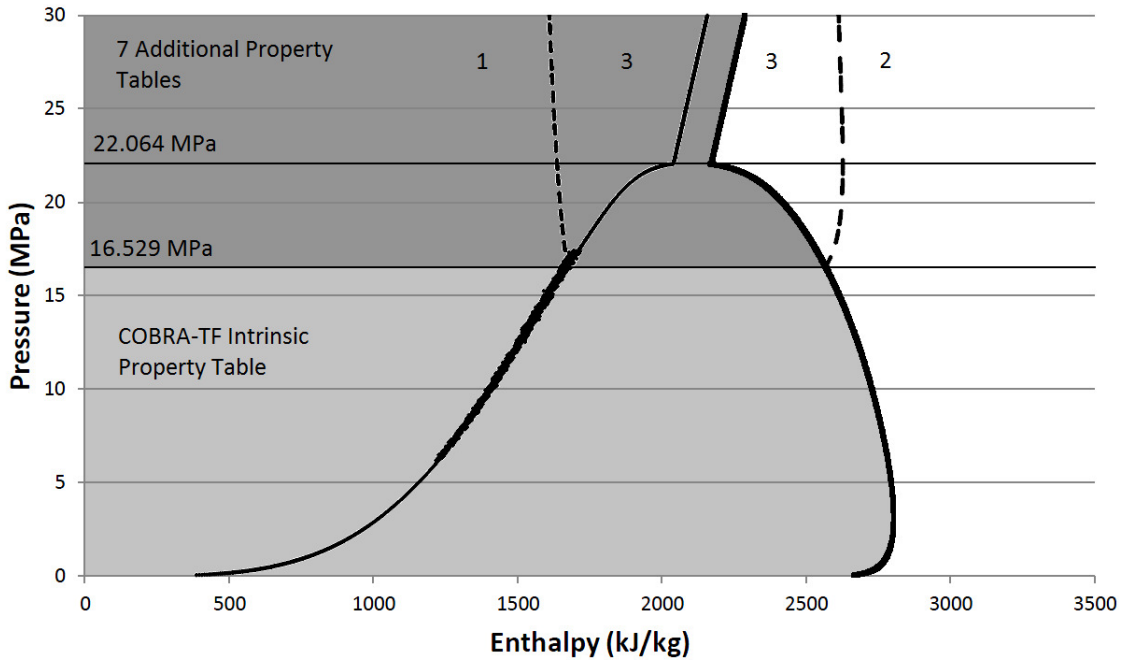

Figure 4.6: Region at which the 7 additional property tables are used to calculate water properties in the modified code.

Modifications done to the IPROP subroutine source code are given in Appendix C.2.

4.1.3 Property Formulations

TGAS subroutine

The TGAS subroutine uses the IAPWS-IF97 region 2 property formulations to determine the temperature and specific isobaric heat capacity of vapour as a function of enthalpy and pressure. This is only acceptable to determine vapour properties upto a pressure of 16.529 MPa, the starting point of IAPWS-IF97 region 3 [28]. Therefore, the IAPWS-IF97 region 3 property formulations need to be included to determine vapour properties at pressures above 16.529 MPa. The modified COBRA-TF-SC adds the IAPWS-IF97 region 3 property formulations to the TGAS subroutine. The

IAPWS-IF97 divides region 3 into two subregions 3a and 3b as illustrated in Figure 4.7.

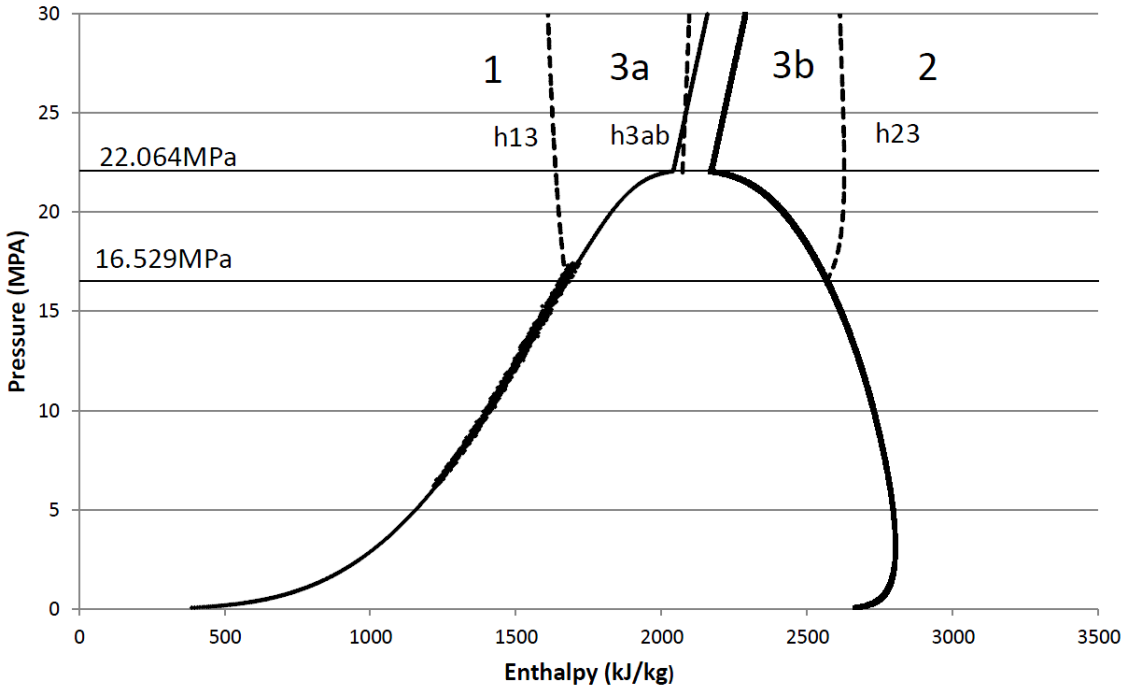

Figure 4.7: IAPWS-IF97 subregions 3a and 3b.

The boundary between subregions 3a and 3b is defined in Section 3.2 and is added to the VBOUNDARY subroutine in modified COBRA-TF-SC. The temperature of water in subregions 3a and 3b can be expressed as a function of pressure and enthalpy using the backward equations 3.46 and 3.47 given in Section 3.2.

The specific isobaric heat capacity of water in region 3 can be determined using the appropriate combinations of the basic equation for region 3 and its derivatives. The basic equation for region 3 and its derivatives can only be formulated as a function of density and temperature. Therefore, the density of water is required to calculate the specific isobaric heat capacity of water in region 3. The density of water can be

determined using the specific volume of water, which can be formulated as a function of pressure and enthalpy in subregions 3a and 3b. The specific volume of water in subregion 3a and 3b can be expressed as a function of pressure and enthalpy using the backward equations 3.44 and 3.45 in Section 3.2 respectively. Then the density of water can be determined using the relation,

$$\rho = \frac{1}{\nu} \tag{4.4}$$

After obtaining the density and temperature of water, the specific isobaric heat capacity of water in region 3 can be calculated using,

$$\frac{c_p\left(\delta,\tau\right)}{R} = -\tau^2\phi_{\tau\tau} + \frac{\left(\delta\phi_\delta - \delta\tau\phi_{\delta\tau}\right)^2}{2\delta\phi_\delta + \delta^2\phi_{\delta\delta}} \tag{4.5}$$

where $\delta = \rho/\rho^*$ and $\tau = T^*/T$ with $\rho^* = \rho_c = 322\ kg/m^3$, $T^* = T_c = 647.096$ K and $R = 0.461526\ kJ/kgK$. The coefficients n_i and exponents I_i and J_i are listed in the IAPWS-IF97 and are omitted here for conciseness.

Figures 4.8 and 4.9 illustrate the absolute percentage error in temperature and specific isobaric heat capacity of water calculated using the original TGAS subroutine and the modified TGAS subroutine at a pressure of 25 MPA. The absolute percentage error in temperature and specific isobaric heat capacity of water reduces significantly after introducing the IAPWS-IF97 region 3 property formulations to the TGAS subroutine.

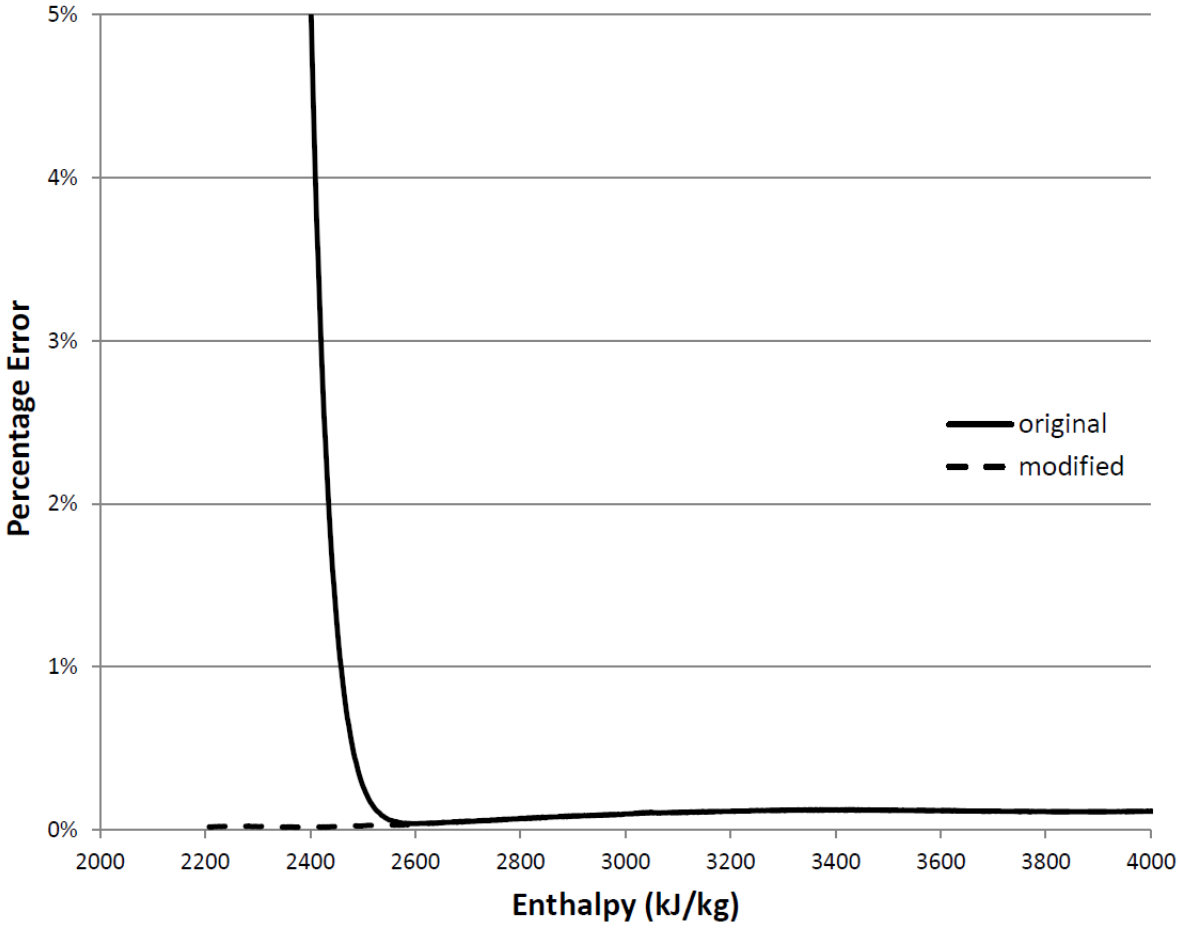

Figure 4.8: Absolute percentage error in temperature of water calculated using the original TGAS subroutine and the modified TGAS subroutine at a pressure of 25 MPA.

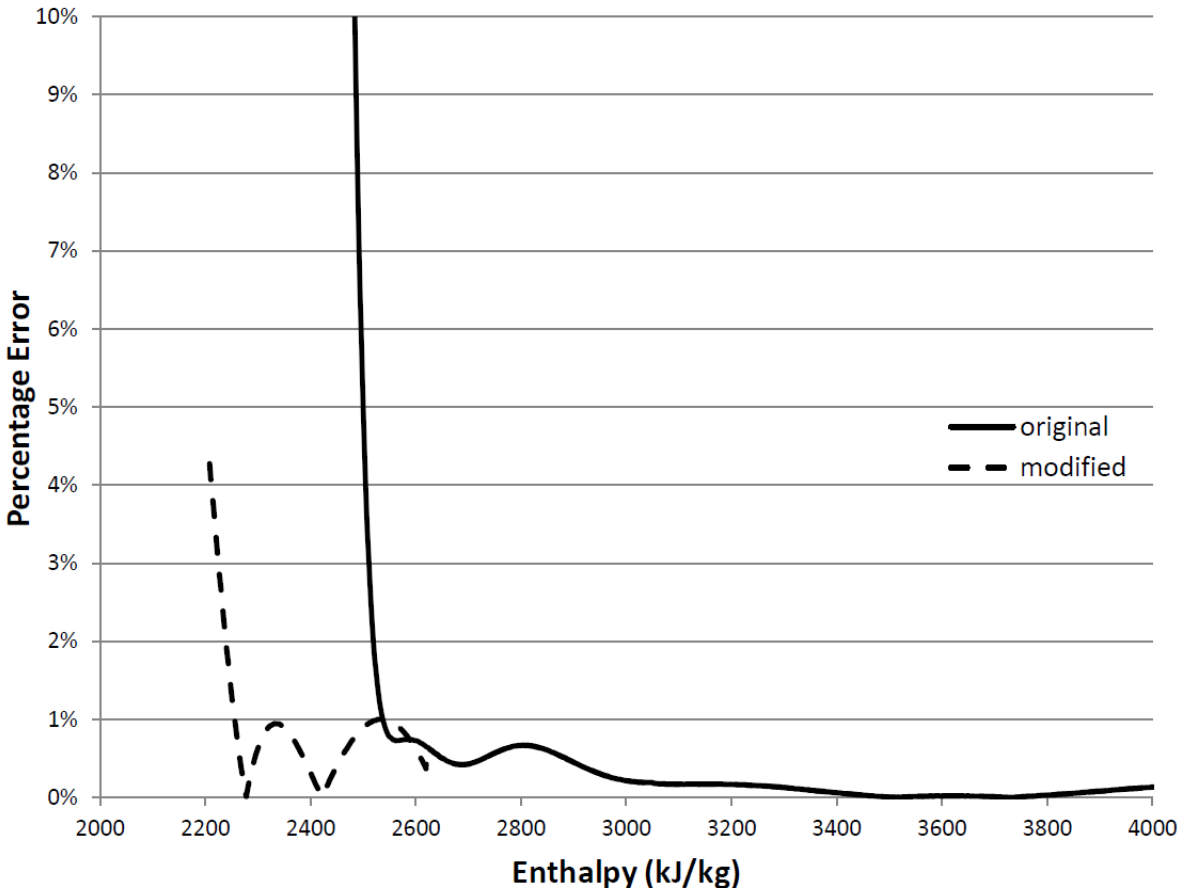

Figure 4.9: Absolute percentage error in specific isobaric heat capacity of water calculated using the original TGAS subroutine and the modified TGAS subroutine at a pressure of 25 MPA.

Modifications done to the TGAS subroutine source code are given in Appendix C.3.

TRANSP subroutine

The TRANSP subroutine calculates thermal conductivity and viscosity of superheated vapour as a function of temperature and density. Table 4.3 shows the absolute percentage error in calculated dynamic viscosity at different points in the pressure-temperature surface for water.

Table 4.3: Absolute percentage error in calculated dynamic viscosity using the TRANSP subroutine at different points in the pressure-temperature surface for water.

Pressure (MPa)	Temperature (°C)	Density ($kg \cdot m^{-}3$)	Viscosity ($Pa \cdot s$)	Viscosity calc ($Pa \cdot s$)	Percentage error
5.0	324.79	20.51	2.10E-05	2.14E-05	1.88
10.0	370.31	41.35	2.32E-05	2.47E-05	6.59
15.0	405.95	62.33	2.53E-05	2.70E-05	6.90
22.5	382.40	167.88	2.83E-05	3.15E-05	11.27
22.5	448.19	93.62	2.84E-05	3.02E-05	6.26
25.0	394.77	185.19	3.01E-05	3.30E-05	9.78
25.0	460.14	103.91	2.94E-05	3.12E-05	5.91

According to Table 4.3 the correlation used to calculate the dynamic viscosity of superheated vapour in the TRANSP subroutine is not valid at supercritical pressures. Therefore, the property formulation for dynamic viscosity is replaced with the IAPWS-IF97 transport property formulation for dynamic viscosity, which is valid for IAPWS-IF97 regions 1,2, and 3. The IAPWS-IF97 dynamic viscosity formulation is given in Equation 3.48 in Section 3.2. Table 4.4 indicates that the absolute percentage error in calculated dynamic viscosity using the modified TRANSP subroutine is acceptable at both subcritical and supercritical pressures.

Table 4.4: Absolute percentage error in calculated dynamic viscosity using the modified TRANSP subroutine at different points in the pressure-temperature surface for water.

Pressure (MPa)	Temperature (°C)	Density ($kg \cdot m^{-}3$)	Viscosity ($Pa \cdot s$)	Viscosity calc ($Pa \cdot s$)	Percentage error
5.0	324.79	20.51	2.10E-05	2.10E-05	0.02
10.0	370.31	41.35	2.32E-05	2.32E-05	0.02
15.0	405.95	62.33	2.53E-05	2.53E-05	0.02
22.5	382.40	167.88	2.83E-05	2.83E-05	0.01
22.5	448.19	93.62	2.84E-05	2.84E-05	0.02
25.0	394.77	185.19	3.01E-05	3.01E-05	0.01
25.0	460.14	103.91	2.94E-05	2.94E-05	0.02

Table 4.5 indicates the absolute percentage error in calculated thermal conductivity using the TRANSP subroutine at different points in the pressure-temperature surface for water. The absolute percentage error in thermal conductivity is not very significant; therefore the correlation used to calculate the thermal conductivity of superheated vapour in the TRANSP subroutine is not altered.

Table 4.5: Absolute percentage error in calculated thermal conductivities using the TRANSP subroutine at different points in the pressure-temperature surface for water.

Pressure (MPa)	Temperature (°C)	Density ($kg \cdot m^{-}3$)	Thermal conductivity ($W/(m \cdot K)$)	Thermal conduc. calc. ($W/(m \cdot K)$)	Percentage error
5.0	324.79	20.51	5.46E-02	5.35E-02	0.02
10.0	370.31	41.35	6.74E-02	6.78E-02	0.01
15.0	405.95	62.33	8.01E-02	8.16E-02	0.02
22.5	382.40	167.88	1.86E-01	1.83E-01	0.02
22.5	448.19	93.62	9.93E-02	1.01E-01	0.02
25.0	394.77	185.19	1.93E-01	1.95E-01	0.01
25.0	460.14	103.91	1.06E-01	1.08E-01	0.02

Modifications done to the TRANSP subroutine source code are given in Appendix C.4.

VOLLIQ subroutine

The specific volume of liquid water is calculated using a simplified version of the IAPWS-IF97 region 1 specific volume property formulation in the VOLLIQ subroutine. This simplified equation does not work well at supercritical pressures. Therefore the simplified specific volume property formulation is replaced with the original IAPWS-IF97 region 1 specific volume property formulation. The original IAPWS-IF97 region 1 specific volume property formulation can be expressed using the appropriate combination of the basic equation for region 1 and its derivatives. The basic equation for region 1 and its derivatives are expressed as a function of pressure and temperature. The VOLLIQ subroutine takes pressure and enthalpy as inputs to determine the specific volume of water. First the temperature of water is calculated as a function of pressure and enthalpy using the backward equation 3.38 in Section 3.2. After determining the temperature, the specific volume can be calculated as a function of pressure and temperature using,

$$\nu(\pi,\tau) = \left(\frac{\partial g}{\partial p}\right)_T = \frac{RT}{p}\pi\gamma_\pi \tag{4.6}$$

The IAPWS-IF97 subregion 3a must also be taken into account for pressures above 16.529 MPa, the starting point of region 3. The IAPWS-IF97 subregion 3a specific volume property formulation is added to the modified VOLLIQ subroutine. The specific volume of water in subregion 3a can be expressed as a function of pressure and enthalpy using the backward equation given in Equation 3.44. The absolute percentage error in specific volume of water calculated using the original and modified VOLLIQ subroutines at a pressure of 25 MPa is illustrated in Figure 4.10. The

absolute percentage error in specific volume of water decreases in both IAPWS-IF97 region 1 and subregion 3a after modifying the VOLLIQ subroutine.

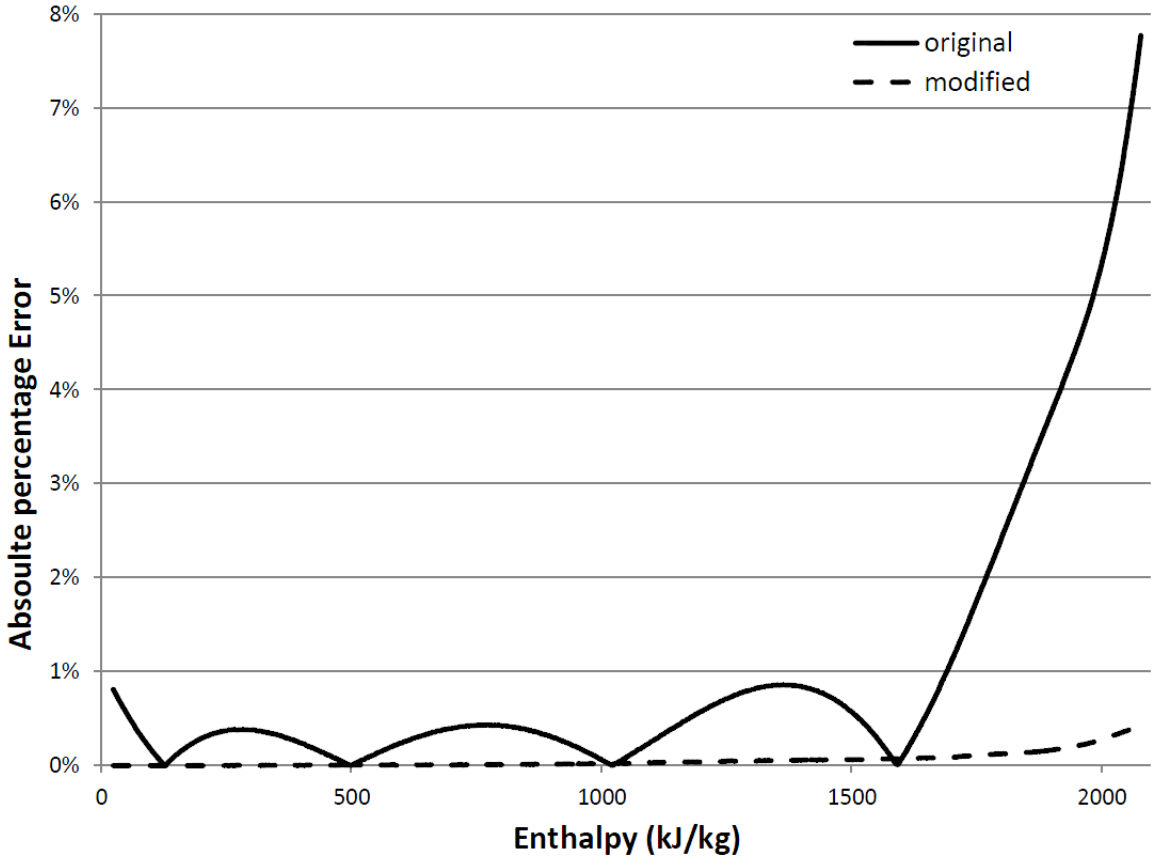

Figure 4.10: Absolute percentage error in specific volume of water calculated using the original and the modified VOLLIQ subroutine at a pressure of 25 MPA.

Modifications done to the VOLLIQ subroutine source code are given in Appendix C.5.

XTRA1 subroutine

After updating the liquid specific volume property formulation , the partial derivatives of this formulation need to be updated. The XTRA1 subroutine calculates the partial derivative of specific volume of liquid water with respect to pressure. The partial

derivative of simplified specific volume property formulation is replaced with the partial derivative of IAPWS-IF97 region 1 specific volume property formulation. The partial derivative of specific volume with respect to pressure can be defined as,

$$\left(\frac{\partial \nu}{\partial p}\right)_T = -\nu\kappa_T \tag{4.7}$$

For IAPWS-IF97 region 1, the specific volume, ν, is calculated using Equation 4.6 and the isothermal conductivity, κ_T, is calculated using the appropriate combination of the basic equation for region 1 and its derivatives.

$$\kappa_T(\pi,\tau) = \frac{1}{p}\frac{1-\pi^2\gamma^r_{\pi\pi}}{1+\pi\gamma^r_{\pi}} \tag{4.8}$$

The partial derivative of specific volume with respect to pressure in IAPWS-97 region 3 is added to the XTRA1 subroutine. The partial derivative of specific volume with respect to pressure in region 3 is determined using Equation 4.7, where ν is calculated using the VOLLIQ subroutine and κ_T is calculated using the appropriate combination of the basic equation for region 3 and its derivatives.

$$\kappa_T(\delta,\tau) = \frac{1}{\rho RT}\frac{1}{2\delta\phi_\delta + \delta^2\phi_{\delta\delta}} \tag{4.9}$$

Modifications done to the XTRA1 subroutine source code are given in Appendix C.7.

DVDHL subroutine

The DVDHL subroutine calculates the partial derivative of specific volume of liquid water with respect to enthalpy. The partial derivative of specific volume with respect

to enthalpy in subregion 3a is added to the DVDHL subroutine. This is obtained by differentiating the backward equation for specific volume for subregion 3a with respect to enthalpy.

$$\left(\frac{\partial \nu_{3a}}{\partial h}\right)_p = \nu^* \sum_{i=1}^{32} n_i \left(\pi + 0.128\right)^{I_i} \frac{J_i}{h^*} \left(\eta - 0.727\right)^{J_i - 1} \tag{4.10}$$

Modifications done to the DVDHL subroutine source code are given in Appendix C.9.

VOLVAP subroutine

The specific volume of vapour is calculated using a simplified version of the IAPWS-IF97 region 2 specific volume property formulation in the VOLVAP subroutine. This simplified equation does not work well at supercritical pressures. The simplified specific volume property formulation is replaced with the IAPWS-IF97 region 2 specific volume property formulation. The IAPWS-IF97 region 2 specific volume property formulation can be expressed using the appropriate combination of the basic equation for region 2 and its derivatives. The basic equation for region 2 and its derivatives are expressed as a function of pressure and temperature. The VOLVAP subroutine takes pressure and enthalpy as inputs to calculate the specific volume of vapour; therefore the water temperature for region 2 need to be calculated to determine the specific volume of vapour for region 2. The water temperature for region 2 is calculated using the TGAS subroutine, which takes pressure and enthalpy as inputs. After determining the water temperature, the specific volume of water for region 2 can be expressed as a function of pressure and temperature using,

$$\nu\left(\pi, \tau\right) = \left(\frac{\partial g}{\partial p}\right)_T = \frac{RT}{p} \pi \left(\gamma_\pi^0 + \gamma_\pi^r\right) \tag{4.11}$$

The IAPWS-IF97 subregion 3b must also be taken into account for pressures above 16.529 MPa, the starting point of region 3. The IAPWS-IF97 subregion 3b specific volume property formulation is added to the modified VOLVAP subroutine. The specific volume of water in subregion 3b can be expressed as a function of pressure and enthalpy using the backward equation given in Equation 3.45. The absolute percentage error in specific volume of water calculated using the original and modified VOLVAP subroutines at a pressure of 25 MPa is illustrated in Figure 4.11. The absolute percentage error in specific volume of water decreases in both IAPWS-IF97 region 2 and subregion 3b after modifying the VOLVAP subroutine.

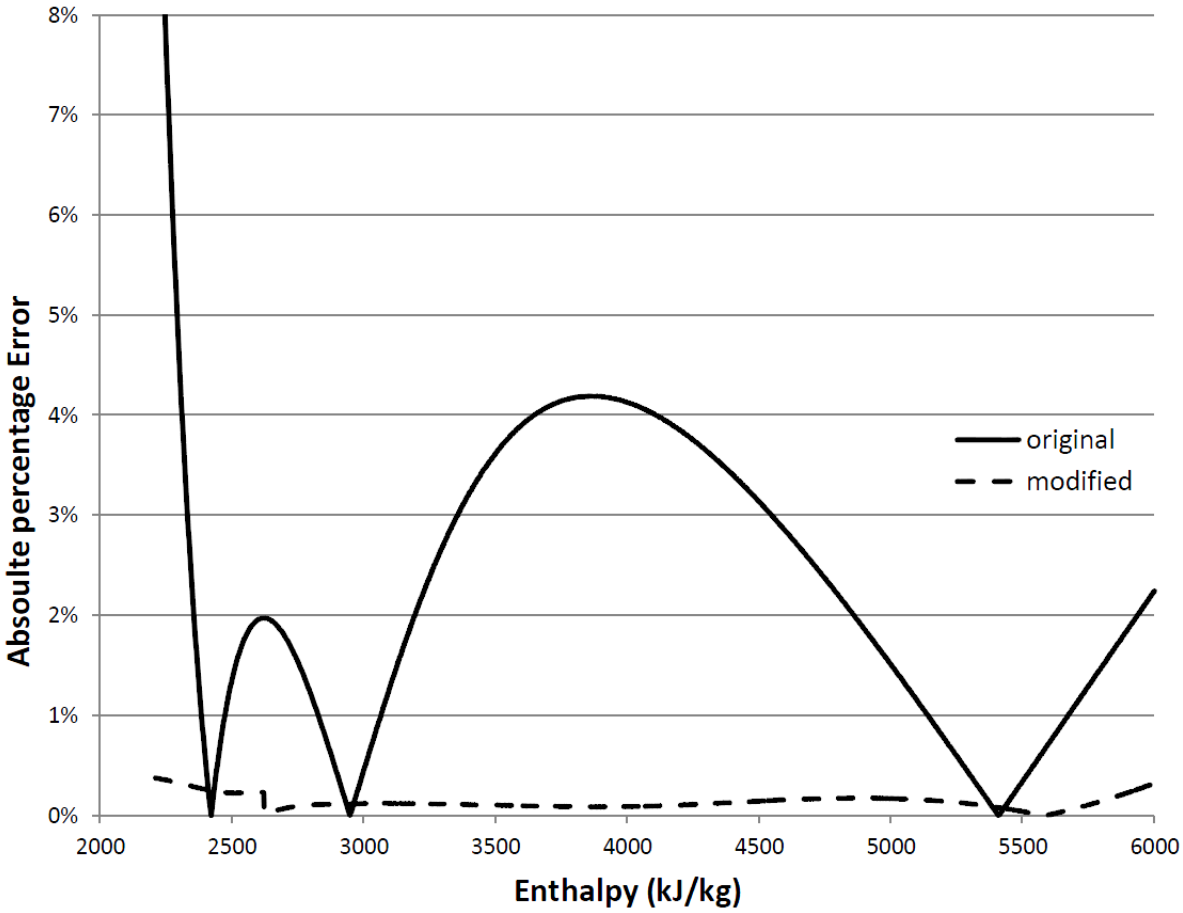

Figure 4.11: Absolute percentage error in specific volume of water calculated using the original and the modified VOLVAP subroutine at a pressure of 25 MPA.

Modifications done to the VOLVAP subroutine source code are given in Appendix C.6.

DVDPV subroutine

After updating the vapour specific volume property formulation , the partial derivatives of this formulation need to be updated. The DVDPV subroutine calculates the partial derivative of specific volume of vapour with respect to pressure. The partial derivative

of simplified specific volume property formulation is replaced with the partial derivative of IAPWS-IF97 region 2 specific volume property formulation. The partial derivative of specific volume with respect to pressure in region 2 is determined using Equation 4.7, where ν is calculated using Equation 4.11 and κ_T is calculated using the appropriate combination of the basic equation for region 2 and its derivatives.

$$\kappa_T(\pi,\tau) = \frac{1}{p}\frac{1-\pi^2\gamma^r_{\pi\pi}}{1+\pi\gamma^r_{\pi}} \tag{4.12}$$

The partial derivative of specific volume of water with respect to pressure in region 3 is added to the DVDPV subroutine. The partial derivative of specific volume with respect to pressure in region 3 is determined using Equation 4.7, where ν is calculated using the VOLVAP subroutine and κ_T is calculated using Equation 4.9. Modifications done to the DVDPV subroutine source code are given in Appendix C.8.

DVDHV subroutine

The DVDHV subroutine calculates the partial derivative of specific volume of vapour with respect to enthalpy. The partial derivative of specific volume with respect to enthalpy in IAPWS-97 subregion 3b is added to the DVDHV subroutine. This is obtained by differentiating the backward equation for specific volume for subregion 3b with respect to enthalpy.

$$\left(\frac{\partial\nu_{3b}}{\partial h}\right)_p = \nu^* \sum_{i=1}^{30} n_i \left(\pi + 0.0661\right)^{I_i} \frac{J_i}{h^*} \left(\eta - 0.0.720\right)^{J_i - 1} \tag{4.13}$$

Modifications done to the DVDHV subroutine source code are given in Appendix C.10.

4.2 Wall Shear Loss

The frictional pressure loss behaviour of supercritical water shows great abnormality due to steep property variations specially near the critical and pseudocritical points. The frictional resistance coefficients used in INTFR subroutine to calculate the frictional pressure loss is only valid at subcritical pressures. Therefore, it is necessary to update these frictional resistance coefficients to determine the frictional pressure loss at supercritical pressures.

The modified COBRA-TF-SC uses two separate frictional resistance correlations to determine the frictional resistance coefficients of subcritical water and supercritical water. The frictional resistance coefficients of subcritical water is determined using the correlations provided in COBRA-TF (Section 3.1.4). The frictional resistant coefficients of supercritical water is determined using the Kirillov et al. (1990) correlation.

$$\left(\frac{\xi}{\xi_{iso}}\right)_{fr} = \left(\frac{\rho_w}{\rho_b}\right)^{0.4} \tag{4.14}$$

where ξ_{iso} is calculated using Equation,

$$\xi_{iso} = \frac{1}{\left(1.82 + \log Re_b - 1.64\right)^2} \tag{4.15}$$

The Kirillov et al. correlation is added to the INTFR subroutine. The water density at a given wall temperature ρ_w in Equation 4.14 is determined using the WALLTEMPPROP subroutine. This new subroutine is added to COBRA-TF-SC to calculate water density and specific heat capacity at a given pressure and wall temperature. The modified INTFR subroutine calculates the vapour frictional resistance

coefficient fv and liquid frictional resistance coefficient fl using,

$$fv = sramp * fvsub + (1 - sramp) * fvsup \tag{4.16a}$$

$$fl = sramp * flsub + (1 - sramp) * flsup \tag{4.16b}$$

where $fvsub$ and $flsub$ are vapour and liquid subcritical pressure friction factors and $fvsup$ and $flsup$ are pseudo vapour and pseudo liquid supercritical pressure friction factors. A pressure ramp, $sramp$, is used to ensure that the transition between subcritical pressure and supercritical pressure friction factor correlations is smooth. This pressure ramp is calculated in the newly added SUPERCRITRAMP subroutine. The SUPERCRITRAMP subroutine takes pressure (in psi) as the input and calculates the ramping factor using the expression,

$$sramp = max \begin{cases} 0.0 \\ min \begin{cases} \frac{3300-p}{100} \\ 1.0 \end{cases} \end{cases} \tag{4.17}$$

This ramping factor goes to zero if the pressure is greater than 3300 psi (22.752 MPa) and goes to unity if the pressure is less than 3200 psi (22.063 MPa). If the pressure is greater than 3300 psi (22.752 MPa) only the supercritical pressure friction factor correlations are used to calculate friction factors. If the the pressure is less than 3200 psi (22.063 MPa) only the subcritical pressure friction factor correlations are used to calculate friction factors. Modifications done to the INTFR subroutine source code are given in Appendix C.11.

4.3 Wall Heat Transfer

4.3.1 Heat Transfer Regime

Above the critical pressure water behaves as a single phase fluid and no boiling and condensation is experienced. The only heat transfer mechanism of supercritical flow is single phase convection. It is necessary to understand the heat transfer regimes of subcritical flow to avoid numerical problems during the transition to supercritical flow.

There are two basic heat transfer zones at subcritical pressures; pre-CHF and post-CHF. The pre-CHF heat transfer zone is selected when the wall temperature is below the critical heat flux temperature. The post-CHF heat transfer zone is selected when the wall temperature is above the critical heat flux temperature. There is also a transition zone between the pre-CHF and post-CHF heat transfer zones when the wall temperature is above the critical heat flux temperature but below the minimum film boiling temperature. The single-phase vapour convection heat transfer regime occurs when the void fraction is greater than 0.999 regardless of the heated wall temperature.

There is no critical heat flux above the critical pressure. In the modified BOILING subroutine a large value is assigned to the critical heat flux at supercritical pressures. Then the wall temperature will not reach the critical heat flux temperature and the only prevailing heat transfer regimes for supercritical flow will be pre-CHF heat transfer regimes and single phase vapour convection heat transfer regime. The critical heat flux for subcritical flow , *qchsub*, is calculated using one of the provided CHF correlations in COBRA-TF. The critical heat flux for supercritical flow , *qchsup*, is assigned a large value as shown in Equation 4.18. This large value is chosen arbitrarily

to be large enough so that the wall temperature will not reach the critical heat flux temperature during supercritical flow simulations.

$$qchfsub = \begin{cases} 1 \times 10^{09} \ \frac{BTU}{h \cdot ft^2} \\ \text{COBRA-TF standard correlation} \\ \text{W-3 model} \end{cases} \tag{4.18a}$$

$$qchfsup = 1 \times 10^{20} \ \frac{BTU}{h \cdot ft^2} \tag{4.18b}$$

A pressure ramp, *sramp*, is included to make sure the transition between subcritical flow and supercritical flow critical heat flux correlations is smooth.

$$qchf = sramp * qchfsub + (1 - sramp) * qchfsup \tag{4.19}$$

This pressure ramp is calculated using the SUPERCRITRAMP subroutine and is provided in Equation 4.17 above. The critical heat flux temperature is then calculated iteratively using the calculated critical heat flux. The code has a minimum and a maximum boundary for critical heat flux temperature. The minimum boundary is set at $20°F$ over the liquid saturation temperature and the maximum boundary is set at $200°F$ over the liquid saturation temperature or at $805.3°F$ (702.76 K). The code checks if the calculated CHF exceeds either of the two boundaries. If the calculated CHF does exceed either of the two boundaries, the CHF and the CHF temperature are set to the boundary that is exceeded. In this case, the CHF temperature will be set at $200°F$ over the liquid saturation temperature or at 805.3° (702.76 K) even with a significantly large critical heat flux at supercritical pressures. Therefore, a large value

must also be assigned to the maximum boundary of CHF temperature to ensure that the wall temperature will not reach the calculated CHF temperature. The maximum boundary for CHF temperature for subcritical flow, *tcmaxsub*, is calculated using the correlation given in the BOILING subroutine. The maximum boundary for CHF temperature for supercritical flow, *tcmaxsup*, is assigned a large value as above. This value has to be large enough so that the wall temperature will not reach this value during supercritical flow simulations.

$$tcmaxsub = min \begin{cases} tf + 200°F \\ 805.3°F \end{cases} \tag{4.20a}$$

$$tcmaxsup = 5000°F \tag{4.20b}$$

A pressure ramp, *sramp*, is included to make sure that the transition between subcritical flow and supercritical flow CHF temperatures is smooth.

$$tcmax = sramp * tcmaxsub + (1 - sramp) * tcmaxsup \tag{4.21}$$

Modifications done to the BOILING subroutine source code are given in Appendix C.12.

Supercritical water behaves as a single phase fluid and no boiling is experienced. Total heat transfer of subcooled nucleate boiling and saturated nucleate boiling heat transfer regimes is calculated as a sum of the forced convection heat transfer to liquid and the nucleate boiling heat transfer. In modified COBRA-TF-SC the nucleate boiling heat transfer term is set to zero for supercritical flow because evaporation heat does not exist at supercritical pressures. The nucleate boiling heat transfer

term can be neglected by removing the nucleate boiling heat transfer coefficient at supercritical pressures. The HCOOL subroutine calculates the nucleate boiling heat transfer coefficient when the wall temperature is $0.1°F$ above the liquid saturation temperature. In modified COBRA-TF-SC the wall temperature limit to calculate the nucleate boiling heat transfer coefficient is updated so that the wall temperature will not reach this value during supercritical flow simulations. Therefore, the nucleate boiling heat transfer coefficient will not be calculated for supercritical flow resulting in only the forced convection heat transfer term to determine the total heat transfer of subcooled nucleate boiling and saturated nucleate boiling heat transfer regimes at supercritical pressures. The wall temperature limit to calculate the nucleate boiling heat transfer coefficient at subcritical pressures, $tflimitsub$, is set to $0.1°F$ above the liquid saturation temperature and the wall temperature limit to calculate the nucleate boiling heat transfer coefficient at supercritical pressures, $tflimitsup$, is set to a large value.

$$tflimitsub = tf + 0.1°F \tag{4.22a}$$

$$tflimitsup = 5000°F \tag{4.22b}$$

A pressure ramp, $sramp$, is included to make sure that the transition between subcritical flow and supercritical flow wall heat transfer models is smooth.

$$tflimit = sramp * tflimitsub + (1 - sramp) * tflimitsup \tag{4.23}$$

After removing the nucleate boiling heat transfer term, the wall heat transfer for supercritical flow will be single phase liquid convection for pseudo void fractions less

than 0.999 and single phase vapour convection for pseudo void fractions greater than 0.999.

After all the modifications, there are three heat transfer zones at supercritical pressures. If the pseudo void fraction is zero only the single phase liquid convection heat transfer coefficient is used to calculate wall heat transfer. This will be the single phase liquid convection heat transfer zone. If the void fraction is unity only the single phase vapour convection heat transfer coefficient is used to calculate wall heat transfer. This will be the single phase vapour convection heat transfer zone. For supercritical flow, the single phase liquid convection and single phase vapour convection heat transfer coefficients are calculated using the same supercritical water heat transfer coefficient correlation. If the pseudo void fraction is between zero and unity a void fraction ramp between single phase liquid and single phase vapour convection heat transfer coefficients is used to calculate wall heat transfer. This will be the transition zone between single phase liquid and single phase vapour convection heat transfer. The transition zone is introduced to make sure that the transition between single phase liquid and single phase vapour convection heat transfer zones is smooth. Supercritical water behaves as a single phase fluid. Both single phase liquid and single phase vapour convection heat transfer zones are used at supercritical pressure due to the pseudo two-phase scheme used to extend the saturation curve. The single phase liquid *htclsup* and single phase vapour *htcvsup* convection heat transfer coefficients in the transition zone is calculated using,

$$htclsup = (1 - \alpha) * hspl \tag{4.24a}$$

$$htcvsup = \alpha * hspv \tag{4.24b}$$

where *hspl* and *hspv* are single phase liquid and single phase vapour convection heat transfer coefficients. In subcritical flow, the transition between single phase liquid convection *htclsub* and single phase vapour convection *htcvsub* heat transfer coefficients is achieved using a liquid heat flux ramp *xliq*.

$$htclsub = hspl \tag{4.25a}$$

$$htcvsub = (1 - xliq) * hspv \tag{4.25b}$$

where

$$xliq = max \begin{cases} 0.0 \\ \frac{0.9999-\alpha}{0.0009} \end{cases} \tag{4.26}$$

A pressure ramp is used to make sure that the transition between subcritical flow and supercritical flow heat transfer coefficients is smooth.

$$htcl = sramp * htclsub + (1 - sramp) * htclsup \tag{4.27a}$$

$$htcv = sramp * htcvsub + (1 - sramp) * htcvsup \tag{4.27b}$$

Modifications done to the HCOOL subroutine source code are given in Appendix C.13.

4.3.2 Heat Transfer Coefficients

As indicated in Section 2.1.1, a large variation in thermophysical properties occur near the critical and pseudocritical points. This would lead to a strong variation in heat transfer coefficients. There is only single phase liquid convection and single phase

vapour convection heat transfer at supercritical pressures. Therefore, the only heat transfer coefficients to consider are the single phase liquid and single phase vapour convection heat transfer coefficients.

In COBRA-TF the single phase liquid convection and single phase vapour convection heat transfer coefficients are calculated in the BOILING subroutine. The single phase liquid convection heat transfer coefficient for laminar flow is calculated using a model recommended by Sparrow et al. [22].

$$h_{wl,lam} = 7.86\frac{k_l}{D_h} \tag{4.28}$$

The single phase liquid convection heat transfer coefficient for turbulent flow is calculated using the Dittus-Boelter correlation [5].

$$h_{wl,DB} = 0.023\frac{k_l}{D_h}Re^{0.8}Pr^n \tag{4.29}$$

where exponent n is 0.4 for heating and 0.3 for cooling [5]. The single phase vapour convection heat transfer coefficient is determined using the Dittus-Boelter correlation, the Wong and Hochreiter correlation for turbulent forced convection, and a constant Nusselt number value for laminar forced convection [1]. The simplest model to determine the single phase vapour convection heat transfer coefficient is obtained by assuming a constant Nusselt number[1]. This model is applicable to only laminar flows.

$$h_{wv,lam} = 10\frac{k_v}{D_h} \tag{4.30}$$

The Dittus-Boelter correlation provided in Equation 4.29 is used with vapour properties instead of liquid properties. The Wong and Hochreiter correlation can be expressed

as [1],

$$h_{wv,WH} = 0.07907 \frac{k_v}{D_h} Re^{0.6774} Pr^{0.333} \tag{4.31}$$

COBRA-TF utilizes the maximum of the three correlations to determine the single phase vapour convection heat transfer coefficient to make sure that the transition between the heat transfer coefficients calculated by the three models is smooth [1].

$$h_{wv} = max \begin{cases} h_{wv,lam} \\ h_{wv,DB} \\ h_{wv,WH} \end{cases} \tag{4.32}$$

It was agreed in the open literature that the actual heat transfer coefficient deviates from the values calculated using the Dittus-Bolter correlation at supercritical pressures specially near the critical and pseudocritical points. The actual heat transfer coefficient is higher than the values predicted by the Dittus-Boelter correlation at low heat fluxes. The Dittus-Boelter correlation fails to capture the heat transfer enhancement effect at low heat fluxes. The actual heat transfer coefficient is lower than the values predicted by the Dittus-Boelter correlation at high heat fluxes. The Dittus-Boelter correlation fails to capture the heat transfer deterioration effect at high heat fluxes.

Several heat transfer correlations have been developed for various geometries and flow conditions for supercritical water heat transfer. Some of these correlations are given in Section 2.1.2. Currently, there is only one supercritical water heat transfer correlation for fuel bundles, developed by Dydyakin and Popov (1977). This correlation was obtained in a 7-element helically finned bundle. The heat transfer correlations for bundles are usually quite sensitive to a particular bundle design [18]. Therefore, this

correlation cannot be used for predicting heat transfer in other bundle geometries. In order to overcome this problem, heat transfer correlations based on bare tube data can be used as a conservative approach. The conservative approach is based on the fact that heat transfer coefficients in bare tubes are generally lower than those in bundle geometries [18]. The heat transfer is enhanced with appendages in bundle geometries [18]. The bare-tube supercritical water heat transfer correlation chosen for this study is the Mokry et al. (2009) correlation. Table 2.5 indicates that Mokry et al. correlation showed the best prediction for the experimental data within all three sub-regions of supercritical flow investigated. The Mokry et al. (2009) correlation is given as,

$$Nu_b = 0.0061 Re_b^{0.904} \bar{Pr}_b^{0.684} \left(\frac{\rho_w}{\rho_b}\right)^{0.564} \tag{4.33}$$

The Mokry et al. correlation is added to the BOILING subroutine to calculate the single phase liquid convection and single phase vapour convection heat transfer coefficients at supercritical pressures.

A pressure ramp is used to make sure that the transition between subcritical flow and supercritical flow heat transfer coefficients is smooth

$$spvl = sramp * spvlsub + (1 - sramp) * spvlsup \tag{4.34a}$$

$$spvn = sramp * spvnsub + (1 - sramp) * spvnsup \tag{4.34b}$$

where *spvlsub* and *spvlsup* are subcritical and supercritical flow single phase liquid convection heat transfer coefficients and *spvnsub* and *spvnsup* are subcritical and supercritical flow single phase vapour convection heat transfer coefficients. Modifications done to the BOILING subroutine source code are given in Appendix C.12.

4.4 Turbulent Mixing and Void Drift

Supercritical water behaves as a single phase fluid. Therefore, the pseudo void fraction has to be either zero or unity and there is no void drift at supercritical pressures. The void drift mixing model of COBRA-TF is therefore disabled for supercritical flow simulations. The void drift model is turned off by setting the equilibrium distribution weighing factor K_M in void drift model (variable AAAK in Group 12) to zero.

Satisfactory turbulent mixing models have not yet been developed for supercritical flow. Therefore, the existing turbulent mixing model of COBRA-TF is used for supercritical flow simulations.

Chapter 5

Results

This section outlines the code assessment and the thermalhydraulics analysis of the 62-element Canadian SCWR fuel bundle. Code assessment is performed by comparing to the experimental data and other numerical results. The results of the thermalhydraulics analysis of the 62-element Canadian SCWR fuel bundle are presented along with a sensitivity analysis.

5.1 Code Assessment

Data for the validation of the code are obtained from the experimental studies on heat transfer to supercritical water flowing upward in a seven-rod test bundle carried out by the Japanese Atomic Energy Agency (JAEA) [17]. The cross sectional configuration of the seven-rod test bundle is illustrated in Figure 5.1.

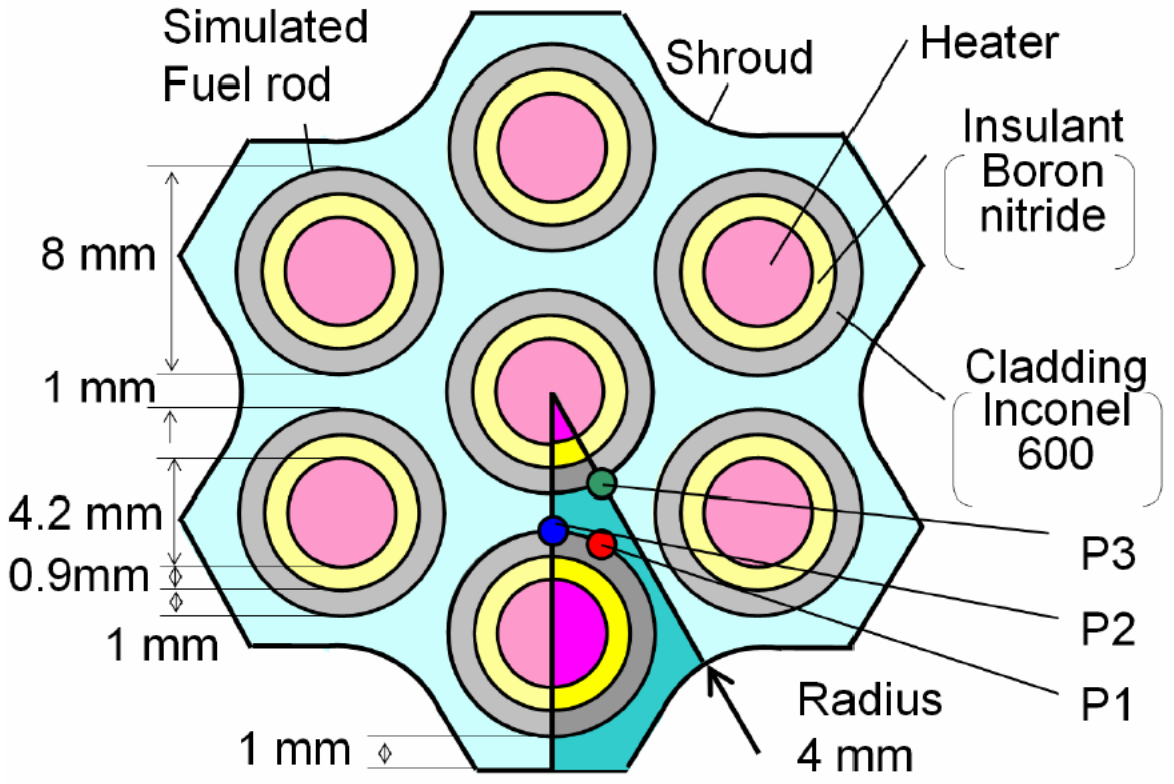

Figure 5.1: Cross-sectional configuration of the test section (Misawa 2009).

The simulated fuel rods are 8 mm in diameter and are arranged in a hexagonal array. The heated length of the test section is 1500 mm. The simulated fuel rods are heated uniformly in the axial direction by indirect-type electrical heat. The rod surface temperatures of each simulated fuel rod are measured with six sheathed thermocouples which are embedded into U-groove at the surface of the rod. The thermocouples are installed on surfaces which face to the center of subchannels (P2 and P3) and on surfaces which face to the narrowest area between rods (P1). The cross-sectional configuration of the test section in Figure 5.2 illustrates where the thermocouples are located in each fuel rod.

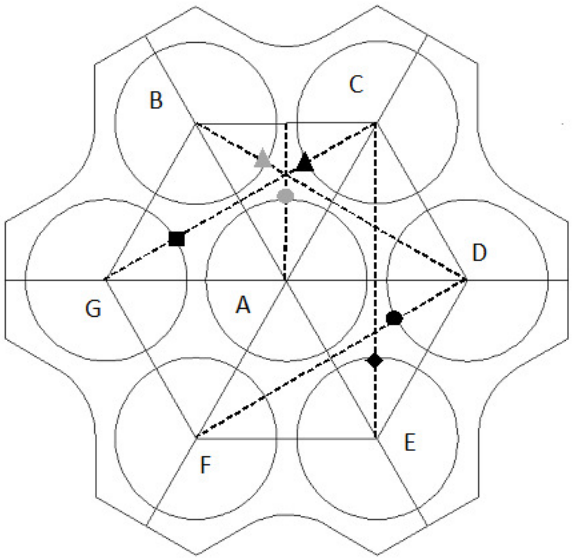

Figure 5.2: Locations of thermocouples (Misawa 2009).

In the heated region of the section, five grid spacers are installed to support the simulated fuel rods. Grid spacers are installed at 0 mm, 300 mm, 700 mm, 900 mm, and 1300 mm from the inlet of the heated region. The grid spacers are ignored in these simulations. The COBRA-TF-SC input files for the seven-rod test bundle simulations are given in Appendix E.1 and E.2.

Two different analyses are performed; low inlet enthalpy condition and high inlet enthalpy condition. In low inlet enthalpy condition, exit enthalpy approaches the inlet enthalpy of high inlet enthalpy condition. In high inlet enthalpy condition, exit enthalpy approaches the pseudocritical enthalpy. The exit pressure, the inlet mass velocity, the inlet enthalpy, and the heat power imposed on the simulated fuel rods for both low and high inlet enthalpy cases are given in Table 5.1.

Table 5.1: Computational cases (Misawa 2009)

Analysis cases	Pressure	Mass velocity	Inlet enthalpy	Heat power per rod
low inlet	25 MPa	1448 kg/m^2s	357 kJ/kg	20 kW (center rod) 23 kW (other rods)
high inlet	25 MPa	1412 kg/m^2s	1033 kJ/kg	34 kW

5.1.1 Validating the Modified COBRA-TF-SC Subchannel Code

Experimental data obtained for the low inlet enthalpy case are given in Figure 5.3. The newly developed COBRA-TF-SC code is used to calculate wall temperatures for the low-inlet enthalpy case. The wall temperatures calculated using the COBRA-TF-SC code are illustrated in Figure 5.3 along with experimental data. The low-inlet enthalpy case is also simulated using the subchannel analysis code ASSERT-PV-SC developed by Atomic Energy of Canada Limited (AECL). The ASSERT-PV-SC results are used to further verify the results obtained from COBRA-TF-SC. The wall temperatures calculated using the ASSERT-PV-SC code are also illustrated in Figure 5.3. For this study, the wall temperatures in both COBRA-TF-SC code and ASSERT-PV-SC code are calculated using the Dittus-Boelter heat transfer correlation. The Mokry et al. correlation used for supercritical water heat transfer calculations in COBRA-TF-SC is not available in ASSERT-PV-SC. The Dittus-Boelter correlation is the only heat transfer correlation available in both codes. Therefore the Dittus-Boelter correlation is used to compare COBRA-TF-SC and ASSERT-PV-SC results. The results for COBRA-TF-SC using the Mokry correlation are presented later.

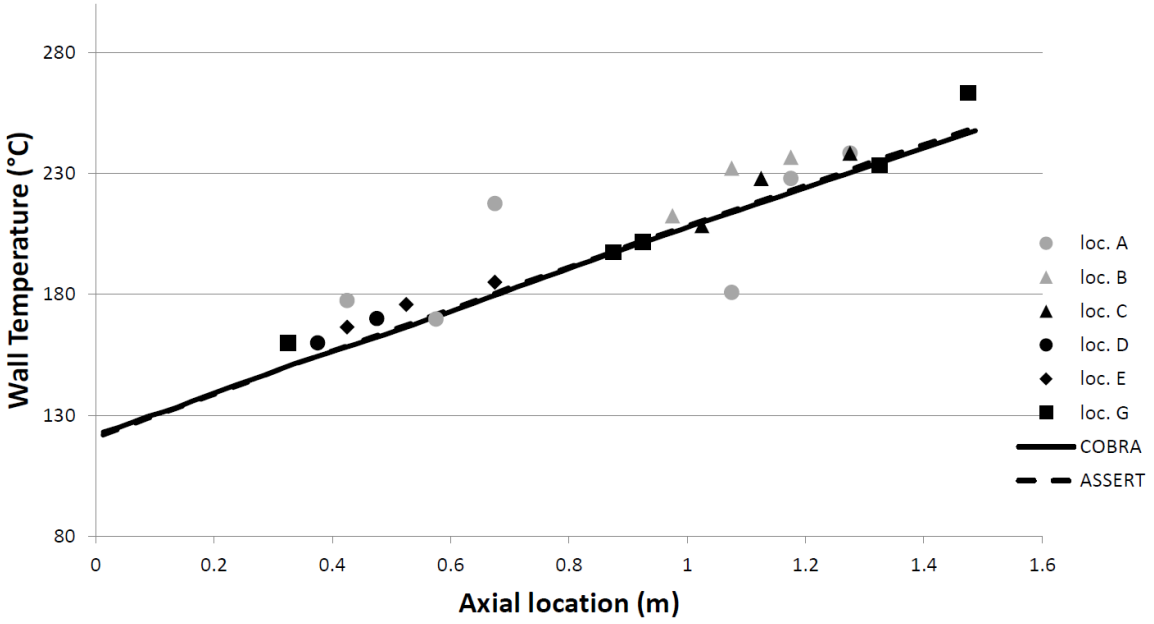

Figure 5.3: Comparison of the rod surface temperatures of low inlet enthalpy case (wall temperatures are calculated using the Dittus-Boelter correlation): Water p=25 MPa, G=1448 kg/m^2s, h_{in}=357 kJ/kg, and power/rod=20 kW (center rod) 23 kW (other rods).

Experimental data for the low-inlet enthalpy case include thermocouple measurements from both rod surfaces facing the gap region of subchannels and rod surfaces facing the center of subchannels. The scatter in experimental data is due to the thermocouple measurements for rod surfaces facing the gap region of subchannels. In this experiment, the gradient of temperature increase in upstream region (height of from 0.3 m to 0.7 m) is slightly larger than that in downstream region (height of from 0.8 m to 1.5 m) [17]. Different temperature gradient between upstream region and downstream region of the experiment maybe caused by axially non-uniform geometry due to displacement of the simulated fuel rods from designed position, or influence of spacers at the height of 0.3 m and 0.9 m.

Subchannel codes calculate one wall temperature for the entire fragment of the

rod surface facing a given subchannel control volume. Subchannel codes are not capable of calculating separate wall temperatures for rod surfaces facing the center of subchannel control volume and facing the gap region of subchannels. The wall temperatures calculated using these subchannel codes are therefore valid only for the rod surfaces facing the center of subchannel control volume. The scatter in wall temperatures observed in experimental data is not seen in both COBRA-TF-SC and ASSERT-PV-SC results as wall temperatures for the rod surfaces facing the gap region of subchannels are not calculated. The calculated rod surface temperatures increase linearly with elevation in channel because the flow field is fully developed and velocity distribution in cross section is hardly varied axially due to axially uniform geometry resulting from neglect of spacers. According to Figure 5.3 COBRA-TF-SC and ASSERT-PV-SC results agree well with thermocouple measurements for rod surfaces facing the center of subchannel control volume. Figure 5.3 also illustrates that COBRA-TF-SC and ASSERT-PV-SC results are identical to each other. This analysis verify that COBRA-TF-SC results agree well with both experimental data and numerical results obtained from ASSERT-PV-SC for the low-inlet enthalpy case.

Experimental data obtained for the high inlet enthalpy case are given in Figure 5.4. The high inlet enthalpy case is simulated with COBRA-TF-SC and ASSERT-PV-SC as above. The wall temperatures calculated using COBRA-TF-SC and ASSERT-PV-SC codes are illustrated in Figure 5.4. The wall temperatures in both COBRA-TF-SC and ASSERT-PV-SC are calculated using the Dittus-Boelter correlation. This correlation is used to compare the results because it is the only correlation available in both COBRA-TF-SC and ASSERT-PV-SC.

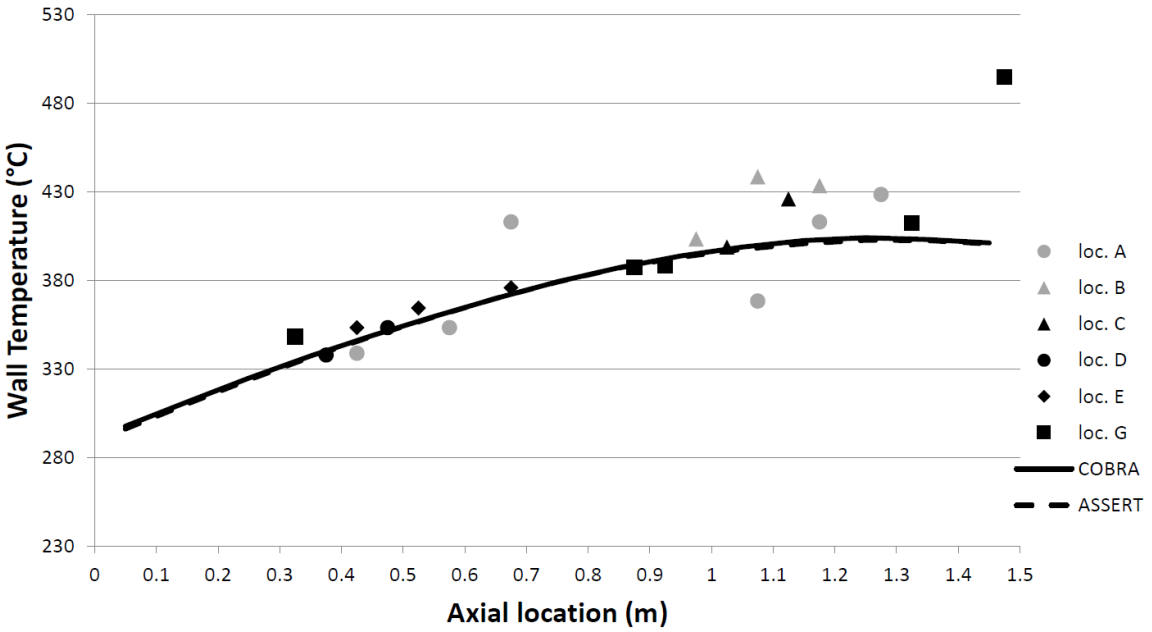

Figure 5.4: Comparison of the rod surface temperatures of high inlet enthalpy case (wall temperatures are calculated using the Dittus-Boelter correlation): Water p=25 MPa, G=1412 kg/m^2s, h_{in} =1033 kJ/kg, and power/rod=34 kW.

In high-inlet enthalpy case, the exit enthalpy approaches the pseudocritical enthalpy. The high-inlet enthalpy case is ended at the onset of wall heat transfer deterioration. The last experimental point signifies the onset of heat transfer deterioration as the enthalpy approaches the pseudocritcal enthalpy. In this experiment, gradient of temperature increase in upstream region (height of from 0.3 m to 0.7 m) is more large than that in downstream region (height of from 0.8 m to 1.5 m) compared to low-inlet enthalpy condition above [17].

According to Figure 5.4 the predicted wall temperatures of COBRA-TF-SC and ASSERT-PV-SC show good agreement with the experimental data in low fluid enthalpy region. However, the predicted wall temperatures underestimate the experimental data as bulk enthalpy approaches the pseudocritical enthalpy. This is due to the

fact that the actual heat transfer coefficient deviates from the value calculated using the Dittus-Bolter correlation at supercritical pressures specially near the critical and pseudocritical points. Figure 5.4 illustrates that COBRA-TF-SC and ASSERT-PV-SC results are identical to each other.

5.1.2 Determining the Appropriate Heat Transfer Correlation for Supercritical Flow Simulations.

The next step is to determine whether Dittus-Boelter or Mokry et. correlation gives better results in COBRA-TF-SC for the thermalhydraulics analysis of the low-inlet and high-inlet enthalpy cases. The low-inlet enthalpy case is simulated using the Mokry et al. correlation, a supercritical water heat transfer correlation, in COBRA-TF-SC. The wall temperatures calculated using both the Dittus-Boelter and the Mokry et al. correlations in COBRA-TF-SC are illustrated in Figure 5.5 along with experimental data.

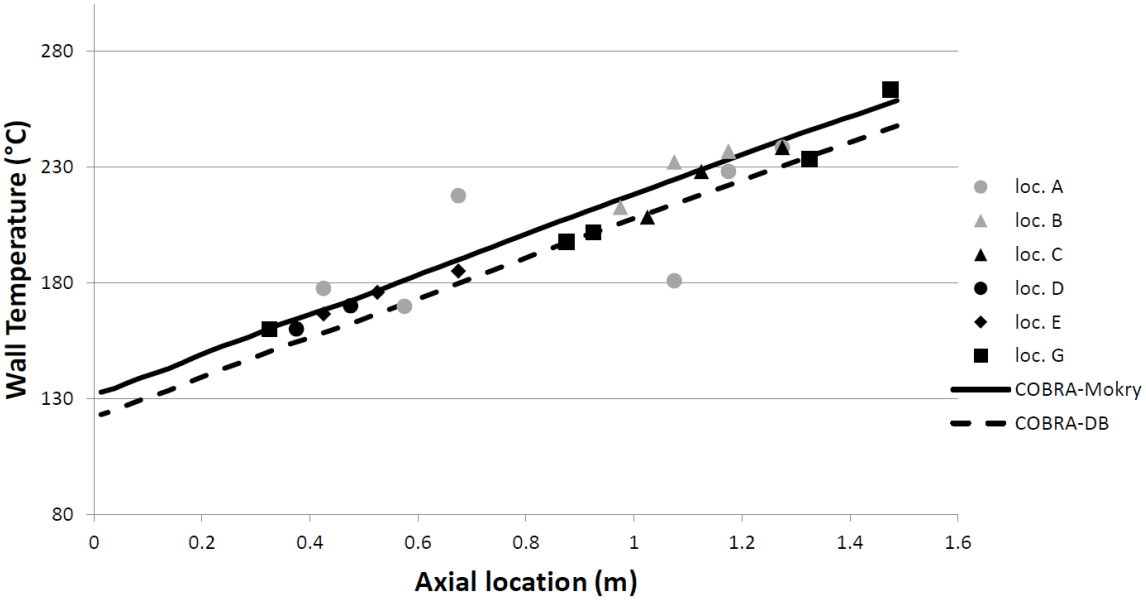

Figure 5.5: Comparison of the rod surface temperatures calculated using the Dittus-Boelter and Mokry et al. correlations for the low inlet enthalpy case: Water p=25 MPa, G=1448 kg/m^2s, h_{in}=357 kJ/kg, and power/rod=20 kW (center rod) 23 kW (other rods).

The wall temperatures calculated using the Mokry et al. correlation are slightly higher than the wall temperatures calculated using the Dittus-Boelter correlation. According to Figure 5.5, the Mokry et al. correlation predicts experimental data better than the Dittus-Boelter correlation. The Dittus-Boelter correlation under-predicts wall temperatures in the low-inlet enthalpy case. Figure 5.6 illustrates the heat transfer coefficients calculated using the Dittus-Boelter and Mokry et al. correlations for rod # 1 facing subchannel # 1 for the low-inlet enthalpy case.

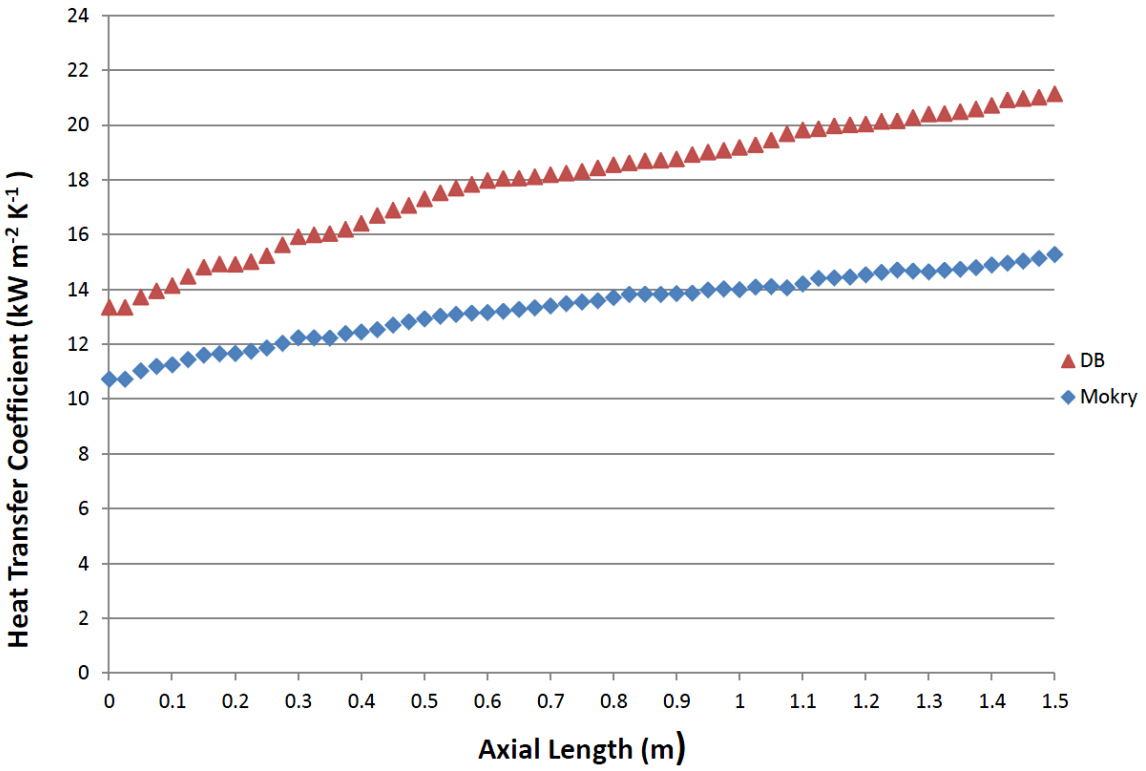

Figure 5.6: Heat transfer coefficients calculated using the Dittus-Boelter and Mokry et al. correlations for rod # 1 facing subchannel # 1 for the low inlet enthalpy case: Water p=25 MPa, G=1448 kg/m^2s, h_{in}=357 kJ/kg, and power/rod=20 kW (center rod) 23 kW (other rods).

The heat transfer coefficients calculated using the Dittus-Boelter correlation are higher than the heat transfer coefficients calculated using the Mokry et al. correlation for the low-inlet enthalpy case. The difference between heat transfer coefficients calculated using the two heat transfer correlations increases with bulk enthalpy along the length of the test section. The Dittus-Boelter correlation over-predicts heat transfer coefficients in the low-inlet enthalpy case.

Then the high-inlet enthalpy case is simulated using the Mokry et al. correlation in COBRA-TF-SC. The wall temperatures calculated using both the Dittus-Boelter

and the Mokry et al. correlations in COBRA-TF-SC for the high-inlet enthalpy case are illustrated in Figure 5.7 along with experimental data.

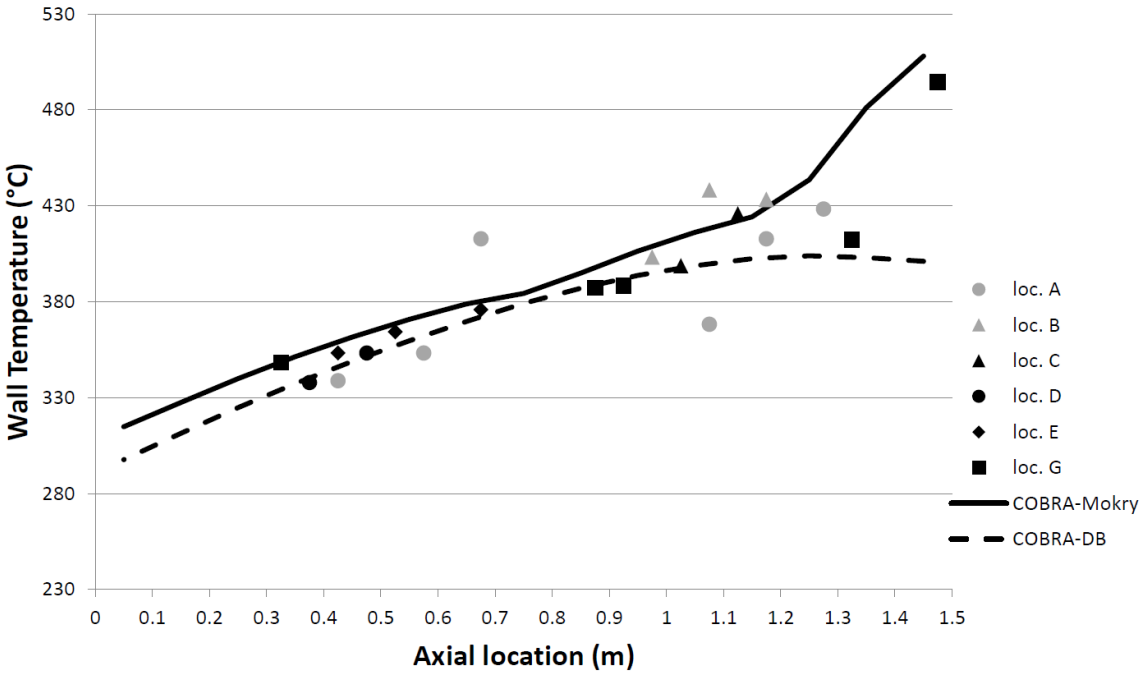

Figure 5.7: Comparison of the rod surface temperatures calculated using the Dittus-Boelter and Mokry et al. correlations for the high inlet enthalpy case: Water p=25 MPa, G=1412 kg/m^2s, h_{in} =1033 kJ/kg, and power/rod=34 kW.

In high-inlet enthalpy case, the difference between wall temperatures calculated using the two heat transfer correlations is not uniform as in the low-inlet enthalpy case. The difference between wall temperatures increases as the bulk enthalpy approaches the pseudocritical enthalpy. The Mokry et al. correlation predicts wall temperatures better than the Dittus-Boelter correlation especially near the pseudocritical point. Figure 5.8 illustrates the heat transfer coefficients calculated using the Dittus-Boelter and Mokry et al. correlations for rod # 1 facing subchannel # 1 for the high-inlet enthalpy case.

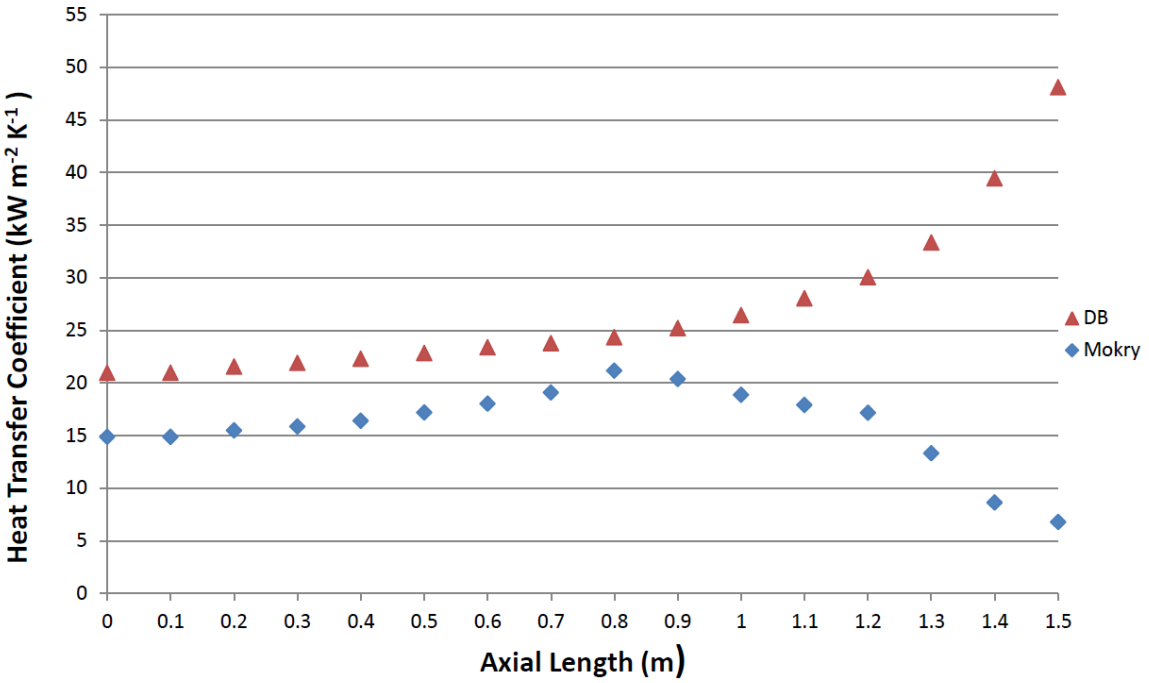

Figure 5.8: Heat transfer coefficients calculated using the Dittus-Boelter and Mokry et al. correlations for rod # 1 facing subchannel # 1 for the high inlet enthalpy case: Water p=25 MPa, G=1412 kg/m^2s, h_{in} =1033 kJ/kg, and power/rod=34 kW.

The heat transfer coefficients calculated using the Dittus-Boelter and the Mokry et al. correlations diverge as the bulk enthalpy approaches the pseudocritical enthalpy. The heat transfer coefficients calculated using the Mokry et al. correlation drops indicating heat transfer deterioration as the bulk enthalpy approaches the pseudocritical enthalpy. The Dittus-Boelter correlation fails to capture this heat transfer deterioration effect and over-predicts heat transfer coefficients near the pseudocritical enthalpy. Therefore the Mokry et al. correlation is more suitable for calculating heat transfer coefficients and in turn wall temperatures at supercritical pressures specially near the pseudocritical points.

5.2 Thermalhydraulics Analysis of The 62-element Canadian Supercritical Water Reactor (SCWR) Fuel Bundle

The 62-element Canadian SCWR fuel bundle is simulated with both COBRA-TF-SC and ASSERT-PV-SC with the Dittus-Boelter heat transfer correlation to verify if the modified COBRA-TF-SC code is capable of simulating this fuel bundle. The results are given in Appendix D. According to Figures 5.5 and 5.7, the COBRA-TF-SC code provides more accurate results when the Mokry et al. correlation is used to calculate supercritical flow heat transfer coefficients rather than the Dittus-Boelter correlation. Therefore, the COBRA-TF-SC code with the Mokry et al. correlation is used to get the detailed thermalhydraulics behaviour of the 62-element Canadian SCWR fuel bundle for the End Of Cycle (EOC) case. The 62-element Canadian SCWR Fuel Bundle and Channel Specifications are provided in Table 2.1 in Section 2.1. Figure 5.9 illustrates the 62-element Canadian SCWR fuel bundle configuration including the rod and subchannel identifications.

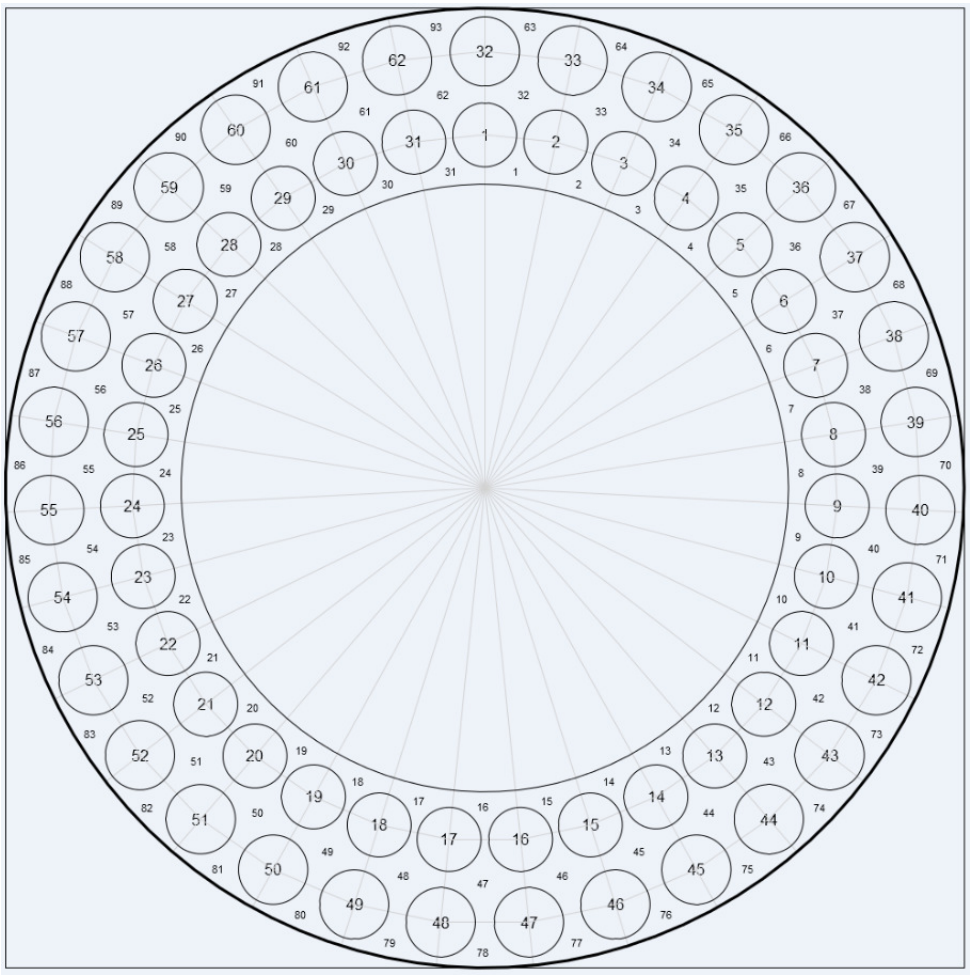

Figure 5.9: Subchannel identification in a 62-element Canadian SCWR fuel bundle.

The model for the 62-element Canadian SCWR fuel bundle includes 62 powered elements and 93 subchannels. Table 5.2 lists flow conditions employed in the current analysis. These are the proposed flow conditions for the 62-element Canadian SCWR fuel bundle design.

Table 5.2: Canadian Supercritical Water Reactor operation parameters (Spencer 2013).

Parameters	Values
Coolant Exit Pressure	25 MPa
Coolant Inlet Temperature	350 $°C$
Average Coolant Mass Flux	975.70 kg/m^2s
Average Heat Flux	851.72 kW/m^2

This analysis investigates the End Of Cycle (EOC) thermalhydraulics behaviour of the 62-element Canadian SCWR fuel bundle. The bundle exhibits a symmetric axial-power profile and a uniform radial power profile. Figure 5.10 illustrates the relative axial heat flux profile (local/average) for the EOC case of the 62-element Canadian SCWR fuel bundle [23]

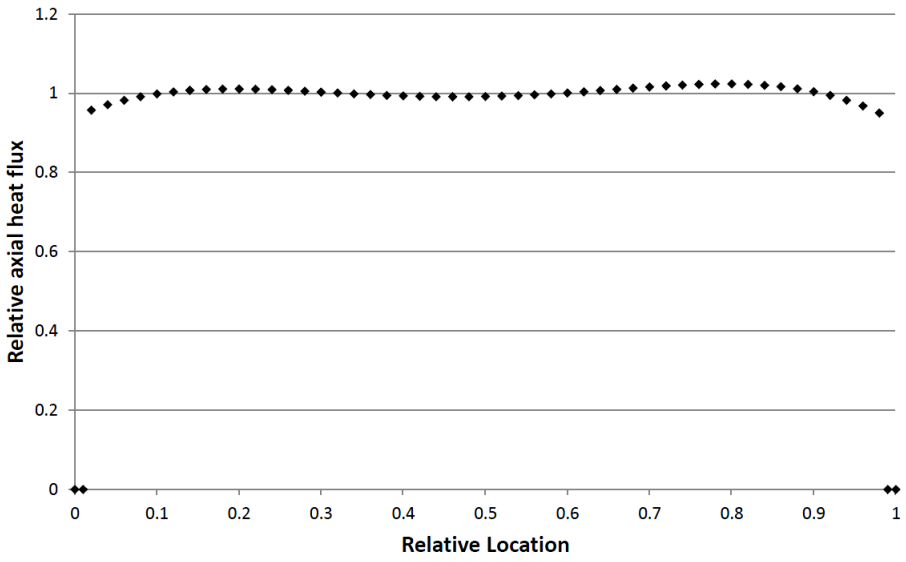

Figure 5.10: Relative Axial Heat Flux.

The COBRA-TF-SC input file for the 62-element Canadian SCWR fuel bundle simulations is given in Appendix E.3.

5.2.1 Mass Flux

The 62-element Canadian SCWR fuel bundle has three subchannel rings; inner ring, intermediate ring, and outer ring. Inner ring spans from subchannel # 1 to subchannel # 31. Intermediate ring spans from subchannel # 32 to subchannel # 62. Outer ring spans from subchannel # 63 to # 93. Subchannels in each ring are identical one another. One subchannel from each ring is selected to present the results. Figure 5.11 shows axial variations of predicted mass flux of the three selected subchannels, one from each subchannel ring, along the bundle.

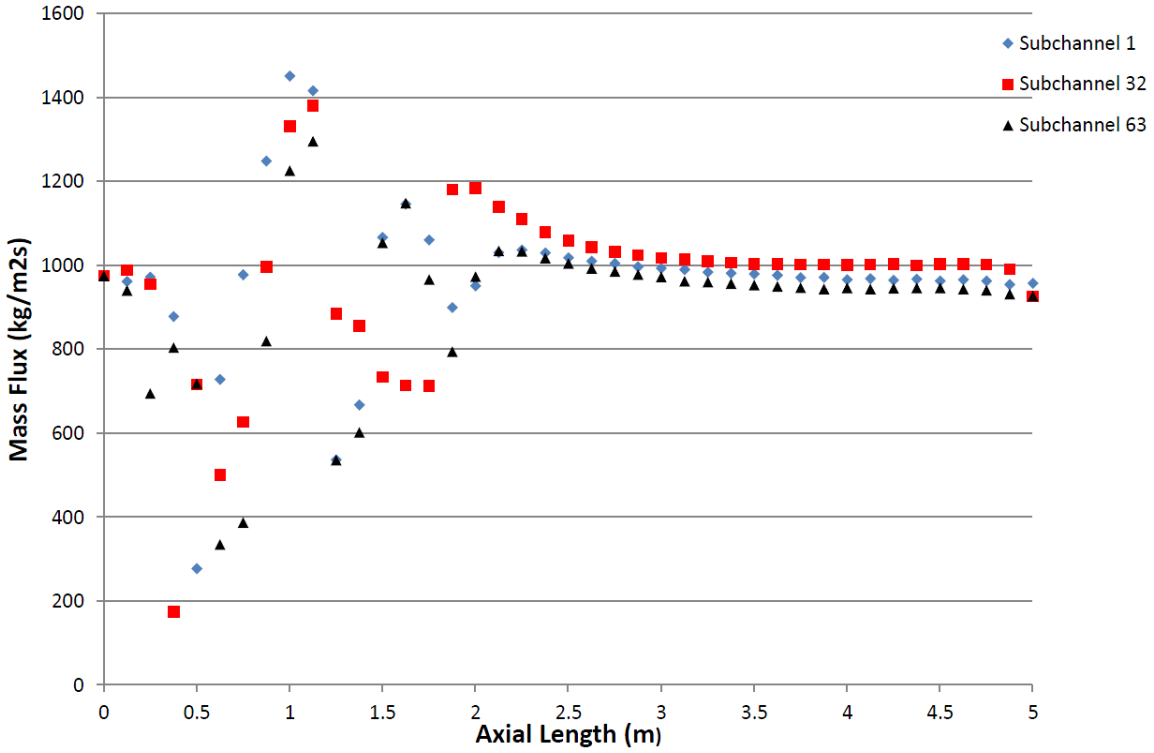

Figure 5.11: Subchannel coolant mass flux distribution along axial nodes: Water, p=25 MPa, G=975.70 kg/m^2s, q=851.72 kW/m^2, and t_{in}=350°C.

The axial mass flux variation is relatively drastic in all three subchannels. This is attributed to the drastic variations of density and viscosity leading to sharp changes in

subchannel mixing as the bulk temperature of the coolant in the subchannel reaches the pseudo-critical temperature. After the pseudocritical transition, the density and viscosity variations dissipate. The subchannels are very well mixed resulting in very little change in subchannel axial mass flux. According to Figure 5.11 subchannel mixing is very important prior to pseudocritical transition and subchannel mixing is not as important after pseudocritical transition. The total mass flux distribution of the Canadian 62-element fuel bundle along axial nodes is illustrated in Figure 5.12.

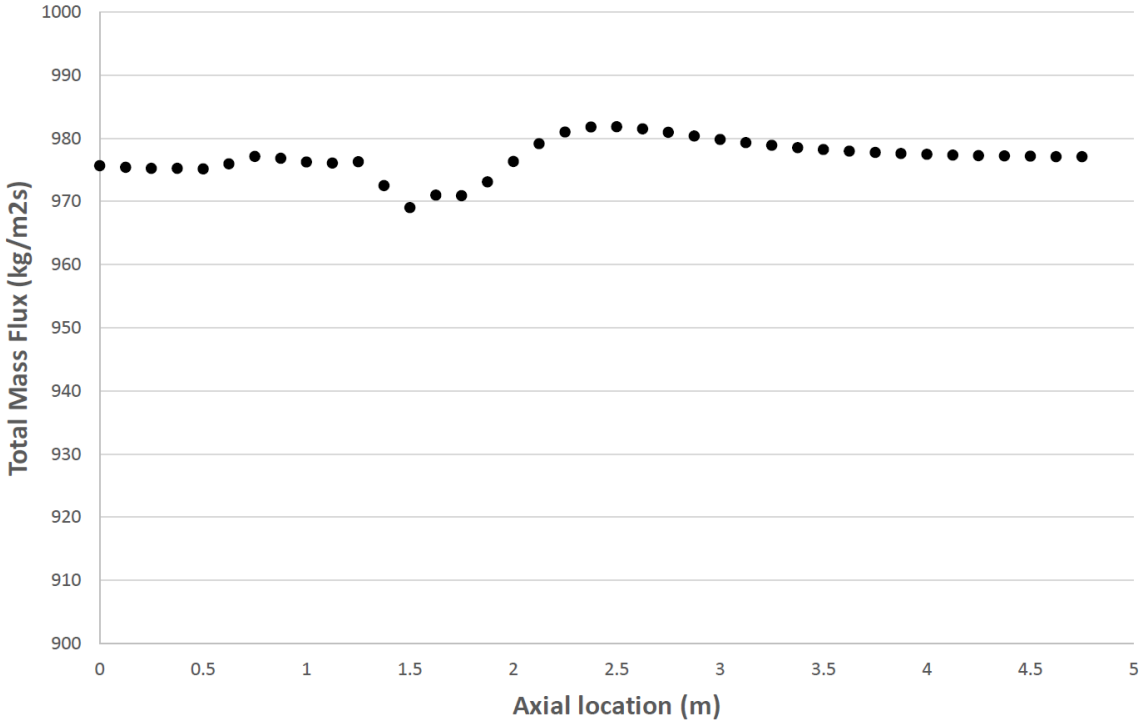

Figure 5.12: Calculated total mass flux distribution of the Canadian 62-element bundle along axial nodes: Water, p=25 MPa, G=975.70 kg/m^2s, q=851.72 kW/m^2, and t_{in}=350°C.

The total mass flux at each axial node need to be conserved for the steady state analysis of the Canadian 62-element fuel bundle. Figure 5.12 shows that the calculated total mass flux is not conserved at each axial node. The calculated total mass flux at

each node can deviate from the inlet mass flux according to the convergence criteria set in the input file. Figure 5.13 shows the deviation in total mass flux at each axial node from the inlet mass flux.

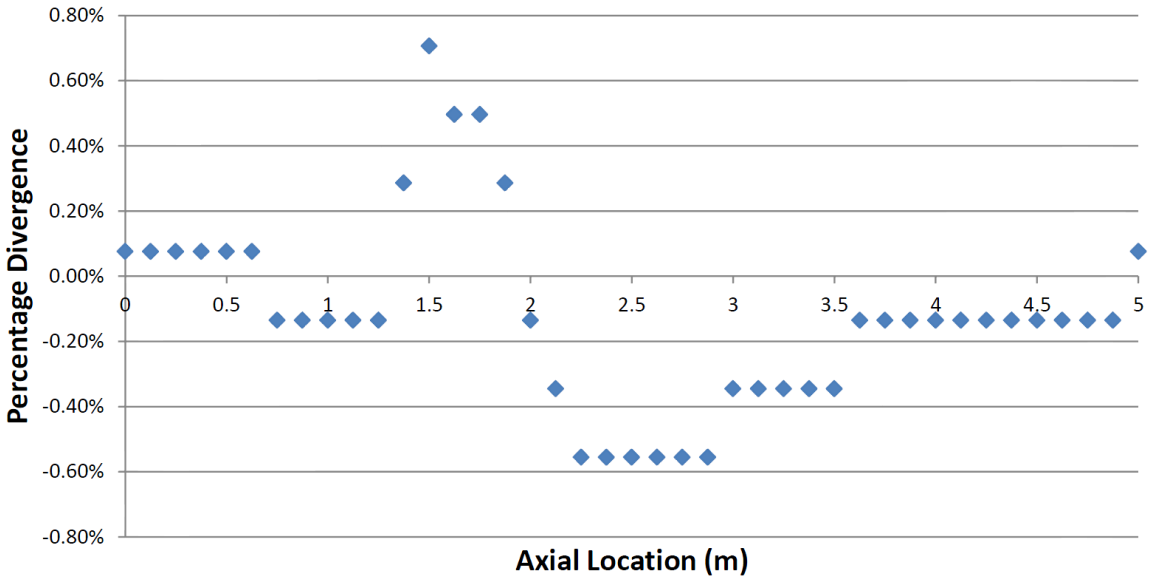

Figure 5.13: Deviation in total mass flux at each axial node: Water, p=25 MPa, G=975.70 kg/m^2s, q=851.72 kW/m^2, and t_{in}=350°C.

The deviation in total mass at each axial node from the inlet mass flux falls within ±1%, which is acceptable.

5.2.2 Bulk Coolant Temperature

Figure 5.14 shows the bulk coolant-temperature distribution of the three selected subchannels along the axial nodes.

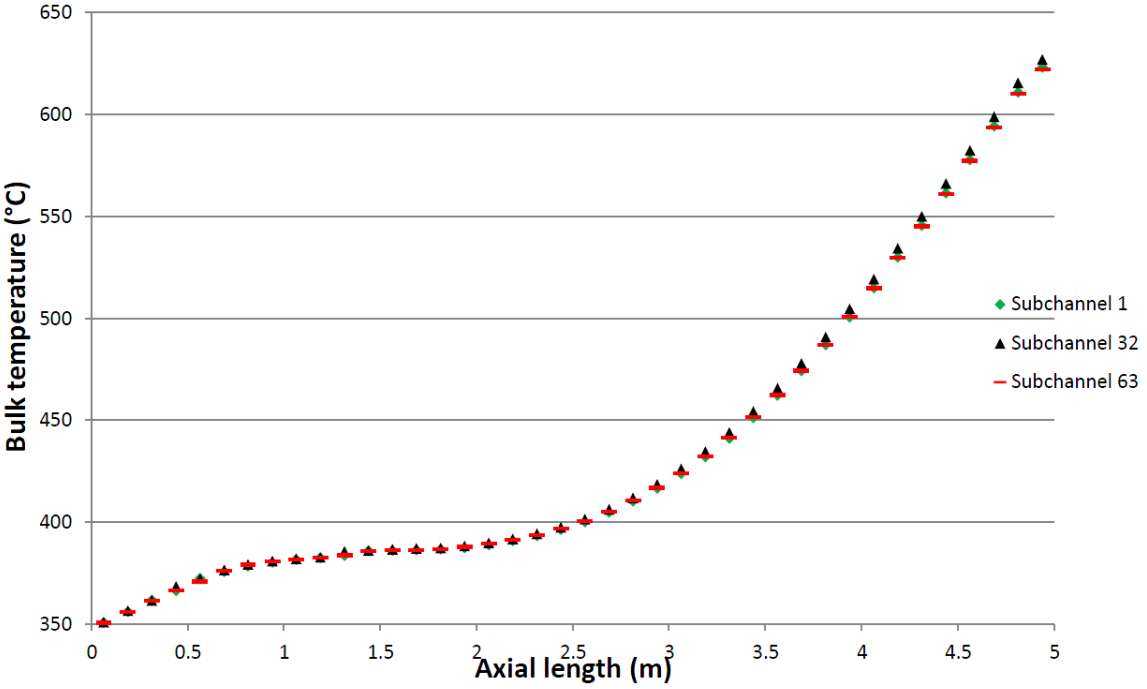

Figure 5.14: Subchannel coolant-temperature distribution along axial nodes: Water, p=25 MPa, G=975.70 kg/m^2s, q=851.72 kW/m^2, and t_{in}=350°C.

The bulk coolant temperature distribution in the three selected subchannels is almost uniform along the axial length of the fuel bundle. The symmetry of the 62-element Canadian SCWR fuel bundle ensures that the bulk coolant temperatures in the subchannels remain uniform along the axial length of the fuel bundle. The maximum bulk coolant temperature occurs in the Subchannel # 62 in the intermediate subchannel ring. The maximum bulk coolant temperature calculated using COBRA-TF-SC is 627.72°C.

5.2.3 Cladding-Surface Temperature

Figures 5.15 and 5.16 illustrate the heat transfer coefficients calculated using the Dittus-Boelter and Mokry et al. correlations respectively in COBRA-TF-SC for rod

32 facing subchannel # 32 in the 62-element Canadian SCWR fuel bundle.

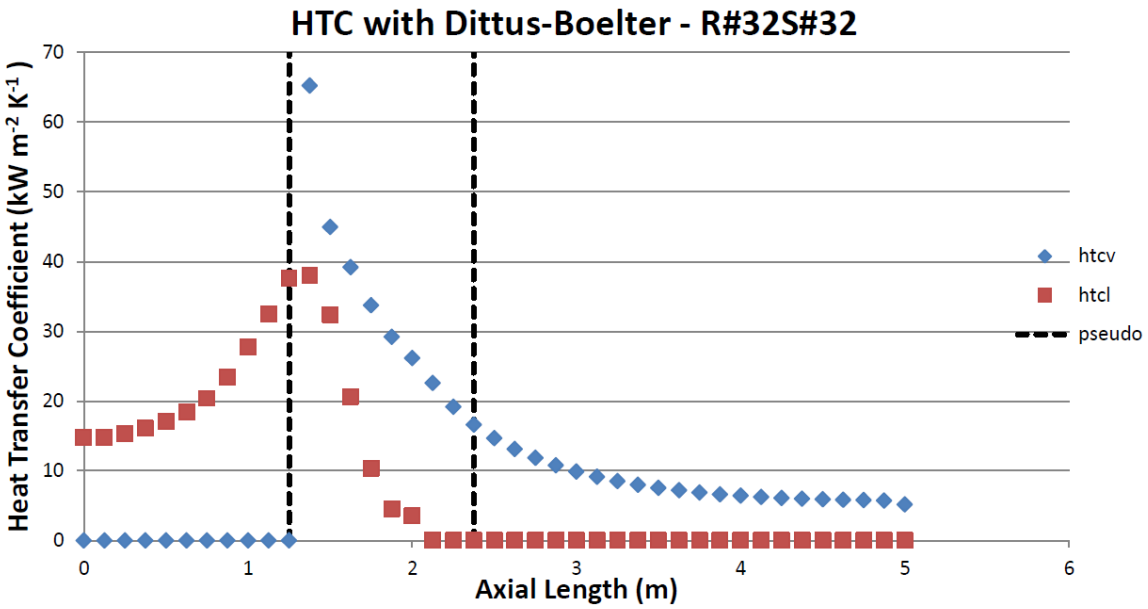

Figure 5.15: Heat transfer coefficient calculated using Dittus-Boelter correlation in COBRA-TF-SC for rod # 32 facing subchannel # 32: Water, p=25 MPa, G=975.70 kg/m^2s, q=851.72 kW/m^2, and t_{in}=350°C.

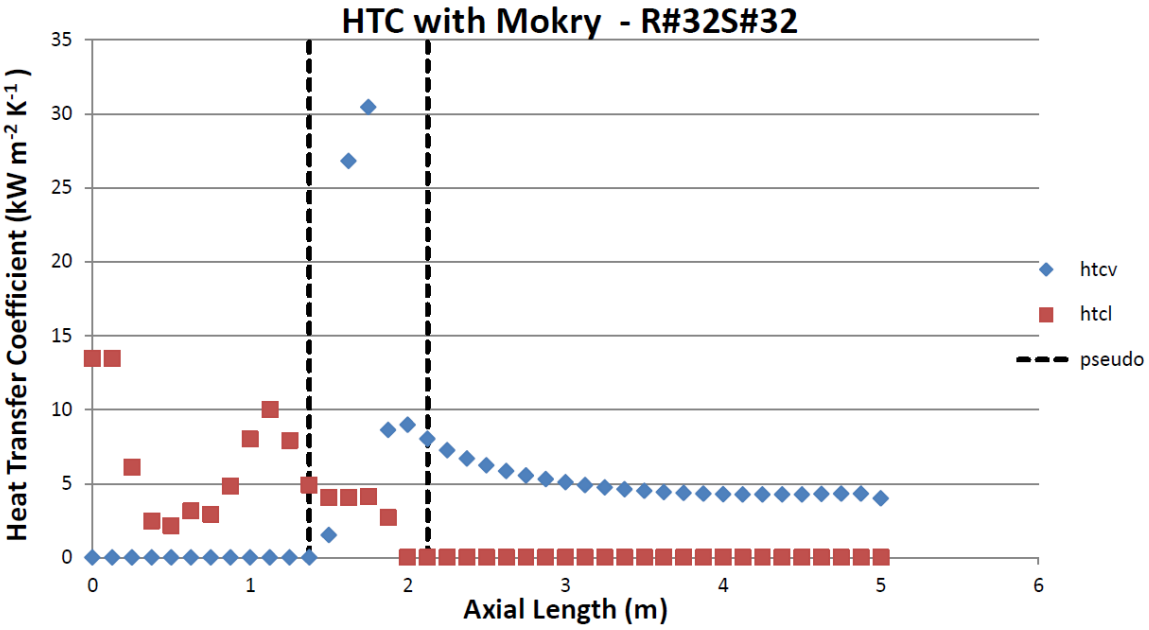

Figure 5.16: Heat transfer coefficient calculated using Mokry et al. correlation in COBRA-TF-SC for rod # 32 facing subchannel # 32: Water, p=25 MPa, G=975.70 kg/m^2s, q=851.72 kW/m^2, and t_{in}=350°C.

Both single phase vapour, hspv, and single phase liquid, hspl, heat transfer coefficients are calculated due to the two-fluid numerical structure of the code. These plots illustrate how the heat transfer coefficient changes from single-phase liquid to single-phase vapour within the pseudo two phase region in COBRA-TF-SC.

Figure 5.15 illustrates that Dittus-Boelter correlation is sensitive to the significant variations in thermophysical properties near the pseudocritical point. The heat transfer coefficient calculated using the Dittus-Boelter correlation peaks at 65.2 kW/m^2K near the pseudocritical point. The Dittus-Boelter correlation significantly overestimates the heat transfer coefficient values within the pseudocritical range. As seen in Figure 5.16, the Mokry et al. correlation is not as sensitive as the Dittus-Boelter correlation to the significant variations in thermophysical properties near the pseudocritical point.

The Mokry et al. correlation is used to calculate supercritical water heat transfer coefficients as it provides the best prediction of heat transfer trends observed within the pseudocritical region out of supercritical water heat transfer correlations available in the literature [18]. The heat transfer coefficient calculated using the Mokry et al. correlation peaks at 30.4 kW/m^2K near the pseudocritical point.

There are four different types of fuel rod surfaces in the 62-element Canadian SCWR fuel bundle as illustrated in Figure 5.17. Inner ring fuel rods facing the inner subchannel ring forms the surface type # 1. Inner ring fuel rods facing the intermediate subchannel ring forms the surface type # 2. Outer ring fuel rods facing the intermediate subchannel ring forms the surface type # 3. Outer ring fuel rods facing the outer subchannel ring forms the surface type # 4.

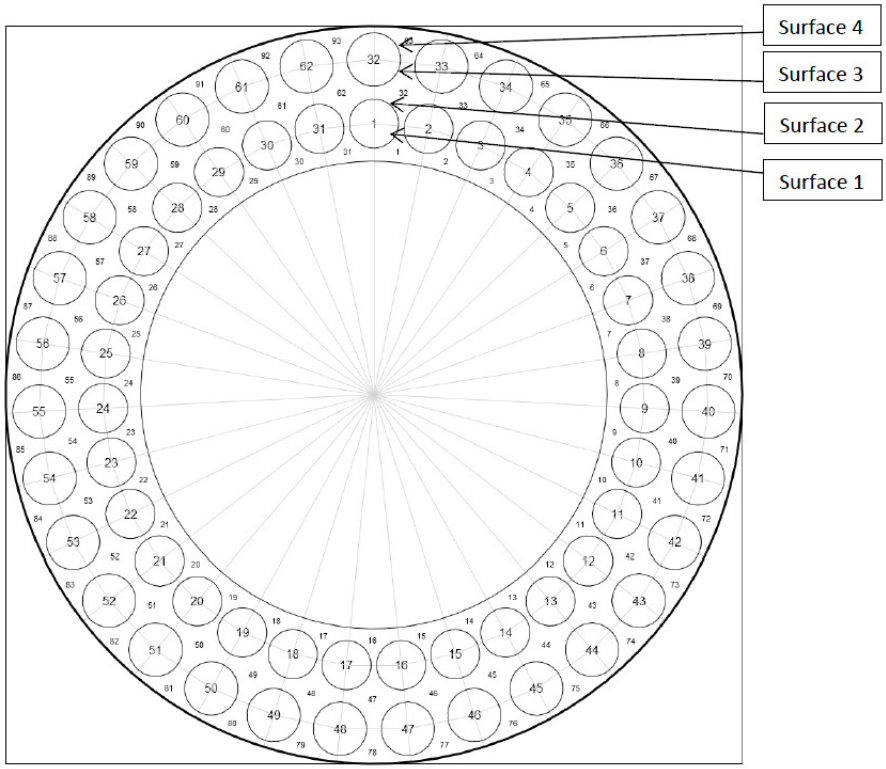

Figure 5.17: Configuration of rod surfaces.

One rod surface from each fuel rod surface type is selected to present the results. The cladding-surface temperature distributions of these surfaces along the bundle are shown in Figure 5.18.

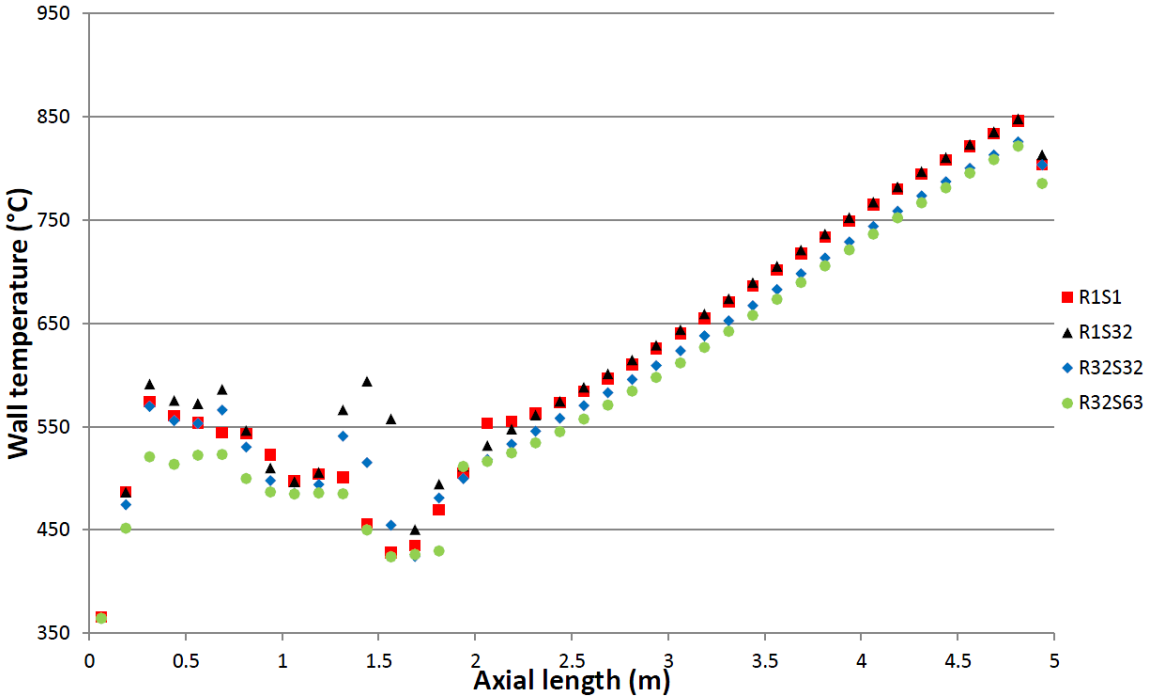

Figure 5.18: Cladding-surface temperature of typical locations along axial nodes using the Mokry et al. coorelation (r1s1 denotes the fragment of rod 1 that facing Subchannel 1): Water, p=25 MPa, G=975.70 kg/m^2s, q=851.72 kW/m^2, and t_{in}=350°C.

Figure 5.10 illustrates that axial heat flux is set to zero at the channel exit. This causes the rod surface temperatures to drop at the last computational node. Figure 5.18 illustrate that the wall temperature changes drastically near the pseudocritical point. The heat transfer coefficient changes drastically due to significant changes in fluid properties near the pseudocritical point. The most significant changes in fluid properties occur within ±25°C from the pseudocritical temperature. Therefore significant variations in heat transfer coefficient and in turn cladding-surface temperature can be expected for bulk fluid temperatures within ±25°C from the pseudocritical temperature. After the pseudocritical transition the drastic changes fluid properties dissipate resulting in equal cladding surface temperatures between rod surfaces. The

cladding-surface temperatures increase gradually along the bundle towards the downstream end. The maximum cladding-surface temperature occurs in the fragment of rod # 32 facing Subchannel # 32. The maximum cladding temperature calculated using COBRA-TF-SC is 848.25°C.

The supercritical water coolant remain single phase at all operating conditions of SCWRs. Therefore, the traditional limiting criteria based on either the dryout or the burnout phenomenon is not applicable. The maximum cladding-surface temperature (MCST) and peak fuel centreline temperature have been adopted as design criterion for the SCWR. Therefore, the design criteria for the Canadian 62-element fuel bundle is the maximum cladding-surface temperature. The design accepted limit for the maximum cladding-surface temperature is 850°C. The calculated maximum cladding-surface temperature above is very close to the accepted limit for the maximum cladding-surface temperature.

5.2.4 Sensitivity Analysis

The Canadian 62-element fuel bundle is simulated with different mass fluxes to observe the behaviour of cladding-surface temperature with mass flux. Figure 5.19 illustrates the change in cladding-surface temperature when the mass flux is increased by 10%.

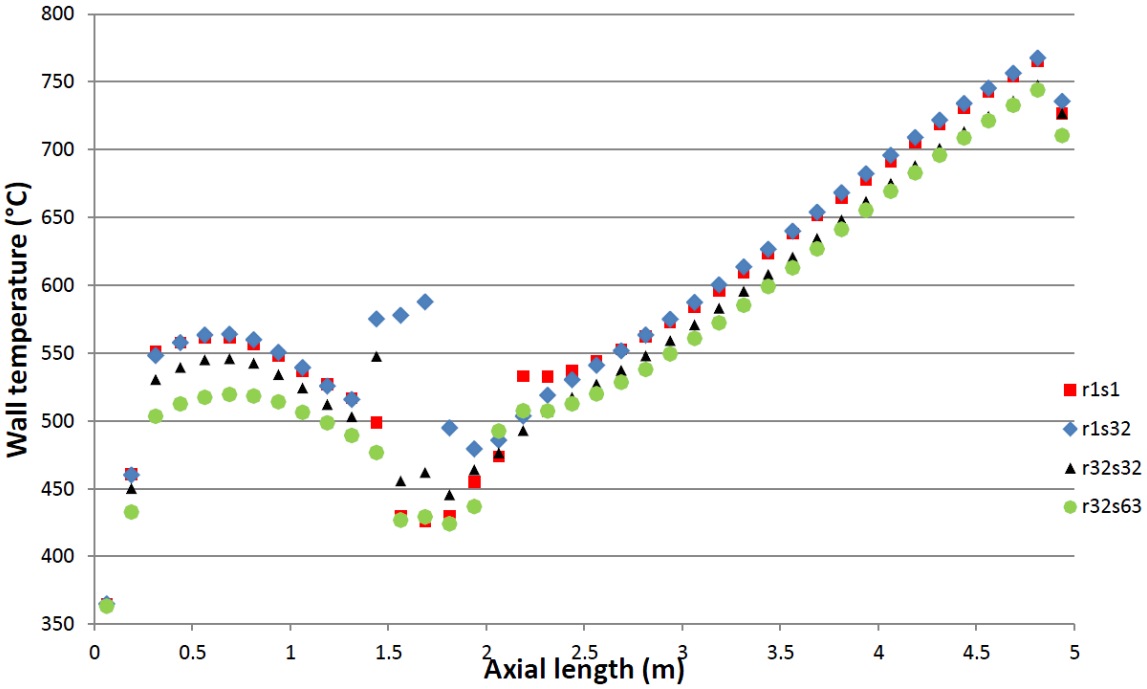

Figure 5.19: Cladding-surface temperature profile when the mass flux is increased by 10%. (r1s1 denotes the fragment of rod 1 that facing Subchannel 1): Water, p=25 MPa, G=1073.27 kg/m^2s, q=851.72 kW/m^2, and t_{in}=350°C.

The maximum cladding-surface temperature occurs in the fragment of rod # 32 facing Subchannel # 32. The maximum cladding-surface temperature drops to 744.25°C when the mass flux is increased by 10%. The maximum cladding-surface temperature decreases by 12.2% when the mass flux is increased by 10%. Figure 5.20 illustrates the change in cladding-surface temperature when the mass flux is increased by 25%.

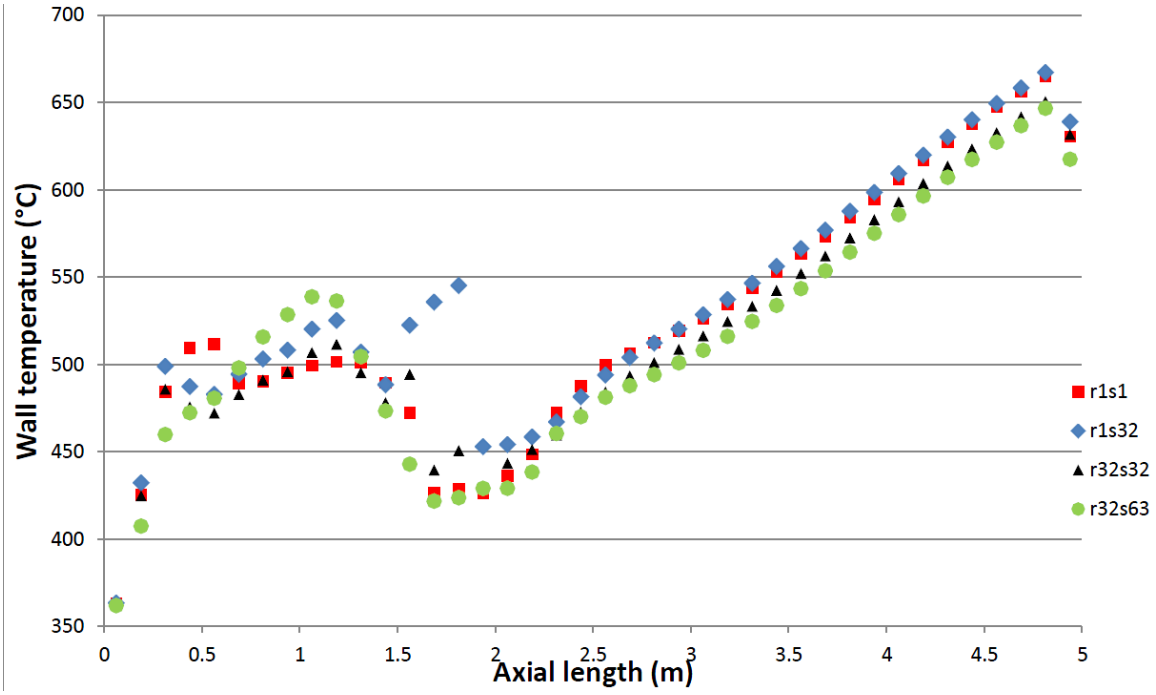

Figure 5.20: Cladding-surface temperature profile when the mass flux is increased by 25%. (r1s1 denotes the fragment of rod 1 that facing Subchannel 1): Water, p=25 MPa, G=1219.63 kg/m^2s, q=851.72 kW/m^2, and t_{in}=350°C.

The maximum cladding-surface temperature occurs in the fragment of rod # 32 facing Subchannel # 32. The maximum cladding-surface temperature drops to 646.72°C when the mass flux is increased by 25%. The maximum cladding-surface temperature decreases by 23.8% when the mass flux is increased by 25%.

Next, the Canadian 62-element fuel bundle is simulated with different heat fluxes to observe the behaviour of cladding-surface temperature with heat flux. Figure 5.21 illustrates the change in cladding-surface temperatures when the heat flux is decreased by 10%.

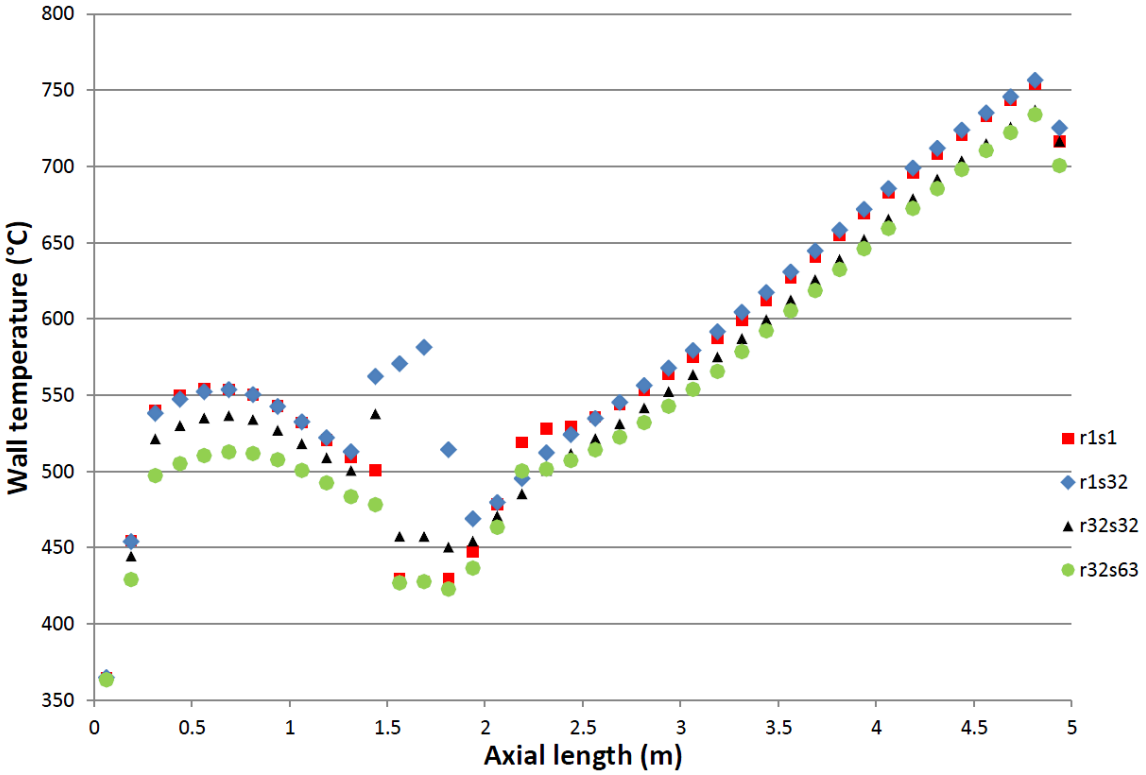

Figure 5.21: Cladding-surface temperature profile when the heat flux is decreased by 10%. (r1s1 denotes the fragment of rod 1 that facing Subchannel 1): Water, p=25 MPa, G=975.70 kg/m^2s, q=851.72 kW/m^2, and t_{in}=350°C.

The maximum cladding-surface temperature occurs in the fragment of rod # 32 facing Subchannel # 32. The maximum cladding-surface temperature drops to 734.02°C when the heat flux is decreased by 10%. The maximum cladding-surface temperature decreases by 13.5% when the heat flux is decreased by 10%.

Chapter 6

Conclusion and Extensions

The main objective of this study is to develop an independent subchannel analysis code that is capable of simulating the 62-element Canadian SCWR fuel bundle. The existing suchannel analysis code COBRA-TF is modified to be able to simulate supercritical water conditions. The modified COBRA-TF-SC code is verified and validated with experimental data and other numerical results. Finally the modified COBRA-TF-SC is code is used to perform thermalhydraulics analysis and sensitivity analysis of the 62-element Canadian SCWR fuel bundle.

6.1 Code Development

A subchannel analysis code COBRA-TF-SC is developed by modifying existing subchannel code COBRA-TF to perform thermalhydraulics analysis of the 62-element Canadian SCWR fuel bundle. Several modifications are introduced to the COBRA-TF code. The operating pressure limit of COBRA-TF is extended by introducing a pseudo two-phase region at supercritical pressures to maintain the two-fluid numerical

structure of the code. The pseudo two-phase region is designed in a way to maintain the numerical stability of the code while minimizing property errors. The pseudo two-phase scheme provides COBRA-TF-SC the ability to perform transcritical flow simulations. Intrinsic property table and property formulations in COBRA-TF are upgraded to simulate supercritical water conditions. Seven additional property tables are added to the code to calculate subcooled liquid and saturated properties of water at supercritical pressures. New property formulations obtained from IAPWS-IF97 are introduced to the code to calculate liquid and vapour volumes and their partial derivatives with respect to pressure and enthalpy at supercritical pressures. New property formulations obtained from IAPWS-IF97 are added to the code to calculate vapour properties at supercritical pressures. The Mokry et al. heat transfer correlation is implemented to the code to determine heat transfer and the Kirillov et al. correlation is implemented to the code to determine hydraulics resistance at supercritical pressures. Finally the heat transfer regime map is modified to take into account that the only heat transfer mechanism of supercritical flow is single phase convection. The void drift mixing model of COBRA-TF is turned off for supercritical flow simulations. The existing turbulent mixing model of COBRA-TF is used for supercritical flow simulations as there are no satisfactory supercritical flow turbulent mixing models.

6.2 Code Assessment

The code is assessed by comparing to the experimental data and other numerical results. The experimental data are obtained from the heat transfer to supercritical water flowing upward in seven-rod test bundle study carried out by the JAEA. This

experiment is simulated with both COBRA-TF-SC and AECL's modified ASSERT-PV-SC. The wall temperatures in both codes are calculated with the Dittus-Boelter correlation for ease of comparison. The experimental data and the calculated wall temperatures agree well with each other. Then the experiment is simulated with COBRA-TF-SC using the Mokry et al. heat transfer correlation. The Mokry et al. correlation predicts wall temperatures better than the Dittus-Boelter correlation especially near the pseudocritical point. Code assessment verified that COBRA-TF-SC is capable of performing supercritical water flow simulations.

6.3 Thermalhydraulics Analysis and Sensitivity Analysis

The Mokry et al. heat transfer correlation is implemented in COBRA-TF-SC to perform thermalhydraulics analysis and sensitivity analysis of the EOC case of 62-element Canadian SCWR fuel bundle. The Mokry et al. correlation is not as sensitive as the Dittus-Boelter correlation to significant changes in fluid properties near the pseudocritical point and it provides the best prediction of heat transfer trends observed within the pseudocritical region.

The axial mass flux changes drastically as the bulk temperature approaches the pseudocritical temperature due to drastic variations in density and viscosity leading to sharp changes in subchannel mixing. After the pseudocritical transition the subchannels are very well mixed leading to very little change in axial mass flux. Subchannel mixing is very important prior to pseudocritical transition and not as important after pseudocritical transition.

The symmetry of the 62-element Canadian SCWR fuel bundle ensures that the subchannel bulk temperatures remain uniform along the axial length of the bundle. The maximum bulk coolant temperature of 627.72°C occurs in the subchannel # 62 in the intermediate subchannel ring.

The heat transfer coefficient changes drastically due to significant changes in fluid properties near the pseudocritical point. This results in drastic changes in cladding surface temperatures within the pseudocritical region. The maximum cladding surface temperature of 848.25°C occurs in the fragment of rod # 32 facing Subchannel # 32. The calculated maximum cladding-surface temperature is very close to the accepted limit for the maximum cladding-surface temperature of 850°C.

The sensitivity analysis determined that the maximum cladding surface temperature decreases by 12.2% and 23.8% when the mass flux is increased by 10% and 25% respectively. The maximum cladding surface temperature decreases by 13.5% when the heat flux is decreased by 10%.

6.4 Recommendations for future work

The following recommendations are offered as possible ways to improve this study and COBRA-TF-SC code.

6.4.1 Incorporate new correlations and models

COBRA-TF-SC is an open source code. This gives the user the ability to incorporate new models and correlations to the code. There are several supercritical water heat transfer and friction factor correlations in literature. These supercritical water heat

transfer and friction factor correlations can be added to the source code for comparison and testing.

The correlations to determine local resistance coefficients for different flow obstructions in COBRA-TF-SC are valid only at subcritical pressures. Currently, there are no satisfactory supercritical flow correlations for local resistance coefficients in the literature. The code can be improved by adding correlations to calculate local resistance coefficients for different flow obstructions at supercritical flow conditions when available.

The turbulent mixing model used in COBRA-TF-SC is only valid at subcritical pressures. Satisfactory turbulent mixing models have not yet been developed for supercritical flow. The subchannel mixing calculations of COBRA-TF-SC can be improved by adding supercritical water turbulent mixing models when available.

6.4.2 Perform trans-critical flow simulations

The pseudo two-phase scheme employed in COBRA-TF-SC gives it the ability to perform trans-critical flow simulations. The trans-critical flow simulation capabilities of COBRA-TF-SC are not tested in this study. This study can be improved by testing the trans-critical flow simulation capabilities of COBRA-TF-SC and verifying the results with experimental data.

6.4.3 Incorporate a model to simulate the moderator channel

The 62-element Canadian SCWR fuel bundle has a high-efficiency re-entrant channel (HERC) in the middle of the fuel channel. COBRA-TF-SC does not incorporate a model to simulate this moderator channel. This study assumes that there is no heat

transfer between the moderator channel and the coolant. This is not true in practice. Therefore a model is required to be added to COBRA-TF-SC to simulate the heat transfer between the coolant and the moderator channel in the 62-element Canadian SCWR fuel bundle.

6.4.4 Develop a coupled code system

System codes and subchannel codes are coupled for calculating the system and local thermalhydraulics behaviour of a nuclear reactor simultaneously. The modified COBRA-TF-SC subchannel analysis code can be coupled with a supercritical water system safety code such as ATHELET to develop a coupled code system to perform thermalhydraulics analysis of the Canadian SCWR.

Appendix A

Nomenclature

General

ρ	Density	G	Mass Flux
μ	Dynamic Viscosity	h	Enthalpy
k	Thermal Conductivity	g	Gravitational Acceleration
c_p	Specific Heat Capacity	h_{fg}	Latent Heat of Vaporization
D	Tube Diameter	α	Void Fraction
p	Pressure	t	Time
T	Temperature	u	Velocity
q	Heat Flux	A	Area
L	Length	σ	Surface Tension

Dimensionless Numbers

Nu	Nusselt Number - Ratio of convective to conductive heat transfer
Re	Reynolds Number - Ratio of inertial to viscous forces
Pr	Prandtl Number - Ratio of viscous to thermal diffusion rates
Gr	Grashof Number - Ratio of buoyant to viscous forces

Subscripts

b	Bulk-fluid Temperature
w	Wall Temperature
pc	Pseudocritical
hy	Hydraulic
in	Inlet
out	Exit
tp	Two-phase

Appendix B

Abbreviation & Acronyms

AECL	Atomic Energy of Canada Limited
ATHAS	Advanced Thermal-Hydraulics Analysis Subchannel
ATHLET	Analysis of Thermal-hydraulics of Leaks and Transients
APROS	Advanced Process Simulation Environment
ASSERT	Advanced Solution of Subchannel Equations in Reactor Thermal-hydraulics
BWR	Boiling Water Reactor
CANFLEX	CANDU FLEXible fuelling
CANDU	CANada Deuterium Uranium
CFD	Computational Fluid Dynamics
CHF	Critical Heat Flux
COBRA	COolant Boiling in Rod Arrays
DOE	Department Of Energy
EOC	End Of Cycle

HERC	High-Efficiency Re-entrant Channel
HPLWR	High Performance Light Water Reactor
HTC	Heat Transfer Coefficient
IAEA	International Atomic Energy Agency
IAPWS	Industrial Formulation for the Thermodynamic Properties of Water and Steam
JAEA	Japanese Atomic Energy Agency
KAERI	Korean Atomic Energy Institute
LOCA	Loss of Coolant Accident
LWR	Light Water Reactor
MATRA	Multichannel Analyzer for steady states and Transients in Rod Arrays
NIST	National Institute of Standards and Technology
NPP	Nuclear Power Plant
PV	Pressure Vessel (reactor)
PWR	Pressurized Water Reactor
REFPROP	REFerence Fluid PROPerties
RBMK	Reaktor Bolshoy Moshchnosti Kanalniy
RMS	Root Mean Square
SC	Supercritical
SCW	Supercritical Water
SCWR	Supercritical Water Reactor
STAFAS	Sub-channel Thermal-hydraulic Analysis of Fuel Assembly under Supercritical Conditions
TF	Two Fluids

VTT	Technical Research Centre of Finland

Appendix C

Modifications to COBRA-TF to Model Supercritical Water Flow

C.1 SAT subroutine

The SAT subroutine calculates liquid and vapour saturation enthalpies and their derivatives with respect to pressure. It is only capable of calculating these variables up to a pressure of 3201 psi. If the pressure is higher than 3201 psi, the simulation stops and returns an error message stating that the pressure is too high. The pressure limit of the algorithm calculating the liquid saturation enthalpy and its derivative is extended by adding the following code segment at line # 43 of the original subroutine.

```
if (ppsia. lt. 4900.)  goto 35
```

If the pressure is greater than 3201 psi the algorithm jumps to 35, where the pseudo liquid saturation enthalpy and its derivative with respect to pressure is calculated using the pseudo two-phase scheme. The following code segment is added at line # 55 of the original subroutine.

```
35 hf = (0.0438*ppsia)+735.3388
   dhfdp = 0.043
```

The SAT subroutine is only capable of calculating the vapour saturation enthalpy and its derivative up to a pressure of 3201 psi. If the pressure is greater than 3201 psi, the simulation stops and returns an error message stating that the pressure is too high. The pressure limit of the algorithm calculating the vapour saturation enthalpy and its derivative is extended by adding the following code segment at line # 61 of the original subroutine.

```
if (ppsia .lt. 3201.)  goto 70
goto 75
```

If the pressure is greater than 3201 psi the algorithm jumps to 75, where the pseudo vapour saturation enthalpy its derivative with respect to pressure is calculated using the pseudo two-phase scheme. The following code segment is added at line # 87 of the original subroutine.

```
75 hg = (0.0438*ppsia)+791.4468
   dhgdp = 0.0438
```

C.2 PROP subroutine

This subroutine calculates liquid and vapour properties of water. The SUPERCRITDATA module is called to obtain all the required supercritical water property data.

```
use supercritdata
```

New local variables are added to calculate supercritical water properties.

```
real  :: tfold    !liq sat temp using the previous property table
real  :: rhofold  !liq sat density using the previous property table
```

```
      real  :: cpfold   !liq sat heat cap using the previous property table
      real  :: kfold    !liq sat thermal con. using the previous property table
      real  :: ufold    !liq sat viscosity using the previous property table
      real  :: sigmaold !surface tension using the previous property table
      real  :: rhogold  !vap sat density using the previous property table
      real  :: kgold    !vap sat thermal con. using the previous property table
      real  :: ugold    !vap sat viscosity using the previous property table
      real  :: tlold    !liq temp. using the previous property table
      real  :: cplold   !liq heat cap. using the previous property table
      real  :: klold    !liq thermal con. using the previous property table
      real  :: ulold    !liq viscosity using the previous property table
      real  :: pramp    !pressure ramp value
      real  :: prange   !pressure ramp range
      real  :: plimitlow!minimum pressure of the pressure ramp range
      real  :: plimithigh!maximum pressure of the pressure ramp range
```

PART 1 of the PROP subroutine determines saturated properties of water and subcooled properties of water at a given enthalpy h . The modified version of COBRA-TF determines saturated and subcooled properties of water at given pressure p and enthalpy h. The continuous pressure range is discretized into 8 different pressure intervals. The liquid and vapour saturation properties are then calculated using 8 intrinsic property tables, one for each pressure interval. The liquid and vapour saturation properties for both subcritical and supercritical flow are calculated by replacing the code segment from line #91 to 152 of the original subroutine with the following code segment.

```
c---- Look-up properties for saturated liquid and saturated vapor
c---- (at saturation enthalpy of liquid hf):
c---- Determine index and fraction for table interpolation
```

```
      if(p.ge.0)then
          iprops = (hf - 10.) / 10 + 1
          iprops = iprops - iprops / nprop
          if(iprops.ge.90)then
              iprops = 89
              fract = 1.0
          else
              fract = (hf - hhf(iprops)) / 10.
          endif
c---- Saturation temperature
          tf = tt(iprops) + fract * (tt(iprops+1)-tt(iprops))
c---- Densities
          rhof = rhoff(iprops) +fract* (rhoff(iprops+1)-rhoff(iprops))
          rhog = rhogg(iprops) +fract* (rhogg(iprops+1)-rhogg(iprops))
c---- Difference of specific volumes for saturated vapor and saturated
c---- liquid
          vfg  = 1./rhog - 1./rhof
c---- Specific heat capacity
          cpf  = cpff(iprops) + fract * (cpff(iprops+1)-cpff(iprops))
c---- Thermal conductivities
          kf   = kkf(iprops)  + fract * (kkf(iprops+1)-kkf(iprops))
          kg   = kkg(iprops)  + fract * (kkg(iprops+1)-kkg(iprops))
c---- Dynamcic viscosities
          uf   = uuf(iprops)  + fract * (uuf(iprops+1)-uuf(iprops))
          ug   = uug(iprops)  + fract * (uug(iprops+1)-uug(iprops))
c---- Surface tension
```

```
          sigma= ssigma(iprops) +fract*(ssigma(iprops+1)-ssigma(iprops))

c---- Auxiliary terms used for several correlations:
c
c---- h11 - used in Chen nucleate boiling correlation:
c         h11 = 0.00122*kf**0.79*cpf**0.45*rhof**0.49/
c               (sqrt(sigma)*uf**0.29*(hfg*rhog)**0.24
c
c---- h22 - used in Berenson film temperature equation:
c         h22 = 0.127*hfg*((rhof-rhog)/(rhof+rhog))**2/3
c               *sqrt(sigma/(rhof-rhog))*(gc/(rhof-rhog))**1/3
c
c---- h33 - used in Bromley film boiling equation:
c         h33 = 0.62*(sqrt((rhof-rhog)/sigma))**0.172*
c               (gc*(rhof-rhog))**0.25/(2*pi)**0.172
c
c---- h44 - used in Forslund-Rohsenow equation:
c         h44 = 0.154*(gc*rhof*rhog**2*hfg*kf**3/(ug*sigma))**0.25
c
c---- h55 - used in Zuber pool boiling equation:
c         h55 = 0.15*hfg*sqrt(gc*rhog)*(sigma*(rhof-rhog))**0.25
c
c---- h66 - used in Henry contact temperature modification:
c         h66 = 0.42*(hfg*sqrt(kf*rhof*cpf)**0.6
          h11  = hh1(iprops)  + fract * (hh1(iprops+1)-hh1(iprops))
          h22  = hh2(iprops)  + fract * (hh2(iprops+1)-hh2(iprops))
```

```
          h33  = hh3(iprops)  + fract * (hh3(iprops+1)-hh3(iprops))
          h44  = hh4(iprops)  + fract * (hh4(iprops+1)-hh4(iprops))
          h55  = hh5(iprops)  + fract * (hh5(iprops+1)-hh5(iprops))
          h66  = hh6(iprops)  + fract * (hh6(iprops+1)-hh6(iprops))

c---- Homogeneous nucleation temperature
          dp  = 3203.6 - p
          dp2 = dp * dp
          dp3 = dp2 * dp
          thn = 705.44 - 4.722e-2 * dp + 2.3907e-5 * dp2 -5.8193e-9*dp3

c---- Inverse derivative of vapor specific volume with respect to enthalpy
          dvidh = c4 + c5 * p + c6 / p

          tfold = tf
          rhofold = rhof
          cpfold = cpf
          kfold = kf
          ufold = uf
          rhogold = rhog
          kgold = kg
          ugold = ug
          sigmaold = sigma
      endif
c----Pressure ABOVE 16.5MPA use the 17MPA property table
      if(p.ge.2393)then
```

```
          plimitlow = 2393
          plimithigh = 2466
          pramp = max(0.0,min(1.0,(p-plimitlow)/(plimithigh-plimitlow)))

          iprops = (hf - 10.) / 10 + 1
          iprops = iprops - iprops / nprop
          fract = (hf - hhlsup(iprops)) / 10.
c---- Saturation temperature
          tf = tlsup17(iprops)+fract*(tlsup17(iprops+1)-tlsup17(iprops))
c---- Densities
          rhof = rsup17(iprops)+fract*(rsup17(iprops+1)-rsup17(iprops))
c---- Specific heat capacity
          cpf  = csup17(iprops)+fract*(csup17(iprops+1)-csup17(iprops))
c---- Thermal conductivities
          kf   = ksup17(iprops)+fract*(ksup17(iprops+1)-ksup17(iprops))
c---- Dynamcic viscosities
          uf   = usup17(iprops)+fract*(usup17(iprops+1)-usup17(iprops))

          if(iprops.ge.90)then
              iprops = 89
              fract = 1.0
          endif
c---- Surface tension
          sigma= ssigma(iprops)+fract*(ssigma(iprops+1)-ssigma(iprops))

          h11  = hh1(iprops)  + fract * (hh1(iprops+1)-hh1(iprops))
```

```
          h22  = hh2(iprops)  + fract * (hh2(iprops+1)-hh2(iprops))
          h33  = hh3(iprops)  + fract * (hh3(iprops+1)-hh3(iprops))
          h44  = hh4(iprops)  + fract * (hh4(iprops+1)-hh4(iprops))
          h55  = hh5(iprops)  + fract * (hh5(iprops+1)-hh5(iprops))
          h66  = hh6(iprops)  + fract * (hh6(iprops+1)-hh6(iprops))

c---- Homogeneous nucleation temperature
          dp  = 3203.6 - p
          dp2 = dp * dp
          dp3 = dp2 * dp
          thn = 705.44 - 4.722e-2 * dp + 2.3907e-5 * dp2 -5.8193e-9*dp3

c---- Inverse derivative of vapor specific volume with respect to enthalpy
          dvidh = c4 + c5 * p + c6 / p

          iprops = (hg - 10.) / 10 + 1
          iprops = iprops - iprops / nprop
          fract = (hg - hhlsup(iprops)) / 10.

          rhog = rsup17(iprops)+fract*(rsup17(iprops+1)-rsup17(iprops))
          kg   = ksup17(iprops)+fract*(ksup17(iprops+1)-ksup17(iprops))
          ug   = usup17(iprops)+fract*(usup17(iprops+1)-usup17(iprops))

          tf = (1-pramp)*tfold + pramp*tf
          rhof = (1-pramp)*rhofold + pramp*rhof
          kf = (1-pramp)*kfold + pramp*kf
```

```
          uf = (1-pramp)*ufold + pramp*uf
          rhog = (1-pramp)*rhogold + pramp*rhog
          kg = (1-pramp)*kgold + pramp*kg
          ug = (1-pramp)*ugold + pramp*ug
          sigma = (1-pramp)*sigmaold + pramp*sigma

          tfold = tf
          rhofold = rhof
          cpfold = cpf
          kfold = kf
          ufold = uf
          rhogold = rhog
          kgold = kg
          ugold = ug
          sigmaold = sigma
c---- Difference of specific volumes for saturated vapor and saturated
c---- liquid
          vfg  = 1./rhog - 1./rhof
      endif
c----Pressure ABOVE 21MPA use the 21.9MPA property table
      if(p.ge.3045)then
          plimitlow = 3045
          plimithigh = 3118
          pramp = max(0.0,min(1.0,(p-plimitlow)/(plimithigh-plimitlow)))

          iprops = (hf - 10.) / 10 + 1
```

```
          iprops = iprops - iprops / nprop
          fract = (hf - hhlsup(iprops)) / 10.
c---- Saturation temperature
          tf = tlsup21(iprops)+fract*(tlsup21(iprops+1)-tlsup21(iprops))
c---- Densities
          rhof = rsup21(iprops)+fract*(rsup21(iprops+1)-rsup21(iprops))
c---- Specific heat capacity
          cpf  = csup21(iprops)+fract*(csup21(iprops+1)-csup21(iprops))
c---- Thermal conductivities
          kf   = ksup21(iprops)+fract*(ksup21(iprops+1)-ksup21(iprops))
c---- Dynamcic viscosities
          uf   = usup21(iprops)+fract*(usup21(iprops+1)-usup21(iprops))

          if(iprops.ge.90)then
              iprops = 89
              fract = 1.0
          endif
c---- Surface tension
          sigma= ssigma(iprops) +fract*(ssigma(iprops+1)-ssigma(iprops))

          h11  = hh1(iprops)  + fract * (hh1(iprops+1)-hh1(iprops))
          h22  = hh2(iprops)  + fract * (hh2(iprops+1)-hh2(iprops))
          h33  = hh3(iprops)  + fract * (hh3(iprops+1)-hh3(iprops))
          h44  = hh4(iprops)  + fract * (hh4(iprops+1)-hh4(iprops))
          h55  = hh5(iprops)  + fract * (hh5(iprops+1)-hh5(iprops))
          h66  = hh6(iprops)  + fract * (hh6(iprops+1)-hh6(iprops))
```

```
c---- Homogeneous nucleation temperature
          dp  = 3203.6 - p
          dp2 = dp * dp
          dp3 = dp2 * dp
          thn = 705.44 - 4.722e-2 * dp + 2.3907e-5 * dp2 -5.8193e-9*dp3

c---- Inverse derivative of vapor specific volume with respect to enthalpy
          dvidh = c4 + c5 * p + c6 / p

          iprops = (hg - 10.) / 10 + 1
          iprops = iprops - iprops / nprop
          fract = (hg - hhlsup(iprops)) / 10.

          rhog = rsup21(iprops)+fract*(rsup21(iprops+1)-rsup21(iprops))
          kg   = ksup21(iprops)+fract*(ksup21(iprops+1)-ksup21(iprops))
          ug   = usup21(iprops)+fract*(usup21(iprops+1)-usup21(iprops))

          tf = (1-pramp)*tfold + pramp*tf
          rhof = (1-pramp)*rhofold + pramp*rhof
          kf = (1-pramp)*kfold + pramp*kf
          uf = (1-pramp)*ufold + pramp*uf
          rhog = (1-pramp)*rhogold + pramp*rhog
          kg = (1-pramp)*kgold + pramp*kg
          ug = (1-pramp)*ugold + pramp*ug
          sigma = (1-pramp)*sigmaold + pramp*sigma
```

```
          tfold = tf
          rhofold = rhof
          cpfold = cpf
          kfold = kf
          ufold = uf
          rhogold = rhog
          kgold = kg
          ugold = ug
          sigmaold = sigma

c---- Difference of specific volumes for saturated vapor and saturated
c---- liquid
          vfg  = 1./rhog - 1./rhof
      endif
c----Pressure ABOVE 22MPA use the 22.1MPA property table
      if(p.ge.3190)then
          plimitlow = 3190
          plimithigh = 3205
          pramp = max(0.0,min(1.0,(p-plimitlow)/(plimithigh-plimitlow)))

          iprops = (hf - 10.) / 10 + 1
          iprops = iprops - iprops / nprop
          fract = (hf - hhlsup(iprops)) / 10.
c---- Saturation temperature
          tf = tlsup22(iprops)+fract*(tlsup22(iprops+1)-tlsup22(iprops))
```

```
c---- Densities
          rhof = rsup22(iprops)+fract*(rsup22(iprops+1)-rsup22(iprops))
c---- Specific heat capacity
          cpf  = csup22(iprops)+fract*(csup22(iprops+1)-csup22(iprops))
c---- Thermal conductivities
          kf   = ksup22(iprops)+fract*(ksup22(iprops+1)-ksup22(iprops))
c---- Dynamcic viscosities
          uf   = usup22(iprops)+fract*(usup22(iprops+1)-usup22(iprops))

          if(iprops.ge.90)then
              iprops = 89
              fract = 1.0
          endif
c---- Surface tension
          sigma= ssigma(iprops) +fract*(ssigma(iprops+1)-ssigma(iprops))

          h11  = hh1(iprops)  + fract * (hh1(iprops+1)-hh1(iprops))
          h22  = hh2(iprops)  + fract * (hh2(iprops+1)-hh2(iprops))
          h33  = hh3(iprops)  + fract * (hh3(iprops+1)-hh3(iprops))
          h44  = hh4(iprops)  + fract * (hh4(iprops+1)-hh4(iprops))
          h55  = hh5(iprops)  + fract * (hh5(iprops+1)-hh5(iprops))
          h66  = hh6(iprops)  + fract * (hh6(iprops+1)-hh6(iprops))

c---- Homogeneous nucleation temperature
          dp  = 0
          dp2 = dp * dp
```

```
          dp3 = dp2 * dp
          thn = 705.44 - 4.722e-2 * dp + 2.3907e-5 * dp2 -5.8193e-9*dp3

c---- Inverse derivative of vapor specific volume with respect to enthalpy
          dvidh = c4 + c5 * p + c6 / p

          iprops = (hg - 10.) / 10 + 1
          iprops = iprops - iprops / nprop
          fract = (hg - hhlsup(iprops)) / 10.

          rhog = rsup22(iprops)+fract*(rsup22(iprops+1)-rsup22(iprops))
          kg   = ksup22(iprops)+fract*(ksup22(iprops+1)-ksup22(iprops))
          ug   = usup22(iprops)+fract*(usup22(iprops+1)-usup22(iprops))

          tf = (1-pramp)*tfold + pramp*tf
          rhof = (1-pramp)*rhofold + pramp*rhof
          kf = (1-pramp)*kfold + pramp*kf
          uf = (1-pramp)*ufold + pramp*uf
          rhog = (1-pramp)*rhogold + pramp*rhog
          kg = (1-pramp)*kgold + pramp*kg
          ug = (1-pramp)*ugold + pramp*ug
          sigma = (1-pramp)*sigmaold + pramp*sigma

          tfold = tf
          rhofold = rhof
          cpfold = cpf
```

```
          kfold = kf
          ufold = uf
          rhogold = rhog
          kgold = kg
          ugold = ug
          sigmaold = sigma

c---- Difference of specific volumes for saturated vapor and saturated
c---- liquid
          vfg  = 1./rhog - 1./rhof
      endif
c----Pressure ABOVE 22.5MPA use the 23MPA property table
      if(p.ge.3263)then
          plimitlow = 3263
          plimithigh = 3336
          pramp = max(0.0,min(1.0,(p-plimitlow)/(plimithigh-plimitlow)))

          iprops = (hf - 10.) / 10 + 1
          iprops = iprops - iprops / nprop
          fract = (hf - hhlsup(iprops)) / 10.
c---- Saturation temperature
          tf = tlsup23(iprops)+fract*(tlsup23(iprops+1)-tlsup23(iprops))
c---- Densities
          rhof = rsup23(iprops)+fract*(rsup23(iprops+1)-rsup23(iprops))
c---- Specific heat capacity
          cpf  = csup23(iprops)+fract*(csup23(iprops+1)-csup23(iprops))
```

```
c---- Thermal conductivities
          kf   = ksup23(iprops)+fract*(ksup23(iprops+1)-ksup23(iprops))
c---- Dynamcic viscosities
          uf   = usup23(iprops)+fract*(usup23(iprops+1)-usup23(iprops))


          if(iprops.ge.90)then
              iprops = 89
              fract = 1.0
          endif
c---- Surface tension
          sigma= ssigma(iprops) +fract*(ssigma(iprops+1)-ssigma(iprops))


          h11  = hh1(iprops)  + fract * (hh1(iprops+1)-hh1(iprops))
          h22  = hh2(iprops)  + fract * (hh2(iprops+1)-hh2(iprops))
          h33  = hh3(iprops)  + fract * (hh3(iprops+1)-hh3(iprops))
          h44  = hh4(iprops)  + fract * (hh4(iprops+1)-hh4(iprops))
          h55  = hh5(iprops)  + fract * (hh5(iprops+1)-hh5(iprops))
          h66  = hh6(iprops)  + fract * (hh6(iprops+1)-hh6(iprops))


c---- Homogeneous nucleation temperature
          dp  = 0
          dp2 = dp * dp
          dp3 = dp2 * dp
          thn = 705.44 - 4.722e-2 * dp + 2.3907e-5 * dp2 -5.8193e-9*dp3


c---- Inverse derivative of vapor specific volume with respect to enthalpy
```

```
dvidh = c4 + c5 * p + c6 / p


iprops = (hg - 10.) / 10 + 1
iprops = iprops - iprops / nprop
fract = (hg - hhlsup(iprops)) / 10.


rhog = rsup23(iprops)+fract*(rsup23(iprops+1)-rsup23(iprops))
kg   = ksup23(iprops)+fract*(ksup23(iprops+1)-ksup23(iprops))
ug   = usup23(iprops)+fract*(usup23(iprops+1)-usup23(iprops))


tf = (1-pramp)*tfold + pramp*tf
rhof = (1-pramp)*rhofold + pramp*rhof
kf = (1-pramp)*kfold + pramp*kf
uf = (1-pramp)*ufold + pramp*uf
rhog = (1-pramp)*rhogold + pramp*rhog
kg = (1-pramp)*kgold + pramp*kg
ug = (1-pramp)*ugold + pramp*ug
sigma = (1-pramp)*sigmaold + pramp*sigma


tfold = tf
rhofold = rhof
cpfold = cpf
kfold = kf
ufold = uf
rhogold = rhog
kgold = kg
```

```
          ugold = ug
          sigmaold = sigma

c---- Difference of specific volumes for saturated vapor and saturated
c---- liquid
          vfg  = 1./rhog - 1./rhof

      endif
c----Pressure ABOVE 23.5MPA use the 24MPA property table
      if(p.ge.3408)then
          plimitlow = 3408
          plimithigh = 3481
          pramp = max(0.0,min(1.0,(p-plimitlow)/(plimithigh-plimitlow)))

          iprops = (hf - 10.) / 10 + 1
          iprops = iprops - iprops / nprop
          fract = (hf - hhlsup(iprops)) / 10.
c---- Saturation temperature
          tf = tlsup24(iprops)+fract*(tlsup24(iprops+1)-tlsup24(iprops))
c---- Densities
          rhof = rsup24(iprops)+fract*(rsup24(iprops+1)-rsup24(iprops))
c---- Specific heat capacity
          cpf  = csup24(iprops)+fract*(csup24(iprops+1)-csup24(iprops))
c---- Thermal conductivities
          kf   = ksup24(iprops)+fract*(ksup24(iprops+1)-ksup24(iprops))
c---- Dynamcic viscosities
```

```
          uf   = usup24(iprops)+fract*(usup24(iprops+1)-usup24(iprops))

          if(iprops.ge.90)then
              iprops = 89
              fract = 1.0
          endif
c---- Surface tension
          sigma= ssigma(iprops) +fract*(ssigma(iprops+1)-ssigma(iprops))

          h11  = hh1(iprops)  + fract * (hh1(iprops+1)-hh1(iprops))
          h22  = hh2(iprops)  + fract * (hh2(iprops+1)-hh2(iprops))
          h33  = hh3(iprops)  + fract * (hh3(iprops+1)-hh3(iprops))
          h44  = hh4(iprops)  + fract * (hh4(iprops+1)-hh4(iprops))
          h55  = hh5(iprops)  + fract * (hh5(iprops+1)-hh5(iprops))
          h66  = hh6(iprops)  + fract * (hh6(iprops+1)-hh6(iprops))

c---- Homogeneous nucleation temperature
          dp  = 0
          dp2 = dp * dp
          dp3 = dp2 * dp
          thn = 705.44 - 4.722e-2 * dp + 2.3907e-5 * dp2 -5.8193e-9*dp3

c---- Inverse derivative of vapor specific volume with respect to enthalpy
          dvidh = c4 + c5 * p + c6 / p

          iprops = (hg - 10.) / 10 + 1
```

```
iprops = iprops - iprops / nprop
fract = (hg - hhlsup(iprops)) / 10.

rhog = rsup24(iprops)+fract*(rsup24(iprops+1)-rsup24(iprops))
kg   = ksup24(iprops)+fract*(ksup24(iprops+1)-ksup24(iprops))
ug   = usup24(iprops)+fract*(usup24(iprops+1)-usup24(iprops))



tf = (1-pramp)*tfold + pramp*tf
rhof = (1-pramp)*rhofold + pramp*rhof
kf = (1-pramp)*kfold + pramp*kf
uf = (1-pramp)*ufold + pramp*uf
rhog = (1-pramp)*rhogold + pramp*rhog
kg = (1-pramp)*kgold + pramp*kg
ug = (1-pramp)*ugold + pramp*ug
sigma = (1-pramp)*sigmaold + pramp*sigma

tfold = tf
rhofold = rhof
cpfold = cpf
kfold = kf
ufold = uf
rhogold = rhog
kgold = kg
ugold = ug
sigmaold = sigma
```

```
c---- Difference of specific volumes for saturated vapor and saturated
c---- liquid
          vfg  = 1./rhog - 1./rhof
      endif
c----Pressure ABOVE 24.5MPA use the 25MPA property table
      if(p.ge.3553)then
          plimitlow = 3553
          plimithigh = 3626
          pramp = max(0.0,min(1.0,(p-plimitlow)/(plimithigh-plimitlow)))

          iprops = (hf - 10.) / 10 + 1
          iprops = iprops - iprops / nprop
          fract = (hf - hhlsup(iprops)) / 10.
c---- Saturation temperature
          tf = tlsup25(iprops)+fract*(tlsup25(iprops+1)-tlsup25(iprops))
c---- Densities
          rhof = rsup25(iprops)+fract*(rsup25(iprops+1)-rsup25(iprops))
c---- Specific heat capacity
          cpf  = csup25(iprops)+fract*(csup25(iprops+1)-csup25(iprops))
c---- Thermal conductivities
          kf   = ksup25(iprops)+fract*(ksup25(iprops+1)-ksup25(iprops))
c---- Dynamcic viscosities
          uf   = usup25(iprops)+fract*(usup25(iprops+1)-usup25(iprops))

          if(iprops.ge.90)then
```

```
              iprops = 89
              fract = 1.0
          endif
c---- Surface tension
          sigma= ssigma(iprops) +fract*(ssigma(iprops+1)-ssigma(iprops))

          h11  = hh1(iprops)  + fract * (hh1(iprops+1)-hh1(iprops))
          h22  = hh2(iprops)  + fract * (hh2(iprops+1)-hh2(iprops))
          h33  = hh3(iprops)  + fract * (hh3(iprops+1)-hh3(iprops))
          h44  = hh4(iprops)  + fract * (hh4(iprops+1)-hh4(iprops))
          h55  = hh5(iprops)  + fract * (hh5(iprops+1)-hh5(iprops))
          h66  = hh6(iprops)  + fract * (hh6(iprops+1)-hh6(iprops))

c---- Homogeneous nucleation temperature
          dp  = 0
          dp2 = dp * dp
          dp3 = dp2 * dp
          thn = 705.44 - 4.722e-2 * dp + 2.3907e-5 * dp2 -5.8193e-9*dp3

c---- Inverse derivative of vapor specific volume with respect to enthalpy
          dvidh = c4 + c5 * p + c6 / p

          iprops = (hg - 10.) / 10 + 1
          iprops = iprops - iprops / nprop
          fract = (hg - hhlsup(iprops)) / 10.
```

```
          rhog = rsup25(iprops)+fract*(rsup25(iprops+1)-rsup25(iprops))
          kg   = ksup25(iprops)+fract*(ksup25(iprops+1)-ksup25(iprops))
          ug   = usup25(iprops)+fract*(usup25(iprops+1)-usup25(iprops))

          tf = (1-pramp)*tfold + pramp*tf
          rhof = (1-pramp)*rhofold + pramp*rhof
          kf = (1-pramp)*kfold + pramp*kf
          uf = (1-pramp)*ufold + pramp*uf
          rhog = (1-pramp)*rhogold + pramp*rhog
          kg = (1-pramp)*kgold + pramp*kg
          ug = (1-pramp)*ugold + pramp*ug
          sigma = (1-pramp)*sigmaold + pramp*sigma

          tfold = tf
          rhofold = rhof
          cpfold = cpf
          kfold = kf
          ufold = uf
          rhogold = rhog
          kgold = kg
          ugold = ug
          sigmaold = sigma

c---- Difference of specific volumes for saturated vapor and saturated
c---- liquid
          vfg  = 1./rhog - 1./rhof
```

```
      endif


c----Pressure ABOVE 25.5MPA use the 26MPA property table
      if(p.ge.3698)then
          plimitlow = 3698
          plimithigh = 3771
          pramp = max(0.0,min(1.0,(p-plimitlow)/(plimithigh-plimitlow)))


          iprops = (hf - 10.) / 10 + 1
          iprops = iprops - iprops / nprop
          fract = (hf - hhlsup(iprops)) / 10.
c---- Saturation temperature
          tf = tlsup26(iprops)+fract*(tlsup26(iprops+1)-tlsup26(iprops))
c---- Densities
          rhof = rsup26(iprops)+fract*(rsup26(iprops+1)-rsup26(iprops))
c---- Specific heat capacity
          cpf  = csup26(iprops)+fract*(csup26(iprops+1)-csup26(iprops))
c---- Thermal conductivities
          kf   = ksup26(iprops)+fract*(ksup26(iprops+1)-ksup26(iprops))
c---- Dynamcic viscosities
          uf   = usup26(iprops)+fract*(usup26(iprops+1)-usup26(iprops))


          if(iprops.ge.90)then
              iprops = 89
              fract = 1.0
          endif
```

```
c---- Surface tension
          sigma= ssigma(iprops) +fract*(ssigma(iprops+1)-ssigma(iprops))

          h11  = hh1(iprops)  + fract * (hh1(iprops+1)-hh1(iprops))
          h22  = hh2(iprops)  + fract * (hh2(iprops+1)-hh2(iprops))
          h33  = hh3(iprops)  + fract * (hh3(iprops+1)-hh3(iprops))
          h44  = hh4(iprops)  + fract * (hh4(iprops+1)-hh4(iprops))
          h55  = hh5(iprops)  + fract * (hh5(iprops+1)-hh5(iprops))
          h66  = hh6(iprops)  + fract * (hh6(iprops+1)-hh6(iprops))

c---- Homogeneous nucleation temperature
          dp  = 0
          dp2 = dp * dp
          dp3 = dp2 * dp
          thn = 705.44 - 4.722e-2 * dp + 2.3907e-5 * dp2 -5.8193e-9*dp3

c---- Inverse derivative of vapor specific volume with respect to enthalpy
          dvidh = c4 + c5 * p + c6 / p

          iprops = (hg - 10.) / 10 + 1
          iprops = iprops - iprops / nprop
          fract = (hg - hhlsup(iprops)) / 10.

          rhog = rsup26(iprops)+fract*(rsup26(iprops+1)-rsup26(iprops))
          kg   = ksup26(iprops)+fract*(ksup26(iprops+1)-ksup26(iprops))
          ug   = usup26(iprops)+fract*(usup26(iprops+1)-usup26(iprops))
```

```
          tf = (1-pramp)*tfold + pramp*tf
          rhof = (1-pramp)*rhofold + pramp*rhof
          kf = (1-pramp)*kfold + pramp*kf
          uf = (1-pramp)*ufold + pramp*uf
          rhog = (1-pramp)*rhogold + pramp*rhog
          kg = (1-pramp)*kgold + pramp*kg
          ug = (1-pramp)*ugold + pramp*ug
          sigma = (1-pramp)*sigmaold + pramp*sigma

          tfold = tf
          rhofold = rhof
          cpfold = cpf
          kfold = kf
          ufold = uf
          rhogold = rhog
          kgold = kg
          ugold = ug
          sigmaold = sigma

c---- Difference of specific volumes for saturated vapor and saturated
c---- liquid
          vfg  = 1./rhog - 1./rhof
      endif
```

In modified COBRA-TF the subcooled liquid properties are calculated similar to the liquid and vapour saturation properties mentioned above. The subcooled liquid properties are

determined using 8 intrinsic property tables, one for each pressure interval mentioned above. The subcooled liquid properties for both subcritical and supercritical flow are calculated by replacing the code segment from line #154 to 179 of the original subroutine with the code segment,

```
c-----------------------------------------------------------------
c---- Subcooled liquid properties
c---- (only as a function of enthalpy h /
c----  dependence from pressure p neglected, because very small)
c-----------------------------------------------------------------
c---- Determine index and fraction for table interpolation
      if(p.ge.0)then
          iprops = (hliq-10.)/10 + 1
          if (iprops.lt.1)  write(iout,10000)
10000 format(//,5x,'***** trouble calculating subcooled liquid',
     &       ' properties in subroutine prop *****',//,
     &       10x,'- liquid enthalpy is less than 10.0',/,
     &       10x,'- partial pressure of vapor is probably too low',/,
     &       10x,'- make sure vfrac(2)*pref is a partial pressure',
     &       10x,'  that gives a reasonable relative humidity (30%)')
          if(iprops.ge.90)then
            iprops = 89
            fracs = 1.0
          else
            fracs = (hliq - hhf(iprops)) / 10.
          endif
c---- Temperature (must not be greater than saturation temperature)
```

```
          tl  = tt(iprops) + fracs * (tt(iprops+1)-tt(iprops))
          tl  = min(tl,tf)
c---- Specific heat capacity
          cpl = cpff(iprops) + fracs * (cpff(iprops+1)-cpff(iprops))
c---- Thermal conductivity
          kl  = kkf(iprops)  + fracs * (kkf(iprops+1)-kkf(iprops))
c---- Dynamic viscosity
          ul  = uuf(iprops)  + fracs * (uuf(iprops+1)-uuf(iprops))

          tlold = tl
          cplold = cpl
          klold = kl
          ulold = ul
      endif
c----Pressure ABOVE 16.5MPA use the 17MPA property table
      if(p.ge.2393)then
          iprops = (hliq-10.)/10 + 1
          if (iprops.lt.1)  write(iout,10001)
10001 format(//,5x,'***** trouble calculating subcooled liquid',
     &       ' properties in subroutine prop *****',//,
     &       10x,'- liquid enthalpy is less than 10.0',/,
     &       10x,'- partial pressure of vapor is probably too low',/,
     &       10x,'- make sure vfrac(2)*pref is a partial pressure',
     &       10x,'  that gives a reasonable relative humidity (30%)')
          fracs = (hliq - hhlsup(iprops)) / 10.
c---- Temperature (must not be greater than saturation temperature)
```

```
          tl  =tlsup17(iprops)+fracs*(tlsup17(iprops+1)-tlsup17(iprops))
          tl  =min(tl,tf)
c---- Specific heat capacity
          cpl = csup17(iprops) + fracs*(csup17(iprops+1)-csup17(iprops))
c---- Thermal conductivity
          kl  = ksup17(iprops) + fracs*(ksup17(iprops+1)-ksup17(iprops))
c---- Dynamic viscosity
          ul  = usup17(iprops) + fracs*(usup17(iprops+1)-usup17(iprops))

          tl = (1-pramp)*tlold + pramp*tl
          cpl = (1-pramp)*cplold + pramp*cpl
          kl = (1-pramp)*klold + pramp*kl
          ul = (1-pramp)*ulold + pramp*ul

          tlold = tl
          cplold = cpl
          klold = kl
          ulold = ul
      endif
c----Pressure ABOVE 21MPA use the 21.9MPA property table
      if(p.ge.3045)then
          iprops = (hliq-10.)/10 + 1
          if (iprops.lt.1)  write(iout,10006)
10006 format(//,5x,'***** trouble calculating subcooled liquid',
     &       ' properties in subroutine prop *****',//,
     &       10x,'- liquid enthalpy is less than 10.0',/,
```

```
     &       10x,'- partial pressure of vapor is probably too low',/,
     &       10x,'- make sure vfrac(2)*pref is a partial pressure',
     &       10x,'  that gives a reasonable relative humidity (30%)')
          fracs = (hliq - hhlsup(iprops)) / 10.
c---- Temperature (must not be greater than saturation temperature)
          tl  =tlsup21(iprops)+fracs*(tlsup21(iprops+1)-tlsup21(iprops))
          tl  =min(tl,tf)
c---- Specific heat capacity
          cpl = csup21(iprops) + fracs*(csup21(iprops+1)-csup21(iprops))
c---- Thermal conductivity
          kl  = ksup21(iprops) + fracs*(ksup21(iprops+1)-ksup21(iprops))
c---- Dynamic viscosity
          ul  = usup21(iprops) + fracs*(usup21(iprops+1)-usup21(iprops))


          tl = (1-pramp)*tlold + pramp*tl
          cpl = (1-pramp)*cplold + pramp*cpl
          kl = (1-pramp)*klold + pramp*kl
          ul = (1-pramp)*ulold + pramp*ul


          tlold = tl
          cplold = cpl
          klold = kl
          ulold = ul
      endif
c----Pressure ABOVE 22MPA use the 22.1MPA property table
      if(p.ge.3190)then
```

```
          iprops = (hliq-10.)/10 + 1
          if (iprops.lt.1)  write(iout,10002)
10002 format(//,5x,'***** trouble calculating subcooled liquid',
     &       ' properties in subroutine prop *****',//,
     &       10x,'- liquid enthalpy is less than 10.0',/,
     &       10x,'- partial pressure of vapor is probably too low',/,
     &       10x,'- make sure vfrac(2)*pref is a partial pressure',
     &       10x,'  that gives a reasonable relative humidity (30%)')
          fracs = (hliq - hhlsup(iprops)) / 10.
c---- Temperature (must not be greater than saturation temperature)
          tl  =tlsup22(iprops)+fracs*(tlsup22(iprops+1)-tlsup22(iprops))
          tl  =min(tl,tf)
c---- Specific heat capacity
          cpl = csup22(iprops) + fracs*(csup22(iprops+1)-csup22(iprops))
c---- Thermal conductivity
          kl  = ksup22(iprops) + fracs*(ksup22(iprops+1)-ksup22(iprops))
c---- Dynamic viscosity
          ul  = usup22(iprops) + fracs*(usup22(iprops+1)-usup22(iprops))


          tl = (1-pramp)*tlold + pramp*tl
          cpl = (1-pramp)*cplold + pramp*cpl
          kl = (1-pramp)*klold + pramp*kl
          ul = (1-pramp)*ulold + pramp*ul


          tlold = tl
          cplold = cpl
```

```
          klold = kl
          ulold = ul
      endif
c----Pressure ABOVE 22.5MPA use the 23MPA property table
      if(p.ge.3263)then
          iprops = (hliq-10.)/10 + 1
          if (iprops.lt.1)  write(iout,10003)
10003 format(//,5x,'***** trouble calculating subcooled liquid',
     &       ' properties in subroutine prop *****',//,
     &       10x,'- liquid enthalpy is less than 10.0',/,
     &       10x,'- partial pressure of vapor is probably too low',/,
     &       10x,'- make sure vfrac(2)*pref is a partial pressure',
     &       10x,'  that gives a reasonable relative humidity (30%)')
          fracs = (hliq - hhlsup(iprops)) / 10.
c---- Temperature (must not be greater than saturation temperature)
          tl  =tlsup23(iprops)+fracs*(tlsup23(iprops+1)-tlsup23(iprops))
          tl  =min(tl,tf)
c---- Specific heat capacity
          cpl = csup23(iprops) + fracs*(csup23(iprops+1)-csup23(iprops))
c---- Thermal conductivity
          kl  = ksup23(iprops) + fracs*(ksup23(iprops+1)-ksup23(iprops))
c---- Dynamic viscosity
          ul  = usup23(iprops) + fracs*(usup23(iprops+1)-usup23(iprops))

          tl = (1-pramp)*tlold + pramp*tl
          cpl = (1-pramp)*cplold + pramp*cpl
```

```
          kl = (1-pramp)*klold + pramp*kl
          ul = (1-pramp)*ulold + pramp*ul

          tlold = tl
          cplold = cpl
          klold = kl
          ulold = ul
      endif
c----Pressure ABOVE 23.5MPA use the 24MPA property table
      if(p.ge.3408)then
          iprops = (hliq-10.)/10 + 1
          if (iprops.lt.1)  write(iout,10005)
10005 format(//,5x,'***** trouble calculating subcooled liquid',
     &       ' properties in subroutine prop *****',//,
     &       10x,'- liquid enthalpy is less than 10.0',/,
     &       10x,'- partial pressure of vapor is probably too low',/,
     &       10x,'- make sure vfrac(2)*pref is a partial pressure',
     &       10x,'  that gives a reasonable relative humidity (30%)')
          fracs = (hliq - hhlsup(iprops)) / 10.
c---- Temperature (must not be greater than saturation temperature)
          tl  =tlsup24(iprops)+fracs*(tlsup24(iprops+1)-tlsup24(iprops))
          tl  =min(tl,tf)
c---- Specific heat capacity
          cpl = csup24(iprops) + fracs*(csup24(iprops+1)-csup24(iprops))
c---- Thermal conductivity
          kl  = ksup24(iprops) + fracs*(ksup24(iprops+1)-ksup24(iprops))
```

```
c---- Dynamic viscosity
          ul  = usup24(iprops) + fracs*(usup24(iprops+1)-usup24(iprops))


          tl = (1-pramp)*tlold + pramp*tl
          cpl = (1-pramp)*cplold + pramp*cpl
          kl = (1-pramp)*klold + pramp*kl
          ul = (1-pramp)*ulold + pramp*ul


          tlold = tl
          cplold = cpl
          klold = kl
          ulold = ul
      endif
c----Pressure ABOVE 24.5MPA use the 25MPA property table
      if(p.ge.3553)then
          iprops = (hliq-10.)/10 + 1
          if (iprops.lt.1)  write(iout,10004)
10004 format(//,5x,'***** trouble calculating subcooled liquid',
     &       ' properties in subroutine prop *****',//,
     &       10x,'- liquid enthalpy is less than 10.0',/,
     &       10x,'- partial pressure of vapor is probably too low',/,
     &       10x,'- make sure vfrac(2)*pref is a partial pressure',
     &       10x,'  that gives a reasonable relative humidity (30%)')
          fracs = (hliq - hhlsup(iprops)) / 10.
c---- Temperature (must not be greater than saturation temperature)
          tl  =tlsup25(iprops)+fracs*(tlsup25(iprops+1)-tlsup25(iprops))
```

```
          tl  =min(tl,tf)
c---- Specific heat capacity
          cpl = csup25(iprops) + fracs*(csup25(iprops+1)-csup25(iprops))
c---- Thermal conductivity
          kl  = ksup25(iprops) + fracs*(ksup25(iprops+1)-ksup25(iprops))
c---- Dynamic viscosity
          ul  = usup25(iprops) + fracs*(usup25(iprops+1)-usup25(iprops))

          tl = (1-pramp)*tlold + pramp*tl
          cpl = (1-pramp)*cplold + pramp*cpl
          kl = (1-pramp)*klold + pramp*kl
          ul = (1-pramp)*ulold + pramp*ul

          tlold = tl
          cplold = cpl
          klold = kl
          ulold = ul
      endif
c----Pressure ABOVE 25.5MPA use the 26MPA property table
      if(p.ge.3698)then
          iprops = (hliq-10.)/10 + 1
          if (iprops.lt.1)  write(iout,10007)
10007 format(//,5x,'***** trouble calculating subcooled liquid',
     &       ' properties in subroutine prop *****',//,
     &       10x,'- liquid enthalpy is less than 10.0',/,
     &       10x,'- partial pressure of vapor is probably too low',/,
```

```
     &       10x,'- make sure vfrac(2)*pref is a partial pressure',
     &       10x,'  that gives a reasonable relative humidity (30%)')
          fracs = (hliq - hhlsup(iprops)) / 10.
c---- Temperature (must not be greater than saturation temperature)
          tl  =tlsup26(iprops)+fracs*(tlsup26(iprops+1)-tlsup26(iprops))
          tl  =min(tl,tf)
c---- Specific heat capacity
          cpl = csup26(iprops) + fracs*(csup26(iprops+1)-csup26(iprops))
c---- Thermal conductivity
          kl  = ksup26(iprops) + fracs*(ksup26(iprops+1)-ksup26(iprops))
c---- Dynamic viscosity
          ul  = usup26(iprops) + fracs*(usup26(iprops+1)-usup26(iprops))

          tl = (1-pramp)*tlold + pramp*tl
          cpl = (1-pramp)*cplold + pramp*cpl
          kl = (1-pramp)*klold + pramp*kl
          ul = (1-pramp)*ulold + pramp*ul

          tlold = tl
          cplold = cpl
          klold = kl
          ulold = ul
      endif
c---- Prandtl number
          prl = cpl * ul / kl
```

PART 2 of the PROP subroutine determines vapour properties at a pressure p and enthalpy h. The PART 2 of the subroutine also requires the calculation of saturation temperature and saturation density of water. These properties are also determined using the 8 intrinsic property tables mentioned above by replacing the code segment from line # 182 to 196 of the original subroutine with the code segment,

```
c=====================================================================
c     Part 2 (ipart = 1 or ipart = 2)
c     ------
c     - vapor properties at pressure p and enthalpy h
c=====================================================================
c---- Set saturation temperature
 200  continue
      if (ipart.eq.2) then
        hvap = param3
        if(p.lt.2393)then
            call curve(hf,p,hhf,pp,nprop,ierror,1)
            iprops = (hf-10.) / 10 + 1
            if(iprops.ge.90)then
                iprops = 89
                fracs = 1.0
            else
                fracs  = (hf-hhf(iprops)) / 10.
            endif
            tf     = tt(iprops) + fracs * (tt(iprops+1)-tt(iprops))
            rhog   = rhogg(iprops)+fracs*(rhogg(iprops+1)-rhogg(iprops))
        endif
```

```
if(p.ge.2393)then
    iprops = (hf-10.) / 10 + 1
    fracs  = (hf-hhlsup(iprops)) / 10.
    tf=tlsup17(iprops)+fracs*(tlsup17(iprops+1)-tlsup17(iprops))
    iprops = (hg-10.) / 10 + 1
    fracs  = (hg-hhlsup(iprops)) / 10.
    rhog=rsup17(iprops)+fracs*(rsup17(iprops+1)-rsup17(iprops))

    tfold = tf
    rhogold = rhog
endif
if(p.ge.3045)then
    plimitlow = 3045
    plimithigh = 3118
    prange = (plimithigh-plimitlow)
    pramp = max(0.0,min(1.0,(p-plimitlow)/prange))

    iprops = (hf-10.) / 10 + 1
    fracs  = (hf-hhlsup(iprops)) / 10.
    tf=tlsup21(iprops)+fracs*(tlsup21(iprops+1)-tlsup21(iprops))
    iprops = (hg-10.) / 10 + 1
    fracs  = (hg-hhlsup(iprops)) / 10.
    rhog=rsup21(iprops)+fracs*(rsup21(iprops+1)-rsup21(iprops))

    tf = (1-pramp)*tf + pramp*tf
    rhog = (1-pramp)*rhogold + pramp*rhog
```

```
        tfold = tf
        rhogold = rhog
    endif
    if(p.ge.3190)then
        plimitlow = 3190
        plimithigh = 3205
        prange = (plimithigh-plimitlow)
        pramp = max(0.0,min(1.0,(p-plimitlow)/prange))

        iprops = (hf-10.) / 10 + 1
        fracs  = (hf-hhlsup(iprops)) / 10.
        tf=tlsup22(iprops)+fracs*(tlsup22(iprops+1)-tlsup22(iprops))
        iprops = (hg-10.) / 10 + 1
        fracs  = (hg-hhlsup(iprops)) / 10.
        rhog=rsup22(iprops)+fracs*(rsup22(iprops+1)-rsup22(iprops))

        tf = (1-pramp)*tf + pramp*tf
        rhog = (1-pramp)*rhogold + pramp*rhog

        tfold = tf
        rhogold = rhog
    endif
    if(p.ge.3263)then
        plimitlow = 3263
        plimithigh = 3336
```

```
        prange = (plimithigh-plimitlow)
        pramp = max(0.0,min(1.0,(p-plimitlow)/prange))

        iprops = (hf-10.) / 10 + 1
        fracs  = (hf-hhlsup(iprops)) / 10.
        tf=tlsup23(iprops)+fracs*(tlsup23(iprops+1)-tlsup23(iprops))
        iprops = (hg-10.) / 10 + 1
        fracs  = (hg-hhlsup(iprops)) / 10.
        rhog=rsup23(iprops)+fracs*(rsup23(iprops+1)-rsup23(iprops))

        tf = (1-pramp)*tf + pramp*tf
        rhog = (1-pramp)*rhogold + pramp*rhog

        tfold = tf
        rhogold = rhog
    endif
    if(p.ge.3408)then
        plimitlow = 3408
        plimithigh = 3481
        prange = (plimithigh-plimitlow)
        pramp = max(0.0,min(1.0,(p-plimitlow)/prange))

        iprops = (hf-10.) / 10 + 1
        fracs  = (hf-hhlsup(iprops)) / 10.
        tf=tlsup24(iprops)+fracs*(tlsup24(iprops+1)-tlsup24(iprops))
        iprops = (hg-10.) / 10 + 1
```

```
        fracs  = (hg-hhlsup(iprops)) / 10.
        rhog=rsup24(iprops)+fracs*(rsup24(iprops+1)-rsup24(iprops))

        tf = (1-pramp)*tf + pramp*tf
        rhog = (1-pramp)*rhogold + pramp*rhog

        tfold = tf
        rhogold = rhog
    endif
    if(p.ge.3553)then
        plimitlow = 3553
        plimithigh = 3626
        prange = (plimithigh-plimitlow)
        pramp = max(0.0,min(1.0,(p-plimitlow)/prange))

        iprops = (hf-10.) / 10 + 1
        fracs  = (hf-hhlsup(iprops)) / 10.
        tf=tlsup25(iprops)+fracs*(tlsup25(iprops+1)-tlsup25(iprops))
        iprops = (hg-10.) / 10 + 1
        fracs  = (hg-hhlsup(iprops)) / 10.
        rhog=rsup25(iprops)+fracs*(rsup25(iprops+1)-rsup25(iprops))

        tf = (1-pramp)*tf + pramp*tf
        rhog = (1-pramp)*rhogold + pramp*rhog

        tfold = tf
```

```
            rhogold = rhog
        endif
        if(p.ge.3698)then
            plimitlow = 3698
            plimithigh = 3771
            prange = (plimithigh-plimitlow)
            pramp = max(0.0,min(1.0,(p-plimitlow)/prange))

            iprops = (hf-10.) / 10 + 1
            fracs  = (hf-hhlsup(iprops)) / 10.
            tf=tlsup26(iprops)+fracs*(tlsup26(iprops+1)-tlsup26(iprops))
            iprops = (hg-10.) / 10 + 1
            fracs  = (hg-hhlsup(iprops)) / 10.
            rhog=rsup26(iprops)+fracs*(rsup26(iprops+1)-rsup26(iprops))

            tf = (1-pramp)*tf + pramp*tf
            rhog = (1-pramp)*rhogold + pramp*rhog
          endif
      endif
```

C.3 TGAS subroutine

The TGAS subroutine calculates the temperature and specific heat capacity of vapour using pressure and enthalpy as inputs. This subroutine is modified to determine supercritical water temperature and specific heat capacity as a function of pressure and enthalpy. The VOLUMEDATA module is called by the TGAS subroutine to obtain the required coefficients

and exponents for IAPWS-IF97 property formulations.

```
      use volumedata
```

New local variables added to determine supercritical water properties.

```
      integer :: superprops
      real :: frac
      real :: diff
      real :: tv
      real :: cpv
```

Temperature calculation for IAPWS-IF97 region 3 is added to the subroutine after the temperature calculation for region 2 at line # 238 of the original subroutine.

```
c=====================================================================
c     Temperature calculation for region 3
c=====================================================================

      call vboundary(p,h13,h3ab,h23)
!-----temperature for region 3b (p,h)
      if(h_SI.lt.h23)then
      ttt = 0
      do i = 1,33
        ttt= ttt + n3tb(i)* ((ppp/100)+0.298)**i3tb(i)
     &                     *((h_SI/2800)-0.720)**j3tb(i)
      enddo
      ttt = ttt*860
      endif
```

```
!-----temperature for region 3a (p,h)
      if(h_SI.lt.h3ab)then
      ttt = 0
      do i = 1,31
        ttt= ttt + n3ta(i)* ((ppp/100)+0.240)**i3ta(i)
     &                      *((h_SI/2300)-0.615)**j3ta(i)
      enddo
      ttt = ttt*760
      endif
```

Then the specific heat calculation for region 3 is added after the specific heat calculation for region 2 at line # 268 of the original subroutine.

```
c=====================================================================
c     Specific heat calculation for region 3 (rho,t)
c=====================================================================

!----volume for region 3b v(p,h)
      if(h_SI.lt.h23)then
      v = 0
      do i = 1,30
       v=v+n3b(i)*((ppp/100)+0.0661)**i3b(i)*((h_SI/2800)-0.720)**j3b(i)
      enddo
      vol = v*0.0088*16.0184634
      endif
!----volume for region 3a v(p,h)
      if(h_SI.lt.h3ab)then
      v = 0
```

```
      do i = 1,32
       v=v+n3a(i)*((ppp/100)+0.128)**i3a(i)*((h_SI/2100)-0.727)**j3a(i)
      enddo
      vol = v*0.0028*16.0184634
      endif
!-----density for region 3
       dSI = 1/(vol*0.06242796)
!-----specific heat capacity for region 3 (rho,t)
      if(h_SI.lt.h23)then
      theta_31 = 0
      do i = 2,40
         theta_31 = theta_31 + n3(i)*i3(i)*(dSI/322)**(i3(i)-1)
     &                          *(647.096/t_SI)**j3(i)
      enddo
      theta_31 = theta_31 + n3(1)*(dSI/322)**-1

      theta_32 = 0
      do i = 2,40
         theta_32 =theta_32 + n3(i)*i3(i)*(i3(i)-1)*(dSI/322)**(i3(i)-2)
     &                          *(647.096/t_SI)**j3(i)
      enddo
      theta_32 = theta_32 - n3(1)*(dSI/322)**-2

      theta_33 = 0
      do i = 2,40
         theta_33 =theta_33 + n3(i)*i3(i)*(dSI/322)**(i3(i)-1)
```

```
&                          *j3(i)*(647.096/t_SI)**(j3(i)-1)
 enddo

 theta_34 = 0
 do i = 2,40
    theta_34 =theta_34 + n3(i)*(dSI/322)**i3(i)
&                  *j3(i)*(j3(i)-1)*(647.096/t_SI)**(j3(i)-2)
 enddo

 cp_SI =(((dSI/322)*theta_31-(dSI/322)*(647.096/t_SI)*theta_33)**2)
&        /(2*(dSI/322)*theta_31+(dSI/322)**2*theta_32)
 cp_SI = (cp_SI - (647.096/t_SI)**2 * theta_34) *Rg
 endif
```

C.4 TRANSP subroutine

The TRANSP subroutine calculates thermal conductivities and viscosity for superheated steam as a function of temperature and density. This subroutine is modified to determine thermal conductivity and viscosity of supercritical water as a function of temperature and density. This subroutine also calls the VOLUMEDATA module to obtain the required coefficients and exponents for IAPWS-IF97 property formulations.

```
use volumedata
```

New local variables are added to determine supercritical water properties.

```
real :: tSI, dSI, psi_0, psi_1, lamda_0, lamda_1, lamda_2, ATC,BTC
real :: delta_t
```

```
      integer :: i
```

The property formulation for viscosity calculation is replaced with the IAPWS-IF97 viscosity property formulation by replacing the code segment from line # 53 to 67 of the original subroutine with the code segment,

```
!---- convert to degree kelvin and kg/m3
      tSI = ((t-32)/t_K_F)+273
      dSI = r*16.0184634
!---- viscosity calculation for all regions

      psi_0 = 0
      do i = 1,4
         psi_0 = psi_0 + nv0(i)*(tSI/647.096)**(1-i)
      enddo
      psi_0 = (tSI/647.096)**0.5 * psi_0**(-1)

      psi_1 = 0
      do i = 1,21
         psi_1 = psi_1 + nv1(i)*(dSI/322 - 1)**iv1(i)
     &                  *((tSI/647.096)**(-1)-1)**jv1(i)
      enddo
      psi_1 = exp((dSI/322)*psi_1)
      u = (psi_0*psi_1)*1e-06
!---- convert from (Pa  s) to [lb / (ft  h)]
      u = u *2419.088153749502
```

C.5 VOLLIQ subroutine

The VOLLIQ subroutine calculates the specific volume of liquid. This subroutine is modified to determine the specific volume of liquid at supercritical pressures. The VOLUMEDATA module is called to obtain the required coefficients and exponents for IAPWS-IF97 regions 1 and 3 property formulations.

```
      use volumedata
```

New local variables are added to determine the specific volume of supercritical water.

```
      integer :: i
      real :: pSI, hSI, tSI, v, h13, h3ab, h23
```

The algorithm used in the VOLLIQ subroutine to determine the specific volume of water is replaced with the IAPWS-IF97 region 1 and region 3 specific volume property formulations. In order to determine the specific volume of water for region 1 the temperature of water for region 1 is required. Temperature for region 1 is calculated using a backward equation.

```
      pSI = t_psi_bar * ppsia/10
      hSI = hh * 2.326
!-----temperature for region 1 (p,h)
      tSI = 0
      do i = 1,20
        tSI = tSI + n1t(i) * pSI**i1t(i) * ((hSI/2500)+1)**j1t(i)
      enddo
```

Then the specific volume of water for region 1 is calculated using the IAPWS-IF97 region 1 specific volume formulation.

```
!-----volume for region 1 (p,t)
```

```
      v = 0
      do i = 1,34
        v=v-n1(i)*i1(i)*(7.1-(pSI/16.53))**(i1(i)-1)
     &            *((1386/tSI)-1.222)**j1(i)
      enddo

      vij = v*Rg*tSI*16.0184634/(16.53*1000)
```

The IAPWS-IF97 region boundaries for specific volume calculations are obtained by calling the VBOUNDARY subroutine.

```
!----region boundaries for volume calculation
      call vboundary(ppsia,h13,h3ab,h23)
```

After obtaining the region boundaries the specific volume for IAPWS-IF97 subregion 3a is calculated.

```
!-----volume for region 3a (p,h)
      if(hSI.gt.h13)then
      v = 0
      do i = 1,32
         v=v+n3a(i)*((pSI/100)+0.128)**i3a(i)*((hSI/2100)-0.727)**j3a(i)
      enddo
      vij = v*0.0028*16.0184634
      endif
```

Then the specific volume for subregion 3b is calculated.

```
!-----volume for region 3b (p,h)
      if(hSI.gt.h3ab)then
```

```
      v = 0
      do i = 1,30
        v=v+n3b(i)*((pSI/100)+0.0661)**i3b(i)*((hSI/2800)-0.720)**j3b(i)
      enddo
      vij = v*0.0088*16.0184634
      endif
```

C.6 VOLVAP subroutine

The VOLVAP subroutine calculates the specific volume of vapour. The VOLVAP subroutine is modified to calculate the specific volume of water at supercritical pressures. The VOLUMEDATA module is called to obtain the required coefficients and exponents for IAPWS-IF97 regions 2 and 3 property formulations.

```
      use volumedata
```

New local variables are added determine the specific volume of water at supercritical pressures.

```
      integer :: i
      real :: pSI, hSI, tSI, t,c, v, h13,h3ab,h23
      real :: gam_20, gam_2r
```

The algorithm used in the VOLVAP subroutine to determine the specific volume of water is replaced with the IAPWS-IF97 region 2 and region 3 specific volume property formulations. In order to determine the specific volume for region 2 the temperature for region 2 is required. Temperature for region 2 is obtained by calling the TGAS subroutine.

```
!----temperature for region 2 (p,h)
      call tgas(ppsia,hh,t,c,3)
```

Then the specific volume of water for region 2 is calculated using the IAPWS-IF97 region 2 specific volume formulation.

```
!----volume for region 2 v(p,t)
      pSI = t_psi_bar * ppsia/10
      hSI = hh * 2.326
      tSI = ((t-32)/t_K_F)+273

      gam_20 = pSI**-1

      gam_2r = 0.
      do i = 1, 43
        gam_2r = gam_2r + nr2(i)* ir2(i)*pSI**(ir2(i)-1)
     &                  *((540/tSI)-0.5)**jr2(i)
      enddo

      vij = 16.0184634*tSI*Rg*(gam_20+gam_2r)/1000
```

The IAPWS-IF97 region boundaries for specific volume calculations are obtained by calling the VBOUNDARY subroutine.

```
!----region boundaries for volume calculation
      call vboundary(ppsia,h13,h3ab,h23)
```

After obtaining the region boundaries the specific volume for IAPWS-IF97 subregion 3b is calculated.

```
!----volume for region 3b v(p,h)
      if(hSI.lt.h23)then
```

```
      v = 0
      do i = 1,30
        v=v+n3b(i)*((pSI/100)+0.0661)**i3b(i)*((hSI/2800)-0.720)**j3b(i)
      enddo
      vij = v*0.0088*16.0184634
      endif
```

Then the specific volume for subregion 3a is calculated.

```
!----volume for region 3a v(p,h)
      if(hSI.lt.h3ab)then
      v = 0
      do i = 1,32
         v=v+n3a(i)*((pSI/100)+0.128)**i3a(i)*((hSI/2100)-0.727)**j3a(i)
      enddo
      vij = v*0.0028*16.0184634
      endif
```

C.7 XTRA1 subroutine

The XTRA1 subroutine calculates the partial derivative of specific volume of liquid water with respect to pressure. The XTRA1 subroutine is modified to determine the partial derivative of specific volume of supercritical water with respect to pressure. The VOLUMEDATA module is called to obtain all the required coefficients and exponents to calculate the partial derivative of specific volume of water with respect to pressure for IAPWS-IF97 regions 1 and 3.

```
      use volumedata
```

New local variables are added to the modified XTRA1 subroutine.

```
integer :: i
real :: pSI, hSI, tSI, dSI, t,c, h13,h3ab,h23,vol
real :: gam_11, gam_12, theta_31, theta_32
```

The partial derivative formulation used in the XTRA1 subroutine is replaced with the partial derivatives of IAPWS-IF97 regions 1 and 3 specific volume formulations with respect to pressure. The specific volume of water is required to determine the partial derivative of IAPWS-IF97 regions 1 and 3 specific volume formulations with respect to pressure. The specific volume of water is obtained by calling the VOLLIQ subroutine.

```
call volliq(hh,vol,ppsia)
```

The water temperature is required to calculate the partial derivative of region 1 specific volume formulation with respect to pressure. The water temperature is determined using,

```
pSI = t_psi_bar * ppsia/10
hSI = hh * 2.326


tSI = 0
do i = 1,20
    tSI = tSI + n1t(i) * pSI**i1t(i) * ((hSI/2500)+1)**j1t(i)
enddo
```

Then the partial derivative of region 1 specific volume formulation with respect to pressure is added to the subroutine.

```
c---- Region 1
```

```
      gam_11 = 0
      do i = 1,34
          gam_11 = gam_11 - n1(i) * i1(i) * (7.1-(pSI/16.53))**(i1(i)-1)
     &                      *((1386/tSI)-1.222)**j1(i)
      enddo

      gam_12 = 0
      do i = 1,34
          gam_12 = gam_12 + n1(i) * i1(i) * (i1(i)-1)
     &            *(7.1-(pSI/16.53))**(i1(i)-2)*((1386/tSI)-1.222)**j1(i)
      enddo

      dvpl = -((pSI/16.53)*gam_12)/(gam_11*pSI)
      dvpl =  -vol*vol*dvpl*100/145.037738
```

The IAPWS-IF97 region boundaries for partial derivative calculations are obtained by calling the VBOUNDARY subroutine.

```
!----region boundaries
      call vboundary(ppsia,h13,h3ab,h23)
```

Then the partial derivative of region 3 specific volume formulation with respect to pressure is added to the XTRA1 subroutine.

```
!----Region 3
      if(hSI.gt.h13)then
      tSI = 0
      do i = 1,31
        tSI= tSI + n3ta(i)* ((pSI/100)+0.240)**i3ta(i)
```

```
&                      *((hSI/2300)-0.615)**j3ta(i)
 enddo
 tSI = tSI*760

 if(hSI.gt.h3ab)then
   tSI = 0
 do i = 1,33
   tSI = tSI + n3tb(i)* ((pSI/100)+0.298)**i3tb(i)
&                      *((hSI/2800)-0.720)**j3tb(i)
 enddo
 tSI = tSI*860
 endif

 dSI = 1/(vol*0.06242796)
 theta_31 = 0
 do i = 2,40
     theta_31 = theta_31 + n3(i)*i3(i)*(dSI/322)**(i3(i)-1)
&                         *(647.096/tSI)**j3(i)
 enddo
 theta_31 = theta_31 + n3(1)*(dSI/322)**-1

 theta_32 = 0
 do i = 2,40
    theta_32 =theta_32 + n3(i)*i3(i)*(i3(i)-1)*(dSI/322)**(i3(i)-2)
&                         *(647.096/tSI)**j3(i)
 enddo
```

```
theta_32 = theta_32 - n3(1)*(dSI/322)**-2
dvpl = 1/(2*(dSI/322)*theta_31 + (dSI/322)**2*theta_32)
dvpl = dvpl*1000/(dSI*Rg*tSI)
dvpl =  -vol*vol*dvpl*100/145.037738
endif
```

C.8 DVDPV subroutine

The DVDPV subroutine calculates the partial derivative of vapour specific volume with respect to pressure. The DVDPV subroutine is modified to determine the partial derivative of specific volume of supercritical water with respect to pressure.The VOLUMEDATA module is called to obtain all the required coefficients and exponents to calculate the partial derivative of specific volume with respect to pressure for IAPWS-IF97 regions 2 and 3.

```
use volumedata
```

New local variables are added to the modified DVDPV subroutine.

```
integer :: i
real :: pSI, hSI, tSI, dSI,t,c, v, v1, v2, h13,h3ab,h23,vol
real :: gam_21r, gam_22r, theta_31, theta_32
```

The partial derivative formulation used in the DVDPV subroutine is replaced with the partial derivatives of IAPWS-IF97 regions 2 and 3 specific volume formulations with respect to pressure. The specific volume of water is required to determine the partial derivative of IAPWS-IF97 regions 2 and 3 specific volume formulations with respect to pressure. The specific volume of water is obtained by calling the VOLVAP subroutine.

```
call volvap(hh,ppsia,vol)
```

The water temperature is required to calculate the partial derivative of region 2 specific volume formulation with respect to pressure. The water temperature is determined by calling the TGAS subroutine.

```
!-----temperature for region 2 (p,h)
      call tgas(ppsia,hh,t,c,3)
```

Then the partial derivative of region 2 specific volume formulation with respect to pressure is added to the subroutine.

```
     !----dv/dp for region 2 (p,t)
      pSI = t_psi_bar * ppsia/10
      hSI = hh * 2.326
      tSI = ((t-32)/t_K_F)+273

      gam_21r = 0.
      do i = 1, 43
        gam_21r = gam_21r + nr2(i)* ir2(i)*pSI**(ir2(i)-1)
     &                  *((540/tSI)-0.5)**jr2(i)
      enddo

      gam_22r = 0.
      do i = 1, 43
        gam_22r = gam_22r + nr2(i)* ir2(i)*(ir2(i)-1)*pSI**(ir2(i)-2)
     &                  *((540/tSI)-0.5)**jr2(i)
      enddo

      dvdp = (1-pSI**2*gam_22r)/(pSI+pSI**2*gam_21r)
```

```
!-----convert from isothermal compressibility to dv/dp (*volume)


      dvdp =  -dvdp*vol/145.037738
```

The IAPWS-IF97 region boundaries for partial derivative calculations are obtained by calling the VBOUNDARY subroutine.

```
!----obtain region boundaries
      call vboundary(ppsia,h13,h3ab,h23)
```

Then the partial derivative of region 3 specific volume formulation with respect to pressure is added to the DVDPV subroutine.

```
!----dv/dp for region 3 (rho,t)
      if(hSI.lt.h23)then
!----obtain density for region 3 (rho,t)
      dSI = 1/(vol*0.06242796)
      theta_31 = 0
      do i = 2,40
         theta_31 = theta_31 + n3(i)*i3(i)*(dSI/322)**(i3(i)-1)
     &                         *(647.096/tSI)**j3(i)
      enddo
      theta_31 = theta_31 + n3(1)*(dSI/322)**-1


      theta_32 = 0
      do i = 2,40
         theta_32 =theta_32 + n3(i)*i3(i)*(i3(i)-1)*(dSI/322)**(i3(i)-2)
     &                         *(647.096/tSI)**j3(i)
      enddo
```

```
      theta_32 = theta_32 - n3(1)*(dSI/322)**-2
      dvdp = 1/(2*(dSI/322)*theta_31 + (dSI/322)**2*theta_32)
      dvdp = dvdp*1000/(dSI*Rg*tSI)
!-----convert from isothermal compressibility to dv/dp (*volume)
      dvdp =  -dvdp*vol/145.037738
      endif
```

C.9 DVDHL subroutine

The DVDHL subroutine calculates the partial derivative of specific volume of liquid water with respect to enthalpy. The DVDHL subroutine is modified to determine the partial derivative of specific volume of supercritical water with respect to enthalpy. The VOLUMEDATA module is called to obtain all the required coefficients and exponents to calculate the partial derivative of specific volume with respect to enthalpy for IAPWS-IF97 region 3.

```
      use volumedata
```

New local variables are added to the modified DVDHL subroutine.

```
      integer :: i
      real :: pSI, hSI, v1, v2, v, h13,h3ab,h23
```

The partial derivative formulation used in the DVDHL subroutine is used to determine the partial derivative of specific volume of water with respect to enthalpy in IAPWS-IF97 region 1. The IAPWS-IF97 region boundaries for partial derivative calculations are obtained by calling the VBOUNDARY subroutine at line # 25 of the original subroutine.

```
!----obtain region boundaries
      call vboundary(ppsia,h13,h3ab,h23)
```

Then the partial derivative of region 3 specific volume formulation with respect to enthalpy is added to the DVDHL subroutine.

```
      pSI = t_psi_bar * ppsia/10
      hSI = hh * 2.326


c---- Region 3a
      if(hSI.gt.h13)then
      v = 0
      do i = 1,32
         v1 = n3a(i)*((pSI/100)+0.128)**i3a(i)
         v2 = j3a(i)*((hSI/2100)-0.727)**(j3a(i)-1)/2100
         v = v + (v1*v2)
      enddo
      dvd = v*0.0028*37.25891241
      endif
c---- Region 3b
      if(hSI.gt.h3ab)then
      v = 0
      do i = 1,30
        v1 = n3b(i)*((pSI/100)+0.0661)**i3b(i)
        v2 = j3b(i)*((hSI/2800)-0.720)**(j3b(i)-1)/2800
        v = v + (v1*v2)
      enddo
      dvd = v*0.0088*37.25891241
      endif
```

C.10 DVDHV subroutine

The DVDHV subroutine calculates the partial derivative of specific volume of vapour with respect to enthalpy. The DVDHV subroutine is modified to determine the partial derivative of specific volume of supercritical water with respect to enthalpy. The VOLUMEDATA module is called to obtain all the required coefficients and exponents to calculate the partial derivative of specific volume with respect to enthalpy for IAPWS-IF97 region 3.

```
      use volumedata
```

New local variables are added to the modified DVDHV subroutine.

```
      integer :: i
      real :: pSI, hSI, v1, v2, v, h13,h3ab,h23
```

The partial derivative formulation used in the DVDHV subroutine is used to determine the partial derivative of specific volume of water with respect to enthalpy in IAPWS-IF97 region 2. The IAPWS-IF97 region boundaries for partial derivative calculations are obtained by calling the VBOUNDARY subroutine at line # 19 of the original subroutine.

```
!----obtain region boundaries
      call vboundary(ppsia,h13,h3ab,h23)
```

Then the partial derivative of region 3 specific volume formulation with respect to enthalpy is added to the DVDHV subroutine.

```
      pSI = t_psi_bar * ppsia/10
      hSI = hh * 2.326


c---- Region 3b
      if(hSI.lt.h23)then
```

```
      v = 0
      do i = 1,30
        v1 = n3b(i)*((pSI/100)+0.0661)**i3b(i)
        v2 = j3b(i)*((hSI/2800)-0.720)**(j3b(i)-1)/2800
        v = v + (v1*v2)
      enddo
      dvd = v*0.0088*37.25891241
      endif
c---- Region 3a
      if(hSI.lt.h3ab)then
      v = 0
      do i = 1,32
         v1 = n3a(i)*((pSI/100)+0.128)**i3a(i)
         v2 = j3a(i)*((hSI/2100)-0.727)**(j3a(i)-1)/2100
         v = v + (v1*v2)
      enddo
      dvd = v*0.0028*37.25891241
      endif
```

C.11 INTFR subroutine

The INTFR subroutine determines the current flow regime for the continuity mesh cell and the interfacial drag and wall friction factors. New variables are added to the INTFR subroutine to modify the wall friction factors.

```
! New variables for the supercritical pressure modification
      real :: rhow   ! density at wall temperature
```

```
      real :: cpw    ! heat capacity at wall temperature
      real :: hhw    ! enthalpy at wall temperature
      real :: tsurf1 !surface temperature
      real :: tsurf2 !surface temperature
      real :: fvsub ! subcritical vapour friction factor
      real :: fvsup ! supercritical vapour friction factor
      real :: flsub ! subcritical liquid friction factor
      real :: flsup ! supercritical liquid friction factor
      real :: sramp ! supercritical ramp calculated using subroutine sramp
```

The INTFR subroutine calculates wall friction factors at two different places. The wall friction factors for rods are modified first by introducing a supercritical friction factor correlation. The supercritical friction factor correlation requires the determination of surface temperature of the continuity mesh cell i,j. The following code segment is added at line # 884 of the original subroutine to determine the surface temperature of the continuity mesh cell i,j.

```
c-----------------------------------------------------------------------
c------ Determine maximum surface temperature tsurf in the sub-channel
c------ continuity cell i,j in order to calculate the supercritical
c------ friction factor.
c-----------------------------------------------------------------------
        tsurf = 0.0
c------ Loop over all rods connected to the current sub-channel (max. 6)
        do l = 1, 6
          ns = lr(i,l)
          if (ns.eq.0) exit
          if (ns.gt.0) then
```

```
c---------- Channel on outside surface of rod
            nr = nrodns(ns)
            it = iftyp(nr)
            iclad = nnodes(it)
          else
c---------- Channel on inside surface of rod
            iclad = 1
            ns = iabs(ns)
          endif
          jh1 = jht(jabs1,nr) + 1
          jh2 = jht(jabs2,nr)
          do jh = jh1, jh2
            tsurf = max(tsurf,trod(iclad,jh,ns))
          enddo
        enddo
c------ Loop over all unheated conductors connected to the current
c------ sub-channel (max. 8)
        do l = 1, 8
          n = ls(i,l)
          if (n.eq.0) exit
          if (n.gt.0) then
c---------- Channel on outside surface of unheated conductor
            it = istyp(n)
            iclad = nnodes(it)
          else
c---------- Channel on inside surface of unheated conductor
```

```
            iclad = 1
            n = iabs(n)
          endif
          tsurf = max(tsurf,tstr(iclad,j,n))
        enddo
```

Then the WALLTEMPPROP subroutine is called to obtain the density and specific heat capacity of water at the calculated surface temperature.

```
        call walltempprop(pll,tsurf,rhow,hhw,cpw)
```

The SUPERCRITRAMP subroutine is called to obtain the pressure ramp value for the transition between subcritical and supercritical flow friction factor correlations.

```
        call supercritramp(pll,sramp)
```

The Kirillov friction factor correlation is added to the algorithm calculating rod wall friction factors by replacing the code segment from line # 884 to 897 of the original subroutine with the following segment.

```
c------ Determine rod friction factor
        if (irfc.eq.0) then
c--------- No wall friction
          fv = 0.0
          fl = 0.0
        elseif (irfc.eq.1) then
c-------- Original COBRA-TF correlation:
          fvsub = max(64.0/rev,frfa(rev))
          flsub = max(64.0/rel,frfa(rel))
          fvsup = ((rhow/rvp)**0.4)* (0.55/log10(rev/8))**2
```

```
          fvsup = max(64.0/rev,fvsup)
          flsup = ((rhow/rlp)**0.4)* (0.55/log10(rel/8))**2
          flsup = max(64.0/rel,flsup)
          fv = sramp*fvsub + (1-sramp)*fvsup
          fl = sramp*flsub + (1-sramp)*flsup
        elseif (irfc.eq.2) then
c-------- Additional correlation:
          fvsub = max(64.0/rev,frfa_new(rev))
          flsub = max(64.0/rel,frfa_new(rel))
          fvsup = ((rhow/rvp)**0.4) / ((1.82*log10(rev)-1.64)**2)
          fvsup = max(64.0/rev,fvsup)
          flsup = ((rhow/rlp)**0.4) / ((1.82*log10(rel)-1.64)**2)
          flsup = max(64.0/rel,flsup)
          fv = sramp*fvsub + (1-sramp)*fvsup
          fl = sramp*flsub + (1-sramp)*flsup
        endif
```

The wall friction factors for gaps are modified next. This requires the determination of surface temperatures between continuity mesh cells that form the gap. This is done by adding the following code segment at line # 1964 of the original subroutine.

```
c-----------------------------------------------------------------------
c------ Determine maximum surface temperature tsurf in the sub-channel
c------ continuity cells ii,j and jj,j to calculate the supercritical
c------ friction factor
c-----------------------------------------------------------------------
          tsurf1 = 0.0
          tsurf2 = 0.0
```

```
          tsurf = 0.0
c------ Loop over all rods connected to the current sub-channel (max. 6)
          do l = 1, 6
            ns = lr(ii,l)
            if (ns.eq.0) exit
            if (ns.gt.0) then
c---------- Channel on outside surface of rod
            nr = nrodns(ns)
            it = iftyp(nr)
            iclad = nnodes(it)
            else
c---------- Channel on inside surface of rod
            iclad = 1
            ns = iabs(ns)
            endif
            jh1 = jht(jabs1,nr) + 1
            jh2 = jht(jabs2,nr)
            do jh = jh1, jh2
            tsurf1 = max(tsurf1,trod(iclad,jh,ns))
            enddo
          enddo
c------ Loop over all unheated conductors connected to the current
c------ sub-channel (max. 8)
          do l = 1, 8
            n = ls(ii,l)
            if (n.eq.0) exit
```

```
            if (n.gt.0) then
c---------- Channel on outside surface of unheated conductor
            it = istyp(n)
            iclad = nnodes(it)
            else
c---------- Channel on inside surface of unheated conductor
            iclad = 1
            n = iabs(n)
            endif
            tsurf1 = max(tsurf1,tstr(iclad,j,n))
          enddo

c------ Loop over all rods connected to the current sub-channel (max. 6)
          do l = 1, 6
            ns = lr(jj,l)
            if (ns.eq.0) exit
            if (ns.gt.0) then
c---------- Channel on outside surface of rod
            nr = nrodns(ns)
            it = iftyp(nr)
            iclad = nnodes(it)
            else
c---------- Channel on inside surface of rod
            iclad = 1
            ns = iabs(ns)
            endif
```

```
            jh1 = jht(jabs1,nr) + 1
            jh2 = jht(jabs2,nr)
            do jh = jh1, jh2
            tsurf2 = max(tsurf2,trod(iclad,jh,ns))
            enddo
          enddo
c------ Loop over all unheated conductors connected to the current
c------ sub-channel (max. 8)
          do l = 1, 8
            n = ls(jj,l)
            if (n.eq.0) exit
            if (n.gt.0) then
c---------- Channel on outside surface of unheated conductor
            it = istyp(n)
            iclad = nnodes(it)
            else
c---------- Channel on inside surface of unheated conductor
            iclad = 1
            n = iabs(n)
            endif
            tsurf2 = max(tsurf2,tstr(iclad,j,n))
          enddo
          tsurf = (tsurf1+tsurf2)/2
```

Then the WALLTEMPPROP subroutine is called to obtain the density and specific heat capacity of water at this calculated surface temperature.

```
          call walltempprop(pll,tsurf,rhow,hhw,cpw)
```

The wall friction factors for the gaps are modified by replacing the code segment from line # 1964 to 1975 of the original subroutine with the code segment given below.

```
c----------------------------
c-------- Rod Friction Factor
c----------------------------
          if(irfc.eq.1) then
c-------- Original COBRA-TF correlation:
            fvsub = max(64.0/rev,frfa(rev))
            flsub = max(64.0/rel,frfa(rel))
            fvsup = ((rhow/rvp)**0.4)* (0.55/log10(rev/8))**2
            fvsup = max(64.0/rev,fvsup)
            flsup = ((rhow/rlp)**0.4)* (0.55/log10(rel/8))**2
            flsup = max(64.0/rel,flsup)
            fv = sramp*fvsub + (1-sramp)*fvsup
            fl = sramp*flsub + (1-sramp)*flsup
          else
c-------- Additional correlation:
            fvsub = max(64.0/rev,frfa_new(rev))
            flsub = max(64.0/rel,frfa_new(rel))
            fvsup = ((rhow/rvp)**0.4) / ((1.82*log10(rev)-1.64)**2)
            fvsup = max(64.0/rev,fvsup)
            flsup = ((rhow/rlp)**0.4) / ((1.82*log10(rel)-1.64)**2)
            flsup = max(64.0/rel,flsup)
            fv = sramp*fvsub + (1-sramp)*fvsup
            fl = sramp*flsub + (1-sramp)*flsup
          endif
```

C.12 BOILING subroutine

The boiling subroutine calculates the heat transfer coefficient to liquid, the heat transfer coefficient to vapour, the critical heat flux, and the critical heat flux temperature. New local variables are added to the BOILING subroutine to modify the wall heat transfer model at supercritical pressures.

```
! New variables for the supercritical pressure modification
      real :: tsurf        !wall temperature
      integer :: l         !terms to calculate wall temprature
      integer :: n         !terms to calculate wall temprature
      integer :: ns        !terms to calculate wall temprature
      integer ::nr         !terms to calculate wall temprature
      integer :: it        !terms to calculate wall temprature
      integer :: iclad     !terms to calculate wall temprature
      integer :: jabs1     !terms to calculate wall temprature
      integer :: jabs2     !terms to calculate wall temprature
      integer :: jh1       !terms to calculate wall temprature
      integer :: jh2       !terms to calculate wall temprature
      integer :: jh        !terms to calculate wall temprature
      real :: rhow         !density of water at wall temperature
      real :: cpw          !specific heat capacity of water  at wall temperature
      real :: hhw          !specific enthalpy of water at wall temperature
      real :: cpavg        !average specific heat capacity
      real :: prlsup       !Prandtl number for supercritical flow
      real :: prvsup       !Prandtl number for supercritical flow
      real :: superfac     !terms of Mokry correlation
```

```
      real :: spvlsub      !subcritical single phase liquid convection htc
      real :: spvlsup      !supercritical single phase liquid convection htc
      real :: spvnsub      !subcritical single phase vapour convection htc
      real :: spvnsup      !supercritical single phase vapour convection htc
      real :: qchfsub      !subcritical critical heat flux
      real :: qchfsup      !supercritical critical heat flux
      real :: tcmaxsup     !subcritical max temp for chf temperature
      real :: tcmaxsub     !supercritical max temp for chf temperature
      real :: sramp        !pressure ramp value
```

The Mokry et al. correlation is used to determine the supercritical wall heat transfer coefficients. The Mokry et al. correlation requires the determination of surface temperatures of fuel rods. This is calculated by adding the following code segment at line #323 of the original code.

```
c-----------------------------------------------------------------------
c------ Determine maximum surface temperature tsurf in the sub-channel
c------ continuity cell i,j
c-----------------------------------------------------------------------
      tsurf = 0.0
c------ Loop over all rods connected to the current sub-channel (max. 6)
      do l = 1, 6
        ns = lr(i,l)
        if (ns.eq.0) exit
        if (ns.gt.0) then
c---------- Channel on outside surface of rod
        nr = nrodns(ns)
        it = iftyp(nr)
```

```
        iclad = nnodes(it)
        else
c---------- Channel on inside surface of rod
        iclad = 1
        ns = iabs(ns)
        endif
        jabs1 = max0(1,j-1) + isects(isect,4)
        jabs2 = jabs1 + 1
        jh1 = jht(jabs1,nr) + 1
        jh2 = jht(jabs2,nr)
        do jh = jh1, jh2
        tsurf = max(tsurf,trod(iclad,jh,ns))
        enddo
      enddo
c------ Loop over all unheated conductors connected to the current
c------ sub-channel (max. 8)
      do l = 1, 8
        n = ls(i,l)
        if (n.eq.0) exit
        if (n.gt.0) then
c---------- Channel on outside surface of unheated conductor
        it = istyp(n)
        iclad = nnodes(it)
        else
c---------- Channel on inside surface of unheated conductor
        iclad = 1
```

```
        n = iabs(n)
        endif
        tsurf = max(tsurf,tstr(iclad,j,n))
      enddo
```

The WALLTEMPPROP subroutine is called to obtain the density and specific heat capacity of water at this calculated surface temperature.

```
        call walltempprop(pll,tsurf,rhow,hhw,cpw)
```

The SUPERCRITRAMP subroutine is called to obtain the pressure ramp value for the transition between subcritical and supercritical heat transfer coefficients.

```
        call supercritramp(pll,sramp)
```

Bulk fluid properties are required to determine the supercritical water heat transfer coefficients using the Mokry et al. correlation.

```
      hbulk = aliq(i,j)*hl(i,j) + al(i,j)*hv(i,j)
      tbulk = aliq(i,j)*tl + al(i,j)*tg
      rhobulk = aliq(i,j)*rl(i,j) + al(i,j)*rv(i,j)
      kbulk = aliq(i,j)*kl + al(i,j)*kfilm
      ubulk = aliq(i,j)*ul + al(i,j)*ufilm
      cpbulk = aliq(i,j)*cpl + al(i,j)*cpfilm
```

Then the heat transfer correlation for single phase liquid convection is modified for supercritical flow by replacing the code segment from line # 324 to 334 of the original subroutine with the following code segment.

```
c=======================================================================
c     Heat transfer coefficient for
```

```
c     --> single phase liquid hspl
c=====================================================================
c---- Calculate Nusselt number
c---- Subcritical heat transfer coefficient to liquid
c---- maximum of:
c----  o) Nu = 7.86 for laminar flow
c----  o) approximation according to Dittus and Boelter
      spvlsub = max(7.86, ((0.023 * rel**0.8) * (prl**0.4)))

c---- Supercritical heat transfer coefficient to liquid
c---- maximum of:
c----  o) Nu = 7.86 for laminar flow
c----  o) approximation according to Jackson
      cpavg = (hhw-hbulk)/(tsurf-tbulk)
      prlsup = cpavg*ubulk/kbulk
      rsup = rel*ul/ubulk
      superfac = (rhow/rhobulk)**0.564
      spvlsup = max(7.86, 0.0053*(rsup**0.914)*(prlsup**0.654)*superfac)

      spvl = (sramp*spvlsub) + ((1-sramp)*spvlsup)
c---- Calculate heat transfer coefficient
      hspl = spvl * kbulk / de
```

The heat transfer correlation for single phase vapour convection is modified for supercritical flow by replacing the code segment from line # 337 to 354 of the original subroutine with the following code segment.

```
c=====================================================================
```

```
c     Heat transfer coefficient for
c     --> single phase vapor hspv
c=====================================================================
c---- Calculate Nusselt number
      if (reg.le.25200.0) then
c---- ... for Re <= 25200
c----   Subcritical heat transfer coefficient for vapor
c----   maximum of:
c----   o) Nu = 10 for laminar flow
c----   o) approximation according to Wong and Hochreiter FLECHT-SEASET
        spvnsub = max(10.0, 0.0797 * reg**0.6774 * prfilm**0.333)
c----   Supercritical heat transfer coefficient for vapor
c----   maximum of:
c----   o) Nu = 10 for laminar flow
c----   o) approximation according Jackson
        cpavg = (hhw-hbulk)/(tsurf-tbulk)
        prvsup = cpavg*ubulk/kbulk
        rsup = regu / ubulk
        superfac = (rhow/rhobulk)**0.564
        spvnsup =max(10.0,0.0053*(rsup**0.914)*(prvsup**0.654)*superfac)
      else
c---- ... for Re > 25200
c----   Subcritical heat transfer coefficient for vapor
c----   o) approximation according to Dittus and Boelter
        spvnsub = 0.023 * reg**0.8 * prfilm**0.4
c----   Supercritical heat transfer coefficient for vapor
```

```
c----   o) approximation according to Jackson
        cpavg = (hhw-hbulk)/(tsurf-tbulk)
        prvsup = cpavg*ubulk/kbulk
        rsup = regu / ubulk
        superfac = (rhow/rhobulk)**0.564
        spvnsup = 0.0053*(rsup**0.914)*(prvsup**0.654)*superfac
      endif
      spvn = (sramp*spvnsub) + ((1-sramp)*spvnsup)
c---- Calculate heat transfer coefficient
      hspv = spvn * kbulk / de
```

The critical heat flux for supercritical flow is modified by adding the following code segment at line # 554 of the original subroutine.

```
      qchfsub = qchf
      qchfsup = 1.e+20
      qchf = sramp*qchfsub + (1-sramp)*qchfsup
```

The maximum critical heat flux temperature for supercritical flow is modified by inserting the following code segment at line # 568 of the original subroutine.

```
      tcmaxsub = min(tf+200.,805.3)
      tcmaxsup = 5000
      tcmax = sramp*tcmaxsub + (1-sramp)*tcmaxsup
```

C.13 HCOOL subroutine

The HCOOL subroutine determines the heat transfer coefficients for fuel rods and unheated structures. New local variables are added to the HCOOL subroutine to modify the wall heat

transfer model at supercritical pressures.

```
      real :: sramp      !pressure ramp values
      real :: tflimit    !temp limit to calculate nucleate boiling htc
      real :: tflimitsub !subcritical temp limit to calculate nb htc
      real :: tflimitsup !supercritical temp limit to calculate nb htc
      real :: htcvsub    !subcritical single phase vapour convection htc
      real :: htcvsup    !supercritical single phase  vapour convection htc
      real :: htclsub    !subcritical single phase liquid convection htc
      real :: htclsup    !supercritical single phase liquid convection htc
```

The nucleate boiling heat transfer coefficient in subcooled nucleate boiling and saturated nucleate boiling heat transfer regimes is eliminated for supercritical flow by replacing the code segment from line # 197 to 240 of the original subroutine with the code segment given below.

```
      call supercritramp(pl,sramp)
      tflimitsub = tf+0.1
      tflimitsup = 5000
      tflimit = sramp*tflimitsub + (1-sramp)*tflimitsup
c---- Pre-CHF heat transfer
c---- Check alfl (continuous liquid volume fraction)
      if (alfl.ge.0.001) then
        htclsub = hspl
        htclsup = (1-al(i,j))*hspl
        htcl = sramp*htclsub + (1-sramp)*htclsup
        imode = 1
        if (twall.ge.(tflimit)) then
```

```
c-------- Evaluate nucleate boiling heat transfer
c-------- (Chen correlation - saturated boiling, pressure term)
          chen3 = chen1 + chen2 * max(0.0,dtf-5.)
          dpf = dpdtc * dtf**chen3
c-------- Heat transfer coefficent for nucleate boiling in the Chen
c-------- correlation
          htcf = supf * h11 * dtf**0.24 * dpf**0.75
c-------- Modify heat transfer coefficient by a ramp (only relevant for
c-------- volume fractions of continous liquid between 0.00 and 0.01)
          ramp = min(1.0,100*alfl)
          htcf = ramp * htcf
          dhtc = (chen3 + 0.24) * htcf / dtf
c-------- Heat flux due to nucleate boiling (Chen correlation)
          qnb = htcf * dtf
cmna----- Saturation predicted by enthalpies. So, saturated nucleate
c-------- boiling has a similar logic to subcooled nucleate boiling.
          if (hl(i,j).ge.(hf+0.01)) then
            qcw = 0.0
            imode = 5
          else
c---------- Subcooled nucleate boiling
c---------- Heat flux dissipated in near wall condensation
            qcw = max(0.0,qhn-hspl*dtl)
            imode = 4
          endif
          fgama = max(0.01,(qnb-qcw)/qnb*scbmod)
```

```
          htcl = htcl + (1.0 - fgama) * qnb / dtl
          htcb = fgama * htcf
        endif
c------ Ramp for heat transfer coefficient to vapor
c------   htcv = 0,    for volume fraction of vapor <= 0.999
c------   htcv = hspv, for volume fraction of vapor = 1
        htcvsub = (1.0 - xliq) * hspv
        htcvsup = al(i,j) * hspv
        htcv = sramp*htcvsub + (1-sramp)*htcvsup
      else
c------ Liquid deficient heat transfer
        imode = 2
        htcv = hspv
      endif
```

Appendix D

Simulating the 62-element Canadian Supercritical Water Reactor (SCWR) Fuel Bundle with COBRA-TF-SC and ASSERT-PV-SC

The COBRA-TF-SC and the ASSERT-PV-SC codes are used to simulate the 62-element Canadian Supercritical Water Reactor (SCWR) fuel bundle. The Dittus-Boelter correlation is used in both COBRA-TF-SC and ASSERT-PV-SC to calculate heat transfer coefficients for ease of comparison. Figures D.1, D.2, and D.3 illustrate the subchannel bulk coolant temperatures calculated using COBRA-TF-SC and ASSERT-PV-SC for subchannel # 1, subchannel # 32, and subchannel # 63 respectively.

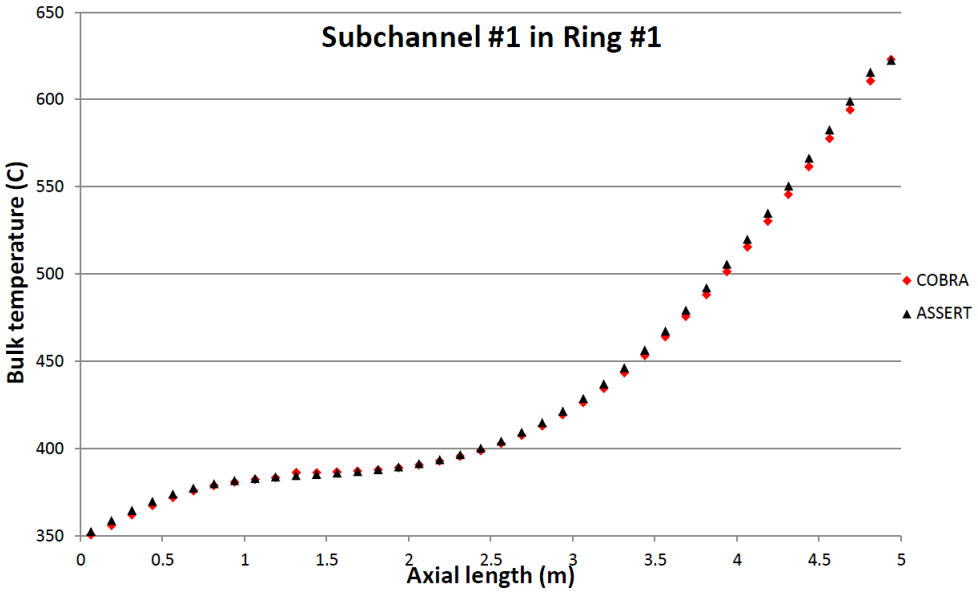

Figure D.1: Bulk coolant temperature profile for subchannel # 1 calculated using COBRA-TF-SC and ASSERT-PV-SC using the Dittus-Boelter correlation: Water, p=25 MPa, G=975.70 kg/m^2s, q=851.72 kW/m^2, and t_{in}=350°C.

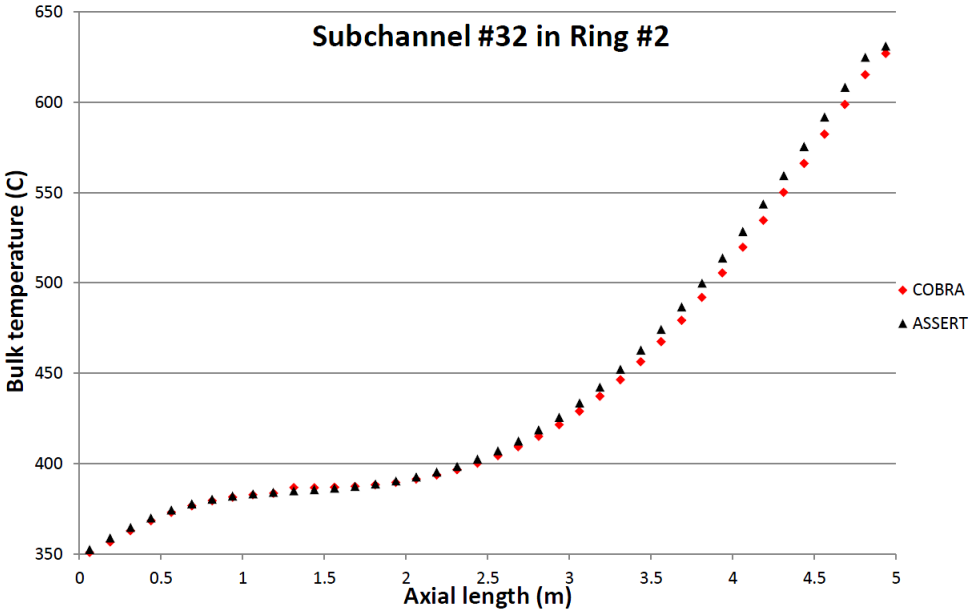

Figure D.2: Bulk coolant temperature profile for subchannel # 32 calculated using COBRA-TF-SC and ASSERT-PV-SC using the Dittus-Boelter correlation: Water, p=25 MPa, G=975.70 kg/m^2s, q=851.72 kW/m^2, and t_{in}=350°C.

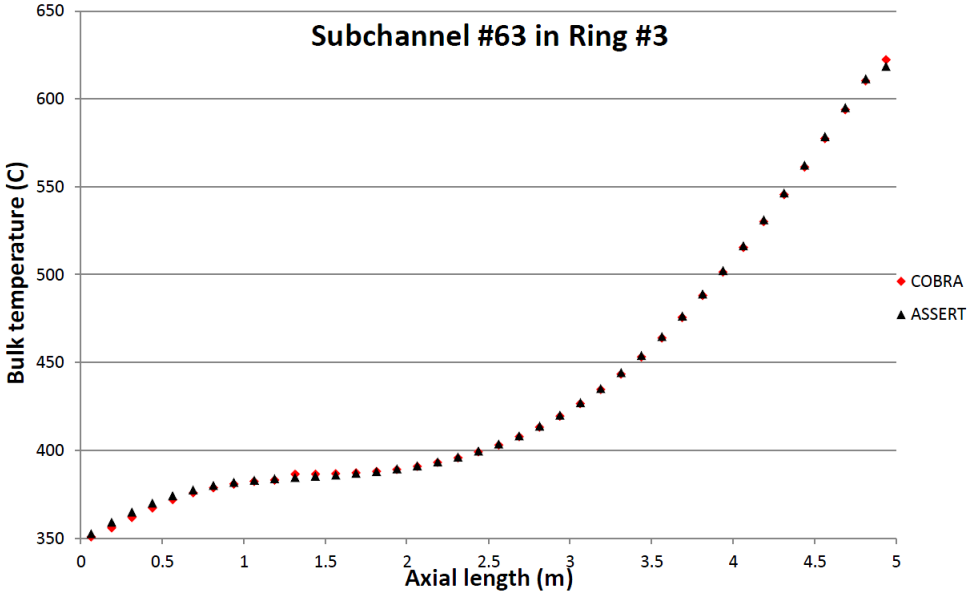

Figure D.3: Bulk coolant temperature profile for subchannel # 63 calculated using COBRA-TF-SC and ASSERT-PV-SC using the Dittus-Boelter correlation: Water, p=25 MPa, G=975.70 kg/m^2s, q=851.72 kW/m^2, and t_{in}=350°C.

The percentage difference between bulk coolant temperatures calculated using COBRA-TF-SC and ASSERT-PV-SC for the subchannels listed above is shown in Figure D.4.

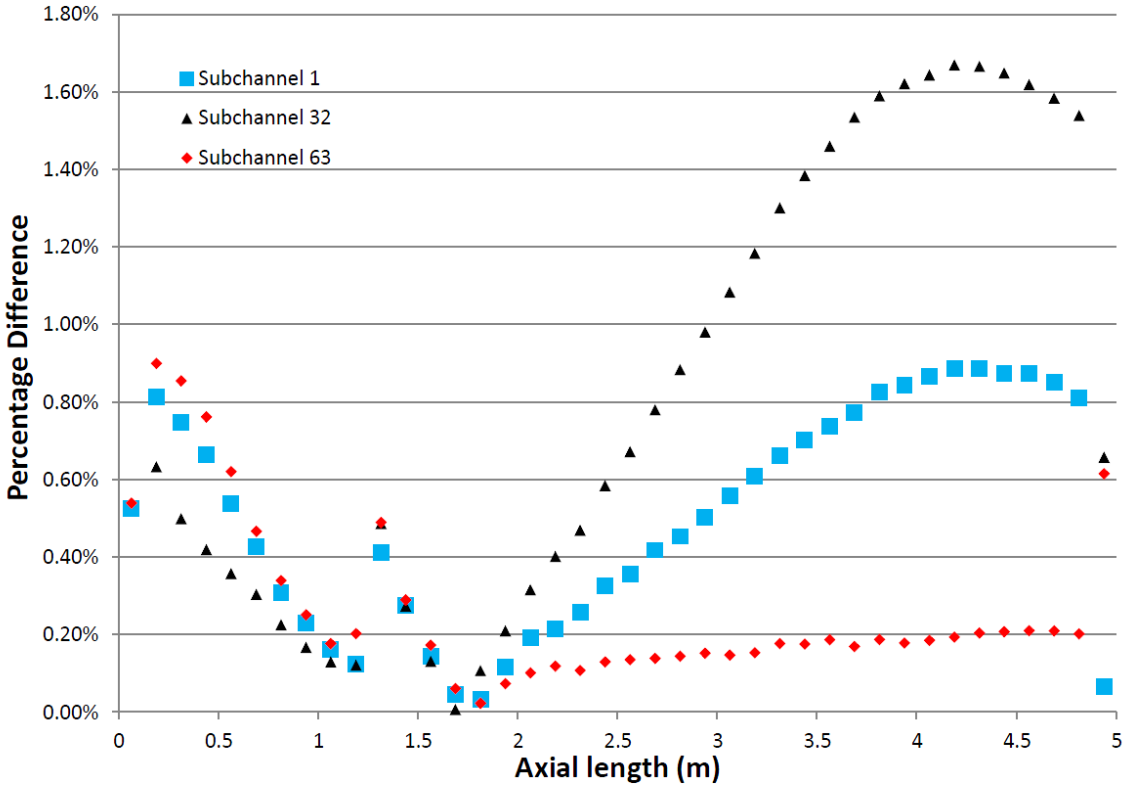

Figure D.4: Percentage difference between subchannel bulk coolant temperatures calculated using COBRA-TF-SC and ASSERT-PV-SC.

The bulk coolant temperatures calculated using COBRA-TF-SC and ASSERT-PV-SC agree well with each other. The highest percentage difference in bulk coolant temperatures occurs in subchannels located in the outermost subchannel ring of the fuel bundle. The lowest percentage difference in bulk coolant temperatures occurs in subchannels located in the innermost subchannel ring of the fuel bundle. The maximum bulk coolant temperature occurs in the intermediate subchannel ring. The maximum bulk coolant temperature calculated using COBRA-TF-SC is 627.45°C and the maximum bulk coolant temperature calculated using ASSERT-PV-SC is 631.20°C. The difference in maximum bulk coolant temperatures calculated using the two codes, is 3.75°C, which is not significant.

Figures D.5, D.6, D.7, and D.8 illustrate the rod surface temperatures calculated using

COBRA-TF-SC and ASSERT-PV-SC for fuel rod surface types # 1, # 2, # 3, and # 4 respectively.

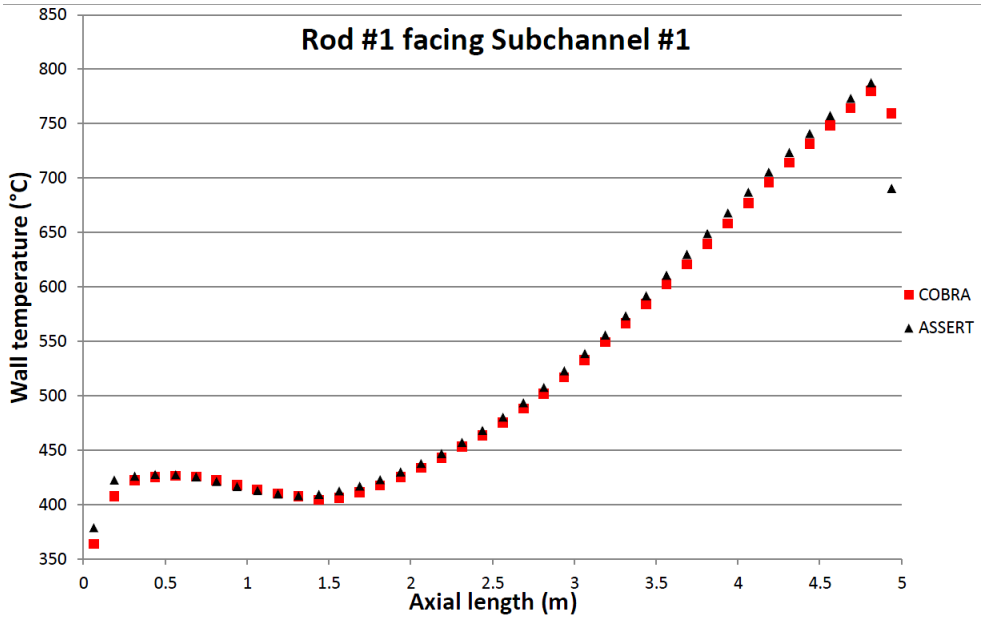

Figure D.5: Rod surface temperature profile for rod # 1 facing subchannel # 1 calculated using COBRA-TF-SC and ASSERT-PV-SC using the Dittus-Boelter correlation: Water, p=25 MPa, G=975.70 kg/m^2s, q=851.72 kW/m^2, and t_{in}=350°C.

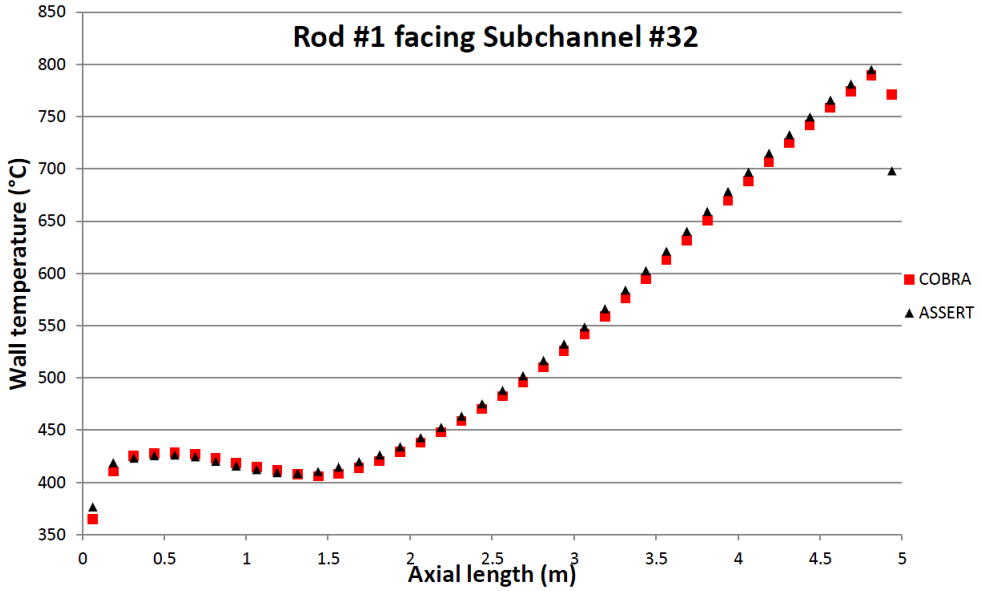

Figure D.6: Rod surface temperature profile for rod # 1 facing subchannel # 32 calculated using COBRA-TF-SC and ASSERT-PV-SC using the Dittus-Boelter correlation: Water, p=25 MPa, G=975.70 kg/m^2s, q=851.72 kW/m^2, and t_{in}=350°C.

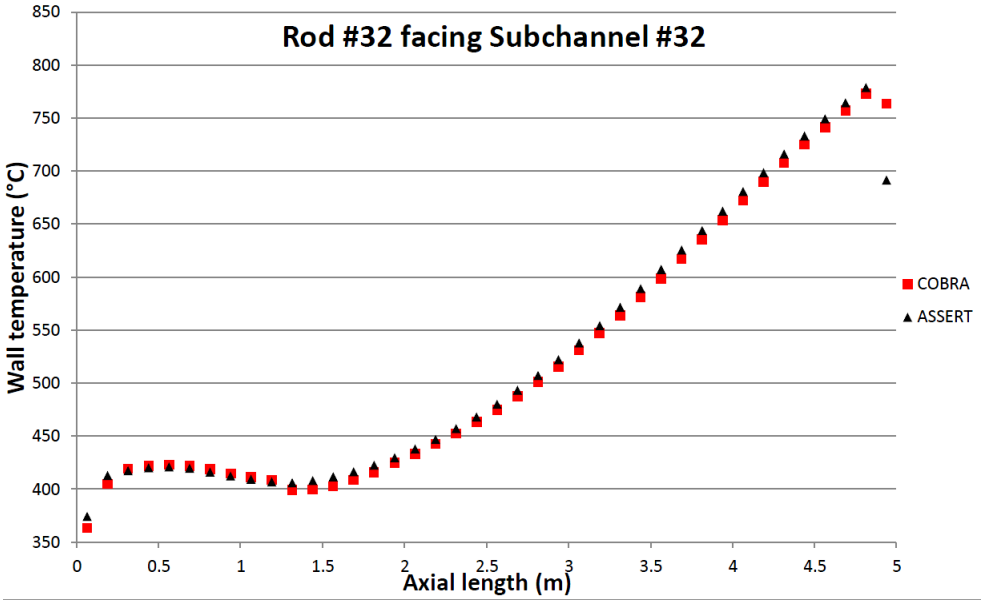

Figure D.7: Rod surface temperature profile for rod # 32 facing subchannel # 32 calculated using COBRA-TF-SC and ASSERT-PV-SC using the Dittus-Boelter correlation: Water, p=25 MPa, G=975.70 kg/m^2s, q=851.72 kW/m^2, and t_{in}=350°C.

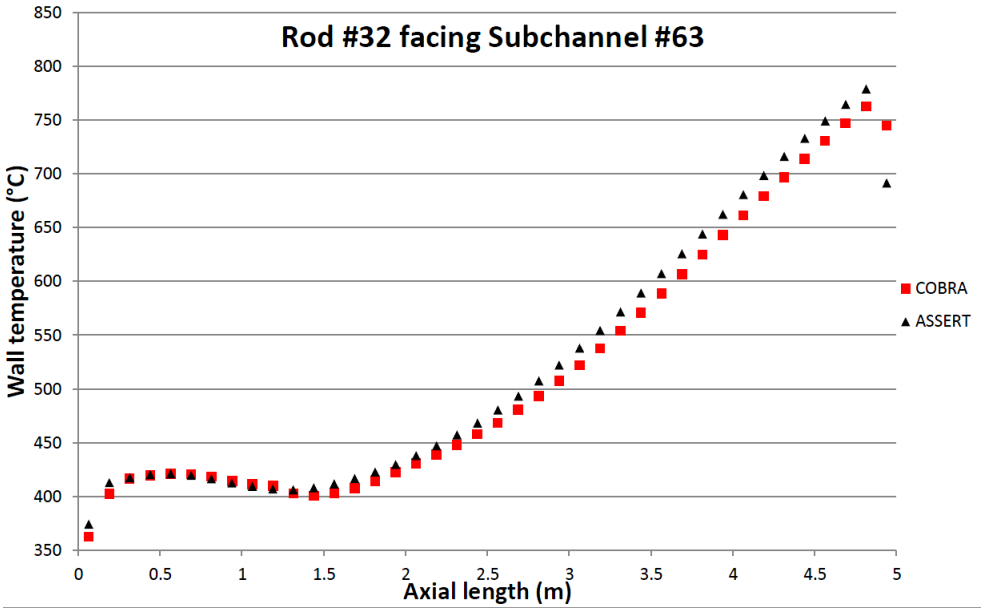

Figure D.8: Rod surface temperature profile for rod # 32 facing subchannel # 63 calculated using COBRA-TF-SC and ASSERT-PV-SC using the Dittus-Boelter correlation: Water, p=25 MPa, G=975.70 kg/m^2s, q=851.72 kW/m^2, and t_{in}=350°C.

The percentage difference between rod surface temperatures calculated using COBRA-TF-SC and ASSERT-PV-SC for the rod surfaces listed above is shown in Figure D.9.

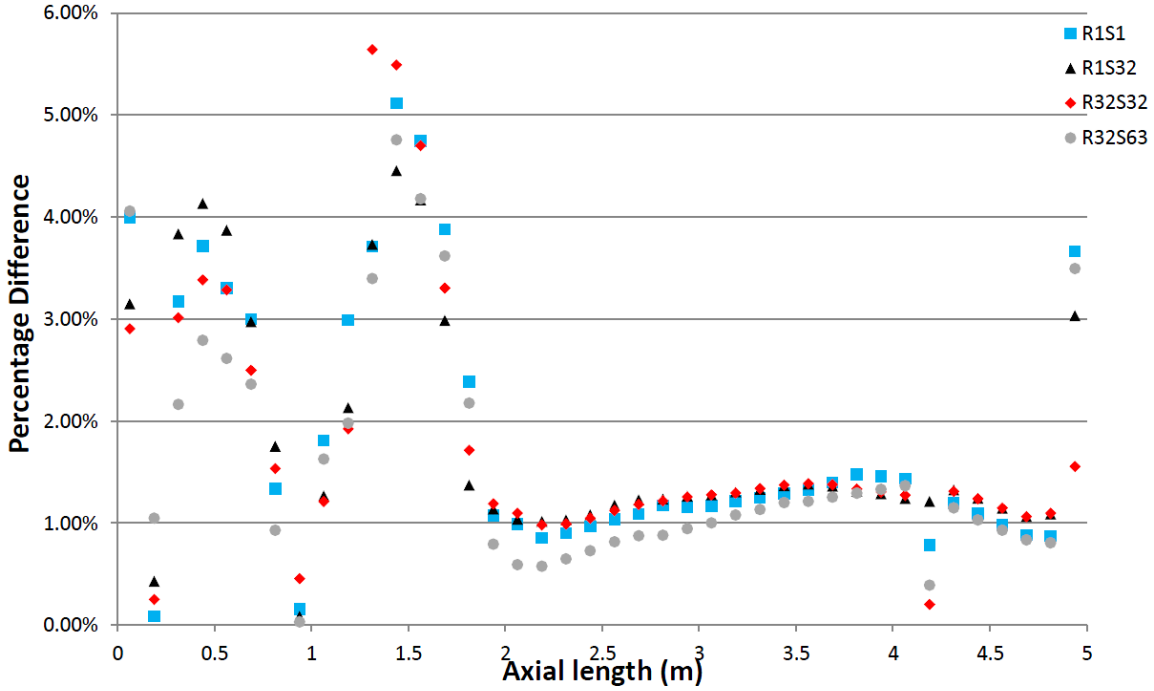

Figure D.9: Percentage difference between rod surface temperatures calculated using COBRA-TF-SC and ASSERT-PV-SC.

The rod surface or cladding temperatures calculated using COBRA-TF-SC and ASSERT-PV-SC agree well with each other. The highest percentage difference in rod surface temperatures calculated using the two codes occurs in rod surfaces of inner ring fuel rods facing the intermediate subchannel ring. The lowest percentage difference in rod surface temperatures calculated using the two codes occurs in rod surfaces of outer ring fuel rods facing the outermost subchannel ring. The maximum rod surface temperature occurs in rod surfaces of inner ring fuel rods facing the intermediate subchannel ring. The maximum rod surface temperature calculated using COBRA-TF-SC is 790.00°C and the maximum cladding temperature calculated using ASSERT-PV-SC is 795.30°C. The difference in maximum rod surface temperatures calculated using the two codes is 5.30°C, which is not significant.

The total pressure drop in the 62-element Canadian SCWR fuel bundle is compared next. Figure D.10 illustrates the relative pressure drop in the 62-element Canadian SCWR fuel

bundle calculated using COBRA-TF-SC and ASSERT-PV-SC. Figure D.11 illustrates the difference in relative pressure drop calculated using COBRA-TF-SC and ASSERT-PV-SC.

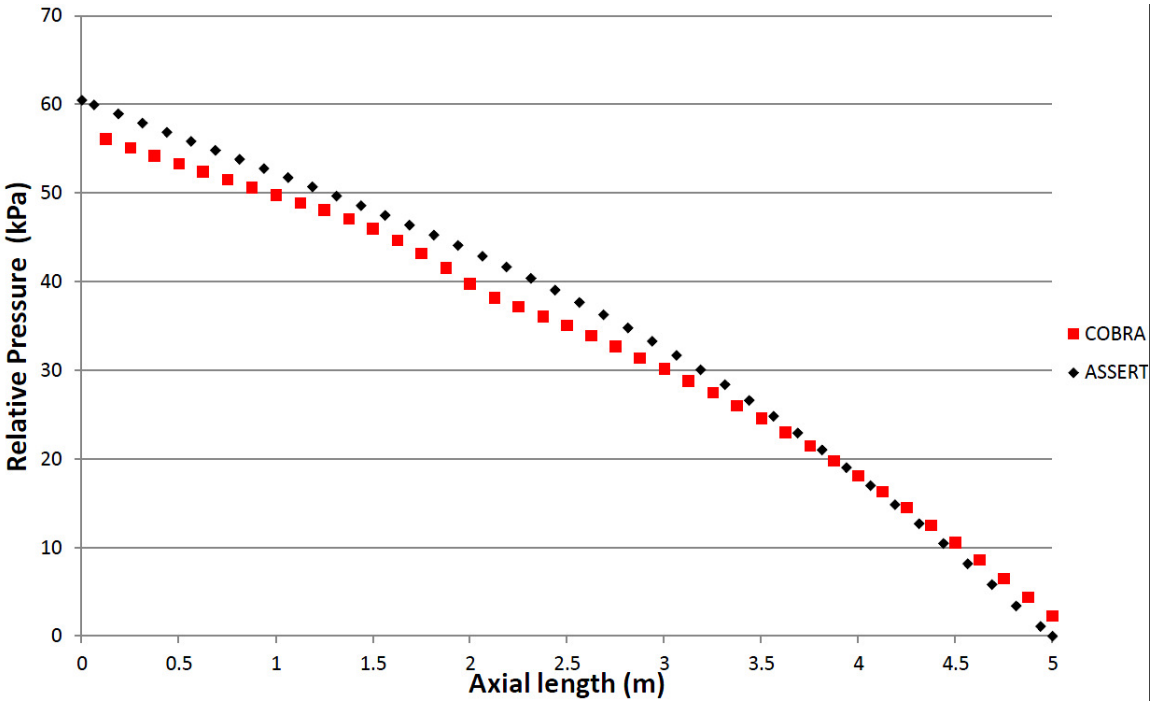

Figure D.10: Relative pressure drop in the 62-element Canadian SCWR fuel bundle calculated using COBRA-TF-SC and ASSERT-PV-SC: Water, p=25 MPa, G=975.70 kg/m^2s, q=851.72 kW/m^2, and t_{in}=350°C.

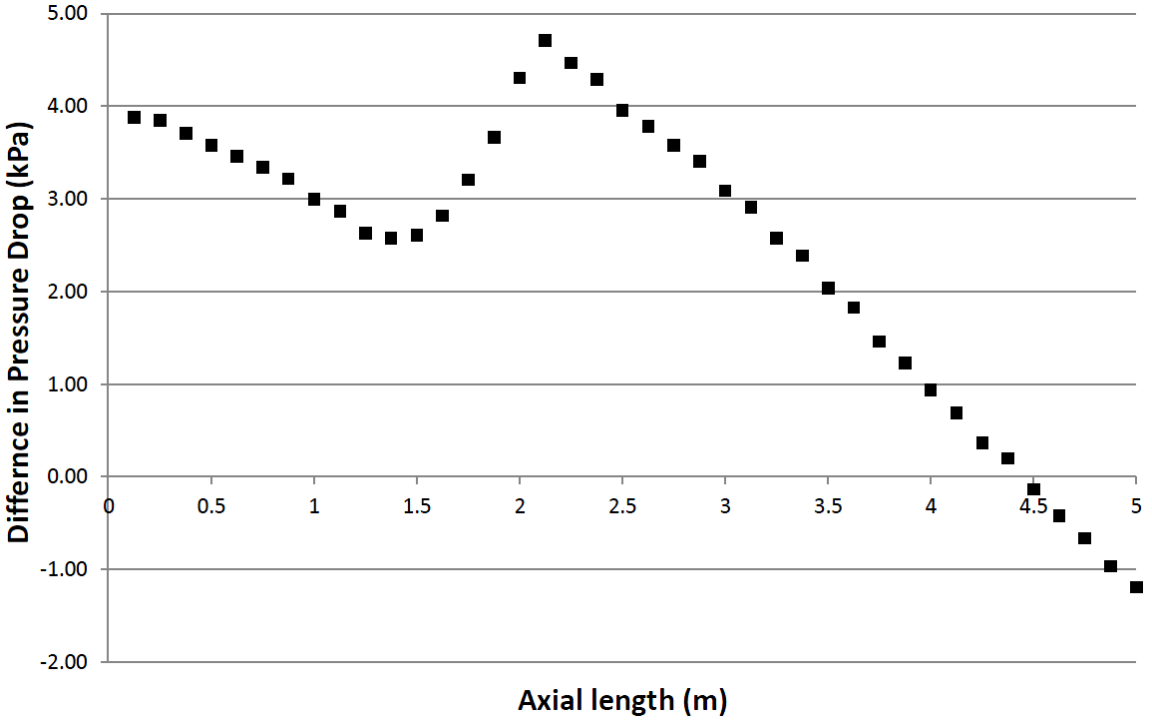

Figure D.11: Difference in relative pressure drop calculated using COBRA-TF-SC and ASSERT-PV-SC.

The relative pressure drop in the 62-element Canadian SCWR fuel bundle calculated using COBRA-TF-SC and ASSERT-PV-SC agree well with each other. The difference in relative pressure drop reaches its maximum near the center of the fuel bundle and then decreases along the bundle. This analysis verifies that COBRA-TF-SC is capable of simulating the 62-element Canadian SCWR fuel bundle successfully.

The slight difference between COBRA-TF-SC and ASSERT-PV-SC results can be attributed to the difference in water property calculations and pressure drop calculations between the two codes.

Appendix E

Input Files

E.1 COBRA-TF-SC input file for the Seven-rod test bundle - low inlet enthalpy.

```
********************************************************************************
* Heat Transfer Experiments and Numerical Analysis of Supercritical  Pressure  *
* Water in Seven-rod Test Bundle - Mishawa et. al                               *
* CTF input deck for test case 1A                                              *
********************************************************************************
* MAIN PROBLEM CONTROL DATA                                                    *
********************************************************************************
* CARD INPUT 1
*       ICOBRA
             1
* CARD INPUT 2
*      INITIAL         DUMPF
             1             1
* CARD INPUT 3
*         EPSO        OITMAX        IITMAX
         0.001            10            40
* CARD COBRA 1
*---------- TEXT ------------>
```

```
  *** 7ROD IAEA BENCHMARK PART 1 ***
*******************************************************************************
* GROUP 1 - Calculation Variables and Initial Conditions                       *
*******************************************************************************
* CARD GROUP 1
* NGR
    1
* Card 1.1
* NGAS IRFC EDMD IMIX ISOL NDM6 NDM7 NDM8 NDM9 NM10 NM11 NM12 NM13 NM14
     1    2    0    2    0    0    0    0    0    0    0    0    0    0
* Card 1.2
*     GTOT     AFLUX    DHFRAC
     0.277    15.048       0.0
* Card 1.3
*     PREF       HIN      HGIN    VFRAC1    VFRAC2
    250.00    357.00     288.4       1.0    0.9999
* Card 1.4
* GTP(1)    VFRAC(3)  GTP(2)    VFRAC(4)  GTP(3)    VFRAC(5)  GTP(4)    VFRAC(6)
air            .0001
*******************************************************************************
* GROUP 2.0 - Channel Description                                              *
*******************************************************************************
* CARD GROUP 2
* NGR
    2
* Card 2.1
* NCHA NDM2 NDM3 NDM4 NDM5 NDM6 NDM7 NDM8 NDM9 NM10 NM11 NM12 NM13 NM14
    12    0    0    0    0    0    0    0    0    0    0    0    0    0
* Card 2.2
*    I         AN         PW ABOT ATOP NMGP
     1 0.00000987 0.01256637  0.0  0.0  0.0
     2 0.00000987 0.01256637  0.0  0.0  0.0
     3 0.00000987 0.01256637  0.0  0.0  0.0
     4 0.00000987 0.01256637  0.0  0.0  0.0
     5 0.00000987 0.01256637  0.0  0.0  0.0
     6 0.00000997 0.01256637  0.0  0.0  0.0
     7 0.00002207 0.03248395  0.0  0.0  0.0
```

```
     8 0.00002207 0.03248395  0.0  0.0  0.0
     9 0.00002207 0.03248395  0.0  0.0  0.0
    10 0.00002207 0.03248395  0.0  0.0  0.0
    11 0.00002207 0.03248395  0.0  0.0  0.0
    12 0.00002207 0.03248395  0.0  0.0  0.0
*
*******************************************************************************
* GROUP 3.0 - Transverse Channel Connection (Gap) Data                         *
*******************************************************************************
* CARD GROUP 3
* NGR
    3
* Card 3.1
*  NK NDM2 NDM3 NDM4 NDM5 NDM6 NDM7 NDM8 NDM9 NM10 NM11 NM12 NM13 NM14
   18    0    0    0    0    0    0    0    0    0    0    0    0    0
* Card 3.2
*   K    IK    JK    GAPN   LNGTH  WKR FWL  IGPB  IGPA FACT  IGAP  JGAP  IGAP  JGAP  IGAP  JGAP
    1     1     2 0.00100 0.00520 0.50 0.0     0     0  1.0     0    0     0     0     0     0
* Card 3.3
* GMLT  ETNR
 1.000 0.000
* Cards 3.2 and 3.3 continued
   2     2     3 0.00100 0.00520 0.50 0.0     0     0  1.0    0     0     0     0     0     0
1.000 0.000
    3     3     4 0.00100 0.00520 0.50 0.0     0     0  1.0    0     0     0     0     0     0
1.000 0.000
    4     4     5 0.00100 0.00520 0.50 0.0     0     0  1.0    0     0     0     0     0     0
1.000 0.000
    5     5     6 0.00100 0.00520 0.50 0.0     0     0  1.0    0     0     0     0     0     0
1.000 0.000
    6     1     6 0.00100 0.00520 0.50 0.0     0     0  1.0    0     0     0     0     0     0
1.000 0.000
    7     1     7 0.00100 0.00484 0.50 0.0     0     0  1.0    0     0     0     0     0     0
1.000 0.000
    8     2     8 0.00100 0.00484 0.50 0.0     0     0  1.0    0     0     0     0     0     0
1.000 0.000
    9     3     9 0.00100 0.00484 0.50 0.0     0     0  1.0    0     0     0     0     0     0
```

```
1.000 0.000
   10     4    10 0.00100 0.00484 0.50 0.0     0     0  1.0    0     0     0     0     0     0
1.000 0.000
   11     5    11 0.00100 0.00484 0.50 0.0     0     0  1.0    0     0     0     0     0     0
1.000 0.000
   12     6    12 0.00100 0.00484 0.50 0.0     0     0  1.0    0     0     0     0     0     0
1.000 0.000
   13     7     8 0.00100 0.00288 0.50 0.5     0     0  1.0    0     0     0     0     0     0
1.000 0.000
   14     8     9 0.00100 0.00288 0.50 0.5     0     0  1.0    0     0     0     0     0     0
1.000 0.000
   15     9    10 0.00100 0.00288 0.50 0.5     0     0  1.0    0     0     0     0     0     0
1.000 0.000
   16    10    11 0.00100 0.00288 0.50 0.5     0     0  1.0    0     0     0     0     0     0
1.000 0.000
   17    11    12 0.00100 0.00288 0.50 0.5     0     0  1.0    0     0     0     0     0     0
1.000 0.000
   18     7    12 0.00100 0.00288 0.50 0.5     0     0  1.0    0     0     0     0     0     0
1.000 0.000
*
* Card 3.4
* NLGP
     0
*
*******************************************************************************
* GROUP 4.0 - Vertical Channel Connection Data                                 *
*******************************************************************************
* CARD GROUP 4
* NGR
    4
* Card 4.1
* NSEC NSIM IREB NDM4 NDM5 NDM6 NDM7 NDM8 NDM9 NM10 NM11 NM12 NM13 NM14
     1    1    1    0    0    0    0    0    0    0    0    0    0    0
* Card 4.2
* ISEC  NCHN  NONO     DXS  IVAR
     1    12    60 0.02500     0
* Card 4.3
```

```
*    I  KCHA  KCHA  KCHA  KCHA  KCHA  KCHA  KCHB  KCHB  KCHB  KCHB  KCHB  KCHB
     1     1     0     0     0     0     0     1     0     0     0     0     0
     2     2     0     0     0     0     0     2     0     0     0     0     0
     3     3     0     0     0     0     0     3     0     0     0     0     0
     4     4     0     0     0     0     0     4     0     0     0     0     0
     5     5     0     0     0     0     0     5     0     0     0     0     0
     6     6     0     0     0     0     0     6     0     0     0     0     0
     7     7     0     0     0     0     0     7     0     0     0     0     0
     8     8     0     0     0     0     0     8     0     0     0     0     0
     9     9     0     0     0     0     0     9     0     0     0     0     0
    10    10     0     0     0     0     0    10     0     0     0     0     0
    11    11     0     0     0     0     0    11     0     0     0     0     0
    12    12     0     0     0     0     0    12     0     0     0     0     0
* Card 4.5
* IWDE
    12
* Card 4.6
* MSIM
   720
*
*******************************************************************************
* GROUP 8.0 - Rod and Unheated Conductor Data                                  *
*******************************************************************************
* CARD GROUP 8
* NGR
    8
* Card 8.1
* NRRD  NSRD   NC NRTB NRAD NLTY NSTA  NXF NCAN RADF   W3 NM12 NM13 NM14
     7     6    3    1    0    0    1    1    0    0   -1    0    0    0
* Card 8.2
*   N IFTY IAXP NRND  DAXMIN   RMULT    HGAP ISECR   HTAMB    TAMB
    1    1    1    0 0.00000   1.000 0.00000     1   0.000   0.000
* Card 8.3
* NSCH   PIE  NSCH   PIE  NSCH   PIE  NSCH   PIE  NSCH   PIE  NSCH   PIE  NSCH   PIE  NSCH   PIE
     1 0.167     2 0.167     3 0.167     4 0.167     5 0.167     6 0.167     0 0.000     0 0.000
*
* Cards 8.2 and 8.3 continued
```

```
     2    1    1    0 0.00000   1.000 0.00000     1   0.000   0.000
     1 0.167     2 0.167     7 0.333     8 0.333     0 0.000     0 0.000     0 0.000     0 0.000
*
     3    1    1    0 0.00000   1.000 0.00000     1   0.000   0.000
     2 0.167     3 0.167     8 0.333     9 0.333     0 0.000     0 0.000     0 0.000     0 0.000
*
     4    1    1    0 0.00000   1.000 0.00000     1   0.000   0.000
     3 0.167     4 0.167     9 0.333    10 0.333     0 0.000     0 0.000     0 0.000     0 0.000
*
     5    1    1    0 0.00000   1.000 0.00000     1   0.000   0.000
     4 0.167     5 0.167    10 0.333    11 0.333     0 0.000     0 0.000     0 0.000     0 0.000
*
     6    1    1    0 0.00000   1.000 0.00000     1   0.000   0.000
     5 0.167     6 0.167    11 0.333    12 0.333     0 0.000     0 0.000     0 0.000     0 0.000
*
     7    1    1    0 0.00000   1.000 0.00000     1   0.000   0.000
     1 0.167     6 0.167     7 0.333    12 0.333     0 0.000     0 0.000     0 0.000     0 0.000
*
* Card 8.5
*   N ISTY  HPERIM  PERIMI RMULT NOSLCHC  NSLCHC  HTAMBS   TAMBS
    1    2 0.01573 0.00000  1.00       7       0   0.000   0.000
    2    2 0.01573 0.00000  1.00       8       0   0.000   0.000
    3    2 0.01573 0.00000  1.00       9       0   0.000   0.000
    4    2 0.01573 0.00000  1.00      10       0   0.000   0.000
    5    2 0.01573 0.00000  1.00      11       0   0.000   0.000
    6    2 0.01573 0.00000  1.00      12       0   0.000   0.000
*
* Card 8.6
*   I  NRT1  NST1  NRX1
    1     7     6     2
*
* Card 8.7
* IRTAB IRTAB IRTAB IRTAB IRTAB IRTAB IRTAB IRTAB IRTAB IRTAB IRTAB IRTAB
      1     2     3     4     5     6     7     0     0     0     0     0
*
* Card 8.8
* IRTAB IRTAB IRTAB IRTAB IRTAB IRTAB IRTAB IRTAB IRTAB IRTAB IRTAB IRTAB
```

```
      1     2     3     4     5     6     0     0     0     0     0     0
*
* Card 8.9
*   AXIALT     TRINIT
 0.0000000   80.51100
 1.5000000   80.51100
*
*******************************************************************************
* GROUP 9.0 - Conductor Geometry Description                                   *
*******************************************************************************
* CARD GROUP 9
* NGR
    9
* Card 9.1
* NFLT IRLF ICNF IMWR NDM5 NDM6 NDM7 NDM8 NDM9 NM10 NM11 NM12 NM13 NM14
     2    0    0    0    0    0    0    0    0    0    0    0    0    0
*
* Card 9.6
*   I FTYP    DROD     DIN NFUL ITOX ITIX NDM8 NDM9 NM10 NM11 NM12 NM13 NM14
    1 tube 0.00800 0.00600    1    1    1    0    0    0    0    0    0    0
* Card 9.7
* NODR MATR    TREG    QREG
     2    1 0.00100 1.00000
*
* Card 9.6
*   I FTYP    DROD     DIN NFUL ITOX ITIX NDM8 NDM9 NM10 NM11 NM12 NM13 NM14
    2 wall 0.01573 0.00100    1    1    1    0    0    0    0    0    0    0
* Card 9.7
* NODR MATR    TREG    QREG
     2    1 0.00100 0.00000
*
*******************************************************************************
* GROUP 10 - Material Properties Tables                                        *
*******************************************************************************
* CARD GROUP 10
* NGR
   10
```

```
* CArd 10.1
* NMAT NDM2 NDM3 NDM4 NDM5 NDM6 NDM7 NDM8 NDM9 NM10 NM11 NM12 NM13 NM14
     1    0    0    0    0    0    0    0    0    0    0    0    0    0
* Card 10.2
*   N NTDP     RCOLD                        IMATAN
    1    6   8470.57                   Inconel 600
* Card 10.3
*    TPROP     CPF1      THCF
       -73    0.377     13.40
        93    0.464     15.71
       204    0.485     17.44
       427    0.527     20.90
       649    0.586     24.79
       871    0.623     28.83
*
*******************************************************************************
* GROUP 11.0 - Axial Power Tables and Forcing Functions                        *
*******************************************************************************
* CARD GROUP 11
* NGR
   11
* Card 11.1
* NQA NAXP MNXN   NQ NGPF  NQR NDM7 NDM8 NDM9 NM10 NM11 NM12 NM13 NM14
    1    1    2    0    0    1    0    0    0    0    0    0    0    0
*
* Axial Power Forcing Functions
* Card 11.2
*      YQA
       0.0
* Card 11.3
*  I NAXN
   1    2
* Card 11.4
*        Y      AXIAL
  0.000000   1.000000
  1.500000   1.000000
*
```

```
* Total Power Forcing Functions
* Card 11.5
*       YQ         FQ
*    0.0000     0.0000
*    1.0000     1.0000
*  100.0000     1.0000
*
* Radial Power Forcing Functions
* Card 11.7
*      YQR
       0.0
* Card 11.8
*      FQR        FQR        FQR        FQR        FQR        FQR        FQR        FQR
    0.8861     1.0190     1.0190     1.0190     1.0190     1.0190     1.0190     0.0000
*
*******************************************************************************
* GROUP 12 - Turbulent mixing data                                             *
*******************************************************************************
* CARD GROUP 12
* NGR
   12
* Card 12.2
* AAAK      DFRD  THEM
   0.0   0.00800   5.0
*
*******************************************************************************
* GROUP 13.0 - Boundary Condition Data                                         *
*******************************************************************************
* CARD GROUP 13
* NGR
   13
* Card 13.1
* NBND NKBD NFUN NGBD NDM5 NDM6 NDM7 NDM8 NDM9 NM10 NM11 NM12 NM13 NM14
    24    0    1    0    0    0    0    0    0    0    0    0    0    0
* Card 13.2
* NPT
    4
```

```
* Card 13.3
* ABSC ORDINT   ABSC ORDINT   ABSC ORDINT
   0.0  0.000    0.1  0.000    0.2  1.000 1500.0  1.000
* Card 13.4
* Inlet b.c. ----------------------------------------------------------
* IBD1 IBD2 ISPC N1FN N2FN N3FN   BCVALUE1   BCVALUE2   BCVALUE3 INITGAS
     1    1    2    1    0    0        0.0     357.00     0.0000       1
     2    1    2    1    0    0        0.0     357.00     0.0000       1
     3    1    2    1    0    0        0.0     357.00     0.0000       1
     4    1    2    1    0    0        0.0     357.00     0.0000       1
     5    1    2    1    0    0        0.0     357.00     0.0000       1
     6    1    2    1    0    0        0.0     357.00     0.0000       1
     7    1    2    1    0    0        0.0     357.00     0.0000       1
     8    1    2    1    0    0        0.0     357.00     0.0000       1
     9    1    2    1    0    0        0.0     357.00     0.0000       1
    10    1    2    1    0    0        0.0     357.00     0.0000       1
    11    1    2    1    0    0        0.0     357.00     0.0000       1
    12    1    2    1    0    0        0.0     357.00     0.0000       1
* Outlet b.c. ---------------------------------------------------------
* IBD1 IBD2 ISPC N1FN N2FN N3FN   BCVALUE1   BCVALUE2   BCVALUE3 INITGAS
     1   62   1    0    0    0     0.0000     357.00     250.00       1
     2   62   1    0    0    0     0.0000     357.00     250.00       1
     3   62   1    0    0    0     0.0000     357.00     250.00       1
     4   62   1    0    0    0     0.0000     357.00     250.00       1
     5   62   1    0    0    0     0.0000     357.00     250.00       1
     6   62   1    0    0    0     0.0000     357.00     250.00       1
     7   62   1    0    0    0     0.0000     357.00     250.00       1
     8   62   1    0    0    0     0.0000     357.00     250.00       1
     9   62   1    0    0    0     0.0000     357.00     250.00       1
    10   62   1    0    0    0     0.0000     357.00     250.00       1
    11   62   1    0    0    0     0.0000     357.00     250.00       1
    12   62   1    0    0    0     0.0000     357.00     250.00       1
*
*******************************************************************************
* Group 14 - Output Options                                                    *
*******************************************************************************
*NGRP
```

```
   14
*  N1 NOU1 NOU2 NOU3 NOU4 IPRP IOPT IRWR NDM9 NM10 NM11 NM12 NM13 NM14
    5    0    0    0    0    0    2    1    0    0    0    0    0    0
*
*PRCH
*    5  13   17   20
*PRTG
*    9  25   36
*PRTR
*    4  10   12
*PRTS
*    5   8
*
*******************************************************************************
* Group 15 - TIME DOMAIN DATA                                                  *
*******************************************************************************
* CARD GROUP 15
* NGR
   15
* Card 15.1
*        DTMIN         DTMAX          TEND    EDINT   DMPINT       RTWFP
      .0000001         0.001          15.0     15.0      0.1         1.0
* Card 15.2
*        DTMIN (if negative stop)
         -.001           0.0           0.0      0.0      0.0         0.0
*
*******************************************************************************
* END GROUP TIME DOMAIN DATA
*******************************************************************************
*
```

E.2 COBRA-TF-SC input file for the Seven-rod test bundle - high inlet enthalpy.

```
*******************************************************************************
```

```
* Heat Transfer Experiments and Numerical Analysis of Supercritical  Pressure  *
* Water in Seven-rod Test Bundle - Mishawa et. al                               *
* CTF input deck for test case 2A                                               *
*********************************************************************************
* MAIN PROBLEM CONTROL DATA                                                     *
*********************************************************************************
* CARD INPUT 1
*       ICOBRA
             1
* CARD INPUT 2
*      INITIAL         DUMPF
             1             1
* CARD INPUT 3
*         EPSO        OITMAX        IITMAX
         0.001            10            40
* CARD COBRA 1
*---------- TEXT ------------>
  *** 7ROD IAEA BENCHMARK PART 2 ***
*********************************************************************************
* GROUP 1 - Calculation Variables and Initial Conditions                        *
*********************************************************************************
* CARD GROUP 1
* NGR
    1
* Card 1.1
* NGAS IRFC EDMD IMIX ISOL NDM6 NDM7 NDM8 NDM9 NM10 NM11 NM12 NM13 NM14
     1    2    0    2    0    0    0    0    0    0    0    0    0    0
* Card 1.2
*     GTOT     AFLUX    DHFRAC
     0.270    22.667       0.0
* Card 1.3
*     PREF       HIN      HGIN    VFRAC1    VFRAC2
    250.00   1033.00     288.4       1.0    0.9999
* Card 1.4
* GTP(1)    VFRAC(3)  GTP(2)    VFRAC(4)  GTP(3)    VFRAC(5)  GTP(4)    VFRAC(6)
air            .0001
*********************************************************************************
```

```
* GROUP 2.0 - Channel Description                                              *
*******************************************************************************
* CARD GROUP 2
* NGR
    2
* Card 2.1
* NCHA NDM2 NDM3 NDM4 NDM5 NDM6 NDM7 NDM8 NDM9 NM10 NM11 NM12 NM13 NM14
    12    0    0    0    0    0    0    0    0    0    0    0    0    0
* Card 2.2
*    I         AN          PW ABOT ATOP NMGP
     1 0.00000987 0.01256637  0.0  0.0  0.0
     2 0.00000987 0.01256637  0.0  0.0  0.0
     3 0.00000987 0.01256637  0.0  0.0  0.0
     4 0.00000987 0.01256637  0.0  0.0  0.0
     5 0.00000987 0.01256637  0.0  0.0  0.0
     6 0.00000997 0.01256637  0.0  0.0  0.0
     7 0.00002207 0.03248395  0.0  0.0  0.0
     8 0.00002207 0.03248395  0.0  0.0  0.0
     9 0.00002207 0.03248395  0.0  0.0  0.0
    10 0.00002207 0.03248395  0.0  0.0  0.0
    11 0.00002207 0.03248395  0.0  0.0  0.0
    12 0.00002207 0.03248395  0.0  0.0  0.0
*
*******************************************************************************
* GROUP 3.0 - Transverse Channel Connection (Gap) Data                         *
*******************************************************************************
* CARD GROUP 3
* NGR
    3
* Card 3.1
*  NK NDM2 NDM3 NDM4 NDM5 NDM6 NDM7 NDM8 NDM9 NM10 NM11 NM12 NM13 NM14
   18    0    0    0    0    0    0    0    0    0    0    0    0    0
* Card 3.2
*   K    IK    JK    GAPN   LNGTH  WKR FWL  IGPB  IGPA FACT  IGAP  JGAP  IGAP  JGAP  IGAP  JGAP
    1     1     2 0.00100 0.00520 0.50 0.0     0     0  1.0     0    0     0     0     0     0
* Card 3.3
* GMLT  ETNR
```

```
 1.000 0.000
* Cards 3.2 and 3.3 continued
   2     2      3 0.00100 0.00520 0.50 0.0     0     0  1.0    0     0     0     0     0     0
1.000 0.000
   3     3      4 0.00100 0.00520 0.50 0.0     0     0  1.0    0     0     0     0     0     0
1.000 0.000
   4     4      5 0.00100 0.00520 0.50 0.0     0     0  1.0    0     0     0     0     0     0
1.000 0.000
   5     5      6 0.00100 0.00520 0.50 0.0     0     0  1.0    0     0     0     0     0     0
1.000 0.000
   6     1      6 0.00100 0.00520 0.50 0.0     0     0  1.0    0     0     0     0     0     0
1.000 0.000
   7     1      7 0.00100 0.00484 0.50 0.0     0     0  1.0    0     0     0     0     0     0
1.000 0.000
   8     2      8 0.00100 0.00484 0.50 0.0     0     0  1.0    0     0     0     0     0     0
1.000 0.000
   9     3      9 0.00100 0.00484 0.50 0.0     0     0  1.0    0     0     0     0     0     0
1.000 0.000
  10     4     10 0.00100 0.00484 0.50 0.0     0     0  1.0    0     0     0     0     0     0
1.000 0.000
  11     5     11 0.00100 0.00484 0.50 0.0     0     0  1.0    0     0     0     0     0     0
1.000 0.000
  12     6     12 0.00100 0.00484 0.50 0.0     0     0  1.0    0     0     0     0     0     0
1.000 0.000
  13     7      8 0.00100 0.00288 0.50 0.5     0     0  1.0    0     0     0     0     0     0
1.000 0.000
  14     8      9 0.00100 0.00288 0.50 0.5     0     0  1.0    0     0     0     0     0     0
1.000 0.000
  15     9     10 0.00100 0.00288 0.50 0.5     0     0  1.0    0     0     0     0     0     0
1.000 0.000
  16    10     11 0.00100 0.00288 0.50 0.5     0     0  1.0    0     0     0     0     0     0
1.000 0.000
  17    11     12 0.00100 0.00288 0.50 0.5     0     0  1.0    0     0     0     0     0     0
1.000 0.000
  18     7     12 0.00100 0.00288 0.50 0.5     0     0  1.0    0     0     0     0     0     0
1.000 0.000
*
```

```
* Card 3.4
* NLGP
     0
*
*******************************************************************************
* GROUP 4.0 - Vertical Channel Connection Data                                 *
*******************************************************************************
* CARD GROUP 4
* NGR
    4
* Card 4.1
* NSEC NSIM IREB NDM4 NDM5 NDM6 NDM7 NDM8 NDM9 NM10 NM11 NM12 NM13 NM14
     1    1    1    0    0    0    0    0    0    0    0    0    0    0
* Card 4.2
* ISEC  NCHN  NONO     DXS  IVAR
     1    12    15 0.10000     0
* Card 4.3
*    I  KCHA  KCHA  KCHA  KCHA  KCHA  KCHA  KCHB  KCHB  KCHB  KCHB  KCHB  KCHB
     1     1     0     0     0     0     0     1     0     0     0     0     0
     2     2     0     0     0     0     0     2     0     0     0     0     0
     3     3     0     0     0     0     0     3     0     0     0     0     0
     4     4     0     0     0     0     0     4     0     0     0     0     0
     5     5     0     0     0     0     0     5     0     0     0     0     0
     6     6     0     0     0     0     0     6     0     0     0     0     0
     7     7     0     0     0     0     0     7     0     0     0     0     0
     8     8     0     0     0     0     0     8     0     0     0     0     0
     9     9     0     0     0     0     0     9     0     0     0     0     0
    10    10     0     0     0     0     0    10     0     0     0     0     0
    11    11     0     0     0     0     0    11     0     0     0     0     0
    12    12     0     0     0     0     0    12     0     0     0     0     0
* Card 4.5
* IWDE
    12
* Card 4.6
* MSIM
   180
*
```

```
*******************************************************************************
* GROUP 8.0 - Rod and Unheated Conductor Data                                  *
*******************************************************************************
* CARD GROUP 8
* NGR
    8
* Card 8.1
* NRRD  NSRD   NC NRTB NRAD NLTY NSTA  NXF NCAN RADF   W3 NM12 NM13 NM14
     7     6    3    1    0    0    1    1    0    0   -1    0    0    0
* Card 8.2
*   N IFTY IAXP NRND  DAXMIN   RMULT    HGAP ISECR   HTAMB    TAMB
    1    1    1    0 0.00000   1.000 0.00000     1   0.000   0.000
* Card 8.3
* NSCH   PIE  NSCH   PIE  NSCH   PIE  NSCH   PIE  NSCH   PIE  NSCH   PIE  NSCH   PIE  NSCH   PIE
     1 0.167     2 0.167     3 0.167     4 0.167     5 0.167     6 0.167     0 0.000     0 0.000
*
* Cards 8.2 and 8.3 continued
     2    1    1    0 0.00000   1.000 0.00000     1   0.000   0.000
     1 0.167     2 0.167     7 0.333     8 0.333     0 0.000     0 0.000     0 0.000     0 0.000
*
     3    1    1    0 0.00000   1.000 0.00000     1   0.000   0.000
     2 0.167     3 0.167     8 0.333     9 0.333     0 0.000     0 0.000     0 0.000     0 0.000
*
     4    1    1    0 0.00000   1.000 0.00000     1   0.000   0.000
     3 0.167     4 0.167     9 0.333    10 0.333     0 0.000     0 0.000     0 0.000     0 0.000
*
     5    1    1    0 0.00000   1.000 0.00000     1   0.000   0.000
     4 0.167     5 0.167    10 0.333    11 0.333     0 0.000     0 0.000     0 0.000     0 0.000
*
     6    1    1    0 0.00000   1.000 0.00000     1   0.000   0.000
     5 0.167     6 0.167    11 0.333    12 0.333     0 0.000     0 0.000     0 0.000     0 0.000
*
     7    1    1    0 0.00000   1.000 0.00000     1   0.000   0.000
     1 0.167     6 0.167     7 0.333    12 0.333     0 0.000     0 0.000     0 0.000     0 0.000
*
* Card 8.5
*   N ISTY  HPERIM  PERIMI RMULT NOSLCHC  NSLCHC  HTAMBS   TAMBS
```

```
    1    2 0.01573 0.00000  1.00       7       0   0.000   0.000
    2    2 0.01573 0.00000  1.00       8       0   0.000   0.000
    3    2 0.01573 0.00000  1.00       9       0   0.000   0.000
    4    2 0.01573 0.00000  1.00      10       0   0.000   0.000
    5    2 0.01573 0.00000  1.00      11       0   0.000   0.000
    6    2 0.01573 0.00000  1.00      12       0   0.000   0.000
*
* Card 8.6
*   I  NRT1  NST1  NRX1
    1     7     6     2
*
* Card 8.7
* IRTAB IRTAB IRTAB IRTAB IRTAB IRTAB IRTAB IRTAB IRTAB IRTAB IRTAB IRTAB
      1     2     3     4     5     6     7     0     0     0     0     0
*
* Card 8.8
* IRTAB IRTAB IRTAB IRTAB IRTAB IRTAB IRTAB IRTAB IRTAB IRTAB IRTAB IRTAB
      1     2     3     4     5     6     0     0     0     0     0     0
*
* Card 8.9
*   AXIALT     TRINIT
 0.0000000  238.17000
 1.5000000  238.17000
*
*******************************************************************************
* GROUP 9.0 - Conductor Geometry Description                                  *
*******************************************************************************
* CARD GROUP 9
* NGR
    9
* Card 9.1
* NFLT IRLF ICNF IMWR NDM5 NDM6 NDM7 NDM8 NDM9 NM10 NM11 NM12 NM13 NM14
     2    0    0    0    0    0    0    0    0    0    0    0    0    0
*
* Card 9.6
*   I FTYP    DROD     DIN NFUL ITOX ITIX NDM8 NDM9 NM10 NM11 NM12 NM13 NM14
    1 tube 0.00800 0.00600    1    1    1    0    0    0    0    0    0    0
```

```
* Card 9.7
* NODR MATR    TREG    QREG
     2    1 0.00100 1.00000
*
* Card 9.6
*   I FTYP    DROD     DIN NFUL ITOX ITIX NDM8 NDM9 NM10 NM11 NM12 NM13 NM14
    2 wall 0.01573 0.00100    1    1    1    0    0    0    0    0    0    0
* Card 9.7
* NODR MATR    TREG    QREG
     2    1 0.00100 0.00000
*
*******************************************************************************
* GROUP 10 - Material Properties Tables                                        *
*******************************************************************************
* CARD GROUP 10
* NGR
   10
* CArd 10.1
* NMAT NDM2 NDM3 NDM4 NDM5 NDM6 NDM7 NDM8 NDM9 NM10 NM11 NM12 NM13 NM14
     1    0    0    0    0    0    0    0    0    0    0    0    0    0
* Card 10.2
*   N NTDP     RCOLD                        IMATAN
    1    6   8470.57                   Inconel 600
* Card 10.3
*    TPROP     CPF1      THCF
       -73    0.377     13.40
        93    0.464     15.71
       204    0.485     17.44
       427    0.527     20.90
       649    0.586     24.79
       871    0.623     28.83
*
*******************************************************************************
* GROUP 11.0 - Axial Power Tables and Forcing Functions                        *
*******************************************************************************
* CARD GROUP 11
* NGR
```

```
   11
* Card 11.1
* NQA NAXP MNXN   NQ NGPF  NQR NDM7 NDM8 NDM9 NM10 NM11 NM12 NM13 NM14
    1    1    2    0    0    1    0    0    0    0    0    0    0    0
*
* Axial Power Forcing Functions
* Card 11.2
*      YQA
       0.0
* Card 11.3
*  I NAXN
   1    2
* Card 11.4
*        Y      AXIAL
  0.000000   1.000000
  1.500000   1.000000
*
* Total Power Forcing Functions
* Card 11.5
*       YQ         FQ
*    0.0000     0.0000
*    1.0000     1.0000
*  100.0000     1.0000
*
* Radial Power Forcing Functions
* Card 11.7
*      YQR
       0.0
* Card 11.8
*      FQR        FQR        FQR        FQR        FQR        FQR        FQR        FQR
    1.0000     1.0000     1.0000     1.0000     1.0000     1.0000     1.0000     0.0000
*
*********************************************************************************
* GROUP 12 - Turbulent mixing data                                              *
*********************************************************************************
* CARD GROUP 12
* NGR
```

```
   12
* Card 12.2
* AAAK      DFRD  THEM
   0.0   0.00800   5.0
*
*******************************************************************************
* GROUP 13.0 - Boundary Condition Data                                         *
*******************************************************************************
* CARD GROUP 13
* NGR
   13
* Card 13.1
* NBND NKBD NFUN NGBD NDM5 NDM6 NDM7 NDM8 NDM9 NM10 NM11 NM12 NM13 NM14
    24    0    1    0    0    0    0    0    0    0    0    0    0    0
* Card 13.2
* NPT
    4
* Card 13.3
* ABSC ORDINT   ABSC ORDINT   ABSC ORDINT
   0.0  0.000    0.1  0.000    0.2  1.000 1500.0  1.000
* Card 13.4
* Inlet b.c. ----------------------------------------------------------
* IBD1 IBD2 ISPC N1FN N2FN N3FN   BCVALUE1   BCVALUE2   BCVALUE3 INITGAS
     1    1    2    1    0    0        0.0    1033.00     0.0000       1
     2    1    2    1    0    0        0.0    1033.00     0.0000       1
     3    1    2    1    0    0        0.0    1033.00     0.0000       1
     4    1    2    1    0    0        0.0    1033.00     0.0000       1
     5    1    2    1    0    0        0.0    1033.00     0.0000       1
     6    1    2    1    0    0        0.0    1033.00     0.0000       1
     7    1    2    1    0    0        0.0    1033.00     0.0000       1
     8    1    2    1    0    0        0.0    1033.00     0.0000       1
     9    1    2    1    0    0        0.0    1033.00     0.0000       1
    10    1    2    1    0    0        0.0    1033.00     0.0000       1
    11    1    2    1    0    0        0.0    1033.00     0.0000       1
    12    1    2    1    0    0        0.0    1033.00     0.0000       1
* Outlet b.c. ---------------------------------------------------------
* IBD1 IBD2 ISPC N1FN N2FN N3FN   BCVALUE1   BCVALUE2   BCVALUE3 INITGAS
```

```
     1   17   1    0    0    0     0.0000    1033.00     250.00       1
     2   17   1    0    0    0     0.0000    1033.00     250.00       1
     3   17   1    0    0    0     0.0000    1033.00     250.00       1
     4   17   1    0    0    0     0.0000    1033.00     250.00       1
     5   17   1    0    0    0     0.0000    1033.00     250.00       1
     6   17   1    0    0    0     0.0000    1033.00     250.00       1
     7   17   1    0    0    0     0.0000    1033.00     250.00       1
     8   17   1    0    0    0     0.0000    1033.00     250.00       1
     9   17   1    0    0    0     0.0000    1033.00     250.00       1
    10   17   1    0    0    0     0.0000    1033.00     250.00       1
    11   17   1    0    0    0     0.0000    1033.00     250.00       1
    12   17   1    0    0    0     0.0000    1033.00     250.00       1
*
*******************************************************************************
* Group 14 - Output Options                                                    *
*******************************************************************************
*NGRP
   14
*  N1 NOU1 NOU2 NOU3 NOU4 IPRP IOPT IRWR NDM9 NM10 NM11 NM12 NM13 NM14
    5    0    0    0    0    0    2    1    0    0    0    0    0    0
*
*PRCH
*    5  13   17   20
*PRTG
*    9  25   36
*PRTR
*    4  10   12
*PRTS
*    5   8
*
*******************************************************************************
* Group 15 - TIME DOMAIN DATA                                                  *
*******************************************************************************
* CARD GROUP 15
* NGR
   15
* Card 15.1
```

```
*        DTMIN         DTMAX          TEND    EDINT   DMPINT       RTWFP
      .0000001         0.001          15.0     15.0      0.1         1.0
* Card 15.2
*        DTMIN (if negative stop)
         -.001           0.0           0.0      0.0      0.0         0.0
*
********************************************************************************
* END GROUP TIME DOMAIN DATA
********************************************************************************
*
```

E.3 COBRA-TF-SC input file for the 62-element Canadian Supercritical Water Reactor (SCWR) Fuel Bundle

```
********************************************************************************
* The 62-element Canadian SCWR Fuel Bundle: AECL, 2013                         *
* CTF input deck for the EOC case                                              *
********************************************************************************
* MAIN PROBLEM CONTROL DATA                                                    *
********************************************************************************
* CARD INPUT 1
*       ICOBRA
             1
* CARD INPUT 2
*      INITIAL         DUMPF
             1             1
* CARD INPUT 3
*         EPSO        OITMAX        IITMAX
         0.001            10            40
* CARD COBRA 1
*---------- TEXT ------------>
  *** 62-element Canadian SCWR CASE ***
********************************************************************************
```

```
* GROUP 1 - Calculation Variables and Initial Conditions                    *
*****************************************************************************
* CARD GROUP 1
* NGR
    1
* Card 1.1
* NGAS IRFC EDMD IMIX ISOL NDM6 NDM7 NDM8 NDM9 NM10 NM11 NM12 NM13 NM14
     1    2    0    1    0    0    0    0    0    0    0    0    0    0
* Card 1.2
*     GTOT     AFLUX    DHFRAC
     4.7535   30.694       0.0
* Card 1.3
*     PREF       HIN      HGIN    VFRAC1    VFRAC2
    250.00   1623.90     288.4       1.0    0.9999
* Card 1.4
* GTP(1)    VFRAC(3)  GTP(2)    VFRAC(4)  GTP(3)    VFRAC(5)  GTP(4)    VFRAC(6)
air            .0001
*****************************************************************************
* GROUP 2.0 - Channel Description                                           *
*****************************************************************************
* CARD GROUP 2
* NGR
    2
* Card 2.1
* NCHA NDM2 NDM3 NDM4 NDM5 NDM6 NDM7 NDM8 NDM9 NM10 NM11 NM12 NM13 NM14
    93    0    0    0    0    0    0    0    0    0    0    0    0    0
* Card 2.2
*    I         AN         PW ABOT ATOP NMGP
     1 0.00003884 0.02320200  0.0  0.0  0.0
     2 0.00003884 0.02320200  0.0  0.0  0.0
     3 0.00003884 0.02320200  0.0  0.0  0.0
     4 0.00003884 0.02320200  0.0  0.0  0.0
     5 0.00003884 0.02320200  0.0  0.0  0.0
     6 0.00003884 0.02320200  0.0  0.0  0.0
     7 0.00003884 0.02320200  0.0  0.0  0.0
     8 0.00003884 0.02320200  0.0  0.0  0.0
     9 0.00003884 0.02320200  0.0  0.0  0.0
```

```
10 0.00003884 0.02320200  0.0  0.0  0.0
11 0.00003884 0.02320200  0.0  0.0  0.0
12 0.00003884 0.02320200  0.0  0.0  0.0
13 0.00003884 0.02320200  0.0  0.0  0.0
14 0.00003884 0.02320200  0.0  0.0  0.0
15 0.00003884 0.02320200  0.0  0.0  0.0
16 0.00003884 0.02320200  0.0  0.0  0.0
17 0.00003884 0.02320200  0.0  0.0  0.0
18 0.00003884 0.02320200  0.0  0.0  0.0
19 0.00003884 0.02320200  0.0  0.0  0.0
20 0.00003884 0.02320200  0.0  0.0  0.0
21 0.00003884 0.02320200  0.0  0.0  0.0
22 0.00003884 0.02320200  0.0  0.0  0.0
23 0.00003884 0.02320200  0.0  0.0  0.0
24 0.00003884 0.02320200  0.0  0.0  0.0
25 0.00003884 0.02320200  0.0  0.0  0.0
26 0.00003884 0.02320200  0.0  0.0  0.0
27 0.00003884 0.02320200  0.0  0.0  0.0
28 0.00003884 0.02320200  0.0  0.0  0.0
29 0.00003884 0.02320200  0.0  0.0  0.0
30 0.00003884 0.02320200  0.0  0.0  0.0
31 0.00003884 0.02320200  0.0  0.0  0.0
32 0.00007086 0.03131500  0.0  0.0  0.0
33 0.00007086 0.03131500  0.0  0.0  0.0
34 0.00007086 0.03131500  0.0  0.0  0.0
35 0.00007086 0.03131500  0.0  0.0  0.0
36 0.00007086 0.03131500  0.0  0.0  0.0
37 0.00007086 0.03131500  0.0  0.0  0.0
38 0.00007086 0.03131500  0.0  0.0  0.0
39 0.00007086 0.03131500  0.0  0.0  0.0
40 0.00007086 0.03131500  0.0  0.0  0.0
41 0.00007086 0.03131500  0.0  0.0  0.0
42 0.00007086 0.03131500  0.0  0.0  0.0
43 0.00007086 0.03131500  0.0  0.0  0.0
44 0.00007086 0.03131500  0.0  0.0  0.0
45 0.00007086 0.03131500  0.0  0.0  0.0
46 0.00007086 0.03131500  0.0  0.0  0.0
```

```
47 0.00007086 0.03131500  0.0  0.0  0.0
48 0.00007086 0.03131500  0.0  0.0  0.0
49 0.00007086 0.03131500  0.0  0.0  0.0
50 0.00007086 0.03131500  0.0  0.0  0.0
51 0.00007086 0.03131500  0.0  0.0  0.0
52 0.00007086 0.03131500  0.0  0.0  0.0
53 0.00007086 0.03131500  0.0  0.0  0.0
54 0.00007086 0.03131500  0.0  0.0  0.0
55 0.00007086 0.03131500  0.0  0.0  0.0
56 0.00007086 0.03131500  0.0  0.0  0.0
57 0.00007086 0.03131500  0.0  0.0  0.0
58 0.00007086 0.03131500  0.0  0.0  0.0
59 0.00007086 0.03131500  0.0  0.0  0.0
60 0.00007086 0.03131500  0.0  0.0  0.0
61 0.00007086 0.03131500  0.0  0.0  0.0
62 0.00007086 0.03131500  0.0  0.0  0.0
63 0.00004746 0.03215100  0.0  0.0  0.0
64 0.00004746 0.03215100  0.0  0.0  0.0
65 0.00004746 0.03215100  0.0  0.0  0.0
66 0.00004746 0.03215100  0.0  0.0  0.0
67 0.00004746 0.03215100  0.0  0.0  0.0
68 0.00004746 0.03215100  0.0  0.0  0.0
69 0.00004746 0.03215100  0.0  0.0  0.0
70 0.00004746 0.03215100  0.0  0.0  0.0
71 0.00004746 0.03215100  0.0  0.0  0.0
72 0.00004746 0.03215100  0.0  0.0  0.0
73 0.00004746 0.03215100  0.0  0.0  0.0
74 0.00004746 0.03215100  0.0  0.0  0.0
75 0.00004746 0.03215100  0.0  0.0  0.0
76 0.00004746 0.03215100  0.0  0.0  0.0
77 0.00004746 0.03215100  0.0  0.0  0.0
78 0.00004746 0.03215100  0.0  0.0  0.0
79 0.00004746 0.03215100  0.0  0.0  0.0
80 0.00004746 0.03215100  0.0  0.0  0.0
81 0.00004746 0.03215100  0.0  0.0  0.0
82 0.00004746 0.03215100  0.0  0.0  0.0
83 0.00004746 0.03215100  0.0  0.0  0.0
```

```
    84 0.00004746 0.03215100  0.0  0.0  0.0
    85 0.00004746 0.03215100  0.0  0.0  0.0
    86 0.00004746 0.03215100  0.0  0.0  0.0
    87 0.00004746 0.03215100  0.0  0.0  0.0
    88 0.00004746 0.03215100  0.0  0.0  0.0
    89 0.00004746 0.03215100  0.0  0.0  0.0
    90 0.00004746 0.03215100  0.0  0.0  0.0
    91 0.00004746 0.03215100  0.0  0.0  0.0
    92 0.00004746 0.03215100  0.0  0.0  0.0
    93 0.00004746 0.03215100  0.0  0.0  0.0
*
*******************************************************************************
* GROUP 3.0 - Transverse Channel Connection (Gap) Data                         *
*******************************************************************************
* CARD GROUP 3
* NGR
    3
* Card 3.1
*  NK NDM2 NDM3 NDM4 NDM5 NDM6 NDM7 NDM8 NDM9 NM10 NM11 NM12 NM13 NM14
  155    0    0    0    0    0    0    0    0    0    0    0    0    0
* Card 3.2
*   K    IK    JK    GAPN   LNGTH  WKR FWL  IGPB  IGPA FACT  IGAP  JGAP  IGAP  JGAP  IGAP  JGAP
    1     1     2 0.00265 0.00968 0.50 0.5     0     0  1.0     0     0     0     0     0     0
* Card 3.3
* GMLT  ETNR
 1.000 0.000
* Cards 3.2 and 3.3 continued
    2     1    31 0.00265 0.00968 0.50 0.5     0     0  1.0     0     0     0     0     0     0
1.000 0.000
    3     1    32 0.00122 0.01141 0.50 0.0     0     0  1.0     0     0     0     0     0     0
1.000 0.000
    4     2     3 0.00265 0.00968 0.50 0.5     0     0  1.0     0     0     0     0     0     0
1.000 0.000
    5     2    33 0.00122 0.01141 0.50 0.0     0     0  1.0     0     0     0     0     0     0
1.000 0.000
    6     3     4 0.00265 0.00968 0.50 0.5     0     0  1.0     0     0     0     0     0     0
1.000 0.000
```

```
    7     3    34 0.00122 0.01141 0.50 0.0     0     0  1.0     0     0     0     0     0     0
1.000 0.000
    8     4     5 0.00265 0.00968 0.50 0.5     0     0  1.0     0     0     0     0     0     0
1.000 0.000
    9     4    35 0.00122 0.01141 0.50 0.0     0     0  1.0     0     0     0     0     0     0
1.000 0.000
   10     5     6 0.00265 0.00968 0.50 0.5     0     0  1.0     0     0     0     0     0     0
1.000 0.000
   11     5    36 0.00122 0.01141 0.50 0.0     0     0  1.0     0     0     0     0     0     0
1.000 0.000
   12     6     7 0.00265 0.00968 0.50 0.5     0     0  1.0     0     0     0     0     0     0
1.000 0.000
   13     6    37 0.00122 0.01141 0.50 0.0     0     0  1.0     0     0     0     0     0     0
1.000 0.000
   14     7     8 0.00265 0.00968 0.50 0.5     0     0  1.0     0     0     0     0     0     0
1.000 0.000
   15     7    38 0.00122 0.01141 0.50 0.0     0     0  1.0     0     0     0     0     0     0
1.000 0.000
   16     8     9 0.00265 0.00968 0.50 0.5     0     0  1.0     0     0     0     0     0     0
1.000 0.000
   17     8    39 0.00122 0.01141 0.50 0.0     0     0  1.0     0     0     0     0     0     0
1.000 0.000
   18     9    10 0.00265 0.00968 0.50 0.5     0     0  1.0     0     0     0     0     0     0
1.000 0.000
   19     9    40 0.00122 0.01141 0.50 0.0     0     0  1.0     0     0     0     0     0     0
1.000 0.000
   20    10    11 0.00265 0.00968 0.50 0.5     0     0  1.0     0     0     0     0     0     0
1.000 0.000
   21    10    41 0.00122 0.01141 0.50 0.0     0     0  1.0     0     0     0     0     0     0
1.000 0.000
   22    11    12 0.00265 0.00968 0.50 0.5     0     0  1.0     0     0     0     0     0     0
1.000 0.000
   23    11    42 0.00122 0.01141 0.50 0.0     0     0  1.0     0     0     0     0     0     0
1.000 0.000
   24    12    13 0.00265 0.00968 0.50 0.5     0     0  1.0     0     0     0     0     0     0
1.000 0.000
   25    12    43 0.00122 0.01141 0.50 0.0     0     0  1.0     0     0     0     0     0     0
```

```
1.000 0.000
   26    13    14 0.00265 0.00968 0.50 0.5     0     0  1.0     0     0     0     0     0     0
1.000 0.000
   27    13    44 0.00122 0.01141 0.50 0.0     0     0  1.0     0     0     0     0     0     0
1.000 0.000
   28    14    15 0.00265 0.00968 0.50 0.5     0     0  1.0     0     0     0     0     0     0
1.000 0.000
   29    14    45 0.00122 0.01141 0.50 0.0     0     0  1.0     0     0     0     0     0     0
1.000 0.000
   30    15    16 0.00265 0.00968 0.50 0.5     0     0  1.0     0     0     0     0     0     0
1.000 0.000
   31    15    46 0.00122 0.01141 0.50 0.0     0     0  1.0     0     0     0     0     0     0
1.000 0.000
   32    16    17 0.00265 0.00968 0.50 0.5     0     0  1.0     0     0     0     0     0     0
1.000 0.000
   33    16    47 0.00122 0.01141 0.50 0.0     0     0  1.0     0     0     0     0     0     0
1.000 0.000
   34    17    18 0.00265 0.00968 0.50 0.5     0     0  1.0     0     0     0     0     0     0
1.000 0.000
   35    17    48 0.00122 0.01141 0.50 0.0     0     0  1.0     0     0     0     0     0     0
1.000 0.000
   36    18    19 0.00265 0.00968 0.50 0.5     0     0  1.0     0     0     0     0     0     0
1.000 0.000
   37    18    49 0.00122 0.01141 0.50 0.0     0     0  1.0     0     0     0     0     0     0
1.000 0.000
   38    19    20 0.00265 0.00968 0.50 0.5     0     0  1.0     0     0     0     0     0     0
1.000 0.000
   39    19    50 0.00122 0.01141 0.50 0.0     0     0  1.0     0     0     0     0     0     0
1.000 0.000
   40    20    21 0.00265 0.00968 0.50 0.5     0     0  1.0     0     0     0     0     0     0
1.000 0.000
   41    20    51 0.00122 0.01141 0.50 0.0     0     0  1.0     0     0     0     0     0     0
1.000 0.000
   42    21    22 0.00265 0.00968 0.50 0.5     0     0  1.0     0     0     0     0     0     0
1.000 0.000
   43    21    52 0.00122 0.01141 0.50 0.0     0     0  1.0     0     0     0     0     0     0
1.000 0.000
```

```
   44    22    23 0.00265 0.00968 0.50 0.5     0     0  1.0     0     0     0     0     0     0
1.000 0.000
   45    22    53 0.00122 0.01141 0.50 0.0     0     0  1.0     0     0     0     0     0     0
1.000 0.000
   46    23    24 0.00265 0.00968 0.50 0.5     0     0  1.0     0     0     0     0     0     0
1.000 0.000
   47    23    54 0.00122 0.01141 0.50 0.0     0     0  1.0     0     0     0     0     0     0
1.000 0.000
   48    24    25 0.00265 0.00968 0.50 0.5     0     0  1.0     0     0     0     0     0     0
1.000 0.000
   49    24    55 0.00122 0.01141 0.50 0.0     0     0  1.0     0     0     0     0     0     0
1.000 0.000
   50    25    26 0.00265 0.00968 0.50 0.5     0     0  1.0     0     0     0     0     0     0
1.000 0.000
   51    25    56 0.00122 0.01141 0.50 0.0     0     0  1.0     0     0     0     0     0     0
1.000 0.000
   52    26    27 0.00265 0.00968 0.50 0.5     0     0  1.0     0     0     0     0     0     0
1.000 0.000
   53    26    57 0.00122 0.01141 0.50 0.0     0     0  1.0     0     0     0     0     0     0
1.000 0.000
   54    27    28 0.00265 0.00968 0.50 0.5     0     0  1.0     0     0     0     0     0     0
1.000 0.000
   55    27    58 0.00122 0.01141 0.50 0.0     0     0  1.0     0     0     0     0     0     0
1.000 0.000
   56    28    29 0.00265 0.00968 0.50 0.5     0     0  1.0     0     0     0     0     0     0
1.000 0.000
   57    28    59 0.00122 0.01141 0.50 0.0     0     0  1.0     0     0     0     0     0     0
1.000 0.000
   58    29    30 0.00265 0.00968 0.50 0.5     0     0  1.0     0     0     0     0     0     0
1.000 0.000
   59    29    60 0.00122 0.01141 0.50 0.0     0     0  1.0     0     0     0     0     0     0
1.000 0.000
   60    30    31 0.00265 0.00968 0.50 0.5     0     0  1.0     0     0     0     0     0     0
1.000 0.000
   61    30    61 0.00122 0.01141 0.50 0.0     0     0  1.0     0     0     0     0     0     0
1.000 0.000
   62    31    62 0.00122 0.01141 0.50 0.0     0     0  1.0     0     0     0     0     0     0
```

```
1.000 0.000
   63    32    33 0.00250 0.01199 0.50 0.0     0     0  1.0     0     0     0     0     0     0
1.000 0.000
   64    32    62 0.00250 0.01199 0.50 0.0     0     0  1.0     0     0     0     0     0     0
1.000 0.000
   65    32    63 0.00275 0.01038 0.50 0.0     0     0  1.0     0     0     0     0     0     0
1.000 0.000
   66    33    34 0.00250 0.01199 0.50 0.0     0     0  1.0     0     0     0     0     0     0
1.000 0.000
   67    33    64 0.00275 0.01038 0.50 0.0     0     0  1.0     0     0     0     0     0     0
1.000 0.000
   68    34    35 0.00250 0.01199 0.50 0.0     0     0  1.0     0     0     0     0     0     0
1.000 0.000
   69    34    65 0.00275 0.01038 0.50 0.0     0     0  1.0     0     0     0     0     0     0
1.000 0.000
   70    35    36 0.00250 0.01199 0.50 0.0     0     0  1.0     0     0     0     0     0     0
1.000 0.000
   71    35    66 0.00275 0.01038 0.50 0.0     0     0  1.0     0     0     0     0     0     0
1.000 0.000
   72    36    37 0.00250 0.01199 0.50 0.0     0     0  1.0     0     0     0     0     0     0
1.000 0.000
   73    36    67 0.00275 0.01038 0.50 0.0     0     0  1.0     0     0     0     0     0     0
1.000 0.000
   74    37    38 0.00250 0.01199 0.50 0.0     0     0  1.0     0     0     0     0     0     0
1.000 0.000
   75    37    68 0.00275 0.01038 0.50 0.0     0     0  1.0     0     0     0     0     0     0
1.000 0.000
   76    38    39 0.00250 0.01199 0.50 0.0     0     0  1.0     0     0     0     0     0     0
1.000 0.000
   77    38    69 0.00275 0.01038 0.50 0.0     0     0  1.0     0     0     0     0     0     0
1.000 0.000
   78    39    40 0.00250 0.01199 0.50 0.0     0     0  1.0     0     0     0     0     0     0
1.000 0.000
   79    39    70 0.00275 0.01038 0.50 0.0     0     0  1.0     0     0     0     0     0     0
1.000 0.000
   80    40    41 0.00250 0.01199 0.50 0.0     0     0  1.0     0     0     0     0     0     0
1.000 0.000
```

```
   81    40    71 0.00275 0.01038 0.50 0.0     0     0  1.0     0     0     0     0     0     0
1.000 0.000
   82    41    42 0.00250 0.01199 0.50 0.0     0     0  1.0     0     0     0     0     0     0
1.000 0.000
   83    41    72 0.00275 0.01038 0.50 0.0     0     0  1.0     0     0     0     0     0     0
1.000 0.000
   84    42    43 0.00250 0.01199 0.50 0.0     0     0  1.0     0     0     0     0     0     0
1.000 0.000
   85    42    73 0.00275 0.01038 0.50 0.0     0     0  1.0     0     0     0     0     0     0
1.000 0.000
   86    43    44 0.00250 0.01199 0.50 0.0     0     0  1.0     0     0     0     0     0     0
1.000 0.000
   87    43    74 0.00275 0.01038 0.50 0.0     0     0  1.0     0     0     0     0     0     0
1.000 0.000
   88    44    45 0.00250 0.01199 0.50 0.0     0     0  1.0     0     0     0     0     0     0
1.000 0.000
   89    44    75 0.00275 0.01038 0.50 0.0     0     0  1.0     0     0     0     0     0     0
1.000 0.000
   90    45    46 0.00250 0.01199 0.50 0.0     0     0  1.0     0     0     0     0     0     0
1.000 0.000
   91    45    76 0.00275 0.01038 0.50 0.0     0     0  1.0     0     0     0     0     0     0
1.000 0.000
   92    46    47 0.00250 0.01199 0.50 0.0     0     0  1.0     0     0     0     0     0     0
1.000 0.000
   93    46    77 0.00275 0.01038 0.50 0.0     0     0  1.0     0     0     0     0     0     0
1.000 0.000
   94    47    48 0.00250 0.01199 0.50 0.0     0     0  1.0     0     0     0     0     0     0
1.000 0.000
   95    47    78 0.00275 0.01038 0.50 0.0     0     0  1.0     0     0     0     0     0     0
1.000 0.000
   96    48    49 0.00250 0.01199 0.50 0.0     0     0  1.0     0     0     0     0     0     0
1.000 0.000
   97    48    79 0.00275 0.01038 0.50 0.0     0     0  1.0     0     0     0     0     0     0
1.000 0.000
   98    49    50 0.00250 0.01199 0.50 0.0     0     0  1.0     0     0     0     0     0     0
1.000 0.000
   99    49    80 0.00275 0.01038 0.50 0.0     0     0  1.0     0     0     0     0     0     0
```

```
1.000 0.000
  100    50    51 0.00250 0.01199 0.50 0.0     0     0  1.0     0     0     0     0     0     0
1.000 0.000
  101    50    81 0.00275 0.01038 0.50 0.0     0     0  1.0     0     0     0     0     0     0
1.000 0.000
  102    51    52 0.00250 0.01199 0.50 0.0     0     0  1.0     0     0     0     0     0     0
1.000 0.000
  103    51    82 0.00275 0.01038 0.50 0.0     0     0  1.0     0     0     0     0     0     0
1.000 0.000
  104    52    53 0.00250 0.01199 0.50 0.0     0     0  1.0     0     0     0     0     0     0
1.000 0.000
  105    52    83 0.00275 0.01038 0.50 0.0     0     0  1.0     0     0     0     0     0     0
1.000 0.000
  106    53    54 0.00250 0.01199 0.50 0.0     0     0  1.0     0     0     0     0     0     0
1.000 0.000
  107    53    84 0.00275 0.01038 0.50 0.0     0     0  1.0     0     0     0     0     0     0
1.000 0.000
  108    54    55 0.00250 0.01199 0.50 0.0     0     0  1.0     0     0     0     0     0     0
1.000 0.000
  109    54    85 0.00275 0.01038 0.50 0.0     0     0  1.0     0     0     0     0     0     0
1.000 0.000
  110    55    56 0.00250 0.01199 0.50 0.0     0     0  1.0     0     0     0     0     0     0
1.000 0.000
  111    55    86 0.00275 0.01038 0.50 0.0     0     0  1.0     0     0     0     0     0     0
1.000 0.000
  112    56    57 0.00250 0.01199 0.50 0.0     0     0  1.0     0     0     0     0     0     0
1.000 0.000
  113    56    87 0.00275 0.01038 0.50 0.0     0     0  1.0     0     0     0     0     0     0
1.000 0.000
  114    57    58 0.00250 0.01199 0.50 0.0     0     0  1.0     0     0     0     0     0     0
1.000 0.000
  115    57    88 0.00275 0.01038 0.50 0.0     0     0  1.0     0     0     0     0     0     0
1.000 0.000
  116    58    59 0.00250 0.01199 0.50 0.0     0     0  1.0     0     0     0     0     0     0
1.000 0.000
  117    58    89 0.00275 0.01038 0.50 0.0     0     0  1.0     0     0     0     0     0     0
1.000 0.000
```

```
  118    59    60 0.00250 0.01199 0.50 0.0     0     0  1.0     0     0     0     0     0     0
1.000 0.000
  119    59    90 0.00275 0.01038 0.50 0.0     0     0  1.0     0     0     0     0     0     0
1.000 0.000
  120    60    61 0.00250 0.01199 0.50 0.0     0     0  1.0     0     0     0     0     0     0
1.000 0.000
  121    60    91 0.00275 0.01038 0.50 0.0     0     0  1.0     0     0     0     0     0     0
1.000 0.000
  122    61    62 0.00250 0.01199 0.50 0.0     0     0  1.0     0     0     0     0     0     0
1.000 0.000
  123    61    92 0.00275 0.01038 0.50 0.0     0     0  1.0     0     0     0     0     0     0
1.000 0.000
  124    62    93 0.00275 0.01038 0.50 0.0     0     0  1.0     0     0     0     0     0     0
1.000 0.000
  125    63    64 0.00125 0.01409 0.50 0.5     0     0  1.0     0     0     0     0     0     0
1.000 0.000
  126    63    93 0.00125 0.01409 0.50 0.5     0     0  1.0     0     0     0     0     0     0
1.000 0.000
  127    64    65 0.00125 0.01409 0.50 0.5     0     0  1.0     0     0     0     0     0     0
1.000 0.000
  128    65    66 0.00125 0.01409 0.50 0.5     0     0  1.0     0     0     0     0     0     0
1.000 0.000
  129    66    67 0.00125 0.01409 0.50 0.5     0     0  1.0     0     0     0     0     0     0
1.000 0.000
  130    67    68 0.00125 0.01409 0.50 0.5     0     0  1.0     0     0     0     0     0     0
1.000 0.000
  131    68    69 0.00125 0.01409 0.50 0.5     0     0  1.0     0     0     0     0     0     0
1.000 0.000
  132    69    70 0.00125 0.01409 0.50 0.5     0     0  1.0     0     0     0     0     0     0
1.000 0.000
  133    70    71 0.00125 0.01409 0.50 0.5     0     0  1.0     0     0     0     0     0     0
1.000 0.000
  134    71    72 0.00125 0.01409 0.50 0.5     0     0  1.0     0     0     0     0     0     0
1.000 0.000
  135    72    73 0.00125 0.01409 0.50 0.5     0     0  1.0     0     0     0     0     0     0
1.000 0.000
  136    73    74 0.00125 0.01409 0.50 0.5     0     0  1.0     0     0     0     0     0     0
```

```
1.000 0.000
  137    74    75 0.00125 0.01409 0.50 0.5     0     0  1.0     0     0     0     0     0     0
1.000 0.000
  138    75    76 0.00125 0.01409 0.50 0.5     0     0  1.0     0     0     0     0     0     0
1.000 0.000
  139    76    77 0.00125 0.01409 0.50 0.5     0     0  1.0     0     0     0     0     0     0
1.000 0.000
  140    77    78 0.00125 0.01409 0.50 0.5     0     0  1.0     0     0     0     0     0     0
1.000 0.000
  141    78    79 0.00125 0.01409 0.50 0.5     0     0  1.0     0     0     0     0     0     0
1.000 0.000
  142    79    80 0.00125 0.01409 0.50 0.5     0     0  1.0     0     0     0     0     0     0
1.000 0.000
  143    80    81 0.00125 0.01409 0.50 0.5     0     0  1.0     0     0     0     0     0     0
1.000 0.000
  144    81    82 0.00125 0.01409 0.50 0.5     0     0  1.0     0     0     0     0     0     0
1.000 0.000
  145    82    83 0.00125 0.01409 0.50 0.5     0     0  1.0     0     0     0     0     0     0
1.000 0.000
  146    83    84 0.00125 0.01409 0.50 0.5     0     0  1.0     0     0     0     0     0     0
1.000 0.000
  147    84    85 0.00125 0.01409 0.50 0.5     0     0  1.0     0     0     0     0     0     0
1.000 0.000
  148    85    86 0.00125 0.01409 0.50 0.5     0     0  1.0     0     0     0     0     0     0
1.000 0.000
  149    86    87 0.00125 0.01409 0.50 0.5     0     0  1.0     0     0     0     0     0     0
1.000 0.000
  150    87    88 0.00125 0.01409 0.50 0.5     0     0  1.0     0     0     0     0     0     0
1.000 0.000
  151    88    89 0.00125 0.01409 0.50 0.5     0     0  1.0     0     0     0     0     0     0
1.000 0.000
  152    89    90 0.00125 0.01409 0.50 0.5     0     0  1.0     0     0     0     0     0     0
1.000 0.000
  153    90    91 0.00125 0.01409 0.50 0.5     0     0  1.0     0     0     0     0     0     0
1.000 0.000
  154    91    92 0.00125 0.01409 0.50 0.5     0     0  1.0     0     0     0     0     0     0
1.000 0.000
```

```
  155    92    93 0.00125 0.01409 0.50 0.5     0     0  1.0     0     0     0     0     0     0
1.000 0.000
*
* Card 3.4
* NLGP
     0
*
*********************************************************************************
* GROUP 4.0 - Vertical Channel Connection Data                                   *
*********************************************************************************
* CARD GROUP 4
* NGR
    4
* Card 4.1
* NSEC NSIM IREB NDM4 NDM5 NDM6 NDM7 NDM8 NDM9 NM10 NM11 NM12 NM13 NM14
     1    1    1    0    0    0    0    0    0    0    0    0    0    0
* Card 4.2
* ISEC  NCHN  NONO     DXS  IVAR
     1    93    40 0.12500     0
* Card 4.3
*    I  KCHA  KCHA  KCHA  KCHA  KCHA  KCHA  KCHB  KCHB  KCHB  KCHB  KCHB  KCHB
     1     1     0     0     0     0     0     1     0     0     0     0     0
      2     2     0     0     0     0     0     2     0     0     0     0     0
     3     3     0     0     0     0     0     3     0     0     0     0     0
     4     4     0     0     0     0     0     4     0     0     0     0     0
     5     5     0     0     0     0     0     5     0     0     0     0     0
     6     6     0     0     0     0     0     6     0     0     0     0     0
     7     7     0     0     0     0     0     7     0     0     0     0     0
     8     8     0     0     0     0     0     8     0     0     0     0     0
     9     9     0     0     0     0     0     9     0     0     0     0     0
    10    10     0     0     0     0     0    10     0     0     0     0     0
    11    11     0     0     0     0     0    11     0     0     0     0     0
    12    12     0     0     0     0     0    12     0     0     0     0     0
    13    13     0     0     0     0     0    13     0     0     0     0     0
    14    14     0     0     0     0     0    14     0     0     0     0     0
    15    15     0     0     0     0     0    15     0     0     0     0     0
    16    16     0     0     0     0     0    16     0     0     0     0     0
```

17	17	0	0	0	0	0	17	0	0	0	0	0
18	18	0	0	0	0	0	18	0	0	0	0	0
19	19	0	0	0	0	0	19	0	0	0	0	0
20	20	0	0	0	0	0	20	0	0	0	0	0
21	21	0	0	0	0	0	21	0	0	0	0	0
22	22	0	0	0	0	0	22	0	0	0	0	0
23	23	0	0	0	0	0	23	0	0	0	0	0
24	24	0	0	0	0	0	24	0	0	0	0	0
25	25	0	0	0	0	0	25	0	0	0	0	0
26	26	0	0	0	0	0	26	0	0	0	0	0
27	27	0	0	0	0	0	27	0	0	0	0	0
28	28	0	0	0	0	0	28	0	0	0	0	0
29	29	0	0	0	0	0	29	0	0	0	0	0
30	30	0	0	0	0	0	30	0	0	0	0	0
31	31	0	0	0	0	0	31	0	0	0	0	0
32	32	0	0	0	0	0	32	0	0	0	0	0
33	33	0	0	0	0	0	33	0	0	0	0	0
34	34	0	0	0	0	0	34	0	0	0	0	0
35	35	0	0	0	0	0	35	0	0	0	0	0
36	36	0	0	0	0	0	36	0	0	0	0	0
37	37	0	0	0	0	0	37	0	0	0	0	0
38	38	0	0	0	0	0	38	0	0	0	0	0
39	39	0	0	0	0	0	39	0	0	0	0	0
40	40	0	0	0	0	0	40	0	0	0	0	0
41	41	0	0	0	0	0	41	0	0	0	0	0
42	42	0	0	0	0	0	42	0	0	0	0	0
43	43	0	0	0	0	0	43	0	0	0	0	0
44	44	0	0	0	0	0	44	0	0	0	0	0
45	45	0	0	0	0	0	45	0	0	0	0	0
46	46	0	0	0	0	0	46	0	0	0	0	0
47	47	0	0	0	0	0	47	0	0	0	0	0
48	48	0	0	0	0	0	48	0	0	0	0	0
49	49	0	0	0	0	0	49	0	0	0	0	0
50	50	0	0	0	0	0	50	0	0	0	0	0
51	51	0	0	0	0	0	51	0	0	0	0	0
52	52	0	0	0	0	0	52	0	0	0	0	0
53	53	0	0	0	0	0	53	0	0	0	0	0

54	54	0	0	0	0	0	54	0	0	0	0	0
55	55	0	0	0	0	0	55	0	0	0	0	0
56	56	0	0	0	0	0	56	0	0	0	0	0
57	57	0	0	0	0	0	57	0	0	0	0	0
58	58	0	0	0	0	0	58	0	0	0	0	0
59	59	0	0	0	0	0	59	0	0	0	0	0
60	60	0	0	0	0	0	60	0	0	0	0	0
61	61	0	0	0	0	0	61	0	0	0	0	0
62	62	0	0	0	0	0	62	0	0	0	0	0
63	63	0	0	0	0	0	63	0	0	0	0	0
64	64	0	0	0	0	0	64	0	0	0	0	0
65	65	0	0	0	0	0	65	0	0	0	0	0
66	66	0	0	0	0	0	66	0	0	0	0	0
67	67	0	0	0	0	0	67	0	0	0	0	0
68	68	0	0	0	0	0	68	0	0	0	0	0
69	69	0	0	0	0	0	69	0	0	0	0	0
70	70	0	0	0	0	0	70	0	0	0	0	0
71	71	0	0	0	0	0	71	0	0	0	0	0
72	72	0	0	0	0	0	72	0	0	0	0	0
73	73	0	0	0	0	0	73	0	0	0	0	0
74	74	0	0	0	0	0	74	0	0	0	0	0
75	75	0	0	0	0	0	75	0	0	0	0	0
76	76	0	0	0	0	0	76	0	0	0	0	0
77	77	0	0	0	0	0	77	0	0	0	0	0
78	78	0	0	0	0	0	78	0	0	0	0	0
79	79	0	0	0	0	0	79	0	0	0	0	0
80	80	0	0	0	0	0	80	0	0	0	0	0
81	81	0	0	0	0	0	81	0	0	0	0	0
82	82	0	0	0	0	0	82	0	0	0	0	0
83	83	0	0	0	0	0	83	0	0	0	0	0
84	84	0	0	0	0	0	84	0	0	0	0	0
85	85	0	0	0	0	0	85	0	0	0	0	0
86	86	0	0	0	0	0	86	0	0	0	0	0
87	87	0	0	0	0	0	87	0	0	0	0	0
88	88	0	0	0	0	0	88	0	0	0	0	0
89	89	0	0	0	0	0	89	0	0	0	0	0
90	90	0	0	0	0	0	90	0	0	0	0	0

```
    91    91     0     0     0     0     0    91     0     0     0     0     0
    92    92     0     0     0     0     0    92     0     0     0     0     0
    93    93     0     0     0     0     0    93     0     0     0     0     0
* Card 4.5
* IWDE
    93
* Card 4.6
* MSIM
  3720
*
*******************************************************************************
* GROUP 8.0 - Rod and Unheated Conductor Data                                  *
*******************************************************************************
* CARD GROUP 8
* NGR
    8
* Card 8.1
* NRRD  NSRD   NC NRTB NRAD NLTY NSTA  NXF NCAN RADF   W3 NM12 NM13 NM14
    62    62    1    1    0    0    1    1    0    0   -1    0    0    0
* Card 8.2
*   N IFTY IAXP NRND  DAXMIN   RMULT    HGAP ISECR   HTAMB    TAMB
    1    1    1    0 0.00000   1.000 0.00000     1   0.000   0.000
* Card 8.3
* NSCH   PIE  NSCH   PIE  NSCH   PIE  NSCH   PIE  NSCH   PIE  NSCH   PIE  NSCH   PIE  NSCH   PIE
     1 0.234    31 0.234    32 0.266    62 0.266     0 0.000     0 0.000     0 0.000     0 0.000
*
* Cards 8.2 and 8.3 continued
     2    1    1    0 0.00000   1.000 0.00000     1   0.000   0.000
     1 0.234     2 0.234    32 0.266    33 0.266     0 0.000     0 0.000     0 0.000     0 0.000
*
     3    1    1    0 0.00000   1.000 0.00000     1   0.000   0.000
     2 0.234     3 0.234    33 0.266    34 0.266     0 0.000     0 0.000     0 0.000     0 0.000
*
     4    1    1    0 0.00000   1.000 0.00000     1   0.000   0.000
     3 0.234     4 0.234    34 0.266    35 0.266     0 0.000     0 0.000     0 0.000     0 0.000
*
     5    1    1    0 0.00000   1.000 0.00000     1   0.000   0.000
```

```
     4 0.234     5 0.234    35 0.266    36 0.266     0 0.000     0 0.000     0 0.000     0 0.000
*
     6    1    1    0 0.00000   1.000 0.00000     1   0.000   0.000
     5 0.234     6 0.234    36 0.266    37 0.266     0 0.000     0 0.000     0 0.000     0 0.000
*
     7    1    1    0 0.00000   1.000 0.00000     1   0.000   0.000
     6 0.234     7 0.234    37 0.266    38 0.266     0 0.000     0 0.000     0 0.000     0 0.000
*
     8    1    1    0 0.00000   1.000 0.00000     1   0.000   0.000
     7 0.234     8 0.234    38 0.266    39 0.266     0 0.000     0 0.000     0 0.000     0 0.000
*
     9    1    1    0 0.00000   1.000 0.00000     1   0.000   0.000
     8 0.234     9 0.234    39 0.266    40 0.266     0 0.000     0 0.000     0 0.000     0 0.000
*
    10    1    1    0 0.00000   1.000 0.00000     1   0.000   0.000
     9 0.234    10 0.234    40 0.266    41 0.266     0 0.000     0 0.000     0 0.000     0 0.000
*
    11    1    1    0 0.00000   1.000 0.00000     1   0.000   0.000
    10 0.234    11 0.234    41 0.266    42 0.266     0 0.000     0 0.000     0 0.000     0 0.000
*
    12    1    1    0 0.00000   1.000 0.00000     1   0.000   0.000
    11 0.234    12 0.234    42 0.266    43 0.266     0 0.000     0 0.000     0 0.000     0 0.000
*
    13    1    1    0 0.00000   1.000 0.00000     1   0.000   0.000
    12 0.234    13 0.234    43 0.266    44 0.266     0 0.000     0 0.000     0 0.000     0 0.000
*
    14    1    1    0 0.00000   1.000 0.00000     1   0.000   0.000
    13 0.234    14 0.234    44 0.266    45 0.266     0 0.000     0 0.000     0 0.000     0 0.000
*
    15    1    1    0 0.00000   1.000 0.00000     1   0.000   0.000
    14 0.234    15 0.234    45 0.266    46 0.266     0 0.000     0 0.000     0 0.000     0 0.000
*
    16    1    1    0 0.00000   1.000 0.00000     1   0.000   0.000
    15 0.234    16 0.234    46 0.266    47 0.266     0 0.000     0 0.000     0 0.000     0 0.000
*
    17    1    1    0 0.00000   1.000 0.00000     1   0.000   0.000
    16 0.234    17 0.234    47 0.266    48 0.266     0 0.000     0 0.000     0 0.000     0 0.000
```

```
*
    18    1    1    0 0.00000   1.000 0.00000     1   0.000   0.000
    17 0.234    18 0.234    48 0.266    49 0.266     0 0.000     0 0.000     0 0.000     0 0.000
*
    19    1    1    0 0.00000   1.000 0.00000     1   0.000   0.000
    18 0.234    19 0.234    49 0.266    50 0.266     0 0.000     0 0.000     0 0.000     0 0.000
*
    20    1    1    0 0.00000   1.000 0.00000     1   0.000   0.000
    19 0.234    20 0.234    50 0.266    51 0.266     0 0.000     0 0.000     0 0.000     0 0.000
*
    21    1    1    0 0.00000   1.000 0.00000     1   0.000   0.000
    20 0.234    21 0.234    51 0.266    52 0.266     0 0.000     0 0.000     0 0.000     0 0.000
*
    22    1    1    0 0.00000   1.000 0.00000     1   0.000   0.000
    21 0.234    22 0.234    52 0.266    53 0.266     0 0.000     0 0.000     0 0.000     0 0.000
*
    23    1    1    0 0.00000   1.000 0.00000     1   0.000   0.000
    22 0.234    23 0.234    53 0.266    54 0.266     0 0.000     0 0.000     0 0.000     0 0.000
*
    24    1    1    0 0.00000   1.000 0.00000     1   0.000   0.000
    23 0.234    24 0.234    54 0.266    55 0.266     0 0.000     0 0.000     0 0.000     0 0.000
*
    25    1    1    0 0.00000   1.000 0.00000     1   0.000   0.000
    24 0.234    25 0.234    55 0.266    56 0.266     0 0.000     0 0.000     0 0.000     0 0.000
*
    26    1    1    0 0.00000   1.000 0.00000     1   0.000   0.000
    25 0.234    26 0.234    56 0.266    57 0.266     0 0.000     0 0.000     0 0.000     0 0.000
*
    27    1    1    0 0.00000   1.000 0.00000     1   0.000   0.000
    26 0.234    27 0.234    57 0.266    58 0.266     0 0.000     0 0.000     0 0.000     0 0.000
*
    28    1    1    0 0.00000   1.000 0.00000     1   0.000   0.000
    27 0.234    28 0.234    58 0.266    59 0.266     0 0.000     0 0.000     0 0.000     0 0.000
*
    29    1    1    0 0.00000   1.000 0.00000     1   0.000   0.000
    28 0.234    29 0.234    59 0.266    60 0.266     0 0.000     0 0.000     0 0.000     0 0.000
*
```

```
    30    1    1    0 0.00000   1.000 0.00000     1   0.000   0.000
    29 0.234    30 0.234    60 0.266    61 0.266     0 0.000     0 0.000     0 0.000     0 0.000
*
    31    1    1    0 0.00000   1.000 0.00000     1   0.000   0.000
    30 0.234    31 0.234    61 0.266    62 0.266     0 0.000     0 0.000     0 0.000     0 0.000
*
    32    4    1    0 0.00000   1.000 0.00000     1   0.000   0.000
    32 0.234    62 0.234    63 0.266    93 0.266     0 0.000     0 0.000     0 0.000     0 0.000
*
    33    4    1    0 0.00000   1.000 0.00000     1   0.000   0.000
    32 0.234    33 0.234    63 0.266    64 0.266     0 0.000     0 0.000     0 0.000     0 0.000
*
    34    4    1    0 0.00000   1.000 0.00000     1   0.000   0.000
    33 0.234    34 0.234    64 0.266    65 0.266     0 0.000     0 0.000     0 0.000     0 0.000
*
    35    4    1    0 0.00000   1.000 0.00000     1   0.000   0.000
    34 0.234    35 0.234    65 0.266    66 0.266     0 0.000     0 0.000     0 0.000     0 0.000
*
    36    4    1    0 0.00000   1.000 0.00000     1   0.000   0.000
    35 0.234    36 0.234    66 0.266    67 0.266     0 0.000     0 0.000     0 0.000     0 0.000
*
    37    4    1    0 0.00000   1.000 0.00000     1   0.000   0.000
    36 0.234    37 0.234    67 0.266    68 0.266     0 0.000     0 0.000     0 0.000     0 0.000
*
    38    4    1    0 0.00000   1.000 0.00000     1   0.000   0.000
    37 0.234    38 0.234    68 0.266    69 0.266     0 0.000     0 0.000     0 0.000     0 0.000
*
    39    4    1    0 0.00000   1.000 0.00000     1   0.000   0.000
    38 0.234    39 0.234    69 0.266    70 0.266     0 0.000     0 0.000     0 0.000     0 0.000
*
    40    4    1    0 0.00000   1.000 0.00000     1   0.000   0.000
    39 0.234    40 0.234    70 0.266    71 0.266     0 0.000     0 0.000     0 0.000     0 0.000
*
    41    4    1    0 0.00000   1.000 0.00000     1   0.000   0.000
    40 0.234    41 0.234    71 0.266    72 0.266     0 0.000     0 0.000     0 0.000     0 0.000
*
    42    4    1    0 0.00000   1.000 0.00000     1   0.000   0.000
```

```
    41 0.234    42 0.234    72 0.266    73 0.266     0 0.000     0 0.000     0 0.000     0 0.000
*
    43    4    1    0 0.00000   1.000 0.00000     1   0.000   0.000
    42 0.234    43 0.234    73 0.266    74 0.266     0 0.000     0 0.000     0 0.000     0 0.000
*
    44    4    1    0 0.00000   1.000 0.00000     1   0.000   0.000
    43 0.234    44 0.234    74 0.266    75 0.266     0 0.000     0 0.000     0 0.000     0 0.000
*
    45    4    1    0 0.00000   1.000 0.00000     1   0.000   0.000
    44 0.234    45 0.234    75 0.266    76 0.266     0 0.000     0 0.000     0 0.000     0 0.000
*
    46    4    1    0 0.00000   1.000 0.00000     1   0.000   0.000
    45 0.234    46 0.234    76 0.266    77 0.266     0 0.000     0 0.000     0 0.000     0 0.000
*
    47    4    1    0 0.00000   1.000 0.00000     1   0.000   0.000
    46 0.234    47 0.234    77 0.266    78 0.266     0 0.000     0 0.000     0 0.000     0 0.000
*
    48    4    1    0 0.00000   1.000 0.00000     1   0.000   0.000
    47 0.234    48 0.234    78 0.266    79 0.266     0 0.000     0 0.000     0 0.000     0 0.000
*
    49    4    1    0 0.00000   1.000 0.00000     1   0.000   0.000
    48 0.234    49 0.234    79 0.266    80 0.266     0 0.000     0 0.000     0 0.000     0 0.000
*
    50    4    1    0 0.00000   1.000 0.00000     1   0.000   0.000
    49 0.234    50 0.234    80 0.266    81 0.266     0 0.000     0 0.000     0 0.000     0 0.000
*
    51    4    1    0 0.00000   1.000 0.00000     1   0.000   0.000
    50 0.234    51 0.234    81 0.266    82 0.266     0 0.000     0 0.000     0 0.000     0 0.000
*
    52    4    1    0 0.00000   1.000 0.00000     1   0.000   0.000
    51 0.234    52 0.234    82 0.266    83 0.266     0 0.000     0 0.000     0 0.000     0 0.000
*
    53    4    1    0 0.00000   1.000 0.00000     1   0.000   0.000
    52 0.234    53 0.234    83 0.266    84 0.266     0 0.000     0 0.000     0 0.000     0 0.000
*
    54    4    1    0 0.00000   1.000 0.00000     1   0.000   0.000
    53 0.234    54 0.234    84 0.266    85 0.266     0 0.000     0 0.000     0 0.000     0 0.000
```

```
*
    55    4    1    0 0.00000   1.000 0.00000     1   0.000   0.000
    54 0.234    55 0.234    85 0.266    86 0.266     0 0.000     0 0.000     0 0.000     0 0.000
*
    56    4    1    0 0.00000   1.000 0.00000     1   0.000   0.000
    55 0.234    56 0.234    86 0.266    87 0.266     0 0.000     0 0.000     0 0.000     0 0.000
*
    57    4    1    0 0.00000   1.000 0.00000     1   0.000   0.000
    56 0.234    57 0.234    87 0.266    88 0.266     0 0.000     0 0.000     0 0.000     0 0.000
*
    58    4    1    0 0.00000   1.000 0.00000     1   0.000   0.000
    57 0.234    58 0.234    88 0.266    89 0.266     0 0.000     0 0.000     0 0.000     0 0.000
*
    59    4    1    0 0.00000   1.000 0.00000     1   0.000   0.000
    58 0.234    59 0.234    89 0.266    90 0.266     0 0.000     0 0.000     0 0.000     0 0.000
*
    60    4    1    0 0.00000   1.000 0.00000     1   0.000   0.000
    59 0.234    60 0.234    90 0.266    91 0.266     0 0.000     0 0.000     0 0.000     0 0.000
*
    61    4    1    0 0.00000   1.000 0.00000     1   0.000   0.000
    60 0.234    61 0.234    91 0.266    92 0.266     0 0.000     0 0.000     0 0.000     0 0.000
*
    62    4    1    0 0.00000   1.000 0.00000     1   0.000   0.000
    61 0.234    62 0.234    92 0.266    93 0.266     0 0.000     0 0.000     0 0.000     0 0.000
*
* Card 8.5
*   N ISTY  HPERIM  PERIMI RMULT NOSLCHC  NSLCHC  HTAMBS   TAMBS
    1    2 0.00000 0.00924  1.00       1       0   0.000   0.000
    2    2 0.00000 0.00924  1.00       2       0   0.000   0.000
    3    2 0.00000 0.00924  1.00       3       0   0.000   0.000
    4    2 0.00000 0.00924  1.00       4       0   0.000   0.000
    5    2 0.00000 0.00924  1.00       5       0   0.000   0.000
    6    2 0.00000 0.00924  1.00       6       0   0.000   0.000
    7    2 0.00000 0.00924  1.00       7       0   0.000   0.000
    8    2 0.00000 0.00924  1.00       8       0   0.000   0.000
    9    2 0.00000 0.00924  1.00       9       0   0.000   0.000
   10    2 0.00000 0.00924  1.00      10       0   0.000   0.000
```

11	2	0.00000	0.00924	1.00	11	0	0.000	0.000
12	2	0.00000	0.00924	1.00	12	0	0.000	0.000
13	2	0.00000	0.00924	1.00	13	0	0.000	0.000
14	2	0.00000	0.00924	1.00	14	0	0.000	0.000
15	2	0.00000	0.00924	1.00	15	0	0.000	0.000
16	2	0.00000	0.00924	1.00	16	0	0.000	0.000
17	2	0.00000	0.00924	1.00	17	0	0.000	0.000
18	2	0.00000	0.00924	1.00	18	0	0.000	0.000
19	2	0.00000	0.00924	1.00	19	0	0.000	0.000
20	2	0.00000	0.00924	1.00	20	0	0.000	0.000
21	2	0.00000	0.00924	1.00	21	0	0.000	0.000
22	2	0.00000	0.00924	1.00	22	0	0.000	0.000
23	2	0.00000	0.00924	1.00	23	0	0.000	0.000
24	2	0.00000	0.00924	1.00	24	0	0.000	0.000
25	2	0.00000	0.00924	1.00	25	0	0.000	0.000
26	2	0.00000	0.00924	1.00	26	0	0.000	0.000
27	2	0.00000	0.00924	1.00	27	0	0.000	0.000
28	2	0.00000	0.00924	1.00	28	0	0.000	0.000
29	2	0.00000	0.00924	1.00	29	0	0.000	0.000
30	2	0.00000	0.00924	1.00	30	0	0.000	0.000
31	2	0.00000	0.00924	1.00	31	0	0.000	0.000
32	3	0.01459	0.00000	1.00	63	0	0.000	0.000
33	3	0.01459	0.00000	1.00	64	0	0.000	0.000
34	3	0.01459	0.00000	1.00	65	0	0.000	0.000
35	3	0.01459	0.00000	1.00	66	0	0.000	0.000
36	3	0.01459	0.00000	1.00	67	0	0.000	0.000
37	3	0.01459	0.00000	1.00	68	0	0.000	0.000
38	3	0.01459	0.00000	1.00	69	0	0.000	0.000
39	3	0.01459	0.00000	1.00	70	0	0.000	0.000
40	3	0.01459	0.00000	1.00	71	0	0.000	0.000
41	3	0.01459	0.00000	1.00	72	0	0.000	0.000
42	3	0.01459	0.00000	1.00	73	0	0.000	0.000
43	3	0.01459	0.00000	1.00	74	0	0.000	0.000
44	3	0.01459	0.00000	1.00	75	0	0.000	0.000
45	3	0.01459	0.00000	1.00	76	0	0.000	0.000
46	3	0.01459	0.00000	1.00	77	0	0.000	0.000
47	3	0.01459	0.00000	1.00	78	0	0.000	0.000

```
   48    3 0.01459 0.00000  1.00      79       0   0.000   0.000
   49    3 0.01459 0.00000  1.00      80       0   0.000   0.000
   50    3 0.01459 0.00000  1.00      81       0   0.000   0.000
   51    3 0.01459 0.00000  1.00      82       0   0.000   0.000
   52    3 0.01459 0.00000  1.00      83       0   0.000   0.000
   53    3 0.01459 0.00000  1.00      84       0   0.000   0.000
   54    3 0.01459 0.00000  1.00      85       0   0.000   0.000
   55    3 0.01459 0.00000  1.00      86       0   0.000   0.000
   56    3 0.01459 0.00000  1.00      87       0   0.000   0.000
   57    3 0.01459 0.00000  1.00      88       0   0.000   0.000
   58    3 0.01459 0.00000  1.00      89       0   0.000   0.000
   59    3 0.01459 0.00000  1.00      90       0   0.000   0.000
   60    3 0.01459 0.00000  1.00      91       0   0.000   0.000
   61    3 0.01459 0.00000  1.00      92       0   0.000   0.000
   62    3 0.01459 0.00000  1.00      93       0   0.000   0.000
*
* Card 8.6
*   I  NRT1  NST1  NRX1
    1    62    62     2
*
* Card 8.7
* IRTAB IRTAB IRTAB IRTAB IRTAB IRTAB IRTAB IRTAB IRTAB IRTAB IRTAB IRTAB
      1     2     3     4     5     6     7     8     9    10    11    12
     13    14    15    16    17    18    19    20    21    22    23    24
     25    26    27    28    29    30    31    32    33    34    35    36
     37    38    39    40    41    42    43    44    45    46    47    48
     49    50    51    52    53    54    55    56    57    58    59    60
     61    62
*
* Card 8.8
* IRTAB IRTAB IRTAB IRTAB IRTAB IRTAB IRTAB IRTAB IRTAB IRTAB IRTAB IRTAB
      1     2     3     4     5     6     7     8     9    10    11    12
     13    14    15    16    17    18    19    20    21    22    23    24
     25    26    27    28    29    30    31    32    33    34    35    36
     37    38    39    40    41    42    43    44    45    46    47    48
     49    50    51    52    53    54    55    56    57    58    59    60
     61    62
```

```
*
* Card 8.9
*   AXIALT     TRINIT
 0.0000000  300.00000
 5.0000000  300.00000
*
*******************************************************************************
* GROUP 9.0 - Conductor Geometry Description                                   *
*******************************************************************************
* CARD GROUP 9
* NGR
    9
* Card 9.1
* NFLT IRLF ICNF IMWR NDM5 NDM6 NDM7 NDM8 NDM9 NM10 NM11 NM12 NM13 NM14
     4    0    0    0    0    0    0    0    0    0    0    0    0    0
*
* Card 9.6
*   I FTYP    DROD     DIN NFUL ITOX ITIX NDM8 NDM9 NM10 NM11 NM12 NM13 NM14
    1 tube 0.00950 0.00850    1    1    1    0    0    0    0    0    0    0
* Card 9.7
* NODR MATR    TREG    QREG
     2    1 0.00050 1.00000
*
* Card 9.6
*   I FTYP    DROD     DIN NFUL ITOX ITIX NDM8 NDM9 NM10 NM11 NM12 NM13 NM14
    2 wall 0.00924 0.00100    1    1    1    0    0    0    0    0    0    0
* Card 9.7
* NODR MATR    TREG    QREG
     2    1 0.00100 0.00000
*
* Card 9.6
*   I FTYP    DROD     DIN NFUL ITOX ITIX NDM8 NDM9 NM10 NM11 NM12 NM13 NM14
    3 wall 0.01459 0.00100    1    1    1    0    0    0    0    0    0    0
* Card 9.7
* NODR MATR    TREG    QREG
     2    1 0.00100 0.00000
*
```

```
* Card 9.6
*   I FTYP    DROD     DIN NFUL ITOX ITIX NDM8 NDM9 NM10 NM11 NM12 NM13 NM14
    4 tube 0.01050 0.00950    1    1    1    0    0    0    0    0    0    0
* Card 9.7
* NODR MATR    TREG    QREG
     2    1 0.00050 1.00000
*
*******************************************************************************
* GROUP 10 - Material Properties Tables                                       *
*******************************************************************************
* CARD GROUP 10
* NGR
   10
* CArd 10.1
* NMAT NDM2 NDM3 NDM4 NDM5 NDM6 NDM7 NDM8 NDM9 NM10 NM11 NM12 NM13 NM14
     1    0    0    0    0    0    0    0    0    0    0    0    0    0
* Card 10.2
*   N NTDP     RCOLD                        IMATAN
    1    6   8470.57                   Inconel 600
* Card 10.3
*    TPROP     CPF1      THCF
       -73    0.377     13.40
        93    0.464     15.71
       204    0.485     17.44
       427    0.527     20.90
       649    0.586     24.79
       871    0.623     28.83
*
*******************************************************************************
* GROUP 11.0 - Axial Power Tables and Forcing Functions                       *
*******************************************************************************
* CARD GROUP 11
* NGR
   11
* Card 11.1
* NQA NAXP MNXN   NQ NGPF  NQR NDM7 NDM8 NDM9 NM10 NM11 NM12 NM13 NM14
    1    1  101    0    0    1    0    0    0    0    0    0    0    0
```

```
*
* Axial Power Forcing Functions
* Card 11.2
*      YQA
       0.0
* Card 11.3
*  I NAXN
   1   52
* Card 11.4
*        Y      AXIAL
  0.000000   0.000000
  0.100000   0.239400
  0.200000   0.964600
  0.300000   0.977200
  0.400000   0.987400
  0.500000   0.995400
  0.600000   1.001400
  0.700000   1.005900
  0.800000   1.008800
  0.900000   1.010500
  1.000000   1.011200
  1.100000   1.010900
  1.200000   1.010000
  1.300000   1.008600
  1.400000   1.006800
  1.500000   1.004700
  1.600000   1.002500
  1.700000   1.000400
  1.800000   0.998200
  1.900000   0.996300
  2.000000   0.994700
  2.100000   0.993300
  2.200000   0.992400
  2.300000   0.991800
  2.400000   0.991700
  2.500000   0.992000
  2.600000   0.992800
```

```
  2.700000   0.994000
  2.800000   0.995700
  2.900000   0.997800
  3.000000   1.000200
  3.100000   1.002800
  3.200000   1.005700
  3.300000   1.008700
  3.400000   1.011800
  3.500000   1.014800
  3.600000   1.017500
  3.700000   1.019900
  3.800000   1.021900
  3.900000   1.023300
  4.000000   1.024000
  4.100000   1.023500
  4.200000   1.022000
  4.300000   1.019100
  4.400000   1.014500
  4.500000   1.008200
  4.600000   0.999800
  4.700000   0.989100
  4.800000   0.975800
  4.900000   0.959600
  5.000000   0.237700
  5.000000   0.000000
*
* Total Power Forcing Functions
* Card 11.5
*       YQ         FQ
*    0.0000     0.0000
*    1.0000     1.0000
*  100.0000     1.0000
*
* Radial Power Forcing Functions
* Card 11.7
*      YQR
       0.0
```

```
* Card 11.8
*      FQR        FQR        FQR        FQR        FQR        FQR        FQR        FQR
    1.0000     1.0000     1.0000     1.0000     1.0000     1.0000     1.0000     1.0000
    1.0000     1.0000     1.0000     1.0000     1.0000     1.0000     1.0000     1.0000
    1.0000     1.0000     1.0000     1.0000     1.0000     1.0000     1.0000     1.0000
    1.0000     1.0000     1.0000     1.0000     1.0000     1.0000     1.0000     1.0000
    1.0000     1.0000     1.0000     1.0000     1.0000     1.0000     1.0000     1.0000
    1.0000     1.0000     1.0000     1.0000     1.0000     1.0000     1.0000     1.0000
    1.0000     1.0000     1.0000     1.0000     1.0000     1.0000     1.0000     1.0000
    1.0000     1.0000     1.0000     1.0000     1.0000     1.0000
*
*******************************************************************************
* GROUP 12 - Turbulent mixing data                                             *
*******************************************************************************
* CARD GROUP 12
* NGR
   12
* Card 12.1
* AAAK BETA
   0.0 0.04
*
*******************************************************************************
* GROUP 13.0 - Boundary Condition Data                                         *
*******************************************************************************
* CARD GROUP 13
* NGR
   13
* Card 13.1
* NBND NKBD NFUN NGBD NDM5 NDM6 NDM7 NDM8 NDM9 NM10 NM11 NM12 NM13 NM14
   186    0    1    0    0    0    0    0    0    0    0    0    0    0
* Card 13.2
* NPT
    4
* Card 13.3
* ABSC ORDINT   ABSC ORDINT   ABSC ORDINT
   0.0  0.000    0.1  0.000    0.2  1.000 1500.0  1.000
* Card 13.4
```

```
* Inlet b.c. ----------------------------------------------------------
* IBD1 IBD2 ISPC N1FN N2FN N3FN   BCVALUE1   BCVALUE2   BCVALUE3 INITGAS
     1    1    2    1    0    0        0.0    1623.90     0.0000       1
     2    1    2    1    0    0        0.0    1623.90     0.0000       1
     3    1    2    1    0    0        0.0    1623.90     0.0000       1
     4    1    2    1    0    0        0.0    1623.90     0.0000       1
     5    1    2    1    0    0        0.0    1623.90     0.0000       1
     6    1    2    1    0    0        0.0    1623.90     0.0000       1
     7    1    2    1    0    0        0.0    1623.90     0.0000       1
     8    1    2    1    0    0        0.0    1623.90     0.0000       1
     9    1    2    1    0    0        0.0    1623.90     0.0000       1
    10    1    2    1    0    0        0.0    1623.90     0.0000       1
    11    1    2    1    0    0        0.0    1623.90     0.0000       1
    12    1    2    1    0    0        0.0    1623.90     0.0000       1
    13    1    2    1    0    0        0.0    1623.90     0.0000       1
    14    1    2    1    0    0        0.0    1623.90     0.0000       1
    15    1    2    1    0    0        0.0    1623.90     0.0000       1
    16    1    2    1    0    0        0.0    1623.90     0.0000       1
    17    1    2    1    0    0        0.0    1623.90     0.0000       1
    18    1    2    1    0    0        0.0    1623.90     0.0000       1
    19    1    2    1    0    0        0.0    1623.90     0.0000       1
    20    1    2    1    0    0        0.0    1623.90     0.0000       1
    21    1    2    1    0    0        0.0    1623.90     0.0000       1
    22    1    2    1    0    0        0.0    1623.90     0.0000       1
    23    1    2    1    0    0        0.0    1623.90     0.0000       1
    24    1    2    1    0    0        0.0    1623.90     0.0000       1
    25    1    2    1    0    0        0.0    1623.90     0.0000       1
    26    1    2    1    0    0        0.0    1623.90     0.0000       1
    27    1    2    1    0    0        0.0    1623.90     0.0000       1
    28    1    2    1    0    0        0.0    1623.90     0.0000       1
    29    1    2    1    0    0        0.0    1623.90     0.0000       1
    30    1    2    1    0    0        0.0    1623.90     0.0000       1
    31    1    2    1    0    0        0.0    1623.90     0.0000       1
    32    1    2    1    0    0        0.0    1623.90     0.0000       1
    33    1    2    1    0    0        0.0    1623.90     0.0000       1
    34    1    2    1    0    0        0.0    1623.90     0.0000       1
    35    1    2    1    0    0        0.0    1623.90     0.0000       1
```

36	1	2	1	0	0	0.0	1623.90	0.0000	1
37	1	2	1	0	0	0.0	1623.90	0.0000	1
38	1	2	1	0	0	0.0	1623.90	0.0000	1
39	1	2	1	0	0	0.0	1623.90	0.0000	1
40	1	2	1	0	0	0.0	1623.90	0.0000	1
41	1	2	1	0	0	0.0	1623.90	0.0000	1
42	1	2	1	0	0	0.0	1623.90	0.0000	1
43	1	2	1	0	0	0.0	1623.90	0.0000	1
44	1	2	1	0	0	0.0	1623.90	0.0000	1
45	1	2	1	0	0	0.0	1623.90	0.0000	1
46	1	2	1	0	0	0.0	1623.90	0.0000	1
47	1	2	1	0	0	0.0	1623.90	0.0000	1
48	1	2	1	0	0	0.0	1623.90	0.0000	1
49	1	2	1	0	0	0.0	1623.90	0.0000	1
50	1	2	1	0	0	0.0	1623.90	0.0000	1
51	1	2	1	0	0	0.0	1623.90	0.0000	1
52	1	2	1	0	0	0.0	1623.90	0.0000	1
53	1	2	1	0	0	0.0	1623.90	0.0000	1
54	1	2	1	0	0	0.0	1623.90	0.0000	1
55	1	2	1	0	0	0.0	1623.90	0.0000	1
56	1	2	1	0	0	0.0	1623.90	0.0000	1
57	1	2	1	0	0	0.0	1623.90	0.0000	1
58	1	2	1	0	0	0.0	1623.90	0.0000	1
59	1	2	1	0	0	0.0	1623.90	0.0000	1
60	1	2	1	0	0	0.0	1623.90	0.0000	1
61	1	2	1	0	0	0.0	1623.90	0.0000	1
62	1	2	1	0	0	0.0	1623.90	0.0000	1
63	1	2	1	0	0	0.0	1623.90	0.0000	1
64	1	2	1	0	0	0.0	1623.90	0.0000	1
65	1	2	1	0	0	0.0	1623.90	0.0000	1
66	1	2	1	0	0	0.0	1623.90	0.0000	1
67	1	2	1	0	0	0.0	1623.90	0.0000	1
68	1	2	1	0	0	0.0	1623.90	0.0000	1
69	1	2	1	0	0	0.0	1623.90	0.0000	1
70	1	2	1	0	0	0.0	1623.90	0.0000	1
71	1	2	1	0	0	0.0	1623.90	0.0000	1
72	1	2	1	0	0	0.0	1623.90	0.0000	1

```
    73    1    2    1    0    0        0.0    1623.90     0.0000       1
    74    1    2    1    0    0        0.0    1623.90     0.0000       1
    75    1    2    1    0    0        0.0    1623.90     0.0000       1
    76    1    2    1    0    0        0.0    1623.90     0.0000       1
    77    1    2    1    0    0        0.0    1623.90     0.0000       1
    78    1    2    1    0    0        0.0    1623.90     0.0000       1
    79    1    2    1    0    0        0.0    1623.90     0.0000       1
    80    1    2    1    0    0        0.0    1623.90     0.0000       1
    81    1    2    1    0    0        0.0    1623.90     0.0000       1
    82    1    2    1    0    0        0.0    1623.90     0.0000       1
    83    1    2    1    0    0        0.0    1623.90     0.0000       1
    84    1    2    1    0    0        0.0    1623.90     0.0000       1
    85    1    2    1    0    0        0.0    1623.90     0.0000       1
    86    1    2    1    0    0        0.0    1623.90     0.0000       1
    87    1    2    1    0    0        0.0    1623.90     0.0000       1
    88    1    2    1    0    0        0.0    1623.90     0.0000       1
    89    1    2    1    0    0        0.0    1623.90     0.0000       1
    90    1    2    1    0    0        0.0    1623.90     0.0000       1
    91    1    2    1    0    0        0.0    1623.90     0.0000       1
    92    1    2    1    0    0        0.0    1623.90     0.0000       1
    93    1    2    1    0    0        0.0    1623.90     0.0000       1
* Outlet b.c. ------------------------------------------------------
* IBD1 IBD2 ISPC N1FN N2FN N3FN   BCVALUE1   BCVALUE2   BCVALUE3 INITGAS
     1   42    1    0    0    0     0.0000     1623.90     250.00       1
     2   42    1    0    0    0     0.0000     1623.90     250.00       1
     3   42    1    0    0    0     0.0000     1623.90     250.00       1
     4   42    1    0    0    0     0.0000     1623.90     250.00       1
     5   42    1    0    0    0     0.0000     1623.90     250.00       1
     6   42    1    0    0    0     0.0000     1623.90     250.00       1
     7   42    1    0    0    0     0.0000     1623.90     250.00       1
     8   42    1    0    0    0     0.0000     1623.90     250.00       1
     9   42    1    0    0    0     0.0000     1623.90     250.00       1
    10   42    1    0    0    0     0.0000     1623.90     250.00       1
    11   42    1    0    0    0     0.0000     1623.90     250.00       1
    12   42    1    0    0    0     0.0000     1623.90     250.00       1
    13   42    1    0    0    0     0.0000     1623.90     250.00       1
    14   42    1    0    0    0     0.0000     1623.90     250.00       1
```

15	42	1	0	0	0	0.0000	1623.90	250.00	1
16	42	1	0	0	0	0.0000	1623.90	250.00	1
17	42	1	0	0	0	0.0000	1623.90	250.00	1
18	42	1	0	0	0	0.0000	1623.90	250.00	1
19	42	1	0	0	0	0.0000	1623.90	250.00	1
20	42	1	0	0	0	0.0000	1623.90	250.00	1
21	42	1	0	0	0	0.0000	1623.90	250.00	1
22	42	1	0	0	0	0.0000	1623.90	250.00	1
23	42	1	0	0	0	0.0000	1623.90	250.00	1
24	42	1	0	0	0	0.0000	1623.90	250.00	1
25	42	1	0	0	0	0.0000	1623.90	250.00	1
26	42	1	0	0	0	0.0000	1623.90	250.00	1
27	42	1	0	0	0	0.0000	1623.90	250.00	1
28	42	1	0	0	0	0.0000	1623.90	250.00	1
29	42	1	0	0	0	0.0000	1623.90	250.00	1
30	42	1	0	0	0	0.0000	1623.90	250.00	1
31	42	1	0	0	0	0.0000	1623.90	250.00	1
32	42	1	0	0	0	0.0000	1623.90	250.00	1
33	42	1	0	0	0	0.0000	1623.90	250.00	1
34	42	1	0	0	0	0.0000	1623.90	250.00	1
35	42	1	0	0	0	0.0000	1623.90	250.00	1
36	42	1	0	0	0	0.0000	1623.90	250.00	1
37	42	1	0	0	0	0.0000	1623.90	250.00	1
38	42	1	0	0	0	0.0000	1623.90	250.00	1
39	42	1	0	0	0	0.0000	1623.90	250.00	1
40	42	1	0	0	0	0.0000	1623.90	250.00	1
41	42	1	0	0	0	0.0000	1623.90	250.00	1
42	42	1	0	0	0	0.0000	1623.90	250.00	1
43	42	1	0	0	0	0.0000	1623.90	250.00	1
44	42	1	0	0	0	0.0000	1623.90	250.00	1
45	42	1	0	0	0	0.0000	1623.90	250.00	1
46	42	1	0	0	0	0.0000	1623.90	250.00	1
47	42	1	0	0	0	0.0000	1623.90	250.00	1
48	42	1	0	0	0	0.0000	1623.90	250.00	1
49	42	1	0	0	0	0.0000	1623.90	250.00	1
50	42	1	0	0	0	0.0000	1623.90	250.00	1
51	42	1	0	0	0	0.0000	1623.90	250.00	1

52	42	1	0	0	0	0.0000	1623.90	250.00	1
53	42	1	0	0	0	0.0000	1623.90	250.00	1
54	42	1	0	0	0	0.0000	1623.90	250.00	1
55	42	1	0	0	0	0.0000	1623.90	250.00	1
56	42	1	0	0	0	0.0000	1623.90	250.00	1
57	42	1	0	0	0	0.0000	1623.90	250.00	1
58	42	1	0	0	0	0.0000	1623.90	250.00	1
59	42	1	0	0	0	0.0000	1623.90	250.00	1
60	42	1	0	0	0	0.0000	1623.90	250.00	1
61	42	1	0	0	0	0.0000	1623.90	250.00	1
63	42	1	0	0	0	0.0000	1623.90	250.00	1
63	42	1	0	0	0	0.0000	1623.90	250.00	1
64	42	1	0	0	0	0.0000	1623.90	250.00	1
65	42	1	0	0	0	0.0000	1623.90	250.00	1
66	42	1	0	0	0	0.0000	1623.90	250.00	1
67	42	1	0	0	0	0.0000	1623.90	250.00	1
68	42	1	0	0	0	0.0000	1623.90	250.00	1
69	42	1	0	0	0	0.0000	1623.90	250.00	1
70	42	1	0	0	0	0.0000	1623.90	250.00	1
71	42	1	0	0	0	0.0000	1623.90	250.00	1
72	42	1	0	0	0	0.0000	1623.90	250.00	1
73	42	1	0	0	0	0.0000	1623.90	250.00	1
74	42	1	0	0	0	0.0000	1623.90	250.00	1
75	42	1	0	0	0	0.0000	1623.90	250.00	1
76	42	1	0	0	0	0.0000	1623.90	250.00	1
77	42	1	0	0	0	0.0000	1623.90	250.00	1
78	42	1	0	0	0	0.0000	1623.90	250.00	1
79	42	1	0	0	0	0.0000	1623.90	250.00	1
80	42	1	0	0	0	0.0000	1623.90	250.00	1
81	42	1	0	0	0	0.0000	1623.90	250.00	1
82	42	1	0	0	0	0.0000	1623.90	250.00	1
83	42	1	0	0	0	0.0000	1623.90	250.00	1
84	42	1	0	0	0	0.0000	1623.90	250.00	1
85	42	1	0	0	0	0.0000	1623.90	250.00	1
86	42	1	0	0	0	0.0000	1623.90	250.00	1
87	42	1	0	0	0	0.0000	1623.90	250.00	1
88	42	1	0	0	0	0.0000	1623.90	250.00	1

```
    89   42    1    0    0    0     0.0000     1623.90     250.00       1
    90   42    1    0    0    0     0.0000     1623.90     250.00       1
    91   42    1    0    0    0     0.0000     1623.90     250.00       1
    92   42    1    0    0    0     0.0000     1623.90     250.00       1
    93   42    1    0    0    0     0.0000     1623.90     250.00       1
*
*******************************************************************************
* Group 14 - Output Options                                                    *
*******************************************************************************
*NGRP
   14
*  N1 NOU1 NOU2 NOU3 NOU4 IPRP IOPT IRWR NDM9 NM10 NM11 NM12 NM13 NM14
    5    0    0    0    0    0    2    1    0    0    0    0    0    0
*
*PRCH
*    5  13   17   20
*PRTG
*    9  25   36
*PRTR
*    4  10   12
*PRTS
*    5   8
*
*******************************************************************************
* Group 15 - TIME DOMAIN DATA                                                  *
*******************************************************************************
* CARD GROUP 15
* NGR
   15
* Card 15.1
*        DTMIN         DTMAX          TEND    EDINT   DMPINT       RTWFP
      .0000001         0.001          10.0     10.0      0.1         1.0
* Card 15.2
*        DTMIN (if negative stop)
         -.001           0.0           0.0      0.0      0.0         0.0
*
*******************************************************************************
```

```
* END GROUP TIME DOMAIN DATA
*******************************************************************************
*
```

Bibliography

[1] M.N. Avramova and R.K. Salko. *CTF Theory Manual*. The Pennsylvania State University, October 2011.

[2] S.G. Beus. A two-phase turbulent mixing model for flow in rod bundles. Technical report, Bettis Atomic Power Laboratory, 1971.

[3] A.A. Bishop, R.O. Sandberg, and L.S. Tong. Forced convection heat transfer to water at near-critical temperatures and supercritical pressures. Technical report, Westinghouse Electric Corp., 1964.

[4] X. Cheng, T. Schulenberg, and D. Bittermann. Design analysis of core assemblies for supercritical pressure conditions. *Nuclear Engineering and Design*, page 279294, 2003.

[5] F.W. Dittus and L.M.K. Boelter. Heat transfer in automobile radiators for the tubular type. In *Publications in Engineering 2*, pages 443– 461, 1930.

[6] B.V. Dyadyakin and A.S. Popov. Heat transfer and thermal resistance of tight seven-rod bundle cooled with water flow at supercritical pressures. *Transactions of VTI*, pages 244–253, 1977.

[7] S.W. Fu, C. Zhou, Z.H. Xu, and X.J. Liu. Modification and application of the athlet code to trans-critical simulations. In *Proceeding of the 5th International Symposium on Supercritical Water-Cooled Reactors*, March 2011.

[8] M. Hänninen and J. Kurki. Simulations of flows at supercritical pressures with a two-fluid code. In *Proceeding of the 7th International Topical Meeting on Nuclear Reactor Thermal Hydraulics, Operation and Safety*, October 2008.

[9] R.E. Henry. A correlation for the minimum film boiling temperature. In *AICHE Symposium Series*, volume 138, pages 81–90, 1974.

[10] J.D. Jackson. Consideration of the heat transfer properties of supercritical pressure water in connection with the cooling of advanced nuclear reactors. In *Proceedings of the 13th Pacific Basin Nuclear Conference*, October 2002.

[11] J.D. Jackson and J. Fewster. Forced convection data for supercritical pressure fluids. Technical report, HTFS 21540, 1975.

[12] P.L. Kirillov, Yu.S. Yurev, and V.P. Bobkov. *Handbook of Thermal-Hydraulics Calculations*. Energoatomizdat Publishing House, 1990.

[13] E.A. Krasnoshchekov, V.S. Protopopov, Van Fen, and I.V. Kuraeva. Experimental investigation of heat transfer for carbon dioxide in the supercritical region. In *Proceedings of the Second All-Soviet Union Conference on Heat and Mass Transfer*, May 1964.

[14] R.T. Lahey and F.J. Moody. The thermal-hydraulics of a boiling water nuclear reactor. Technical report, ANS Monograph, 1977.

[15] W.H. McAdam, W.E. Kennel, and J.N. Addoms. Heat transfer to superheated steam at high pressures. *Trans. ASME 72*, pages 421–428, 1950.

[16] W.H. McAdams. *Heat Transmission*. McGraw-Hill, 2 edition, 1942.

[17] Takeharu Misawa, Toru Nakatsuka, Hiroyuki Yoshida, and Kazuyuki Takase. Heat transfer experiments and numerical analysis of supercritical pressure water in seven-rod test bundle. In *The 13th International Topical Meeting on Nuclear Reactor Thermal Hydraulics*, September 27-October 2, 2009.

[18] S. Mokry, I. Pioro, A. Farah, K. King, S. Gupta, W. Peiman, and P. Kirillov. Development of supercritical water heat-transfer correlation for vertical bare tubes. *Nuclear Engineering and Design*, 241(4):1126–1136, 2011.

[19] Igor L. Pioro and Romney B. Duffey. *Heat Transfer and Hydraulic Resistance at Supercritical Pressures in Power Engineering Applications*. ASME, 2002.

[20] J.T. Rogers and R.G. Rosehart. Mixing by turbulent interchange in fuel bundles correlations and influences. *72-HT-53*, 1972.

[21] J. Q. Shan and B. Zhang et al. Scwr subchannel code athas development and candu-scwr analysis. *Nuclear Engineering and Design*, pages 1979–1987, 2009.

[22] E.M. Sparrow and et al. Heat transfer to longitudinal laminar flow between cylinders. *J. Heat Transfer*, 83(4), 1961.

[23] J. Spencer, D. Watts, A. Colton, X. Wang, L. Blomeley, V. Anghel, and S. Yue. Core neutronics for the canadian scwr conceptual design. In *The 6th International Symposium on Supercritical Water-Cooled Reactors*, March 03-07, 2013.

[24] H.S. Swenson, J.R. Carver, and C.R. Karakala. Heat transfer to supercritical water in smooth-bore tubes. *Heat Transfer*, 1965.

[25] N.E. Todreas and M.S. Kazimi. *Nuclear Systems 2.* Taylor and Francis, 2001.

[26] N.E. Todreas and M.S. Kazimi. *Nuclear Systems Volume 1.* Taylor and Francis, 2 edition, 2012.

[27] L.S. Tong. Heat transfer in water cooled nuclear reactors. *Nuclear Engineering and Design*, 1972.

[28] W. Wagner and H. Kretzchmar. *International Steam Tables-Properties of Water and Steam Based on the Industrial Formulation IAPWS-IF97.* Springer, 2 edition, 2008.

[29] G.B. Wallis. *One-dimensional two-phase flow.* McGraw-Hill, 1969.

[30] C. Zhou, X.J. Liu, Y.H. Yang, and X. Cheng. Scwr subchannel code athas development and candu-scwr analysis. *At. Energy Sci. Technol.*, pages 80–84, 2009.